INFORMATION TO USERS

This manuscript has been reproduced from the microfilm master. UMI films the text directly from the original or copy submitted. Thus, some thesis and dissertation copies are in typewriter face, while others may be from any type of computer printer.

The quality of this reproduction is dependent upon the quality of the copy submitted. Broken or indistinct print, colored or poor quality illustrations and photographs, print bleedthrough, substandard margins, and improper alignment can adversely affect reproduction.

In the unlikely event that the author did not send UMI a complete manuscript and there are missing pages, these will be noted. Also, if unauthorized copyright material had to be removed, a note will indicate the deletion.

Oversize materials (e.g., maps, drawings, charts) are reproduced by sectioning the original, beginning at the upper left-hand corner and continuing from left to right in equal sections with small overlaps.

Photographs included in the original manuscript have been reproduced xerographically in this copy. Higher quality 6" x 9" black and white photographic prints are available for any photographs or illustrations appearing in this copy for an additional charge. Contact UMI directly to order.

ProQuest Information and Learning
300 North Zeeb Road, Ann Arbor, MI 48106-1346 USA
800-521-0600

Functional Neuroanatomy during Language Processing: Correspondence of Cortical Stimulation Mapping, fMRI, PEPSI, and ERP during a Visual Object Naming Task

by

Sandra Serafini

A dissertation submitted in partial fulfillment of the requirements for the degree of

Doctor of Philosophy

University of Washington

2002

Program Authorized to Offer Degree: Department of Speech and Hearing Sciences

UMI Number: 3053554

ProQuest Information and Learning Company
300 North Zeeb Road
P.O. Box 1346
Ann Arbor, MI 48106-1346

Doctoral Dissertation

In presenting this dissertation in partial fulfillment of the requirements for the Doctoral degree at the University of Washington,
I agree that the Library shall make its copies freely available for inspection. I further agree that extensive copying of the dissertation is allowable only for scholarly purposes, consistent with "fair use" as prescribed in the U.S. Copyright Law. Requests for copying or reproduction of this dissertation may be referred to Bell and Howell Information and Learning, 300 North Zeeb Road, P.O. Box 1346, Ann Arbor, MI 48106-1346, to whom the author has granted "the right to reproduce and sell (a) copies of the manuscript in microform and/or (b) printed copies of the manuscript made from microform."

Signature 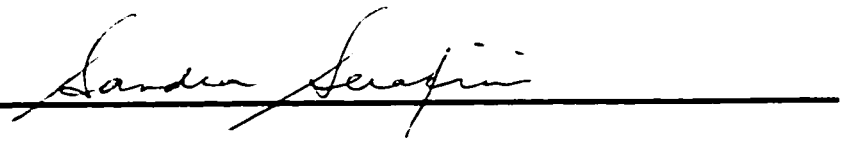

Date 06/12/02

University of Washington
Graduate School

This is to certify that I have examined this copy of a doctoral dissertation by

Sandra Serafini

and have found that it is complete and satisfactory in all respects,
and that any and all revisions required by the final
examining committee have been made.

Chair of Supervisory Committee:

Patricia K. Kuhl

Reading Committee:

Patricia K. Kuhl

George A. Ojemann

Todd L. Richards

Date: 6/13/02

University of Washington

Abstract

Functional Neuroanatomy during Language Processing:

Correspondence of Cortical Stimulation Mapping, fMRI, PEPSI, and ERP during a

Visual Object Naming Task

by Sandra Serafini

Chairperson of the Supervisory Committee

Professor Patricia K. Kuhl
Department of Speech and Hearing Sciences

This study examines the correspondence of functional language maps using Cortical Stimulation Mapping (CSM), functional MRI (fMRI), Proton Echo-Planar Spectroscopic Imaging (PEPSI), and source localizations from Event-Related Potentials (ERP) during a visual object naming task in two patients undergoing treatment for intractable epilepsy. The spatial relationship between fMRI/PEPSI peak activations and CSM language sites was quantitatively analyzed, indicating minimal correspondence across these techniques. Qualitatively, areas of activation that were common across imaging techniques corresponded well with sites of naming disruption in the anterior superior temporal gyrus and posterior middle temporal gyrus. One control subject participated in fMRI, PEPSI, and ERP sessions and is also examined. For all subjects, fMRI/PEPSI activations and ERP sources for N100 and N400 components were consistent with neuroanatomical areas described for visual object naming in the fMRI and

PET literature. Areas most consistently activated across fMRI/PEPSI/ERP techniques were the middle temporal gyrus posteriorly and the superior frontal gyrus and insula anteriorly. ERP scalp distributions for the N100 component across subjects were consistently prominent over anterior sites, while prominent amplitudes for the N400 component varied across subjects in posterior, centro-temporal, and anterior sites. Sources for the N100 component were also consistent across subjects in posterior areas, likely reflecting visual processing, while sources for the N400 component varied across subjects in frontal, temporal, and parietal areas, possibly reflecting not only semantic, but phonological processing as well. Concurrent anterior and posterior fMRI activations appear to be functionally distinguishable based on the ERP source data, again with posterior activations reflecting lower-level visual processing and anterior activations reflecting semantic or phonological processing. Implications for the functional role of specific anatomical structures (e.g. middle temporal gyrus) based on these correspondences are discussed. Theoretical issues pertaining to the physiological mechanisms of CSM disruption, fMRI-BOLD activations, lactate metabolism, and ERP source localizations are also examined to account for matches and mismatches across techniques.

TABLE OF CONTENTS

LIST OF FIGURES

LIST OF TABLES

ACKNOWLEDGEMENTS

I would like to express my sincere appreciation to the Department of Speech and Hearing Sciences and especially to my committee members Professor Patricia Kuhl, Professor David Corina from the Department of Psychology, Professor Todd Richards from the Department of Radiology, and Dr. George Ojemann from the Department of Neurosurgery for their guidance, supervision, vast patience, and extended financial support throughout my degree program and final project. The financial support of Professor Virginia Berninger from the Department of Education is also appreciated. This project could not have been completed without the generous assistance and support from several people, particularly Professor Lee Osterhout and Dr. Mark Allen in the Department of Psychology, who made the ERP portions of this project possible; Professor Jim Brinkley, programming wizard Dr. Andrew Poliakov, and Dr. Richard Martin in the Structural Informatics Group for providing the brain reconstructions and comparison analysis software. An enormous thank you goes to my family for their encouragement, and to my extended family, the soccer players and referees in Washington who have provided me with shelter and transport during this past year, and wonderful friendship since day one.

DEDICATION

To my spouse and love, Daryl Hochman.

Chapter 1 Introduction and Literature Review

Introduction

The functional organization of human language is a topic that has interested researchers and clinicians since the early associations of language disorders and brain lesions by Broca in 1861 and Wernicke in 1874 (Afifi and Bergman, 1998). Since then, technological advancements have been made that allow investigators to link language behaviors not only with specific anatomical areas of the brain, but with its hemodynamic, metabolic, and temporal characteristics as well. Presently, studies that explore functional brain regions of language can be divided into two main categories. The first category comprises studies that attempt to identify anatomical areas activated by a language behavior, including those areas that may be involved, though not necessarily essential, to a particular language behavior. The second category of studies ties deficits in language to anatomical areas that are deemed essential for a specific language behavior, and includes observations from pathological states such as aphasia due to stroke or other trauma, as well as from temporarily and purposefully induced lesion states such as Wada testing and intraoperative or extraoperative cortical stimulation.

This study combines the above two categories by comparing techniques that identify anatomical areas activated by a language behavior within the same subjects, creating a spatiotemporal profile that includes hemodynamic, metabolic, and electrophysiological information for a specific language task. This information is

compared to intraoperative and extraoperative cortical stimulation, currently the gold standard of language localization. Using a visual object-naming task, this profile was assembled with functional magnetic resonance imaging (fMRI), proton echo-planar spectroscopic imaging (PEPSI), and event-related potentials (ERPs). These techniques were performed in one normal control subject and presurgically in two patients who subsequently underwent cortical stimulation mapping (CSM) as part of their clinical treatment for intractable temporal-lobe epilepsy. Data from each technique were analyzed separately, and fMRI and PEPSI data were displayed on 3-D reconstructions of each patient's brain in order to quantitatively analyze the relationship between CSM sites and fMRI/PEPSI volumes.[1] Despite the various physiological mechanisms that are represented by each technique, the hypothesis of this study is that 1) a correlation will be found between CSM sites significant for language disruption and visual object-naming areas identified by fMRI and PEPSI peak activations, and 2) anatomical overlaps will occur between fMRI and PEPSI peak activations and source localizations of the ERP data. Other questions that will be addressed are whether ERP sources for early perceptual processing (N100 component) and semantic processing (N400 component) can functionally distinguish fMRI and PEPSI peak activations, and whether common areas across fMRI, PEPSI, and ERP sources correspond qualitatively to CSM sites of language disruption.

---

[1] The proprietary nature of the source localization software EMSE (SourceSignal Inc., city) did not allow the retrieval of image information necessary to convert the images into magnet space, which is a necessary step in displaying the data on the 3D reconstruction.

Normal language processing

Models of normal language processing divide the system into distinct subcomponents that are necessary for both comprehension and production in visual and auditory modalities. Functional neuroimaging techniques used to examine normal language processing are reviewed briefly, followed by an examination of selected subcomponents of the language processing system: a) orthography – knowledge of letter combinations of written words, b) phonology – knowledge of the sound structure of words, c) semantics – knowledge of concepts that are required for comprehension, and d) visual object naming – knowledge of producing a verbal label for a seen object. Where possible, pertinent lesion evidence is also reported. Insights into language processing from cortical stimulation studies are described, followed by a review of neuroimaging and cortical stimulation direct comparison studies. This assessment will illustrate the functional neuroanatomical correlates of the different types of language processing outlined above, and will show that a great deal of neuroanatomical overlap exists with respect to these processes.

Figure 1 below illustrates some anatomical terms that will be used throughout this study. The terms *anterior, posterior, superior,* and *inferior* refer to the long axis of the body; the terms *dorsal, ventral, rostral,* and *caudal* refer to the long axis of the central nervous system. The major planes of section used in imaging the brain are also shown in Figure 1.

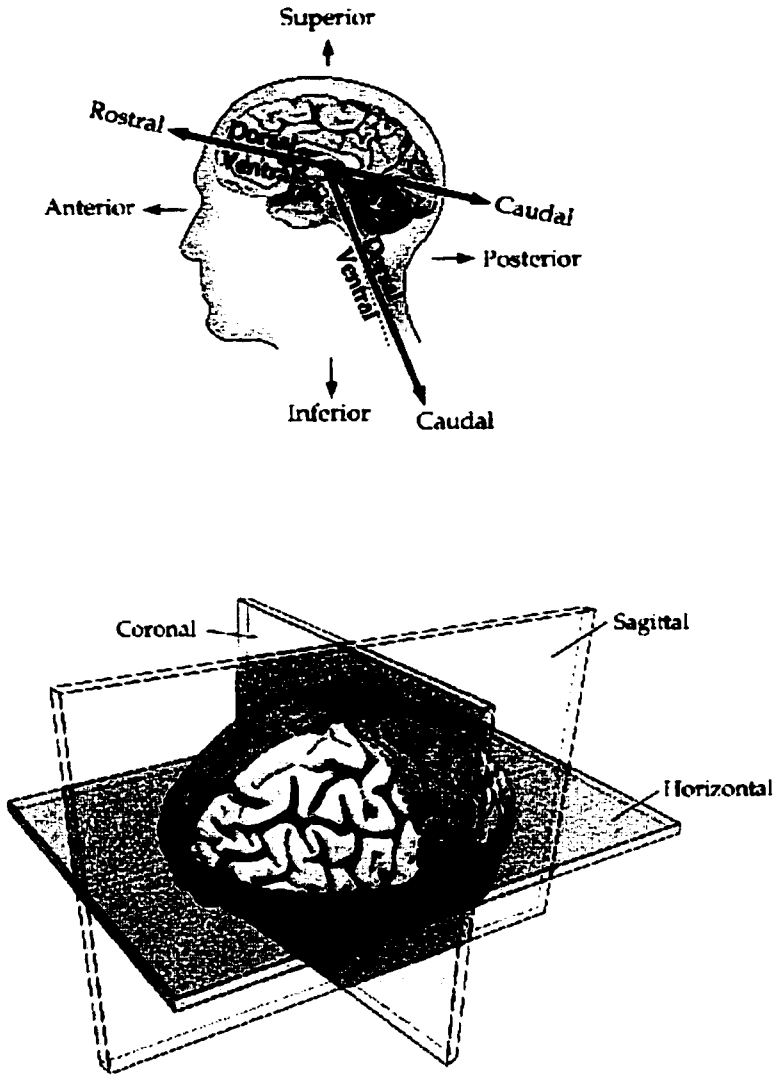

Figure 1. Anatomical terms used throughout this study and the major planes of section used in imaging the brain. From Purves et al. (2001).

The lateral surface of a reconstructed brain (Bavelier et al., 1997) and the regions that will be discussed throughout this study are shown below in Figure 2. Figure 3 shows a map of

cytoarchitectural regions and numbers that refer to Brodmann's areas (BAs), also used in the review.

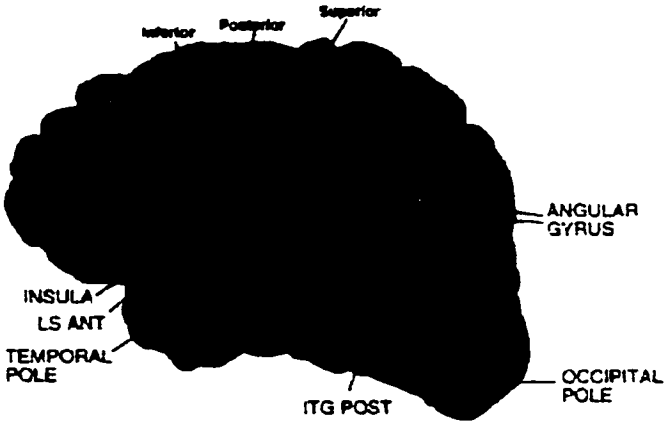

Figure 2. Anatomical regions on the lateral surface of a reconstructed brain. Adapted from Bavelier et al. (1997). SMG—Supramarginal gyrus, S—Superior, M—Middle, I—Inferior, F—frontal, T—temporal, O—Occipital, ANT—anterior, MID—middle, POST—posterior.

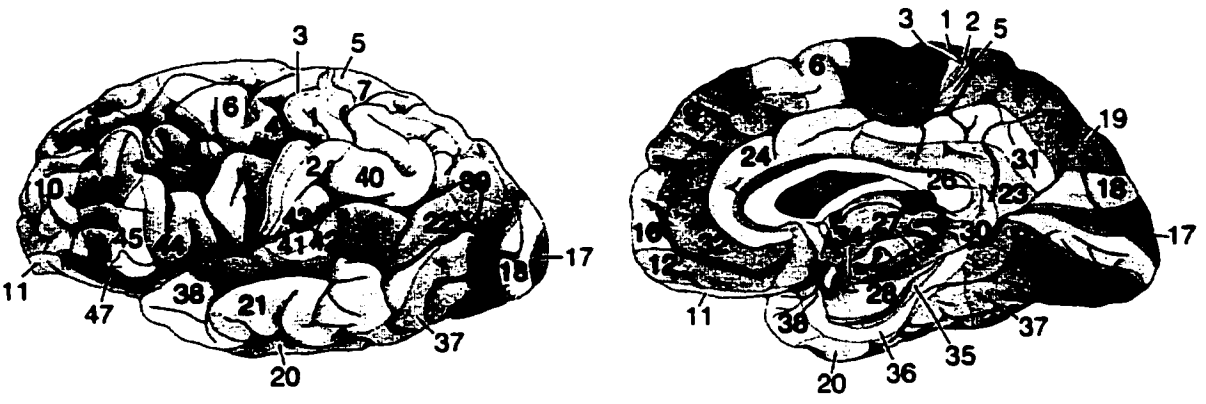

Figure 3. Lateral and midline views of the Brodmann Areas (BAs) (Purves et al., 2001).

Review of functional neuroimaging techniques

Positron Emission Tomography (PET)

Development of Positron Emission Tomography (PET) techniques gave researchers some of the earliest opportunities to relate anatomical areas to cognitive functions in subjects free from neurological damage (Petersen et al., 1989; Wise et al., 1991b; Demonet et al., 1992; Petersen and Fiez, 1993). To image cognitive functions, isotopes of elements with low atomic numbers (e.g. hydrogen, carbon, nitrogen, and oxygen) are required that will decay slowly and emit positrons. Radioactive isotopes of carbon (^{11}C), nitrogen (^{13}N), or oxygen (^{15}O) can be substituted in the structure of any of these compounds, while fluorine (^{18}F) can be substituted for hydrogen. Isotopes are made in a cyclotron by accelerating protons into the nuclei of nitrogen, oxygen, carbon, and fluorine. Incorporating an extra proton into the nucleus (which usually has an equal number of protons and neutrons) produces an unstable isotope. In order to regain stability, the proton is broken down into a neutron, which remains stable in the nucleus, and a positron, which is unstable and travels away from the site of generation, decaying in energy. This positron will eventually collide with an electron, leading to a mutual destruction and the emission of two gamma rays exactly 180° apart from the site. These rays are in turn detected by an array that surrounds the head (see Kandel, Shwartz, and Jessel, 1991 for a brief overview).

Cognitive experiments are based on the assumption that those parts of the brain with a high level of neuronal activity will possess higher levels of blood flow or

metabolism (Lassen et al., 1978, cited in Petersen and Fiez, 1993) than when at rest. The radioactive isotopes described above are injected into the subject usually to image regional cerebral blood flow (rCBF) by using $H_2{}^{15}O$ (radioactive water), but sometimes to image glucose metabolism by using [^{18}F] 2-fluoro-2-deoxyglucose (FDG), which is a competitive substrate for glucose and proportionally accumulates in the brain to the amount of glucose utilized (Petersen and Fiez, 1993). In rCBF measurements, scanning time is limited because of the short half-life of $H_2{}^{15}O$ (approximately 2 minutes). However, several scans can be performed in sequence, and immediate post-injection times can be used to measure resting states. Difference images are then made by subtracting the resting-state scan from the stimulus-scan, and those areas with increased perfusion stand out (Kandel, Shwartz, and Jessel, 1991).

PET methods can also determine oxygen use, or the percentage of the oxygen delivered to the brain that is actually utilized. This utilization is expressed as the oxygen extraction fraction (OEF), which is the ratio of oxygen utilization to blood flow (BF) or oxygen delivered (Gusnard and Raichle, 2001). The OEF is relevant to identifying signal increases versus decreases, which will be discussed further in the fMRI section below.

PEPSI

It has been established that functional MRI (fMRI) is an effective tool to measure Blood Oxygenation Level Dependent (BOLD) changes during language processing (e.g. Binder et al., 1997). These BOLD responses, however, may only provide an indirect

measurement of neuronal activation during cognitive processing. In contrast, *in-vivo* Proton Echo-Planar Spectroscopic Imaging (PEPSI) measures intracellular metabolism of the brain (e.g. lactate), which is perhaps a more direct measurement of cognitive processing (Richards et al., 1999). Previous studies using PEPSI have shown increased lactate levels in auditory monitoring tasks (Steury, 2001), increased lactate in bilateral anterior quadrants in normal adults during verb generation tasks (Richards et al., 1997), greater areas of lactate elevation in the left anterior quadrant of dyslexic boys when compared to controls in a phonological task (Richards et al., 1999).

Researchers have been interested in lactate as a metabolite during brain activation for decades. Since the 1940's, it has been argued that elevated tissue lactate levels indicated hypoxia and anaerobic energy metabolism (Friedmann and Barborka, 1941; Halijamae, 1987). However, many studies now show that lactate is produced aerobically in brain tissue in both animals (Fellows et al., 1993; Fray et al., 1996; Hu and Wilson, 1997; Hyder et al., 1996) and humans (Fox et al., 1988; Frahm et al., 1997; Prichard et al., 1991; Sappey-Marinier et al., 1992). *In vitro*, it has been shown that brain tissue not only produces lactate under aerobic conditions but also is able to support synaptic function in rat hippocampal slices (Izumi et al., 1994; McIlwain, 1953a, 1953b; Schurr et al., 1988; Sittsworth and Lanthorn, 1993), and is a preferred substrate over glucose in sympathetic ganglia (Larrabee, 1995; Larrabee, 1996). Schurr et al. (1999) showed in rat hippocampal slices that when neuronal lactate use was inhibited with 4-CIN, activation by the excitatory neurotransmitter glutamate (Glu) resulted in a permanent loss of neuronal

function plus a large increase in tissue lactate content. Inhibition of glycolysis with 2DG during exposure to Glu significantly lowered neuronal function, except when lactate was added. *In vivo*, lactate is not considered an adequate substrate because it only marginally crosses the blood-brain barrier (Pardridge and Oldendorf, 1977), but it appears that lactate can be formed within the brain parenchyma and transformed by the neurons into pyruvate to serve as an energy fuel (Schurr et al., 1999).

Astrocyte culture studies (Magistretti et al., 1995; Pellerin and Magistretti, 1994) showed that Glu, released from excitatory synapses when modality-specific neuronal pathways are activated, is the key signal for coupling neuronal activity to glucose utilization. Synaptically-released Glu is taken up by astrocytes (i.e., glial cells) via Na^+ cotransport, stimulating aerobic glycolysis (i.e. the transformation of glucose into lactate in the presence of sufficient oxygen). The lactate released from astrocytes during this process is taken up by neurons where it is converted into pyruvate and channeled into oxidative phosphorylation. In other words, the heightened energy demands of activated neurons are met through increased glial glycolytic flux, and lactate is transformed by the neurons into a crucial aerobic energy substrate.

The coupling between lactate production and fMRI signal intensity has received relatively little attention. During photic stimulation in the primary visual area (V1) of human subjects, Menon and Gati (1997) found that lactate concentrations increased immediately upon visual stimulation, mirroring an increase in fMRI signal intensity. A transient dip in lactate during stimulation was also mirrored by a similar decrease in the

fMRI signal. A recent language study comparing fMRI and PEPSI (Serafini et al., 2001) found general consistency between fMRI BOLD activations and PEPSI lactate increases in the left temporal area of normal control boys during a lexical task, but the physiological basis of these consistencies is still unclear.

Clarifying the relationship between lactate, glucose, and oxygen consumption may give insights into this basis, but this relationship has only been recently investigated. During prolonged visual stimulation, Frahm and colleagues (1997) found that lactate concentration rose during the initial phase of stimulation, while glucose concentration decreased (indicating enhanced glucose consumption) and cerebral metabolic rates of oxygen ($CMRO_2$) increased. They interpreted these results as indicating an early prevalence of nonoxidative glycolysis during the initial phase of activation, consistent with the PET studies of Fox and Raichle (1986) and Fox et al. (1988). If a rapid increase in CBF relative to $CMRO_2$ occurs, then a change in the ratio between oxy- and deoxyhemoglobin occurs as well, providing a BOLD-fMRI signal when deoxyhemoglobin decreases. *In vitro* (Magistretti and Pellerin, 1996) and *in vivo* (Sibson et al., 1998) studies also suggest, however, that a recoupling of enhanced $CMRO_2$ and glucose occurs subsequent to this initial phase of nonoxidative glycolysis. PEPSI is believed to capture increases in intracellular lactate concentrations, though the temporal resolution of the PEPSI signal make the relative contributions of the early nonoxidative glycolysis period and later oxidative glycolysis (recoupling) period unclear. The studies showing both anatomical overlap (Serafini et al., 2001) and comparable signal magnitude changes

(Menon and Gati, 1997) between lactate and the BOLD signal suggest that these techniques are measuring different but related aspects of stimulus-induced activation.

Functional Magnetic Resonance Imaging (fMRI)

Functional magnetic resonance imaging (fMRI) is capable of providing information about the location and magnitude of hemodynamic responses to various stimuli, being first demonstrated *in vivo* by Ogawa et al. (1990, 1992) and used to functionally map the human brain by Kwong et al. (1992). There are numerous advantages to using fMRI over PET as a functional imaging tool. As described in a review by LeBihan and Karni (1995), fMRI provides relatively good temporal resolution (seconds) and excellent spatial resolution (up to 1 mm). Unlike PET, contrast agents with fMRI are not necessary, making this technique less physiologically invasive and allowing investigators to take repeated, multiple scans within the same subject. The limitation of fMRI is that signal changes reflect a combination of secondary hemodynamic and metabolic effects that are relatively slower than neuronal or glial changes that occur with cognitive processing. Additionally, the relationship between metabolic/hemodynamic changes and neuronal activity is only recently beginning to be considered (Villringer, 2000; Magistretti and Pellerin, 2000).

Magnetic resonance techniques, including MRI, fMRI, and magnetic resonance spectroscopy (MRS), take advantage of magnetic properties that some atomic nuclei have, particularly hydrogen nuclei (protons) from water molecules, which are abundant in the

human brain and body (see Hashemi and Bradley, 1997 for a review). In the presence of an external magnetic field (B_0), all the proton spins are aligned along its axis (about which they are precessing) and form a net magnetization vector (M_0) in the same direction as B_0, which is the z-direction. When a 90° radiofrequency pulse B_1 is transmitted perpendicular to B_0 (in the x-axis), the magnetization vector is flipped into the x-y plane. When this RF pulse is turned off the spins realign themselves with the main scanner magnetic field, and emit a radiofrequency (RF) signal that can be detected by a receiver coil. The molecular structure, or lattice, surrounding the nuclei influences the speed at which the spins reorient, or relax, back to the main magnetic field after the RF pulse is removed. This relaxation time constant is called T_1, or Longitudinal, relaxation time because it refers to the time it takes for the spins to realign along the longitudinal axis. It is also called the Spin-Lattice relaxation time because it refers to the time it takes for the spins to return the energy received from the RF pulse back to the surrounding lattice as they return to their equilibrium state. T_1 weighted images provide the anatomical detail seen in most structural MR scans.

When many protons are in a large magnetic field such as the scanner, they rotate, or precess, randomly about the axis of this magnetic field. After these protons are excited by an RF pulse, their spins precess in phase with each other. When the RF pulse is turned off, their spins begin to dephase. The signal emitted as the spins lose phase coherence in the transverse (x-y) plane decays exponentially, and is known as the Transverse, or T_2 relaxation time. It is also called the Spin-Spin relaxation time because the magnetic field

of one proton affects the proton (and its spin) next to it, causing interactions inherent in the tissue. The decay of T_2 occurs 5 to 10 times more rapidly than T_1 recovery (Hashemi and Bradley, 1997). A second cause of spin dephasing is caused by external magnetic field inhomogeneity. This inhomogeneity makes protons in different locations precess at different frequencies because each spin is subjected to slightly different magnetic field strengths, resulting in a shorter decay constant, designated T_2^*. Heterogeneities in the main magnetic field are thought to originate from two sources. The first is macroscopic, which can be due to imperfections in the magnet, or heterogeneities produced at interfaces between the brain and large areas that have a different magnetic susceptibility, such as the frontal sinuses or the area surrounding the cerebellum. The second is microscopic, found for example in the erythrocytes of the capillaries, which vary in their magnetic susceptibility as well. The majority of fMRI experiments measure changes in T_2^*, which are thought to be due to changes in the microscopic magnetic environment surrounding the capillaries during brain activity. These changes are usually measured by comparing experimental task images with baseline or control task images using *t*-tests, or by correlating the hemodynamic waveform of the experimental task with a reference waveform. For the voxel intensity to be sensitive to T_2^*, a time delay known as echo time (TE) is put between the RF pulse and the image acquisition, and the signal will then decay at a rate which is dependent on TE.

In 1990, Ogawa and his colleagues demonstrated that an MRI pulse sequence (a combination of RF and gradient pulses) could detect changes in blood oxygenation

(Ogawa et. al., 1990). Blood Oxygen Level Dependent (BOLD) changes are now commonly used as an inherent contrast mechanism in humans to measure cognitive activity. This contrast mechanism is based on differences between oxyhemoglobin, which is diamagnetic (not magnetized), and deoxyhemoglobin, which is paramagnetic (slightly magnetized). Because deoxyhemoglobin at a high concentration is confined to red blood cells, it acts like an inherent and endogenous contrast agent, which fluctuates according to variations in both oxygen supply (blood flow) and utilization (tissue metabolism). Briefly, the basis for the fMRI signal is that during neuronal activation, a relatively large increase in blood flow occurs with a relatively small increase in blood oxygenation, leading to a net decrease in blood deoxyhemoglobin concentration and in turn to a signal increase (Fox and Raichle, 1986; Ogawa et al., 1993). A concern among investigators is that the BOLD contrast signal bears only an indirect relationship to activated neurons, and possibly reflects changes in distant large-draining veins or capillaries in some cases (Lai et al., 1993; Segebarth et al., 1994).

FMRI methods measure the cell activity that is associated with local changes in metabolism, particularly with glucose and oxygen consumption, and changes in neurovascular coupling between cerebral blood flow (CBF) and oxygenation (Villringer, 2000). These changes, however, occur in several types of brain activity, such as synaptic excitation, inhibition, and neuron-glia interactions, and it appears that the fMRI signal may represent changes in metabolism and blood flow in both neuronal and non-neuronal

events that require an increase in energy at a given time (Nudo and Masteron, 1986; Jueptner and Weiller, 1995).

Changes associated with several variables of brain activity are reflected in the fMRI signal: 1) glucose consumption, 2) oxygen consumption ($CMRO_2$), 3) CBF (which is dependent on capillary density and blood velocity), and 4) cerebral oxygenation (dependent on oxy- and deoxyhemoglobin). The classic PET studies of Fox and Raichle (1986) and Fox et al. (1988) found discrepancies between small increases in $CMRO_2$ (oxygen consumption) and large stimulus-induced increases in CBF and glucose consumption. They interpreted the increase in CBF relative to $CMRO_2$ as leading to a rise in cerebral oxygenation and an associated drop in deoxyhemoglobin. The increase in glucose consumption (CMRGlc) relative to $CMRO_2$ led them to interpret that glucose metabolism occurred in a nonoxidative manner, but this view has since been challenged by studies that show increases in oxidative glucose consumption with rat forepaw-stimulation (Hyder et al., 1996, 1997), and by studies that examine lactate accumulation as a marker of nonoxidative glycolysis, which show that such increases in lactate concentrations are transient and too small to account for the total amount of glucose being metabolized (Madsen et al., 1998). In addition, lactate can be produced aerobically as the end-product of glycolysis when $CMRO_2$ does not match glucose utilization (Magistretti and Pellerin, 2000). Together, these studies are consistent with the view that oxidative glucose metabolism is the main mechanism of energy generation for brain activity with only a brief and transient period of nonoxidative glucose utilization following a stimulus.

The view currently held is that following the onset of brain activity, glutamate-mediated adenosine signals the feeding arteriole which then dilates (Meno et al., 2001), leading to an increase in CBF in capillaries. The increase in CBF is relatively larger than the increase in $CMRO_2$, with oxygenation increasing at the venular side of the capillary in the venous vessels (Villringer, 2000). A brief and transient period of nonoxidative glucose utilization occurs, followed by a recoupling of $CMRO_2$ and glucose utilization. The increase in CBF in the capillaries is thought to be due mainly to an increase in blood velocity (Villringer, 2000), which is associated with a decrease in deoxyhemoglobin and an increase in the BOLD-fMRI signal. As these neurovascular events occur, glucose is imported into the brain parenchyma and undergoes a transient glycolysis in astrocytes resulting in lactate production, which is then taken up by the neurons and oxidized. Because the relationship between intracellular lactate measurements made with PEPSI and metabolic/neurovascular events measured with fMRI is unclear, a prediction is made that activations between PEPSI and fMRI should be proximal to each other or perhaps overlap, but is done so conservatively.

Negative correlations, or activation decreases, are seen in most, if not all, studies of fMRI and PET. The interpretation of decreases in signal is uncertain, and has only recently been considered in the PET (Fiez et al., 1995; Shulman et al., 1997) and fMRI (Binder et al., 1994; Raichle et al., 1994; Gusnard and Raichle, 2001) literature, with one study showing congruent increases and decreases in both PET and fMRI in a confrontation naming task (Votaw et al., 1999), suggesting that a similar physiological

mechanism is being measured by both PET and fMRI techniques. One interpretation that has been forwarded involves redistribution, or the shunting of the blood supply from areas of decreased activity to areas of increased activity (Bavelier et al., 1997). This interpretation is unlikely for several reasons. Relative to the overall blood flow to the brain, changes in local blood flow are extremely small, and the hemodynamic reserve of the brain is large enough to compensate for small local increases in blood flow (Gusnard and Raichle, 2001). In addition, Shulman et al. (1997) showed that decreases can occur either independently from increases or at remote areas from increases, making a shunting within a small area an unlikely explanation. Inhibitory processes have also been suggested as explaining areas of decreased activation, although it is now commonly held that inhibition can be as metabolically demanding as excitation, since both conditions produce increases in local glucose utilization (Kandell, Shwartz, and Jessell, 1991; Nudo and Masteron, 1986; Ackerman et al., 1984; Batini et al., 1984). Others have suggested that regions with significant decreases in signal are due to normalization procedures during analysis (Strother et al., 1995; Anderson, 1997), though the normalization procedures of Votaw et al. (1999) reduced the size of the decreased regions, arguing against this interpretation as well.

As mentioned above, PET methods have been used to determine the oxygen extraction fraction (OEF), which is the ratio of oxygen utilization to blood flow (BF) or oxygen delivered. When BF increases more than oxygen utilization and OEF decreases, there is an activation. BF and utilization changes in the opposite direction cause OEF to

increase, and a deactivation results. The physiological mechanism that causes these decreases is still unclear, though it has been suggested that it may reflect a decrease in activity of thalamic or other basal ganglia cells that project to the area of deactivation (Gusnard and Raichle, 2001), or reflect the suppression of information processing in areas not engaged in task performance, such as unattended sensory input (Drevets et al., 1995). Although the first view remains speculative, the second view has been supported in studies that have examined task-specific decreases both within and across sensory modalities (Drevets et al., 1995; Haxby et al., 1994).

Two meta-analyses of PET data by Shulman et al. (1997) and Mazoyer et al. (2001) showed that decreases can also be task-independent. These decreases occur in a consistent set of brain areas which are active at a baseline rate during rest with eyes closed, during visual fixation, and during passive viewing of simple visual stimuli. These areas then become attenuated during a variety of cognitive tasks, and appear as decreases. These areas include medial parietal cortex, posterior cingulate, precuneus, and retrosplenial cortices, which are all associated with different aspects of visuospatial processing. Whether these areas show decreases in the present study will be considered below in Chapter 5 (Discussion).

Event Related Potentials (ERPs)

Imaging modalities described up to now all have the advantage of good spatial resolution, but ERPs provide temporal resolution on the order of milliseconds (msec),

making them an important complement to imaging modalities. ERPs represent scalp-recorded changes during the ongoing EEG when it is time-locked to a presentation of a given event, such as a word, picture, or behavioral response, and averaged over many instances of that event (Friederici, 1997). Averaging is necessary to increase the signal-to-noise ratio against ongoing background EEG activity, and the ERP waveforms are thought to reflect the postsynaptic activity of pools of neurons (particularly the pyramidal cells of the neocortex) that are arranged or oriented in roughly the same direction orthogonal to the scalp and that are polarized or depolarized synchronously.

The localization of these neuronal ensembles, or neural generators, is difficult to pinpoint from scalp-recorded electrical activity because of the inverse problem (see later text), but as the number of recording sites increases, reasonable conjectures can be made from dipole modeling, and from seeding these solutions with fMRI activations (Wang et al. 1999). Algorithms such as Low Resolution Tomographic Analysis (LORETA) have also been recently developed to estimate source localizations from scalp field potentials (Pascual-Marqui et al., 1994). ERPs measured intracranially in clinical settings to localize language functions in patients being evaluated for intractable epilepsy have also been examined in attempts to locate the neural generator of scalp potential components (Nobre & McCarthy, 1994; Luders et al., 1986; Ojemann, 1979; Ojemann et al., 1989).

The variables examined in ERP studies include topography, latency (milliseconds from the stimulus onset), polarity (positive or negative), and amplitude. An early sensory processing peak occurs approximately 100-200msec after stimulus onset, which is

associated with the sensory modality of the stimulus, and enlarged when the stimulus is attended to (Hillyard and Hansen, 1986). The visual N100 component reflects visual perceptual processing and is observed approximately 100msec after stimulus presentation for a variety of stimuli (Mangun & Hillyard, 1991), including objects and pseudo-objects (Schendan et al., 1998). Three major ERP components are associated with different aspects of language processing. The first is an early left anterior negativity (LAN) wave that is seen with early syntactic processes with a peak at approximately 200msec. The second component is a centroparietal negativity that is seen with lexical or semantic integration processes occurring 250-500msec post-stimulus, with a peak at approximately 400 msec (N400), first demonstrated by Kutas and Hillyard (1980). The third is a late centroparietal positivity that is correlated with secondary syntactic processes, whose peak is seen at approximately 600 msec, and is known as the P600 (Osterhout and Holcomb, 1992).

The early left anterior negativity waveform at 200 msec is thought to reflect an initial stage of syntactic parsing (Friederici, 1995; Friederici and Mecklinger, 1996). It has been elicited by various syntactic anomalies, particularly with syntactic violations, such as *Max's of proof the theorem* (Friederici, 1997), but has also been found for violations of phrase structure, such as when a noun in a prepositional phrase has been changed to a verb (Friederici et al., 1993).

Early studies showed that the N400 component was sensitive to a variety of semantic manipulations (Kutas and Hillyard, 1980). This component can be elicited and

affected in semantic priming and memory paradigms with most word types, such as nouns and verbs, as well as with orthographically legal, pronounceable non-words, the presentation of words in sentences, and visual object stimuli (Kutas and Van Petten, 1988, 1994; Hagoort and Kutas, 1995 for reviews). It is sensitive to the modality of presentation and is thought to primarily reflect postlexical processes involved in semantic integration. With word/sentence stimuli, it is larger with unexpected endings of sentences and has the largest amplitude when the last word in a sentence is semantically anomalous. The amplitude of the N400 is reduced under several conditions: a) higher word frequency, b) repetition, orthographic/phonological/semantic priming, c) in word or picture pairs, when the second word or picture of a pair is related to the first word or picture, compared to when it is not related, and d) in sentences, as the predictability of the word in the context increases (Brown and Hagoort, 1993; Osterhout and Holcomb 1992; Kutas et al., 1999).

The P600 is also associated with secondary syntactic processes, and is thought to reflect reanalysis during complex sentence structures (Friederici, 1995; Friederici and Mecklinger, 1996). This component has been observed during sentences with nonpreferred structures, and where the initially assigned structure has not been met by subsequent input, such as in the example: *The broker persuaded to sell the stock met the man*. These sentences are known as "garden-path" sentences, where the initial syntactic structures are ambiguous, and whose resolutions are made with nonpreferred syntactic representations, requiring a reanalysis of the initial phrase (Osterhout and Holcomb,

1992). The P600 has also been seen with morphological violations such as subject-verb agreements, and word order violations (Hagoort et al., 1993). It is unclear whether this component is elicited by anomalies in verb endings, prepositions, conjunctions, or pronouns, which would be consistent with the interpretation of a relationship between sentence reading errors evoked by cortical stimulation and syntactical processing (Ojemann and Mateer, 1979).

In summary, ERP waveforms can be divided into an early sensory or perceptual component and three major components that correspond with distinct language processes. The N100 component reflects early perceptual processing of visual or auditory stimuli (Mangun and Hillyard, 1991). The first language component reflects processing of initial syntactic structure, reflected by an early left anterior negativity seen around 200 msec. The second major language component, the N400, reflects processes associated with lexical and semantic information, and is possibly generated by the anterior medial temporal lobe for words, though the scalp distribution for words and pictures differ, with the N400 for pictures being relatively more anterior, implying that the neural generators responsible for this component may also be dissimilar. The third major language component is where lexical or semantic and syntactic information is mapped onto one another so that a reanalysis takes place when a mismatch or nonpreferred completion of a sentence occurs. This waveform is seen as a centroparietal positivity around 600 ms, and is known as the P600.

Comparing physiological signals across techniques

One of the main novelties of this study is the integrated approach it takes towards examining language processing in the brain. This integrated approach replicates the experimental design for visual object naming across fMRI, PEPSI, and ERP as much as each technique allows given their specific idiosyncrasies. With source localization (LORETA), ERP also has the advantage of considering the entire brain volume for locating neural generators, allowing comparisons with fMRI and PEPSI techniques. In addition to combining different techniques using the same task, this study does so in the same subjects, providing a unique opportunity to examine various neural responses from different physiological measurements within single subjects. Expectations for overlapping areas of activation, however, are conservative. Each method is sensitive to different neurophysiological changes during the given task, and requires certain conditions for these changes to be detected. ERP signals, for example, require that neuronal populations are geometrically configured so that individual dipole moments summate into an open-field; additionally, this population must activate synchronously and be time-locked to a specific event. In contrast, fMRI, PEPSI, and CSM signals do not require distinctive configurations of neuronal populations, nor do they require neural activity to be synchronous. However, changes in fMRI and PEPSI signals do require changes in neural activity that alter metabolic and hemodynamic demands in a way that signals can be detected. CSM is different from the other techniques on several fronts, including: 1) causing a depolarization of a neuronal population from the cortical surface

corresponding to the current spread of the stimulating electrode, and 2) measuring language disruptions in small, localized areas of cortex rather than measuring activations throughout a brain volume. Nevertheless, it is expected that some degree of overlap will occur across these techniques, and that the areas involved will be consistent with areas in the visual object naming network described below.

Normal language processes

Orthography: Visual Word Identification

Definitions of orthographic processing in the literature range widely. Some definitions are exclusionary, where access to lexical representations of printed words is gained without access to other language processes such as phonology (Olson et al., 1990). Other definitions emphasize strictly visual processing, where the features of the visual stimuli are analyzed (Shaywitz et al., 1995). Still other definitions stress the linguistic features of the stimuli, concentrating on patterns of letter-sound invariances, sequential dependencies, structural redundancies, or letter position frequencies (Vellutino et al., 1995).

Functional neuroimaging studies related to visual word processing identify four main areas of activity: 1) lateral and medial extrastriate cortex (BA 18), 2) left inferior frontal cortex (BA 47), 3) left posterior middle and superior temporal gyrus (BA 21 and 22 respectively), and 4) left supramarginal gyrus (BA 40). ERP studies identify a fifth

area, the fusiform gyrus, as being active during the visual processing of word or wordlike stimuli.

The classic PET studies of Petersen et al. (1988, 1989, 1990) places the reading lexicon in the left medial extrastriate cortex, arguing that visual word forms are more related to vision than they are to language. The Petersen et al. (1988) study, confirmed by Wise et al. (1991b), showed that visual presentation of words without additional task demands activated several areas of extrastriate visual cortex (BA 18) bilaterally. These activations could have been due to simple visual features of the stimuli, letter processing, or word-level processing. The Petersen et al. (1990) study addressed these possibilities by giving subjects four experimental conditions compared to the baseline task of fixation on a crosshair. Subjects saw false fonts in one condition, where the letter-like strings were comparable in complexity to real letters. In the second condition, random consonant strings (e.g. NLPFZ) were shown; in the third, pronounceable pseudowords (e.g. TWEAL); and in the fourth, real words (e.g. BOARD) were shown. Relative to the crosshair fixation (baseline) task, all four conditions produced significant activation increases in both the left and right lateral extrastriate cortex. However, when false fonts and random letter strings were compared with pseudowords and real words, they found that pseudowords and real words caused greater activation in the left medial extrastriate cortex (BA 18), while real words activated an area in left inferior frontal cortex (BA 47), which was subsequently questioned as an orthographic processing area and attributed to semantic processing. Petersen and his colleagues suggested that pseudowords and real

words both activated the reading lexicon in the medial extrastriate areas of cortex because they both conformed to the orthographic constraints of English. Pugh et al. (1996) used fMRI to investigate the component processes of reading and also confirmed that lateral extrastriate regions were most strongly associated with orthographic processing while the medial extrastriate region was more responsive to real words than to nonword strings of letters. This distinguishing level of visual processing is consistent with cognitive psychology studies that show the word superiority effect, that is, the effect of letters inside of words and pseudowords being processed differently, in this case more efficiently, than letters inside of random letter strings (Carr and Pollatsek, 1985).

A study by Howard et al. (1992) also showed bilateral activation in both the striate and extrastriate cortex with false fonts, but showed peak activation in the left posterior middle temporal gyrus with the visual presentation of words. This area differs markedly from the left medial extrastriate cortex activation observed in the Petersen et al. (1990), Wise et al. (1991b), and Pugh et al. (1996) studies. There were, however, several procedural differences between the Petersen et al. (1990) and the Howard et al. (1992) studies, including exposure duration (150msec vs. 1000msec) and type of reading task (words viewed silently vs. read aloud) that may have accounted for the discrepancies. These differences were systematically investigated by Price et al. (1994), who found that reading aloud and reading silently both engaged the left middle and superior temporal regions (BA 21 and 22), which was consistent with Howard et al. (1992), but inconsistent with Petersen et al. (1990). In addition, they found that shorter exposure durations

(150msec vs. 981 and 1000msec) significantly increased activity in these temporal areas (plus others) during a reading-aloud condition. In the silent-reading versus false-font condition, longer exposure durations activated the inferior occipital cortex bilaterally, though activity in the medial extrastriate cortex did not reach significance at any of the exposure durations, also inconsistent with Petersen et al. (1990). Rumsey et al. (1997), however, found most regions of the visual cortex, including extrastriate cortex (BA 18), were activated equally in two pronunciation tasks with visually presented words: a) phonological (pseudowords that did not resemble real words) and b) orthographic (words with irregular spellings). The stimuli used in that study, however, were not described thoroughly enough to make a direct comparison with the results described above.

Recording field potentials directly from the inferior temporal lobe, Nobre et al. (1994) compared visual processing of words, pseudowords, and non-pronounceable nonwords, finding responses from two discrete areas of the fusiform (occipitotemporal) gyrus. The fusiform gyrus is highlighted below in Figure 4 on a ventral view of the brain.

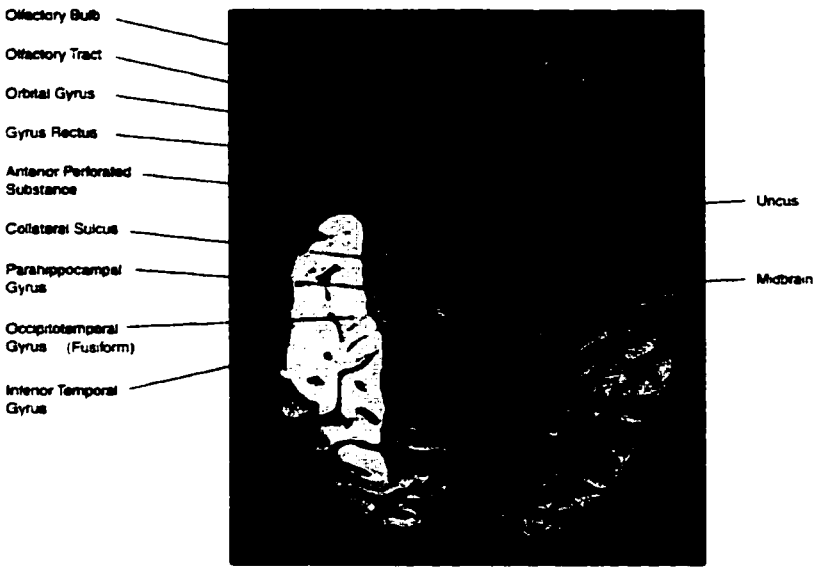

Figure 4. Ventral view of the brain showing major sulci and gyri. The fusiform (occipitotemporal) area is highlighted. Adapted from Afifi and Bergman (1998).

The posterior fusiform gyrus responded equally to words and nonwords, and was also noted to be unaffected by semantic context. The anterior fusiform gyrus, however, did not respond to nonwords and was sensitive to semantic content and context. These results suggest that the N200s seen in posterior fusiform areas are pre-lexical in nature whereas the N400s in anterior fusiform areas were sensitive to words and their semantic contexts (Nobre et al., 1994). Chronically implanted electrodes on the surface of striate and extrastriate cortex in epilepsy patients also shows that letter-strings (words and non-words) evokes the N200 in inferior temporal and posterior fusiform areas (Allison et al., 1994). Consistent with these results is an ERP study by Ziegler et al. (1997) who showed that words and pseudowords differed from non-words at posterior fusiform sites, while words differed from pseudowords and non-words at anterior fusiform sites.

Overall, the neuroimaging studies show that visually presented words consistently activate visual regions, often, though not always, including the extrastriate (BA 18) gyri, plus areas in left inferior frontal cortex (BA 47), left posterior middle and superior temporal cortex (BA 21 and 22), and left supramarginal gyrus (BA 40). The fact that areas outside the extrastriate regions have been identified repeatedly, though inconsistently, across studies suggests that other processes besides orthography are taking place depending on the experimental task and control stimuli. The ERP results show sensitivity to semantic content in the temporal and anterior fusiform gyri activations, adding strength to this suggestion. The studies below provide evidence that in addition to orthography, visual word processing will rely on other language processes such as phonological and semantic processing, and will do so automatically, that is, in the absence of explicit phonological or semantic task demands.

One of the assumptions of the Petersen et al. studies (1988, 1990) was that visual word tasks elicit limited processing from the brain. Evidence from psychological experiments, however, has shown that presenting familiar words will automatically activate semantic and phonological representations even when subjects are not instructed to do so (Van Orden et al., 1988; Macleod, 1991; Coltheart et al., 1994; Price et al., 1996a), and that these automatic activations can interfere with subsequent or concurrent language tasks; the Stroop effect is an example of automatic activation interfering with a

language task.[2] An area in left inferior frontal cortex (BA 47) was found in the Petersen et al. (1990) study during the word condition (but not the pseudoword or nonword conditions), also suggesting that automatic semantic processing took place. The Price et al. (1994) study additionally showed that when subjects silently viewed words, brain activity relative to the false font condition was detected in a widespread network of cortical areas, including bilateral posterior temporal cortices, left inferior frontal cortex, left inferior parietal cortex, both sensorimotor cortices, and the supplementary motor area (SMA). This network strongly suggested the possibility of implicit activation of multiple language processes, which was further investigated by Price et al. (1996a). They had subjects engaged in a nonlinguistic visual feature detection task, using the same stimuli as those in the Petersen et al. (1990) study. They found that words and pseudowords activated the medial extrastriate cortex, the left posterior temporal cortex, the left inferior parietal cortex, and the left prefrontal cortex, all of which have been implicated by both lesion and PET studies to be involved in visual and auditory word processing with *explicit* semantic and phonological task demands (Mesulam, 1990; Wise et al., 1991a; Demonet et al., 1992; Howard et al., 1992; Price et al., 1994). It would appear then, that visual word processing activates not only the orthographic code, but implicitly and automatically activates phonological and semantic codes as well. In addition, anterior fusiform sites may be partly responsible for orthographic to semantic transformations.

---

[2] The Stroop effect is seen when subjects who are required to name the physical color of a word will respond faster if the phonological representation of the word is the same color as the physical color of the

In contrast to orthographic-to-semantic processing, evidence for the localization of orthographic-to-phonological transformations in the anterior portion of left inferior parietal cortex, i.e. the supramarginal gyrus (BA 40), comes from several studies. In addition to the language network they identified for visual word processing, Price et al. (1996a) found that pseudowords, which invoke a strong phonological component for processing, activated this language network more strongly than words, particularly in the left inferior parietal cortex. This area has been consistently associated with phonological tasks, for example in a study by Law et al. (1991) where Japanese subjects read Kana, which has consistent orthographic to phonological links, relative to Kanji, which does not have consistent orthographic to phonological links. The orthography to phonology route can also be examined indirectly by contrasting reading words (letter forms with phonology) with picture naming (non-letter forms with phonology). Several studies that contrasted reading or viewing words with naming or viewing pictures have also shown that increased activation for words has been detected in the left supramarginal gyrus, compared to pictures (Bookheimer et al., 1995; Vandenberghe et al., 1996; Menard et al., 1996). This result suggests that the supramarginal gyrus is involved in orthographic processing that includes a strong phonological component.

Additional evidence for this conclusion comes from lesion studies of acquired alexia. A double dissociation is found in the ability to read unfamiliar nonwords, which uses an orthographic to phonological route, versus the ability to read irregularly spelled

---

word (e.g. the word RED is printed in red ink) than if the phonological representation is a different color

words (e.g. 'debt'), which uses an intermediate semantic stage in the orthography to phonology route (Price, 1998). The deficit in reading unfamiliar words is found with damage to the left inferior parietal cortex while the deficit in reading irregularly spelled words is found with damage to the left inferior temporal region (Vanier and Caplan, 1985; Marin, 1980). These findings, like those in word and word-versus-object studies, indicate that regions within the left inferior parietal cortex are necessary for orthographic to phonological conversion, while evidence from PET, ERP, and lesion studies tenuously suggest that posterior temporal and fusiform regions are involved in orthographic to semantic conversion.

Phonology

Numerous tasks in addition to reading have been used in neuroimaging studies in an attempt to determine the functional localization of phonology and phonological retrieval, including word production, phoneme monitoring of words and nonwords, phoneme discrimination, and various rhyming judgment tasks (Petersen et al., 1989; Demonet et al., 1992, 1994; Zatorre et al., 1992, 1996; Binder et al., 1994, 1997; Fiez et al., 1995; Pugh et al., 1996; Price et al., 1997; Herbster et al., 1997). Perhaps not surprisingly, the presence of so many different experimental and control tasks seems to preclude the unequivocal localization of phonological processing at first glance. Accordingly, a review of eight PET studies and one fMRI study by Poeppel (1996)

---

than the physical color (e.g. the word RED is printed in green ink).

concludes that the unconstrained nature of the tasks and the lack of overlap in neuroanatomical areas they identify prevents drawing any conclusions whatsoever about the functional localization of phonological processing. Figure 5 shows the cortical areas that are argued to mediate phonological processing in the reviewed studies, indicated by anatomical and Brodmann labels, and the research groups who identified them. As seen in the figure, several frontal, temporal, and temporoparietal cortex are identified as mediating phonological processing.

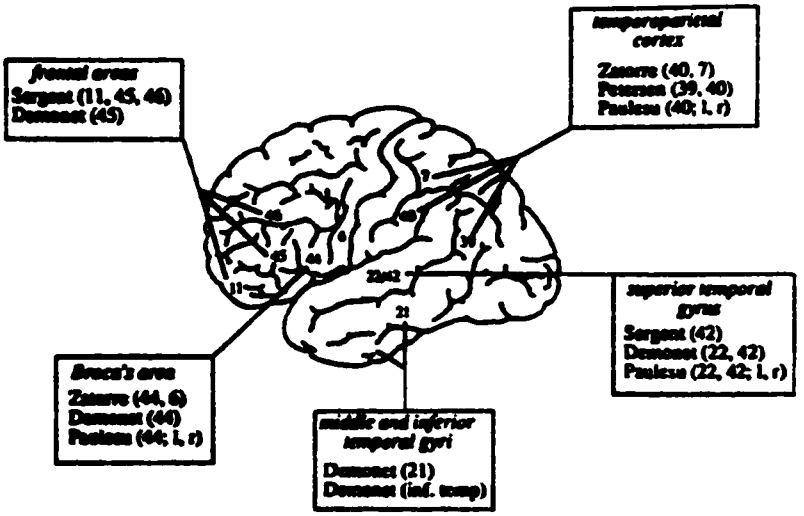

Figure 5. Cortical regions considered crucial for phonological processing. Associated verbal and Brodmann area labels and researchers who identified them are listed. From Poeppel (1996).

On closer examination, however, there are several differences across these studies that would not necessarily evoke consistent areas of activation. These differences are not highlighted in Poeppel's review, but are important because of the different demands they place on attentional, memory, and sensory systems. For example, tasks differed in: 1) the short-term memory load between the Sergent et al. (1992a) and the Paulesu et al (1993) studies; 2) the modality of presentation, which was either auditory (Demonet et al., 1992, 1994; Zatorre et al., 1992), or visual (Petersen et al., 1989; Sergent et al., 1992a; Paulesu et al., 1993)--this difference can vary the types of processing used to perform a phonological task (Baddeley, 1990); 3) the rate of stimulus presentation, which varied from 1 item every 3 seconds (Demonet et al., 1992, 1994) to 1 item every second (Paulesu et al., 1993)--these differences are known by the work of Price et al. (1994) to have an effect on blood flow activity; and 4) the type of stimulus item, which ranged from words (Petersen et al., 1989; Zatorre et al., 1992), to nonwords (Demonet et al., 1992, 1994; Zatorre et al., 1992), to letters (Sergent et al., 1992a; Paulesu et al., 1993)--differences in which have been discussed above.

Contrary to Poeppel's claim, most researchers agree that phonological processing is not a unitary process, but something that reflects a set of related but independent processes (Demonet et al., 1996). These processes include: 1) those related to the perception of spoken words; 2) transformations related to how visual or auditory words sound or are spoken, for example in orthographic to phonological coding; and 3) the generation of the articulatory codes necessary for the production of words (Demonet et

al., 1996). Keeping in mind the differences in experimental and control tasks between studies, as well as the different types of phonological processing that are possible, three main neuroanatomical areas are activated consistently in the reviewed studies: 1) left inferior frontal gyrus (Broca's area) (BA 44/45), 2) left superior temporal gyrus (BA 22), including Wernicke's area (BA 22/39) and 3) left supramarginal gyrus (BA 40).

Broca's area has been considered the motor speech area in the inferior frontal gyrus of the left hemisphere since its naming after Pierre-Paul Broca, a French anthropologist, anatomist, and surgeon who associated lesions of this area with disturbance of speech function in 1861 (Afifi and Bergman, 1998). The inferior frontal gyrus is further subdivided by two sulci into three gyri: the orbital, triangular, and opercular gyri. The triangular gyrus (BA 45) and the adjacent part of the opercular gyrus (BA 44) in the left hemisphere constitute Broca's area of speech (Afifi and Bergman, 1998). Figure 6 below clarifies the anatomical location of Broca's area.

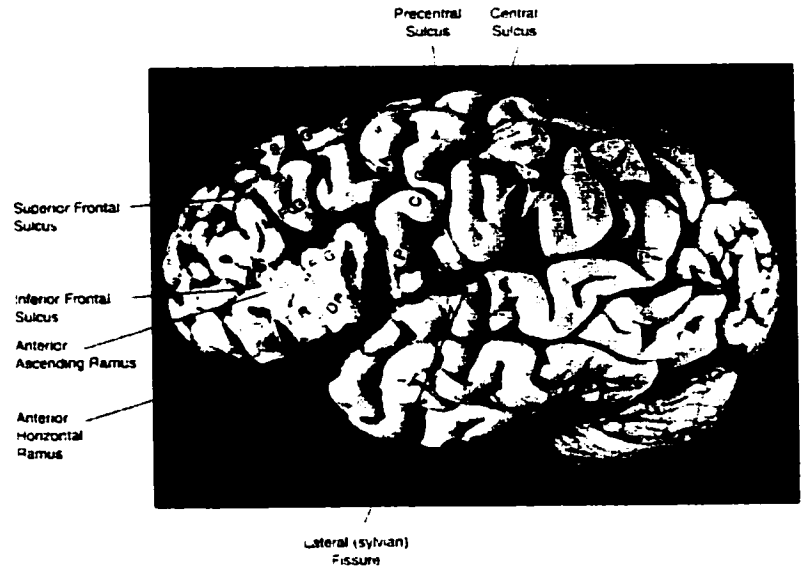

Figure 6. Lateral view of the brain showing the major sulci and gyri in the frontal lobe. Broca's area is highlighted. Adapted from Afifi and Bergman (1998).

It is important to note that Poeppel separates BAs 44 and 45 as non-overlapping activation areas, as seen in Figure 4 (frontal areas vs. Broca's area). As noted above, however, areas 44 and 45 should be considered subregions of Broca's area; doing so reorganizes Poeppel's localization map so that no less than five studies identify this region as having a role in phonological processing. These studies include Zatorre et al. (1992), who asked subjects to compare and judge as the same or different the final consonants in aurally presented pairs of consonant-vowel-consonant (CVC) strings (e.g. 'leb-fab'), and found the largest increase in the opercular gyrus (BA 44). In another study, Sergent et al. (1992a) asked subjects to determine if a single visual letter sounded with "ee" or not, and was compared to either a letter spatial task or an object categorization task. Although

they specifically denied the involvement of Broca's area, they did observe activation of the left inferior frontal gyrus. Also using phoneme monitoring, Demonet et al. (1992) used a phonemic monitoring task where subjects identified a particular phoneme (/b/) in non-words when a preceding phoneme (/d/) was present, and found small activations in BAs 44 and 45, in addition to larger ones in superior temporal areas. However, this study was confounded by perceptually ambiguous stimuli where distractors were phonetically similar to targets, which in turn encouraged various cognitive strategies that seemed to rely more on attentional and memory systems than phonological processes. A follow-up study by Demonet et al. (1994) addressed these confounds and duplicated the Broca's area (BA 44) activations from the 1992 study. Other phonetic tasks were examined by Paulesu et al. (1993), who used rhyming judgments for letters and also found activation of BA 44, while Fiez et al. (1995) identified the left frontal opercular area (BA 45) in several phonetic analysis tasks, including vowel discrimination and detection of CVC target syllables.

The two main (related) theoretical frameworks that could account for the consistent activation of Broca's area during phonological processing in the above studies are: 1) the motor theory of speech perception proposed by Liberman (Liberman and Mattingly, 1985), and 2) the subvocal rehearsal aspect of Baddeley's "articulatory loop" theory (Baddeley, 1986, 1992). Neither of these theories predict precisely which areas of the brain may be active during a given task, but some researchers have attempted to

couch their neuroimaging results in these frameworks (e.g. Zatorre et al., 1992; Paulesu et al., 1993).

The motor theory of speech perception proposes that phonetic decoding depends on access to articulatory gestures associated with a given speech sound. Although left posterior temporal areas that are activated with passive speech may represent the initial stages of phonetic analysis (Petersen et al., 1988, 1989), judgments of phonetic segments of the stimulus are argued as being related to articulation (Wise et al., 1991a), though this idea is difficult to test experimentally.

Related to Liberman's motor theory of speech perception is Baddeley's articulatory loop theory, which includes a subvocal rehearsal system and a phonological store (see Baddeley, 1986 for a review). Strategies of subvocal rehearsal to check the presence of targets in phoneme strings have been forwarded by several researchers as being akin to "inner speech", where subjects access an articulatory representation of the phonetic unit to be judged upon, whether in short-term memory conditions or simple rhyming conditions (Paulesu et al., 1993; Pugh et al., 1996), and whether stimuli are presented visually or aurally (Zatorre et al., 1992; Paulesu et al., 1993; Demonet et al., 1994; Pugh et al., 1996). If such a system exists, Broca's area seems to be crucial to it; lesions in and adjacent to this area can result in deficits of temporal perception, which is considered necessary for resolving rapidly changing acoustic cues in phonemic processing, (Tallal and Newcombe, 1978), resulting in phonetic perceptual disturbances (Blumstein et al., 1977; Ojemann and Mateer, 1979; Ojemann, 1983). Damage to this

area in Japanese-speaking patients, for example, result in impairments in recognizing and writing Kana (which is coded phonologically), but not Kanji (which is coded orthographically) (Sasanuma, 1971, 1975). In summary, Broca's area appears essential to phonological processing according to functional neuroimaging and lesion data, and though difficult to prove, is strongly implicated as the structure responsible for phonetic decoding in the motor-speech perception theory of Liberman as well as the subvocal rehearsal component of Baddeley's articulatory loop theory.

In addition to the inferior frontal areas described above, left superior temporal (BA 22) (Wernicke's area) and supramarginal areas (BA 40) are important to phonological processing as well. Many of the studies that have found superior temporal activation during phonological processing have found supramarginal activation as well (Petersen et al., 1989; Binder et al., 1997; Price et al., 1997), though some studies find supramarginal activation in conjunction with frontal activation (Zatorre et al., 1992; Paulesu et al., 1993) or frontal activation in conjunction with temporal activation (Demonet et al., 1992, 1994; Price et al., 1997), depending on the emphasis of the task. Wernicke's area, named after the German neurologist Karl Wernicke, is considered a secondary auditory region and includes the posterior part of the superior temporal gyrus (BA 22) as well as the inferior portion of the angular gyrus (BA 39) (Afifi and Bergman, 1998). It is located adjacent to the primary auditory area (Heschl's gyrus, BAs 41 and 42) and is crucial for the comprehension of both written and spoken language (Afifi and Bergman, 1998).

Several studies suggest that these secondary auditory regions, including temporoparietal and anterior or superior temporal cortex, are not activated by simple auditory stimuli such as clicks, tones, or noise bursts (Roland et al., 1980; Mazziota et al., 1982; Lauter, et al., 1985). In support of this theory, Binder et al. (1994) showed in an fMRI study that the superior temporal gyrus exhibited significantly greater activation by speech stimuli than by unmodulated noise stimuli, suggesting that a major role of this area (BA 22) is the analysis of highly modulated sounds such as the temporal acoustic features of speech. Consistent with this view are PET studies such as those of Petersen et al. (1989), who found bilateral activation in the posterior superior temporal lobe (BA 22) as well as activation in the left temporoparietal (the supramarginal gyrus, BA 40) area for passive auditory word presentation, but not for auditory clicks or tones. They also found activation in the supramarginal gyrus during a rhyming task with visually presented words, suggesting again that this area is involved in the phonological encoding of words, whether presented aurally or visually. Demonet et al. (1992) used a sequential phonological monitoring task of nonwords and found significant activations in the superior temporal gyrus, from the anterior part of Wernicke's area to the anterior part of the superior temporal gyrus. The study of Zatorre et al. (1992) explored the lateralization of phonetic and pitch discrimination in speech syllables. Again, areas in the superior temporal gyrus were activated bilaterally by speech stimuli but not by noise. They showed that in addition to Broca's area activation during discrimination of phonetic structure, a left parietal area near the superior aspect of the supramarginal gyrus was also

identified. Rumsey et al. (1997) used an auditory rhyme judgment task and also found left temporoparietal increases plus a small increase in the left posterior frontal area. In short, simple acoustic stimuli such as tones, noise, or clicks activate primary auditory areas (BA 41/42), whereas linguistic stimuli are necessary to activate superior temporal (BA 22) and supramarginal (BA 40) regions; even relatively simple linguistic stimuli, such as phonemes, are sufficient to activate these regions.

Cortical stimulation studies are also consistent with Wernicke's and supramarginal areas being involved during phonology (Ojemann, 1983), showing phonemic disruptions during speech output throughout stimulation. Vascular lesions of the left supramarginal gyrus are known to produce speech output disturbances characterized by phonemic paraphasias in repetition (Geschwind, 1965; Damasio and Damasio, 1980) and other phonological deficits (Caplan et al., 1995). Lesions in this area also produce phonological agraphia where patients can write words from dictation but not nonwords (Roeltgen, Sevush, & Heilman, 1983; Shallice, 1981; Benson et al., 1973), also signifying a phonological impairment. Zatorre et al.'s (1992) suggestion that phonological processing is accomplished through a network that includes the left posterior temporal and parietal regions, i.e. Wernicke's area and supramarginal gyrus, as well as Broca's area was well-founded based on both the imaging and lesion evidence at that time (as well as later PET studies such as Zatorre et al., 1996). Beyond a general involvement in phonological processing, however, the specific function of each area remained unresolved and continues to be a source of debate.

Shortly after the Zatorre et al. (1992) study, another research group stipulated that the specific function of the left supramarginal gyrus in phonological processing was the location of the phonological store (Paulesu et al., 1993), and the counterpart to the Broca's area subvocal rehearsal system in Baddeley's "articulatory loop" theory described above. Paulesu and colleagues used fMRI to compare activation levels during a phonological short-term memory task (remembering letters) with a rhyming task and demonstrated that activation in the supramarginal gyrus (BA 40) was found only in the phonological short-term memory task. This result is also consistent with lesion evidence showing that the phonological store plays a fundamental role in phonological short-term memory (Vallar and Baddeley, 1984; Shallice and Vallar, 1990), but not for rhyming tasks that do not require short-term memory to be completed (Burani, et al., 1991; Vallar and Baddeley, 1984). This interpretation could account for the pervasiveness of the supramarginal gyrus activation in auditory tasks, especially those with low presentation rates that require storage during interstimulus intervals, in tasks that require phonological processing of visual information, as well as its absence in several semantic association tasks that require verb generation or retrieval. Paulesu and colleagues concluded that phonological processing that is independent from memory is found in left posterior superior temporal areas (BA 22), and suggested that the anatomical network for Baddeley's articulatory loop theory consisted of the supramarginal gyrus (BA 40), which becomes involved once the phonological store is activated through verbal short-term

memory, and Broca's area (BA 44), which becomes activated during subvocal rehearsal or "inner speech".

A combined Zatorre-Paulesu model, shown in Figure 7 below, summarizes and illustrates the roles of the three areas identified earlier: 1) left inferior frontal gyrus (Broca's area) (BA 44, 45), 2) left superior temporal gyrus (BA 22), including Wernicke's area (BA 22/39) and 3) left supramarginal gyrus (BA 40).

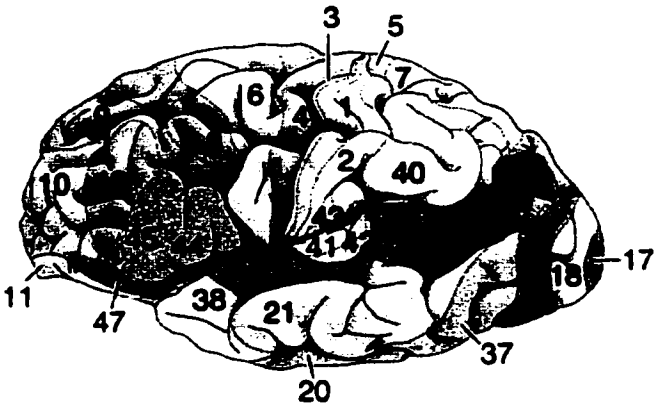

Superior temporal gyri (BA 22) (Bilateral)

- perceptual analysis of incoming speech stream
- anterior regions respond to passive speech
- sensitive to word presentation rate
- ♦ general role: basic perceptual analysis of auditory stimuli

Wernicke's area (BA 22/39) (Left posterior superior temporal gyrus, angular gyrus)

- not responsive to simple auditory stimuli (noise, tones, clicks)
- responsive to speech processing
- not sensitive to word presentation rate
- ♦ general role: higher level analysis of speech stimuli

Broca's area (BA 44/45) (Left triangular and opercular gyri)

- finds similarities in phonetic segments that vary acoustically across larger syllable segments
- ♦ general role: responsible for articulatory recoding and sub-vocal rehearsal ("inner speech")

Supramarginal gyrus (BA 40)

- phonological store
- ♦ general role: phonological processing when short-term memory is involved

Figure 7. The Zatorre-Paulesu model of phonological processing. Brodmann Areas are numbered. Anatomical areas involved in this function are highlighted in bright colors, all others are translucent. Green – superior temporal gyrus, Fuscia – Wernicke's area, Blue – Broca's area, Yellow – Supramarginal gyrus.

Semantics

The conceptual knowledge required for comprehension is referred to as semantics. A variety of cognitive tasks have been used throughout the neuroimaging literature in an attempt to tap into semantic knowledge independently from orthographic and phonological processing. The task most commonly used in this endeavor is word generation, where subjects are given a noun either visually or aurally, and must generate an associated verb (e.g. responding "bake" or "eat" to the noun "cake"). Other tasks include producing words beginning with a designated letter or belonging to a given semantic category (e.g. Frith et al., 1991). The neuroanatomical areas most strongly associated with semantic tasks are: 1) the left frontal cortex, which includes Broca's area (BA 44/45), 2) left prefrontal cortex (BA 46), and 3) left inferior frontal cortex (BA 47), which is inferior and anterior to Broca's area. Other areas associated with semantic processing are left anterior (BA 38) and middle (BA 21) temporal cortices, and Wernicke's area, particularly the angular gyrus (BA 39) in the left posterior temporoparietal cortex. Note that many of these areas overlap with those identified as the neuroanatomical correlates of phonological processing (BA's 39, 44, 45). This overlap has been the topic of much debate in the literature, and competing interpretations of these functional areas are discussed below.

The PET studies of Petersen et al. (1988, 1989) were among the first to identify frontal regions as being involved with semantic processing. By comparing an overt speech verb generation task with an overt noun repetition task, Petersen et al. (1988)

found significantly greater activation in a left inferior frontal region around BA 47. Petersen et al. (1989) used a task where subjects monitored a word list for examples of the semantic category "dangerous animals". They also found activation at or near BA 47 relative to a passive viewing baseline task. A consistent finding was made by McCarthy et al. (1993) in an early fMRI study where subjects generated verbs to given nouns. Compared to simply repeating the nouns, the primary focus of activation was in BA 47, extending to area 10 in prefrontal cortex, although regions of the anterior insula and right frontal cortex were also activated. Little or no activation of BAs 47 or 10 were found for passive listening, covert generation, or mouth-movement control tasks. In contrast to BA 47 activation during verbal fluency tasks, Phelps et al. (1997) used fMRI to compare generating words beginning with a given letter to both a word repetition task and a task where subjects had to generate an antonym to a given word. They found areas of activation in the left inferior frontal gyrus (Broca's area) (BA 45), the superior frontal sulcus bordering the middle frontal gyrus (BA 8), and the anterior cingulate gyrus (BA 32). Activation in BA 8 has been differentially associated with eye movement (Demonet et al., 1992) and effortful searches through memory for words (Demonet et al., 1994), while anterior cingulate activation has long been associated with attentional mechanisms required during cognitive tasks (Petersen et al., 1988; Frith et al., 1991; Raichle et al., 1994). It is unclear why the Phelps et al. (1997) study failed to activate left inferior frontal gyrus (BA 47) in contrast to the Petersen et al. (1988, 1989) and McCarthy et al. (1993) studies, although other frontal areas were activated.

One possible explanation is that the studies of the Petersen and McCarthy groups have a potential confound in that the tasks associated with activation in BA 47 were more difficult than the non-semantic comparison tasks as measured by reaction time or accuracy. Two subsequent studies addressed this confound. Rather than a word generation task, Demb et al. (1995) compared a semantic task where subjects judged whether words were abstract or concrete, to both an "easy" (short response time) and a "difficult" (long response time) orthographic task. In the easy orthographic task, subjects judged whether words were displayed in uppercase or lowercase letters. In the difficult orthographic task, subjects indicated whether the first and last letters in a given word were in ascending or descending alphabetic order. Regardless of task difficulty, areas in left inferior prefrontal cortex, including BAs 45, 46, and 47, showed greater activation during the semantic task than during the orthographic tasks. This result went against the notion that activation of BA 47 was due to task difficulty. Consistent with this interpretation was a study by Roskies et al. (1996), who used two tasks comparable in difficulty: a synonym monitoring experimental task and a rhyme judgment control task. They found greater activation at or near BA 47 for the synonym compared to the rhyme judgment task. Another study by Spitzer et al. (1996) used a word-pair similarity task and compared it to a color similarity task of equal difficulty. They found left frontal activation that overlapped with Broca's area and left fronto-temporal activation, though precisely which areas were activated within these regions were not identified. Overall,

however, it appears that task difficulty does not account for inferior frontal (BA 47) activation during semantic processing.

Semantic processing tasks besides word generation also activate this inferior frontal (BA 47) area. Kapur et al. (1994), for example, found activation in the BA 47 region in a PET study when overt spoken responses were removed (contrary to the Petersen 1988 and 1989 studies) and the verb generation task was replaced with a word categorization task. They found activation at or near BA 47 when subjects viewed a series of nouns and judged whether each noun denoted a living or non-living entity, compared to a task of judging whether each noun contained the letter "a". In short, various types of word generation tasks as well as word categorization tasks produce activation in several areas of frontal cortex, particularly BAs 47, but also 45 and 46.

Evidence also suggests that semantic processing is affected by frontal lesions, especially in semantic priming tasks (Milberg and Blumstein, 1981; Swinney et al, 1989). It is unclear, however, whether these lesions cause difficulties with access to semantic codes for lexical/word items, or difficulties in processing the semantic code itself. Lesions within Broca's area (BA 44/45) have most often been associated with apraxic deficits of articulation (Mohr et al., 1978), and cortical stimulation in some frontal areas can result in total speech arrest (Ojemann, 1983). Lesions outside of Broca's area, in dorsolateral prefrontal cortex and superior frontal gyrus are associated with impaired comprehension for complex syntactic material, agrammatism, paraphasia, inability to formulate narrative discourse, and an inability to generate word lists (Rubens, 1976;

Alexander and Schmitt, 1980; Freedman et al., 1984; Stuss and Benson, 1986; Costello and Warrington, 1989). Additionally, significant naming errors occur in frontal areas of cortical stimulation patients, particularly those who had stimulation in middle or superior frontal gyri (Ojemann, 1992). The term Broca's aphasia is somewhat of a misnomer, as corresponding lesions often extend far outside Broca's area, usually involving the anterior inferior frontal gyrus, the middle frontal gyrus, insula, pre- and post-central gyri, or anterior parietal areas (Mohr, 1976; Mohr et al., 1978).

Despite the above evidence, the semantic processing role of frontal areas been questioned by several researchers, who contend that temporal areas are instead the primary areas involved in this type of processing. For example, in two tasks involving a) aurally presented words/pseudowords and b) generation of a verb in response to a visually presented noun, Fiez et al. (1996) found spatially distinct areas of activation in both temporal and temporoparietal (Wernicke's) areas. Activation in temporoparietal areas for aurally presented words and pseudowords (compared to visual fixation on a crosshair) was consistent with earlier studies of Petersen et al. (1988, 1989) and Wise et al. (1991a). Activation in the verb generation task (compared to reading nouns) that was found in the posterior middle temporal region (BA 37), however, was argued to reflect a different type of semantic processing, contrary to the suggestions of Wise et al. (1991a) that posterior temporal activation simply reflects semantic processing across a variety of tasks. Wise et al. (1991) used aurally presented words in a comprehension and retrieval task, and found that word comprehension activated superior temporal structures (BA 22), which is

consistent with the argument of Fiez et al. (1996). Wernicke's area, however, particularly temporoparietal areas, was also activated during the verb generation task, and unlike other superior temporal regions, was not affected by presentation rate. Fiez et al. (1996) argue that this more parietal activation represents a different type of semantic processing because of its sensitivity to presentation rate, in contrast to more anterior areas of superior temporal cortex.

Additional areas of activation for the verb generation task in the Wise et al. (1991a) study included the left premotor area, known as the supplementary motor area (SMA), the opercular gyrus (BA 44) in Broca's area, and the posterior end of the left middle frontal gyrus (BA 8). Although the SMA is usually activated during overt speech (Petersen et al., 1988), its presence was explained by the argument that retrieving words from memory results in automatic "inner speech", with which the SMA is involved. This argument is consistent with the studies of Price et al. (1994, 1996a). The involvement of the opercular gyrus in Broca's area (BA 44) is an area relatively unemphasized in the semantic studies reviewed above that found inferior frontal gyrus (BA 47) activation during verb generation, and this difference has yet to be explained. As mentioned earlier, the presence of the posterior portion of the left middle frontal gyrus (BA 8) has multiple possible explanations; lesions in this area have been associated with transcortical motor aphasia, which is characterized by nonfluent spontaneous speech but well-preserved repetition (Freedman et al., 1984). Wise et al. (1991a) speculated that this area of the posterior middle frontal gyrus is involved in the task of fluency when multiple words are

generated to a single cue, Demonet et al. (1994) argues that this area is involved with effortful searches through memory for words, and the verbal fluency study by Phelps et al. (1997) using auditory stimuli also found a small area of middle frontal gyrus (BA 8) activation, as did Demonet et al. (1992). This area is also known as the frontal eye field, which triggers voluntary saccades to visible targets in the visual environment, but it also receives cortical inputs from dorsolateral prefrontal cortex (BA 46) (Afifi and Bergman, 1998), which is an area that has been identified above in orthographic semantic tasks (Demb et al., 1995) and verb generation tasks using aural stimuli (Frith et al., 1991). Therefore, it is likely that lesions to BA 8 affect verbal fluency tasks because of disruptions to BA 46 connections, rather than because of deficits in processing visual stimuli.

In summary, Wise et al. (1991a) found that word comprehension activates temporal lobe structures (Wernicke's area) almost exclusively, and that silent word retrieval involves not only Wernicke's area, but two areas in left prefrontal cortex (BAs 44 and 8) and the SMA as well. As noted by Fiez et al. (1996), although Wernicke's area is common to both types of semantic tasks (comprehension and retrieval), there is sufficient separation between temporal and temporoparietal areas of Wernicke's activity that suggests a difference in the type of semantic processing that is necessary to accomplish the demands of each task. Frith et al. (1991) also used verbal fluency tasks, but rather than generating verbs to given nouns, subjects had to name as many jobs as possible in 3 minutes in one task, and had to generate words beginning with the letter "a"

in another task. Subjects gave overt verbal responses in all tasks except for rest. They found activation in the left dorsolateral prefrontal cortex (DLPC) (BA 46) during both verbal fluency tasks and left superior temporal gyrus (BA 22) in a lexical decision (word comprehension) task. These results are generally consistent with Wise et al. (1991), except that Frith et al. (1991) found a decrease in activation in superior temporal cortex activation during the verbal fluency tasks. What is common between these studies, however, is that intrinsic generation or retrieval of words activates frontal areas while word comprehension tasks consistently activate superior temporal areas. A series of studies by Binder and colleagues (1995, 1996, 1997) used a task where subjects heard names of animals and pressed a button when the animal was both "native to the United States" and "used by people". When this task was compared to a tone task, they found activation in inferior and middle frontal gyri, angular gyrus (BA 39), middle temporal (BA 21), and posterior inferior temporal (BA 37) gyri. It is possible that the frontal activations can be explained by the memory components involved with the given semantic task tapping into similar processes as those involved with word retrieval. This view is consistent with Gabrieli et al. (1998), who reviewed both neuroimaging and amnesic studies and concluded that activations in left inferior prefrontal cortex reflect semantic working memory capacity. It is also related to the view of Thompson-Schill et al. (1997), who suggest that rather than retrieval of semantic knowledge *per se*, left inferior frontal gyrus activation is associated with selection of information among competing alternatives from semantic memory.

Adding to the debate of the role of frontal areas are several studies that control for phonological processing or self-generated searches; these studies find exclusive or nearly exclusive temporal or temporoparietal activation for semantic processing. Demonet et al. (1992) used a lexical-semantic auditory task where subjects monitored for nouns of small animals with "positive" attributes (e.g. "kind") in noun-pairs, and compared it to a tone task and a phoneme task. There was widespread activation in frontal, temporal, fusiform, and supramarginal gyrus when the semantic task was compared to the tone task, but when compared to the phonological task, both the angular (BA 39) and supramarginal gyrus (BA 40) were activated, as were the left middle frontal gyrus/frontal eye fields (BA 8), the inferior part of the temporal lobe (BA 20), and areas related to attention such as the cingulate gyrus (BA 32). In a study by Shaywitz et al. (1995), subjects performed a phonological task where they judged whether two visually presented non-words rhymed (using a letter-case monitoring task as a control), and a semantic task, where they judged whether two visually presented words came from the same semantic category. When the letter-case task was subtracted out, the phonological task activated the inferior and middle frontal gyri bilaterally as well as the superior and middle temporal gyri bilaterally. When the phonological task was subtracted out, the semantic task activated the superior and middle temporal gyri bilaterally. These results led the authors to conclude that the inferior frontal gyrus was more strongly associated with phonological processing and temporal sites more strongly associated with semantic processing. In their study of the component processes of reading, Pugh et al. (1996) also found sites in both the middle (BA 21) and

superior (BA 22) temporal gyri that were specialized for semantic category judgments when compared to rhyme judgments. Price et al. (1997) contrasted a semantic decision, where subjects pressed a mouse button when a visually presented word referred to a living object (vs. a nonliving object), with a phonological decision, where subjects made a finger press when the word had a specific number of syllables, and found that relative to the phonological task, the semantic task was associated with activations in the left temporal pole (BA 38) and the angular gyrus (BA 39). Overall, with the exception of the Roskies et al. (1996) study, it appears that when phonological processing is subtracted from semantic tasks, frontal activations are minimized and temporal activations become more prominent.

Lesions in temporal and temporoparietal areas often result in semantic deficits (Hart and Gordon, 1990), including word comprehension and cross-modal word matching (Coughlan and Warrington, 1978; Wise et al., 1991a). Several researchers have argued that it is the stored information itself that is lost rather than the retrieval or access mechanism to these semantic abilities (Hart and Gordon, 1990; Hart et al., 1992; Hillis and Caramazza, 1991; Warrington and Shallice, 1984), similar to the arguments posed relating frontal lesions and semantic processing. Cortical stimulation mapping often uses sentence reading when the posterior temporal lobe needs to be resected (Ojemann, 1983) but errors tend to be syntactic rather than semantic in nature. Errors in reading may include slow, effortful reading, but also fluent reading with mistakes on verb endings,

prepositions, conjunctions, or pronouns, all suggesting a relation to syntax and thereby implicating the temporal areas in syntactic, as well as semantic, processing.

Other studies that explore semantic and syntactic processing find similar frontal and temporal networks despite a variety of tasks and stimuli. Vandenberghe et al. (1996) used both words and pictures in a semantic task and found that a common semantic code existed for words and pictures, which was also consistent with many regions identified during word generation and comprehension: temporoparietal areas, the junction between fusiform and inferior temporal cortex, the left middle temporal gyrus (BA 21), and the left inferior frontal gyrus (BA11/47). Semantic processing differed between words and pictures in specific areas as well. The left superior temporal sulcus, left anterior middle temporal gyrus (BA 21), and left inferior frontal sulcus were activated more when the semantic task was performed with words. Activation specific to pictures of objects was localized to the left posterior inferior temporal sulcus, possibly reflecting ventral pathways that mediate semantic processing in the visual domain. Visual object processing in ventral pathways will be discussed in more detail below.

In a study examining syntactic comprehension and the acceptability of sentences by comparing visually presented center-embedded sentences with right-branching sentences and sentences containing pseudowords, Stromswold et al. (1996) found consistent activation in the opercular gyrus in Broca's area (BA 44) across all condition subtractions. Activation of the frontal eye fields (BA 8) was attributed to differences in eye movements across conditions. It is unclear whether Broca's area activation in these

conditions was due to: 1) an increased memory load in processing center-embedded sentences, 2) general verbal working memory capacity unrelated to syntactic processing, 3) rehearsal of the sentences before responding (i.e. subvocal rehearsal, or "inner speech"), or 4) general syntactic processing. The authors favored a general syntactic processing interpretation, though they did not account for the many studies that identify Broca's area activation with phonological processing or subvocal rehearsal/inner speech. In contrast, temporal and temporoparietal activations were condition-dependent. Subtracting the pseudoword condition from the center-embedded condition showed additional activation in Wernicke's area (BA 22/39), and adjacent areas of the superior temporal gyrus (BA 22). Subtracting the pseudoword condition from the right-branching sentences showed supramarginal gyrus (BA 40) in addition to frontal activation. It has been argued above that during phonological processing, supramarginal gyrus activation tends to be present under conditions of short-term memory load. If the right-branching sentence condition can be considered to possess a greater short-term memory load than center-embedded sentences, it can be argued that the supramarginal activation seen here is also consistent with such an interpretation. To date, however, this interpretation has not been directly tested with respect to either syntactic or semantic processing.

In another study examining sentence reading, Bavelier et al. (1997) used fMRI to compare sentences with consonant strings, and also found both frontal and temporal areas to be active. Individual subject data comparing sentences to consonant strings showed activation that was focal and variable across subjects, a pattern most commonly found in

studies using cortical stimulation (Ojemann et al., 1989; Ojemann 1991, 1992). Activation in individual subjects in the Bavelier et al. (1997) study was distributed in both Broca's and Wernicke's areas (BA 22/39), but also extended into other left prefrontal areas and the left anterior temporal lobe (BA 38). Across subjects, activation was most commonly seen in Broca's and Wernicke's areas, including most of the angular gyrus (BA 39). Broca's area activation in this case appears to be consistent with subvocal rehearsal, or "inner speech" during sentence-reading. The apparent absence of both a short-term memory component in the task and supramarginal gyrus activation is also consistent with the short-term memory interpretation of this structure's role, though this view is still far from conclusive.

Figure 8 below illustrates the neuroanatomical areas identified during semantic processing by various researchers and the accompanying table summarizes the semantic tasks most often identified with a particular anatomical and Brodmann Area. Despite varied experimental and control tasks, it is apparent that as in phonological processing, a network of frontal, temporal, and temporoparietal areas are activated during semantic processing across methodologies.

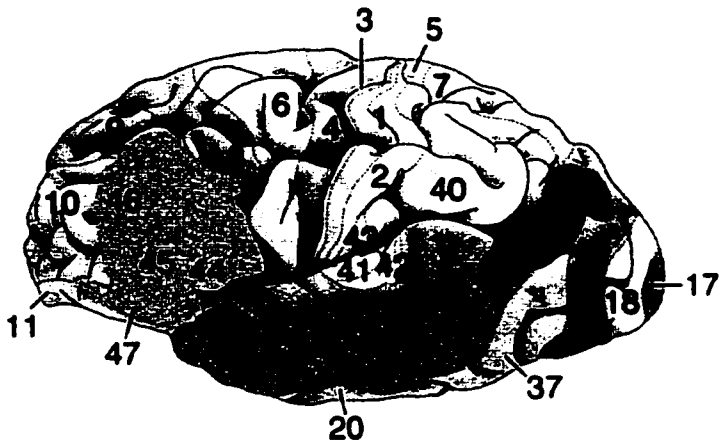

Figure 8. Areas identified with semantic processing. Brodmann Areas are numbered. Anatomical areas involved in this function are highlighted in bright colors, all others are translucent. Green – Temporal Pole (BA 38) and Middle Temporal gyrus (BA 21), Fuscia – Wernicke's area (BA 22/39), Blue – Broca's area (BA 44/45) and Middle Frontal gyrus (BA 46)

Table 1. Experimental and control tasks during semantic processing and the areas and studies associated with them. Abbreviations: generation = gen, repetition = rep, inferior = inf, middle = mid, superior = sup, anterior = ant, posterior = post.

Study	Experimental task	Control task	Activated areas (BA)
Petersen et al. (1988) Petersen et al. (1989)	Overt verb gen Category monitoring	Overt noun rep Passive viewing	Inf frontal (47) Inf frontal (47)
McCarthy et al. (1993)	Covert verb gen	Covert noun rep	Inf frontal (47) prefrontal (10)
Phelps et al. (1997)	Word gen from given letter	Word rep, antonym gen	Broca's (45), frontal eye fields (8), ant cingulate (32)
Demb et al. (1995)	Abstract vs. concrete word categorization	Easy orthograph task Hard orthograph task	Inf prefrontal (45, 46, 47)
Roskies et al. (1996)	Synonym monitoring	Rhyme judgment	Inf frontal (47)
Spitzer et al. (1996)	Word-pair similarity judgment	Color similarity judgment	Frontal (Broca's overlap), frontotemporal (not specified)

Table 1 Continued.

Kapur et al. (1994)	Word categorization (living vs. non-living)	Orthographic monitoring	Inf frontal (47)
Fiez et al. (1996)	Aurally presented words/pseudoword Verb generation	Visual fixation on crosshair Reading nouns	Wernicke's (22/39) Post mid temp (not specified)
Wise et al. (1991a)	Aurally presented comprehension Retrieval (verb generation)	Rest Rest	Superior temporal (22) Wernicke's (22/39), SMA, Broca's (44), frontal eye fields (8)
Frith et al. (1991)	Generate specific category of words (jobs) Generate words from given letter Word comprehension	Rest Rest Rest	Frontal (DLPC) (46) Frontal (DLPC) (46) Superior temporal (22)
Binder et al. (1995, 1996, 1997)	Word categorization (animals)	Tone task	Inf/mid frontal (not specified), angular (39), mid temporal (21), post inf temporal (37)
Demonet et al. (1992)	Category monitoring (same)	Tone task Phoneme task	Frontal, temporal, fusiform, supramarginal (40) Angular (39), supramarginal (40), frontal eye fields (8), inf temporal (20), cingulate (32)
Shaywitz et al. (1995)	Non-word rhyme judgment Word categorization	Letter-case monitoring Non-word rhyme judgment	Inf/mid frontal, sup/mid temporal Sup/mid temporal
Pugh et al. (1996)	Semantic category judgments	Rhyme judgments	Mid/sup temporal (21/22)
Price et al. (1997)	Semantic categorization (living vs. non-living)	Phonological monitoring (# of syllables)	Temporal pole (38), angular (39)

Table 1. Continued.

Vandenburghe et al. (1996)	Semantic judgment (words) Semantic judgment (pictures) Non-semantic judgment (size matching)	Orthogonal design (non-semantic = baseline)	Words/pictures: temporoparietal, fusiform/inf temporal, mid temporal (21), inf frontal (47/11) Words: sup/mid temporal (21), inf frontal Pictures: post inf temporal
Stromswold et al. (1996)	Center-embedded sentences Right-embedded sentences	Sentences with pseudowords (same)	Broca's (44), Wernicke's (22/39), superior temporal (22) Broca's (44), supramarginal (40)
Bavelier et al. (1997)	Sentence reading	Viewing of consonant strings	Broca's & Wernicke's, prefrontal, angular (39)

Semantics and ERP studies

It has been well-documented that the N400 is sensitive to semantic priming (Kutas and Hillyard, 1980; Bentin et al., 1985; Holcomb, 1988; Rugg, 1990). Since picture naming is assumed to be mediated by semantic processes (e.g. Humphreys et al., 1988), it follows that in addition to words, N400 semantic priming effects are also seen for line drawings (Barrett and Rugg, 1990; Holcomb and McPherson, 1994). The picture N400 shows a similar time course as the N400 observed with words, and a similar reduction in amplitude when sentences end with line drawings that are semantically congruous versus line drawings that are semantically anomalous (Ganis et al. 1996; Nigam et al., 1992).

When relatively large electrode arrays are used, the scalp distribution of the N400 to words and pictures is different as well, with the N400 to words being prominent over right centroparietal sites and the N400 to pictures more prominent in left frontal sites (Holcomb and McPherson, 1994; Ganis et al., 1996). The semantic priming study of Barrett and Rugg (1990) used pairs of line drawings of common objects in a relatedness judgment task. They found larger N400s for unrelated than for related objects, and showed negativities for pictures were as large at frontal sites as at more posterior sites, unlike the N400s to visual words. They also found an earlier negativity at approximately 300msec (N300). The N300 component was also larger for unrelated objects, and also more frontally distributed than the verbal N400. Component and distribution differences were interpreted as evidence for multiple semantic stores, where semantic processing for pictures and words occurs in separate systems. Similar results were found by Holcomb and McPherson (1994), with target pictures (line drawings) preceded by semantically related or unrelated pictures. Unrelated targets generated larger N400s and N300s than related targets, and the N300 was more prominent at anterior sites. In this study, one-third of unrelated pictures were unrecognizable nonobjects. The N400 has been seen in response to non-objects or incomplete objects, being more negative with incomplete (Stuss et al., 1992) or unidentified pictures (McPherson and Holcomb, 1999), and with a slightly different distribution than the object N400, with larger negativities at central and anterior sites and more positive-going waveforms at occipital sites than for objects, which is more negative over the left hemisphere (Holcomb and McPherson, 1994).

McPherson and Holcomb (1999) replicated Barrett and Rugg (1990) and found N400 semantic priming effects could also be obtained with color pictures of real objects (as opposed to line drawings), where the N400 was more negative for unrelated than related target pictures, and most negative for unidentifiable pictures at anterior sites. Like Holcomb and McPherson (1994), unidentifiable objects were more positive-going over occipital sites. The scalp distribution for the N400 in this study was largest at temporal, temporal-parietal, and central sites, slightly smaller at anterior temporal and frontal sites, and all but absent at occipital sites. The presence of the N300 component, which is relatively anterior, was suggested as possibly influencing the distribution of the N400 component to more anterior areas relative to that for words, though this study as well as McPherson and Holcomb (1992) suggest that these two components are dissociable.

An attempt to locate the neural generator for the word N400 has been made with intracranial grids. To study the role of the anterior medial temporal lobe in the N400 in epilepsy patients, Nobre and McCarthy (1995) placed an intracranial grid over this region and visually presented several categories of words. Their results also showed that the amplitude of the N400 was reduced when word pairs were related compared to when they were unrelated. They also found that the N400 potentials they measured tended to be larger for concrete nouns with a high visual imagery component, and smaller for orthographically illegal words, unpronounceable nonwords, function words (such as grammatical connectives), and when they were pre-exposed to semantically related words. The N400 ERP from scalp recordings has been shown to respond similarly to

these task manipulations (Nobre and McCarthy, 1994), even though it is considered a volume-conducted representation of anterior medial temporal lobe activity (Nobre and McCarthy, 1995), in contrast to intracranial electrodes that record mostly local activity. Studies that show large attenuations in the N400 following unilateral anterior temporal lobectomy (Rugg et al., 1991; Smith and Halgren, 1988, 1989) also suggest the temporal lobe is involved in generating the N400. There is evidence, however, that other anatomical structures are implicated in the generation of the N400. Guillem et al. (1995) recorded ERPs from intracranial electrodes in medial and lateral aspects of the temporal, frontal, parietal, and occipital lobes during a continuous recognition memory task. They found N400 and P600 components in temporal, frontal, and parietal areas, suggesting that scalp-recorded components represent only the most obvious aspects of synchronous activity that are generated from distributed brain structures or neural systems underpinning a given cognitive mechanism.

The early negative-going perceptual component, the visual N100, and the later negative-going semantic processing component, the N400, are the two components of interest for this study. Since a visual object-naming paradigm is the task being employed across techniques, the association of the sources of these components to visual perceptual and semantic processing will be focused upon both within the ERP technique and in comparisons across ERP, fMRI, and PEPSI. It is expected that sources for the N100 component will be most prominent in posterior areas for both objects and scrambled

objects in occipital areas, while those for the N400 will be more prominent in anterior (frontal/temporal) areas in both conditions.

Phonological vs. Semantic Areas

With the exception of extrastriate areas in orthographic processing, it is obvious from the above review that there is a large amount of overlap in frontal, temporal, and parietal areas for orthographic, phonological and semantic tasks. Experimental and control tasks differ in some respects in every neuroimaging study, and lesion evidence can be found to support the interpretations of each area's role for a particular language process. In attempting to distinguish the function of repeatedly identified areas in semantic tasks, Fiez (1997) suggests that frontal and posterior (temporal) areas have different roles in semantic processing, specifically that the left inferior prefrontal region (BA 47) contributes to the effortful retrieval, maintenance, and/or control of semantic information. Posterior (temporal) areas, on the other hand, are responsible for long-term storage of conceptual and semantic knowledge. Neuropsychological evidence seems to lend support to this hypothesis (e.g. Randolph et al., 1993), but investigations in normals suggest that frontal areas are consistently activated in semantic processing tasks unless those tasks are controlled for phonological or self-generated responses. Regarding frontal area overlap for phonological and semantic processing, Fiez (1997) also suggests that semantic and phonological interpretations of inferior prefrontal activation are not contradictory, but complementary. The inferior prefrontal cortex can be subdivided based

on cytoarchitectonic differences, such as the Brodmann areas, and based on these differences, it does appear that overall, semantic processing is most often localized to the ventral inferior portion of the frontal cortex around BA 47, while phonological processing is more likely to activate more posterior areas in the frontal cortex, such as the triangular and opercular areas of the inferior frontal gyrus (BAs 44 and 45, Broca's area). Still, it has been shown that Broca's area is activated during some types of semantic processing, just as temporal areas are activated during some types of phonological processing. It will be up to future studies to clarify and specify the roles of frontal, temporal, and temporoparietal areas in language processing.

Visual object processing

Stages of Object Processing

Cognitive theories of object identification propose that several stages of processing need to occur from the time the object is viewed until its verbal label is produced. These stages include: 1) early or low-level visual sensory processing that encodes shape, surface details such as color and texture, and/or segments figure from ground (Price et al., 1996b) and 2) matching this encoded perceptual information to a multi-level memory system. This multi-level memory system accesses: i) the stored structural description of the object, ii) semantic descriptions (such as functional and associative properties) of the object, and iii) phonological descriptions. Some models argue that a direct route exists from the structural code to the phonological code (Lupker,

1985), but a more common view is that an abstract stage involving semantic access intervenes (Vitkovich and Humphreys, 1991), and that retrieval of the phonological representation takes place subsequent to semantic access (Humphreys et al., 1997; Humphreys et al., 1999). Some evidence in support of this claim includes studies that compare word processing with picture processing. Such studies show that naming latencies are faster for words than for pictures, while categorization latencies are faster than naming latencies for pictures, both implying that the retrieval of the object name occurs after semantic processing has taken place (Potter and Faulconer, 1975; Snodgrass, 1980). Similarly, picture/word interference tasks have demonstrated the influence of semantic activation in picture naming by showing that picture naming, rather than word naming, is vulnerable in the presence of semantic distractors (Smith and Magee, 1980; Glaser and Glaser, 1989; La Heij et al., 1990).

Starting with the theoretical work of Lissauer (1890) (cited in Op de Beeck et al., 2000), Humphreys and colleagues (Humphreys and Riddoch, 1993; Humphreys and Riddoch, 1987; Humphreys et al., 1988) argue for a distinction between the sensory/perceptual and memory stages outlined above. Disorders of object identification, termed visual agnosia, offers one line of evidence to demonstrate the existence and dissociability of these stages (Bruyer, 1994 (cited in Op de Beeck et al., 2000); Farah, 1990; Humphreys and Riddoch, 1987; Humphreys et al 1988, 1999). Impairments can occur at the level of discrimination of visual attributes (stage 1), or in the various memory systems (stage 2). Deficits in processing visual sensory information, such as shape or

color (stage 1), tend to occur after occipital lobe lesions (Benson and Greenberg, 1969; Meadows, 1974; Weiskrantz, 1980; cited in Murtha et al., 1999), whereas deficits in access to memory systems (stage 2) may involve any of the three levels listed above and will therefore occur after lesions in various sites. Within stage 2, impairments to level (i), i.e. stored structural descriptions, are termed apperceptive agnosia. Apperceptive agnosia tends to occur following right inferior parietal-temporal lesions (Humphreys and Riddoch, 1984; Warrington, 1982; Warrington and Taylor, 1973), and is apparent in poor object decision tasks, which require familiarity discriminations between pictures of real objects and non-objects, poor drawing from memory, and impaired responses to questions about the visual properties of objects or at assigning names to definitions that stress visual properties (Sartori and Job, 1988; Gainotti and Silveri, 1996). These patients may retain good early visual processing, where they are able to perform perceptual matching tasks or are able to adequately copy objects. They may also be proficient in their long-term knowledge about the functional or associative properties of objects, as well as demonstrate the ability to name to verbal definitions or questions (Murtha et al., 1999).

If there is successful access to stored visual knowledge, impairments can also occur with access to semantic representations (level ii), especially following lesions at the junction of the left occipital-temporal lobe (Bub et al., 1988; McCarthy and Warrington, 1986, 1988). Although there is intact performance on object decision tasks, patients are impaired at matching tasks that require access to semantic knowledge from visual stimuli and at object naming. They are able, however, to discriminate between real and plausible

non-objects (Riddoch and Humphreys 1987; Sheridan and Humphreys 1993; Hillis and Caramazza, 1995), and to perform associative matching to names of objects as well as name to verbal definition when auditory rather than visual stimuli are used. The poor object naming, therefore, results from impaired visual access to semantic knowledge, rather than impaired semantic knowledge or name retrieval *per se*; impairments in knowledge about visual properties and access to semantic representations are usually classified as problems in object recognition rather than object naming (Humphreys et al., 1997). Lastly, patients may have specific deficits in name retrieval (level iii). This impairment is termed visual anomia, or optic aphasia in early accounts (Beauvois, 1982). These patients perform well at object decision and associative matching tasks (Kay and Ellis, 1987) since they have good access to both visual and semantic knowledge about objects, but are impaired at retrieving the phonological label for an object (Humphreys et al., 1997, 1999). In short, lesion data indicates that stored knowledge about the visual properties of objects is dissociable from semantic and phonological representations, while semantic representations are dissociable from phonological representations.

Ventral vs. dorsal streams

Evidence for two distinct visual pathways has been well described in the macaque (Ungerleider and Mishkin, 1982; Mishkin et al., 1983): a) a ventral pathway, proceeding from the occipital lobe to the inferior temporal lobe, and b) a dorsal pathway, running from the occipital lobe to the posterior parietal lobe (See Figure 1 above). Both non-

human primate (Levine, 1982; Ungerleider and Mishkin, 1982) and human (Haxby et al., 1991; Sergent et al., 1992b; Haxby et al., 1994; Kosslyn et al., 1994) studies indicate that these two pathways have interconnected but distinct functional properties. The ventral, or occipitotemporal, pathway is mainly concerned with objects when properties like shape or color are encoded, and during object recognition or identification (Malach et al., 1995; Maunsell and Newsome, 1987). When inferior temporal lobes are bilaterally ablated in the macaque, difficulty arises in recognizing the shapes of objects, but performance in registering location remains intact (Levine, 1982; Ungerleider and Mishkin, 1982). In humans, this ventral or visual object processing pathway also includes the processing of letters and words (Ungerleider and Haxby, 1994; Haxby et al., 1991), with posterior (occipital) regions active for visual words and letter-strings, and anterior (temporal) regions active only for words (Nobre et al., 1994). This pattern is seen through direct cortical recordings (Nobre et al., 1994), cortical stimulation (Luders et al., 1986; Burnstine et al., 1990), functional neuroimaging (Bookheimer et al., 1995; Puce et al., 1996), and lesion studies in humans (Damasio and Damasio, 1983; Farah, 1990). Additional distinctions with the ventral area may also exist for faces and colored objects (Allison et al., 1994; Puce et al., 1995; Kanwisher et al., 1997).

The dorsal, or occipitoparietal, pathway is mainly concerned with spatial localization, size, or perceiving the spatial relationships among objects and their parts (Desimone and Ungerleider, 1990; Bly and Kosslyn, 1997; Maunsell and Newsome, 1987). When the posterior lobes are ablated bilaterally in the macaque, performance in

registering location fails but recognition of object shape remains intact (Levine, 1982; Ungerleider and Mishkin, 1982). This dual pattern of visual deficits is similar in humans when focal brain damage is sustained in these two areas (Newcombe et al., 1987; Damasio et al., 1982), suggesting comparable pathways between humans and macaque.

Functional studies of object naming

Functional imaging (PET, fMRI), cortical stimulation, and ERP activity related to object recognition and object naming primarily involve the ventral stream of visual processing. Accordingly, these studies identify three main areas of neural activity: 1) the occipital pole (Brodmann Area (BA) 17) and superior/middle occipital gyri (also termed the Lateral Occipital gyrus or LO) (BAs 18, 19), 2) middle temporal/inferior temporal/left fusiform gyri (BAs 21, 20, 37), and 3) middle/inferior frontal gyri (MFG, IFG) (BAs 46, 47), sometimes including Broca's area (BAs 44, 45). Figure 9 below illustrates the location of these areas:

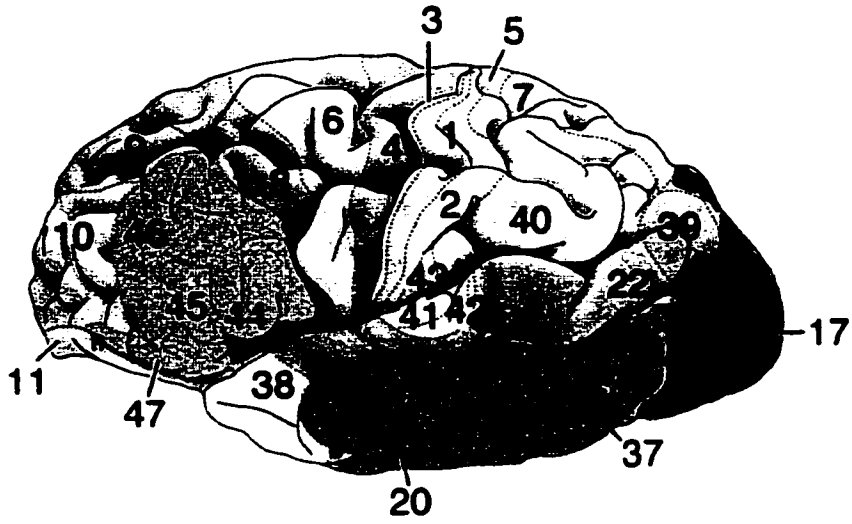

Figure 9. Areas associated with visual object processing. Brodmann Areas are numbered. Anatomical areas most often involved in this function are highlighted in bright colors, all others are translucent. Green – Inferior/Middle Temporal (BA 20, 21) and Fusiform gyri (BA 37), Light Blue – Broca's area (BA 44/45) and Middle Frontal gyrus (BA 46), Dark Blue – Occipital pole (BA 17) and Lateral Occipital gyrus (BA 18, 19).

The ventral stream appears to be activated not only during higher-level semantic and phonological processing, but during lower-level visual/structural processing as well. Puce et al. (1996), for example, found activation in the left inferior occipital temporal regions for letter strings and abstract patterns, while Schacter et al. (1995) found regions in inferotemporal and fusiform gyrus that were more active when subjects evaluated possible objects versus impossible objects. Grill-Spector et al. (1998) found differences in primary retinotopic (V1-3, BA 17) and nonretinotopic (LO) areas (BAs 18, 19) when

subjects had to covertly name objects and objects scrambled to various degrees. Retinotopic primary areas V1-3 remained equally active for objects and scrambled objects, but areas V3a and V4v decreased in activation with highly scrambled objects. The lateral occipital complex (LO) showed the highest sensitivity to object scrambling, reducing in activation to all but the least amount of scrambling. The authors suggested that the LO cortex was involved in the processing of object parts. Malach et al. (1995) also found object-related activation in the lateral occipital (LO) cortex to a wide range of objects, including famous faces, common objects (animate and inanimate), and unfamiliar 3-D abstract sculptures when compared to degraded face pictures and scrambled phase textures, similarly suggesting the LO is involved in the process of object detection. It has been speculated that the final integration of object-part information would occur in the fusiform gyrus, suggesting a higher-level perceptual processing role for the fusiform. The study of Op de Beeck et al. (2000) is consistent with this idea, finding that degrading shape information consistently reduced the amount of activation in the fusiform gyrus. Kanwisher et al. (1997), however, found activation in medial regions of the fusiform when subjects viewed both nonsense objects and familiar drawings, both compared to a baseline of scrambled lines, while Martin et al. (1996) found fusiform activation when viewing nonsense objects compared to a baseline of noise patterns. These two latter studies suggest that ventral occipital-temporal structures such as the fusiform are just as likely to be involved in lower-level stages of visual processing as in higher, more

"semantic" stages of object recognition. These differing interpretations of the role of the fusiform gyrus will be discussed further below.

Other studies with various task demands and control conditions also repeatedly activate the left fusiform/inferior occipitotemporal gyrus as well as the superior/middle occipital gyrus. Haxby et al (1991) had subjects perform face matching, dot-location matching, and sensorimotor control tasks in an attempt to separate the extrastriate visual pathways for object recognition and spatial localization. Results showed that the lateral occipital (LO) cortex was activated for both face-matching and dot-location matching tasks while the occipitotemporal cortex (anterior and inferior to the occipital areas activated by the two visual matching tasks) was activated for the face matching task only. Though the LO was active for both visual tasks, the authors assigned specific occipitotemporal regions to object processing and specific superior parietal regions to spatial visual processing, further demonstrating ventral and dorsal functional distinctions. Sergent et al. (1992b) had subjects perform six tasks involving gratings, faces, and objects with a visual fixation control task during a PET scan. Although the face and object tasks were described as categorization tasks where the specific name of the object/face did not have to produced, the left fusiform and left middle temporal (BA 21) gyri were both active. While the fusiform gyrus is activated bilaterally (but more intensely in the right hemisphere) in other studies using faces as stimuli (e.g. Puce et al. 1995, 1996), the left middle temporal gyrus (BA 21) is implicated by lesion studies to be involved in naming, rather than just categorizing visual objects. For example, lesion

studies by Flude et al. (1989) and Damasio et al. (1990) both describe patients with damage to these temporal areas who were able to recognize faces and objects and describe the object's function, but were unable to retrieve the name. This data suggests that lesions in BA 21 disrupt the ability to assign a label to an object that has been visually recognized, and not the ability to visually recognize an object. Therefore, the involvement of BA 21 during the categorization task in the Sergent et al. (1992b) study probably reflects automatic or implicit naming of the object rather than purely visual and semantic processing. In another study by Sergent et al. (1992a), subjects performed three tasks: a) semantic categorization of visual objects, b) spatial discrimination of visually presented letters, and c) a phonological decision task of visually presented single letters. Activation was found bilaterally in the ventral occipital cortex (BA 19) during all three tasks, but compared to the two letter tasks, activation specific to objects activated BA 18 in the left hemisphere and the posterior region of BA 36 (fusiform gyrus) bilaterally. When the phonological letter task was subtracted from the object task, activation was significant in the left lingual and left fusiform gyrus, whereas the middle temporal gyrus (BA 21) was activated when the object task was compared to the spatial letter task, which is consistent with semantic access during object naming as discussed earlier. Activation in the middle temporal gyrus (BA 21) for the object minus spatial letter task is also consistent with Sergent et al. (1992b), implying that subjects automatically accessed the name of the object during the categorization task. Additionally, the spatial discrimination of letters activated the inferior parietal lobe bilaterally, and the phonological letter task involved the

left prefrontal and superior temporal cortex. In short, the semantic categorization of objects may involve automatic or implicit object naming, activating the ventral pathway, while the letter-spatial task activated the dorsal pathway, consistent with the functional distinctions described earlier.

The above evidence strongly suggests that the ventral and dorsal pathways maintain distinct functions. On some occasions however, these pathways appear to influence each other during object processing as well. A PET study by Kosslyn et al. (1994), for example, compared random line patterns with pictures of objects seen from canonical (typical) or noncanonical (atypical) points of view, and subjects had to decide whether the spoken word named the object. The inferior temporal region was especially active, presumably to encode the visual information needed for recognition and identification, consistent with ventral stream functions. On the other hand, the angular gyrus, considered part of the dorsal stream, was active for noncanonical pictures. This activation was interpreted to be part of an associative memory network, and it has been argued that under certain conditions, the dorsal and ventral brain areas associated with visual processing interact and influence each other (Goodale and Milner, 1992; McIntosh et al., 1994). Tasks involving associative memory could explain why dorsal areas (angular gyrus (BA 39) and/or superior areas of extrastriate cortex (BA 19)) are engaged by object tasks that lack obvious spatial or motion components. One alternative explanation is that spatial properties about the object are encoded automatically during picture naming and result in dorsal activations (Kosslyn et al., 1994), but this pattern of

activation is not seen in the majority of imaging studies examining object processing. Another alternative is that the control tasks involve spatial encoding, such as the random line patterns in this study, thus invoking dorsal structures.

Another PET study by Kosslyn et al. (1995) examined the subprocesses involved in object identification at entry, subordinate, and superordinate levels of birds. Subjects decided whether aurally presented names were appropriate for accompanying pictures or written words. In those tasks involving pictures, the extrastriate (BA 19) area in the left hemisphere was activated for subordinate and superordinate tasks when either entry level pictures or nonsense patterns were subtracted, suggesting spatial and shape encoding (subordinate subtractions) as well as possible higher-level semantic processing (superordinate subtractions). The occipital pole (BA 17) in the left hemisphere was activated when a fixation point was subtracted from subordinate pictures, but this activation is likely due to basic visual processing rather than higher-level semantic access, since the occipital pole is a primary visual area. Besides these occipital areas, left parietal areas were activated for subordinate pictures subtracting either entry level pictures or nonsense patterns, implying spatial encoding, and temporal areas were additionally activated when subordinate pictures were compared with either nonsense patterns or a fixation point, implying both spatial and shape encoding. Again, this group interpreted their results in the context of associative memory, which was predicted to involve both the dorsal and ventral streams in object processing with these particular task demands and subtractions. The middle frontal gyrus (BA 46) was also activated in both studies, which

can be argued as reflecting top-down processing (Kosslyn, 1994, 1995) or knowledge-guided searches during semantic categorization tasks (Murtha et al., 1999). Similar to the temporal areas found in the Kosslyn et al. (1995) study, Gauthier et al. (1997) also found that activity in the fusiform and inferotemporal gyri increased when subjects performed subordinate categorization tasks compared with simpler basic-level categorizations. The study of Op de Beeck et al. (2000), however, shows that activity in the ventral and dorsal visual cortex is present both during object matching at the basic level as well as more specific levels when compared to a shape-orientation matching task, and activity in the fusiform gyrus is not modulated consistently by the abstraction level of the task. Overall, the results can only be interpreted as showing that the processes used in identification and categorization at entry, subordinate, and superordinate taxonomic levels almost always involve occipital and fusiform areas to some degree, although the specific roles of these areas remain unclear. It does appear, however, that parietal (i.e. dorsal) areas become activated when picture identification or categorization tasks are contrasted with tasks that emphasize spatial encoding.

Functional distinctions between ventral and dorsal areas can also be seen when words and pictures are compared. It was shown earlier that an orthography-to-phonology route could be examined by contrasting reading words (letter forms with phonology) with picture naming (non-letter forms with phonology). To summarize, studies that contrast reading or viewing words with naming or viewing pictures show that the left supramarginal gyrus (BA 40), part of the dorsal pathway, tends to be active for words but

not for pictures (Bookheimer et al., 1995; Vandenberghe et al., 1996; Menard et al., 1996), which is consistent with spatial processes involved in orthography. Deficits in reading unfamiliar words occur when damage to the supramarginal gyrus (BA 40) is sustained (Marin, 1980; Vanier and Caplan, 1985), which is also consistent with the interpretation of this area being involved in an orthography-to-phonology route. In contrast, viewing or naming pictures tends to activate more ventral areas. In a study examining the passive viewing of words and pictures, Menard et al. (1996) found that when pictures were subtracted from words, activation occurred in the left angular gyrus (BA 39), supramarginal gyrus (BA 40), and Broca's area. When words were subtracted from pictures, the occipital pole (BA 17) was activated in the right hemisphere, while the lateral occipital gyrus (LO) (BAs 18, 19) was activated bilaterally, along with the middle temporal gyrus (BA 21). As mentioned earlier, middle temporal gyrus (BA 21) activation is consistent with subjects automatically naming an object upon viewing it, even if there are no explicit task demands for doing so (Sergent et al., 1992a, 1992b). Comparing to a visual noise control, Bookheimer et al. (1995) presented subjects with words and objects and found regions both common and specific to reading words and naming objects. Areas common to words and objects included the posterior medial occipital gyrus (BAs 17,18), extrastriate visual cortices (BA 19), and the inferior temporal/fusiform gyri bilaterally. The left inferior frontal gyrus (BA 47) was active in two sub-areas: a) the anterior-lateral IFG near BA 11 for viewing objects, and b) the most anterior and basal portion of the insula (BA 9). Words tended to activate more anterior and lateral regions

of the fusiform compared to objects, which activated regions relatively posterior and medial. Moore and Price (1999b), however, found that the left lateral fusiform was activated in naming both words and objects, while medial anterior regions of the left fusiform (BA 20) were active both for viewing and naming words and objects. Posterior fusiform regions were also active preferentially for naming and viewing objects only. Left superior temporal (BA 22) and supramarginal gyri (BA 40) were more active for words than objects, again consistent with the orthography-to-phonology route mentioned above.

In addition to studies involving various levels of abstraction within a semantic category or the comparison of words and pictures that combine different semantic categories in each class of stimuli, there are a group of studies that examine category-specific object processing. These studies stemmed from several reports in the last decade that have described patients with category-specific deficits in naming natural objects relative to artifacts (DeRenzi and Lucchelli, 1994; Forde et al., 1997; Sartori and Job, 1988; Warrington and Shallice, 1984) as well as the opposite pattern (Hillis and Caramazza, 1991; Sacchett and Humphreys, 1992; Warrington and McCarthy, 1983, 1987). There are three main lines of explanation related to category-specific deficits: a) the semantic system is organized by category, where object knowledge is grouped into natural and man-made categories and localized brain damage causes selective impairments (Hart et al., 1985; Hillis and Caramazza, 1991; Caramazza and Shelton, 1998), b) the semantic system is organized by different types of knowledge, where the

identification of natural objects relies more heavily on perceptual properties while the identification of man-made objects relies more heavily on functional properties (Warrington and Shallice, 1984; Warrington and McCarthy, 1987; Farah and McClelland, 1991), and c) different categories of objects do not segregate into different semantic representations, but place different demands on a shared processing system; in this scenario, natural objects place a higher demand on the system than artifacts because of the high degree of similarity between category exemplars and overlapping perceptual features (Humphreys et al., 1995; Gonnerman et al 1997; Devlin et al 1998). These theories prompted several researchers to make natural (animals, fruit) versus man-made (vehicles, tools) distinctions in their stimuli, but despite the behavioral dissociations seen in patients, regional distinctions for these categories are tenuous and sometimes contradictory across studies. Martin et al. (1996) had subjects either a) silently name line drawings of animals or tools, b) view drawings of structurally plausible non-objects, or c) view random noise patterns. Subtracting noise from non-objects showed bilateral activation in the fusiform gyri and inferior gyri of the occipital lobes, consistent with ventral stream encoding of structural properties. Subtraction of plausible non-objects from object naming in both animal and tool categories activated the temporal lobes bilaterally, somewhat anterior to the fusiform activation in the non-object condition above. Regional distinctions of natural versus man-made objects were therefore not apparent in this study. Perani et al (1995) used animals and artifacts as stimuli, and had subjects judge whether two pictures had the same name, versus a control task that

required viewing two matched random shapes. Animals activated the inferior temporal lobes (fusiform gyri) bilaterally while artifacts activated several left hemisphere regions including the lingual, parahippocampal, and middle occipital gyri (extrastriate cortex (BA 19)), as well as the dorsolateral prefrontal cortex (BA 46). Gerlach et al. (1999) also showed a more widely distributed activation when natural items were processed compared to artifacts in a PET object-decision study. Unlike the Martin et al. (1996) study, some regional distinctions between categories were found in these latter two studies, but why such large-scale regional differences would correspond to relatively subtle differences in object stimuli deserves explanation. One view is that animals and artifacts represent two categories of visual complexity, and that artifacts, though they tend to be relatively more visually complex, activate a less diffuse area than animals, which tend to be relatively less visually complex. This difference may be attributed to the greater differentiation between category exemplars and overlapping perceptual features needed for naming natural objects, making them relatively more demanding than artifacts. Addressing this confound, Moore and Price (1999a) used colored and black-and-white line drawings of animate objects and artifacts, each of which were either visually complex (animals and multi-component artifacts) or visually simple (fruits, vegetables, and simply-shaped artifacts). They found that activation in the left medial occipital lobe (BA 19) reflected both object category and visual complexity. Complex artifacts and animals generated increased activation relative to visually simple artifacts/fruits/vegetables, while animals/fruits/vegetables produced increased activation relative to their matched artifacts,

suggesting that occipital processing is more engaged by complex objects relative to simple ones, and by complex animate or natural objects relative to complex artifacts. Drawings of artifacts (tools) activated the left posterior middle temporal gyrus, while natural objects activated bilateral anterior temporal and right posterior middle temporal gyri. Price et al. (1996b) (see review below), shows that although comparatively posterior areas of cortex, such as the medial occipital lobe (BA 19) and inferior posterior temporal lobe (junction of BA 20 & 37) are activated in object naming in general, posterior areas are especially activated for natural objects relative to artifacts. These results seem best interpreted in the context of explanation "c" above, where it was argued that greater differentiation between category exemplars and overlapping perceptual features is needed for naming natural objects, and identifying natural objects is therefore more relatively demanding (Gonnerman et al 1997; Devlin et al 1998), whereas man-made objects tend to have more distinct visual and semantic attributes, resulting in fewer "competing neighbors", thus allowing for easier identification (also see behavioral evidence in Humphreys et al. (1988) and McRae et al. (1997)). Lastly, this study also found that activation levels in object recognition areas were lower for colored drawings relative to black-and-white line drawings for natural objects, consistent with behavioral studies that show colored drawings of natural objects are named faster than line drawings (Price and Humphreys, 1989). These results are consistent with the argument that neural areas involved with colored object stimuli are more efficient during object recognition because color facilitates the process of differentiating between perceptually overlapping neighbors

in a given category. Additional studies addressing color processing and object naming are reviewed below.

As with the Moore and Price (1999b) study, Damasio et al. (1996) had subjects name animals and tools, versus a control task where subjects had to say "up" or "down" to upright or inverted faces. Relative to this control, both the middle and inferior temporal gyri were activated for tools, but medial and inferior regions of the posterior temporal lobe (anterior to the area found by Martin et al. (1996)) were activated for animals. In contrast, Moore and Price (1999a) found that the left posterior middle temporal gyrus was active for man-made objects, especially tools, while bilateral anterior temporal areas were more active for natural objects such as animals or fruit. During direct cortical stimulation, Ilmberger et al. (2002) found the stimulation of the left superior temporal and inferior/superior frontal gyri increased naming errors for tool items relative to animal items, but the sampled area was restricted to anterior areas only. Overall, the categories of natural and man-made objects do not appear to consistently activate posterior or anterior regions even when visual complexity is controlled for. It does appear, however, that natural categories activate more diffuse or bilateral temporal areas than artifacts, which activate more restricted areas in the left hemisphere.

Damasio et al. (1996) argued that anterior regions of left temporal cortex, such as the temporal pole (BA 38), anterior portions of inferotemporal cortex (BAs 21, 20), and sometimes also relatively more posterior areas (BA 37) are especially crucial for object naming across categories based on their PET data in normals as well as lesion data.

Lesion data indicates that damage to BAs 38, 21, 20, and 37 causes a severe deficit when naming nouns that are either natural or man-made (Damasio and Damasio 1990). There is controversy, however, regarding the importance of the temporal pole (BA 38) in object naming. Murtha et al. (1999) argue that only one other lesion study (Flude et al. 1989) supports the interpretation regarding the temporal pole, and that no other PET study of picture naming has found activation in this left temporal pole region (BA 38). Anterior lobectomy data do not shed additional light on this issue, as some studies report no deficits in picture naming or object recognition (e.g. Biederman et al., 1997) while others claim that word-finding deficits occur and persist after left anterotemporal lobectomy (e.g. Langfitt and Rausch, 1996). In normals, it is possible that the unusual baseline of judging upright and inverted faces in the Damasio et al. (1996) study accounts for the temporal pole activation. Without additional studies using this control task, however, this idea remains speculative. Murtha et al. (1999) also had subjects name animals or carry out a semantic judgment task on pictures of animals and compared these conditions to passively viewing plus signs, abstract patterns, and an anticipation condition where subjects were scanned while waiting for stimuli to appear. Like several of the above studies, picture naming minus baseline activated the inferior/middle occipital (BAs 18, 19) and inferior temporal occipital (BAs 37, 19) gyri bilaterally, as well as the left anterior superior temporal gyrus (BAs 21, 38), and left middle temporal gyrus (BA 22). Semantic judgment minus baseline activated the same bilateral (BAs 18, 19, 37) and left hemisphere regions (BAs 21, 22) as the picture naming task, plus the left inferior frontal

gyrus (BA 44). Subtracting abstract patterns from these conditions did not negate these inferior occipital or fusiform gyri activations, though some additional structures became activated. Anticipating the stimuli did not negate inferior occipital/fusiform activation either, though bilateral hippocampal activation and left inferior and middle frontal gyri activations were seen in addition to these areas, probably reflecting holding instructions in working memory and processing those instructions.

Some studies also address color processing in addition to object identification. Martin et al. (1995) performed a PET study where subjects generated words denoting colors and actions associated either with line drawings or the written names of objects (e.g., shown a drawing or the written word "pencil", the subject would say "yellow" and "write") and compared these tasks to a control task of object naming. In comparison to object naming, generation of color and action words activated the left prefrontal cortex, especially the dorsolateral region (BA 46), reflecting general word retrieval, and left posterior parietal cortex, which the authors attribute to attentional functions. Temporal lobe activation depended on what type of word was generated. Generation of color words activated the fusiform gyrus bilaterally while generation of action words activated the left posterior middle and superior temporal gyri (BA 21, 22). Changing the stimulus from line drawings to their written names did not change the patterns of activation for each type of word. This pattern is consistent with the ventral area processing object attributes such as form and color and the dorsal area processing motion, and extends it to the generation of these attributes from memory. Price et al. (1996b) addressed color and

object naming by using a factorial design where subjects either a) named real objects, b) said "yes" to the occurrence of objects, c) named the color of non-objects, or d) said "yes" to the occurrence of non-objects. In this study, naming tasks for objects and colors (a, c) required the retrieval of phonological labels associated with visual stimuli, while "say yes" tasks required visual analysis and articulation of a response, but not the explicit retrieval of phonological labels. Areas for processing object shapes included the middle occipital cortex, the left middle/inferior temporal lobe, the right anterior temporal lobe, and the left cerebellum, similar to other studies (Kanwisher et al., 1997). Name retrieval in general activated the left inferior occipital gyrus, left lingual, middle fusiform gyri, left middle frontal lobe, plus additional structures, but name retrieval specifically for objects activated the medial anterior temporal lobes bilaterally, the left superior temporal sulcus, the left posterior temporal lobe, left anterior insula, and the right cerebellum, while name retrieval specifically for colors activated the left posterior lingual and fusiform gyri. Particularly in the left posterior inferior temporal lobe, object naming had larger increases in activation than color naming, emphasizing the role of this structure in object identification.

The table below summarizes visual object processing studies reviewed above, indicating experimental and control tasks as well as the main regions that were activated:

Table 2. Summary of visual object processing studies. Abbreviations: inferior = inf, occipital = occ, objects = obj, scrambled = scr, medial = med,

Study	**Experimental task**	**Control task**	**Activated areas (BA)**	**Laterality/ Additional info**
Puce (1995, 1996)	Faces, letter strings	Textures	Fusiform (37) Inf occ temporal (17/18)	Bilateral (faces) Left
Schacter et al. (1995)	Evaluate structures of objects	View abstract structures	Inferotemporal Fusiform (37)	
Grill-Spector et al. (1998)	Object naming	Name progressively scrambled pictures	V1-3 (17) V4v, V3a, Lateral Occipital (LO) (18, 19)	All stimuli Obj & less scrambled images
Malach et al. (1995)	Object viewing (faces, animate, inanimate)	View degraded faces, abstract patterns, and textures	Lateral Occipital (LO) (18, 19)	All obj categories and textures
Op de Beeck et al. (2000)	Object categorization	Shape orientation matching	Occipitotemporal Parietal Fusiform	
Kanwisher et al. (1997)	Viewing objects (familiar/novel)	Scrambled objects, lines	med Fusiform	Left (obj & scr)
Haxby et al. (1991)	Face, dot-location matching	Sensorimotor tasks	Lat Occipital (18, 19) Occipitotemporal (ant/inf to LO) (edge of 19, toward 37)	Both tasks Face task only
Sergent et al (1992b)	Categorization: gratings, faces, objects	Crosshair fixation	Fusiform (37) Middle temporal (21)	Left Left

Table 2. Continued.

Sergent et al. (1992a)	Categorization: objects Spatial discrim: letters Phono decision: letters	Factorial design (tasks compared to each other)	Ventral occipital (19) Sup/Mid Occipital (18) Fusiform (36/37) Middle temporal (21)	Bilateral (all 3 tasks) Left (objects) Bilateral (objects), Left (objects-phono) Left (objects-spatial)
Kosslyn et al. (1994)	Name matching: canonical, non-canonical	Random line patterns	Occipital (17, 18, 19) Fusiform (37) Angular gyrus (39)	Left (17), Right (18), Bilateral (19) Left Bilateral (non-canonical)
Kosslyn et al. (1995)	Category level matching (aural/picture/word) of birds: entry, subordinate (sub), superordinate (sup)	Nonsense (non) line patterns	Occipital (17, 19) Inf/mid temp/fusiform Inf/sup parietal Middle frontal (46)	Left (subord-fix/17) Left (sup/sub-entry/non/19) Left (sub-non/fix) Left (sub-entry/non) Bilateral
Gauthier et al. (1997)	Categorization: Subordinate	Basic-level	Fusiform Inferotemporal	
Menard et al. (1996)	Passive viewing: pictures and words	Passive rest	Occip regions (17, 18, 19) Inf/mid temp (20, 21) Angular gyrus (39) SMG (40) Broca's area (44/45)	Rt (17), Bi (18/19) (p-w) L/Bi (p-w) Left (w-p) Left (w-p) Left (w-p)

Table 2. Continued.

Bookheimer et al. (1995)	Reading words (w) Naming objects (o)	Visual noise	Occip regions (17, 18, 19) Inf temp/Fusiform Inf frontal gyrus (47)	L(17), Bi (18/19) (w & o) Bi (w:ant/lat; o:pos/med) Left
Moore and Price (1999b)	Naming and viewing words and objects (verbal response "ok" with viewing)	False fonts and meaningless shapes	med ant Fusiform (20) lateral Fusiform posterior Fusiform sup Temporal SMG	Left (nam/vw w&o) Left (naming w&o) Bilateral (obj nam/vw) Left (w>o) Left (w>o)
Martin et al. (1996)	Object naming (animals and tools)	Viewing non-objects or noise patterns	Occipital (17) Fusiform (37) Temporal (ant.to fusiform)	Bilateral (n.o.-n) Bilateral (n.o.-n) Bilateral (o-n.o)
Perani et al. (1995)	Objects naming/matching (animals and artifacts)	Viewing matched random shapes	mid Occipital (18) Fusiform (37) Frontal	Left (artifacts) Bilateral (animals) Left (artifacts)
Damasio et al. (1996)	Object naming (animals and tools)	Respond to upright/invertd faces	mid/inf Temporal (21, 20) med/inf post Temporal Temporal Pole (38)	Left? (tools) Left? (animals) Left

Table 2. Continued.

Moore and Price (1999a)	Object naming, word-picture matching: natural [animals/fruit] and man-made [vehicles/tools], color and b&w	Factorial design	pos mid Temporal ant Temporal pos mid Temporal	Left (man-made, esp. tools) Bilateral (natural) Left (b&w of natural) Right (natural)
Murtha et al. (1999)	Object naming (o) or semantic judgment task (s) (animals)	Viewing plus signs (p.s.), abstract patterns (a)	mid/inf Occip (18, 19) inf Temporal (Fusiform)(37) ant/sup Temporal (22, 38) mid Temporal (21) inf Frontal (44)	Bilateral (o/s/a-p.s.) Bilateral (o/s/a-p.s.) Left (o/s-p.s.) Left (o/s-p.s.) Left (s-p.s.)
Martin et al. (1995)	Word generation of colors and actions for object pictures (line drawings) and object names (written word)	Object naming	Fusiform (37) Middle temporal (21) Angular gyrus (39) Supramarginal (40) Dorsolateral prefrontal cortex (44, 45, 46, 47) (same areas for pictures & names)	Bilateral (clr) L (action) L (action) L (action) L (clr & act) Left (clr & action)
Price et al. (1996b)	Object naming and non-object color naming	Respond to occurrence of objects and non-objects (factorial design)	mid Occipital (18) inf Occipital (19) mid Fusiform (37) mid Frontal med ant Temporal sup Temp sulcus (39) pos inf Temporal (37) lat ant inf Temp (20) ant Insula	Left (ob r) Left (nam) Left (nam) Left (nam) Bi (obnam) L (obnam) L (obnam) L (obnam) L (obnam)
Moore and Price (1999b)	Object naming (colored/b&w, animate/artifacts, complex/simple)	Factorial design	med Occipital (18) inf pos Temporal	L (cx/ar/an)

Functional roles of anatomical areas

From these studies, it is possible to tentatively assign roles to the occipital, temporal, and frontal regions involved in visual object processing, and in some cases, to assign roles to smaller Brodmann Areas within these regions as well. Occipital areas are most active during lower-level visual processing and object detection, although some authors argue that these areas play a role in semantic processing as well. The occipital pole (BA 17) (also described as V1 or primary visual cortex) is active during almost all visual tasks, even after lower-level visual control tasks have been subtracted out. For example, it can be active during tasks that involve semantic processing, such as when visual noise is subtracted from reading words or naming objects (Bookheimer et al., 1995), when passively viewing pictures is compared to passively viewing words (Menard et al., 1996), or when matching the names of objects from different viewpoints (Kosslyn et al., 1994). These tasks, however, additionally invoke the lateral occipital gyrus (BAs 18 and 19), making a higher-level linguistic processing role specific to the occipital pole (BA 17) unlikely. Therefore, the role of BA 17 is more likely associated with low-level visual processing, since it is active during a variety of visual processing tasks, such as subtracting textures from faces and letter-strings (Puce et al., 1995, 1996), subordinate-level object matching (Kosslyn et al., 1995), subtracting mildly and severely scrambled objects from whole objects (Grill-Spector et al., 1998), and subtracting noise from non-objects (Martin et al., 1996). These results suggest that low-level visual processing occurs

in this area and that its inclusion in higher-level semantic-type processing is due to the sustained occurrence of low-level visual processing demands. Some studies find the superior or middle occipital gyrus (BA 18) or the inferior occipital gyrus (BA 19) active independently from one another, but many studies find that these areas are active simultaneously, referring to them collectively as the lateral occipital (LO) gyrus. Studies that find only BA 18 active generally emphasize mid-level form or object detection, but actually comprise several different experimental and control tasks. These tasks include categorizing objects compared to making spatial discriminations or phonological decisions for letters (Sergent et al., 1992a), subtracting random shape matching from object matching (Perani et al., 1995), object recognition (Price et al., 1996b), and naming (Moore and Price, 1999b). Studies that find only BA 19 active emphasize general naming (Price et al., 1996b) and category matching at various levels of abstraction (Kosslyn et al., 1995). In contrast, activity in the lateral occipital (LO) gyrus (BAs 18 and 19) is found in studies using both novel and familiar stimuli (Malach et al., 1995; Kanwisher et al., 1997), when textures are subtracted from different object categories (Malach et al., 1995), and when mildly scrambled objects are subtracted from whole objects (Grill-Spector et al., 1998). These results suggest that the LO is involved in perceptual processing of visual forms and object detection. Haxby et al. (1991) illustrates an apparent discrepancy in finding that the LO is also active during both face and dot-location matching tasks. Although one would expect that spatial tasks such as dot-location matching would generally occur more dorsally, their dot-location task seemed

more akin to matching patterns on a die, which could arguably be accomplished by feature detection with a strategy similar to the face-matching task, making the activation of the LO a reasonable result.

In temporal regions, it appears that object naming (including faces) consistently produces activations in BAs 20, 21, 22, 37, and 38, which involve processes related to the structural and semantic aspects of object recognition during object naming and/or to the phonological retrieval of object names (Price et al., 1996b). Previous and subsequent studies have shown some of these temporal regions also to be involved during the identification of visual words (Nobre and McCarthy, 1995; Shaywitz et al., 1995), semantic processing of auditory words (Demonet et al., 1992), and sentence comprehension (Mazoyer et al., 1993; Bavelier et al., 1997). Activation specific to naming objects, however, is usually found bilaterally in the medial anterior temporal lobes, the left superior temporal sulcus (just inferior to the angular gyrus), the left anterior insula, the left lateral anterior inferior temporal lobe (BA 20), and the left posterior inferior temporal cortex (BA 37).

Many studies that compare words to objects activate both ventral and dorsal pathways, particularly the left superior temporal gyrus (BA 22) and the left supramarginal gyrus (BA 40) (Bookheimer et al., 1995; Menard et al., 1996; Vandenberghe et al., 1996). As mentioned earlier, the left supramarginal gyrus appears to be crucial for orthographic-to-phonologic conversion (see Price, 1998), as evidenced by its activation when subjects read unfamiliar pseudowords relative to familiar real words (Price et al., 1996a; Rumsey

et al., 1997) and when reading Kana versus Kanji (Law et al., 1991); both pseudowords and Kana rely heavily on links between orthography and phonology that do not depend on the subject's lexicon. Consistent with this interpretation are the results of Moore and Price (1999b), where activation of the left superior temporal and supramarginal gyrus was found for words but not objects, even when subjects made an unrelated overt verbal response to viewing words, suggesting that words are implicitly subject to an orthographic-to-phonological processing strategy to a greater extent than are objects.

Corbetta et al. (1990) argued that the middle temporal gyrus (BA 21) was responsible for perceptual processes specific to visual shape analysis; Martin et al. (1995) similarly suggested that the middle temporal gyrus was a critical site for stored knowledge about the visual patterns of motion associated with the use of objects. Lesions of left middle temporal gyrus (BA 21), however, do not appear to result in visual agnosia (the disruption of visually presented object recognition), prosopagnosia (the disruption of face recognition), or a deficit in describing an object's function, but rather the naming of these objects (Flude et al., 1989; Damasio et al., 1990). Citing this evidence, Sergent et al. (1992a, 1992b) assigns the middle temporal gyrus (BA 21) with the role of accessing the name of an object, letter, or face during the recognition process rather than visual processes inherent in the recognition of an object or face. Cortical stimulation data in 117 patients shows this area to evoke naming errors in approximately 55% of patients who were stimulated in that region (Ojemann et al., 1989), adding only tenuous support to this view.

The fusiform gyrus is comprised of both BA 20 and BA 37. This area is activated in almost all the experimental paradigms reviewed above, with two main competing interpretations for this structure emerging: a) visual perceptual processing and b) semantic processing. Studies that argue in favor of a visual perceptual role for the fusiform gyrus show that activation occurs when visual noise or random lines are subtracted from scrambled or degraded objects (Kanwisher et al., 1997; Martin et al., 1996) or when color names need to be retrieved (Martin et al., 1995; Price et al., 1996b). The study of Op de Beeck et al. (2000), however, showed that activation in the middle fusiform was reduced as shape degradation became more severe, indicating that only relatively intact final integrations or representations of stimuli are being processed by this area. The activity in the fusiform did not vary reliably with the abstraction level of the task in the Op de Beeck et al. study, which is also consistent with assigning a greater visual perceptual role to this area relative to a semantic role. Several studies, however, point to the fusiform, particularly the anterior portion of the left fusiform (BA 20), as being involved in a larger semantic network for a variety of stimuli. Moore and Price (1999b), for example, showed that regardless of the task, visually presented words or objects (versus meaningless visual controls) activated the medial anterior fusiform, invoking implicit semantic processing. They point out that this area is also more active for several other semantic conditions, including: a) semantic relative to perceptual decisions on visually presented words and objects (Vandenberghe et al., 1996), b) semantic relative to phonological decisions on aurally presented words (Demonet et al.,

1992, 1994), c) naming words and objects (implicit semantic processing) relative to naming letters and colors (Moore et al., 1996), d) retrieving semantic knowledge (Martin et al., 1995), and e) generating visual mental images of heard object words (implicit semantic processing) relative to passive listening of abstract words (D'Esposito et al., 1997). In short, it appears that both visual perceptual and semantic processes are carried out by the fusiform gyrus, and that the anterior portion is particularly involved during semantic tasks.

The part of the fusiform gyrus referred to as the left lateral posterior inferior temporal cortex (posterior part of BA 20/medial portion of BA 37), also known as the basal temporal language area, also appears to carry a semantic processing load from imaging studies of naming, although lesion evidence raises the possibility that it may instead be involved in assigning a verbal label to a stimulus subsequent to semantic processing. Sometimes together with the frontal operculum, the basal temporal language area is activated when subjects perform name retrieval tasks during auditory (sentences, prose) (Warburton et al., 1996), tactile (Braille) (Buchel et al., 1998), and visual (words, letters, objects, and colors) (Price and Friston, 1997) stimuli. Since this area does not appear to be modality-specific, it is considered to be involved at relatively early stages of naming, such as the intermediate step between the recognition of an object and its semantic association (Bookheimer et al., 1995). Neuropsychological evidence, however, shows that lesions in this area produce anomia, and that the subject retains intact object recognition (Bookheimer et al., 1995; Moore and Price 1999b), suggesting that assigning

a name to an object is impaired although some level of semantic knowledge remains; cortical stimulation data in epilepsy patients also shows interruption in name retrieval abilities when this area is stimulated (Luders et al., 1986, 1991; Burnstine et al., 1990), but it is unclear at what point deficits emerge when this area is resected, since all but the most radical resections seem to produce no lasting naming deficits (Luders et al., 1991; Gordon et al., 1991). Although this area does not appear to be modality-specific, both imaging studies and direct cortical recordings show that for visual stimuli, anterior and lateral portions of BA 37 appear to be relatively more word-specific (Bookheimer et al., 1995; Moore and Price 1999b; Price et al., 1996a) than posterior and medial portions of BA 37, which is variably argued as being either nonspecific (Nobre and McCarthy, 1994; Buchel et al., 1998) or relatively more object-specific (Bookheimer et al., 1995; Moore and Price, 1999b) in both viewing and naming. Intracranial ERP studies by Puce and colleagues (see Puce et al., 1999 for a review), however, describe a posterior-to-anterior trend in the location of functional "patches" in the order letter-strings (words and non-words), form, hands, objects, faces, and face parts. Despite this inconsistency, it appears that activation for words, which can be read either via semantics or via sublexical links between orthography and phonology, can be found in a network of regions including the fusiform as well as left superior temporal (BA 22) and supramarginal (BA 40) gyri, whereas activation for objects, which relies more heavily on a semantic route to name retrieval, emphasizes fusiform areas in conjunction with frontal regions (Moore and Price, 1999b). The Puce et al. (1999) results notwithstanding, the fusiform gyrus can tentatively

be divided into three general functional regions: a) an anterior region (anterior portion of BA 20) that is associated with semantic knowledge, b) a medial region spanning the posterior portion of BA 20 and the anterior portion of BA 37 that is associated with multimodal name retrieval and relatively greater word-specific processing, and c) a posterior region (posterior portion of BA 37) that is associated with relatively greater object-specific processing.

Frontal areas of activation are also found during a variety of object recognition and naming tasks. According to Murtha et al. (1999), the activations of the left middle and left inferior frontal gyri (BAs 44, 45, 46, 47) merit four possible explanations: a) anticipation, preparation, and response planning – the authors point out, however, that no activation was found during the anticipation minus baseline condition of their study, so this explanation was immediately ruled out, b) phonology – implicit activation of articulatory mechanisms argues for frontal involvement during the passive viewing of words and pictures (Menard et al., 1996), as well as reading words, naming colors, or naming objects (Bookheimer et al., 1995; Martin et al., 1995; Perani et al, 1995; Price et al., 1996b), c) top-down processing during semantic categorization tasks, as seen in the Kosslyn et al. (1994, 1995) tasks, consistent with the argument that dorsal lateral prefrontal cortex plays a role in knowledge-guided searches, d) semantic retrieval – Demonet et al. (1992) and Petersen et al. (1988) both argue that localization of semantic knowledge and processing is in these frontal areas, Vandenberghe et al. (1996) show an increase in the left inferior frontal area during both visual and associative semantics

during picture naming alone, Murtha et al. (1999) show an increase in inferior frontal gyrus during a semantic judgment on a picture, and the object naming task of Menard et al. (1996) all suggest that an argument for implicit semantic retrieval can be made to explain these activations, although others have argued that these areas reflect semantic "working memory" rather than semantic storage (Demb et al., 1995; Gabrielli et al., 1996). Taken together, it appears that these frontal areas can be considered part of both an articulatory, phonological network along with superior temporal (BA 22) and supramarginal (BA 40) regions and a semantic network, involving left middle and inferior temporal gyri (BA 21 and 20), and left fusiform (BA 20/37) regions.

Language processing in cortical stimulation populations

Cortical Stimulation and Language Localization

Cortical stimulation was initially developed by Penfield (Penfield and Roberts, 1959) to map motor, memory, and language functions in patients with intractable epilepsy. Since then, cortical stimulation is also used in other types of patients, such as those with brain tumors, AVMs, or other types of pathology where resection provides the best clinical outcome for the patient, but is complicated by the pathology's proximity to putative language areas. Cortical stimulation can be performed either intraoperatively or extraoperatively. Intraoperative cortical stimulation is primarily used for mapping function in the same session as the surgical resection. Extraoperative cortical stimulation

utilizes subdural grids that are positioned in a separate surgical procedure to define the degree and extent of the epileptogenic zone as well as to locate critical functional areas for sensation, motor, and language outside the operating room environment, such as at the patient's bedside. Depending on circumstances such as the patient's age or disease process, intraoperative and extraoperative techniques each offer their own set of advantages. One advantage of intraoperative stimulation is that the stimulating electrode can be applied to a location on the surface of the cortex with more control than that offered by a subdural grid array; such an array has electrodes in a fixed relationship to one another, implying that some electrodes may be over unwanted structures such as blood vessels. Another advantage of intraoperative stimulation is that the electrodes are smaller in diameter, thereby allowing a smaller area of brain tissue to receive maximal current density. There are also specific advantages, however, to using a subdural grid array over intracortical stimulation to localize function. Pediatric patients, for example, do not tolerate awake intraoperative mapping well, and a grid allows such patients to be tested at bedside in short intervals and over several days if necessary. Another advantage of localizing language with subdural grids is that the time constraints of the operating room are eased, allowing for more thorough and complex language testing to take place.

In both cases, cortical stimulation induces a temporary and reversible lesion by applying an electrical current to a small area of the surface of the cortex. In the case of intraoperative stimulation, this current comes from a pair of 1mm bipolar electrodes with a 5mm tip separation (Haglund et al., 1994). With extraoperative stimulation, subdural

grid arrays are comprised of electrodes with a 3mm diameter and a center-to-center interelectrode distance of 1cm (~7mm separates the borders of adjacent electrodes) (Schaffler et al., 1996). Parameters for intraoperative stimulation are set at 60Hz, with biphasic square wave pulses with variable peak-to-peak current amplitudes between 2-15mA. The current necessary to produce after-discharges (AD's) from the temporal cortex is found, often in the range of 2-8mA, and the current for mapping language is then adjusted to 0.5-1mA below the AD threshold. Grid arrays can range from 4 x 6 to 8 x 8, and these grids usually cover the frontotemporoparietal region of the language-dominant hemisphere. Electrodes are individually stimulated starting at an intensity of 1mA, and consist of 5-20 second trains of 25Hz biphasic square-wave pulses. Stimulus intensity is also increased in 0.5-1mA steps until AD's are elicited or sensations or motor effects occur. Language disruption is usually performed at 0.5mA below the AD threshold up to a maximum of 15mA, and can vary within a patient across stimulation sites. In both intraoperative and extraoperative settings, it is believed that the general effect of applying an electrical current to the surface of the cortex is that both excitatory and inhibitory synaptic systems will be activated in some neurons and en passage fibers, while other functions will become blocked by depolarization (Ojemann, 1993). Stimulation of primary motor and sensory areas, for example, usually elicits positive responses such as tongue movement or tingling. In contrast, higher cognitive functions such as language will be disrupted during the active performance of a specific task, either because of depolarization or activation of inhibitory systems.

Because anatomic landmarks such as the perisylvian cortex or the inferior frontal gyrus do not have a reliable relationship to language localization, it is necessary to map language for each individual patient. Often, the hemisphere of language dominance is determined preoperatively by intracarotid sodium amytal (Wada) testing (Wada and Rasmussen, 1960), which anaesthetizes one hemisphere at a time while the patient performs language production and comprehension tasks. Disruptions during these tasks, such as speech arrest, naming errors, or the inability to read or comprehend aural commands determines the hemisphere of language dominance (Desmond et al., 1995). Wada testing has revealed that the left hemisphere is most likely to be essential for language in both left- and right-handers, though right or bilateral dominance is slightly more common in left-handers. An fMRI study by Springer et al. (1999) compared language dominance in neurologically normal and epilepsy subjects using a semantic task and found that 94% of normal subjects were left hemisphere dominant and 6% had bilateral language representation, while epileptic subjects showed greater variability of language dominance, with 78% left hemisphere dominant, 16% bilateral, and 6% right hemisphere dominant. They concluded that atypical language dominance in the epilepsy group was associated with early onset of brain injury and weaker right hand dominance.

As mentioned earlier, language paradigms used in intraoperative and extraoperative settings may differ for reasons such as relative time restrictions. Though reading tasks have been used in some studies (Ojemann and Mateer, 1979), the task used most often during intracortical mapping has been visual object naming (e.g. Ojemann and

Whitaker, 1978; Ojemann and Mateer, 1979; Berger et al., 1989; Ojemann, 1983, 1991, 1992, 1993; Ojemann et al., 1989; Haglund et al., 1994) since it is well established that such word-finding tasks can be sensitive to language deficits in several types of aphasia (Benson, 1985). Visual object naming is also used in grid patients (Malow et al., 1996; Luders et al., 1991; Lesser et al., 1994; Devinsky et al., 2000), but lighter time constraints have allowed object naming to be supplemented by tasks involving reading (Luders et al., 1991), sentence completion (Devinsky et al., 2000), picture selection (Malow et al., 1996), visual semantic tasks (Schaffler et al., 1996), auditory comprehension (Schaffler et al., 1996), and auditory naming (Malow et al., 1996). Despite these different settings and tasks, it appears that specific patterns of disruptions emerge according to the region stimulated. The most consistent disruption is that of orofacial motor pathways and speech arrest following stimulation of the posterior inferior frontal area, although studies also report phoneme disruption (Ojemann and Mateer, 1979), speech alterations (Lebrun and Leleux, 1993), variable degrees of anomia in both visual (Ojemann and Whitaker, 1978; Lebrun and Leleux, 1993) and auditory (Malow et al., 1996) domains when this region, usually referred to as Broca's area, is stimulated. The temporal lobe region encompassing putative Wernicke's area shows both language production and comprehension disturbances (Schaffler et al., 1996), as well as variable naming disruptions (Ojemann and Whitaker, 1978; Berger et al., 1989), reading comprehension disruptions (Lesser et al., 1994), and short-term verbal memory disturbances (Ojemann and Mateer, 1979). However, it also appears to be modality-

sensitive, being especially prone to disturbances in auditory naming paradigms when compared to visual naming paradigms (Malow et al., 1996; Hamberger and Tamny, 1999). The basal temporal, or fusiform area also shows variable naming disturbances during stimulation (Schaffler et al., 1996; Luders et al., 1991; Lesser et al., 1994), and though it is a separate entity from Wernicke's area, white matter underlying this basal temporal region is in direct contact with the white matter underlying Wernicke's area (Luders et al., 1991). This contact may explain why naming errors in the basal temporal area and Wernicke's area during stimulation are similar, though the basal temporal area may be resected for several centimeters without any apparent post-operative consequences (Gordon et al., 1991) while resections within 2cm of a positive language site in Wernicke's area produce severe fluent aphasias (Ojemann, 1983; Haglund et al., 1994).

In general, sites with repeated errors in object naming are highly localized and discrete within a patient, but the exact location of these sites varies greatly across patients (Ojemann, 1993). Furthermore, this variation in functional localization is greater than the morphological variability in the perisylvian cortex (Steinmetz et al., 1990; Steinmetz and Seitz, 1991), which is substantial in the gyral patterns, the planum temporale, and the cytoarchitectonic areas within these structures (Ojemann, 1991). In a study of 117 patients, Ojemann (1989) found essential sites in traditional Broca's area only 70% of the time in approximately 80% of subjects, while essential sites in the superior temporal gyrus were identified in only 65% of subjects, and no region of traditional Wernicke's

area in the posterior portion of the cortex showed essential sites in over 36% of subjects. Two explanations emerged which could account for this large variability: 1) age of seizure onset, and 2) verbal IQ. An early age of seizure onset would seem to predict increased variability because of language regions being displaced from traditional sites to nontraditional sites in order to circumvent the diseased tissue. Although language does not seem to dramatically reorganize and fully relocate to the opposite hemisphere unless the disorder is acquired before the age of 5 years, destroying prenatally determined language cortex outright (Duchowny et al., 1996), some reorganization within the dominant hemisphere does appear to occur with early-onset seizure activity (Springer et al., 1999). Evidence is also accumulating for the correlation between more spatially distributed and atypical language sites and lower preoperative verbal IQ's. Ojemann (1991, 1993) found that higher verbal IQ's are associated with a mosaic of areas related only to object naming in the middle temporal gyrus and areas related to reading in the superior temporal gyrus, with the reverse pattern in subjects with lower verbal IQ's; higher verbal IQ subjects also had a smaller total surface area related to object naming. In another study, Devinsky et al. (2000) used grid patients to examine sentence completion and object naming disruptions from a) anterior or inferior temporal cortex (< 4.5 cm from the temporal pole), labeled "atypical" language sites, and b) posterosuperior temporal and inferior parietal perisylvian areas (> 4.5 cm from the temporal pole), labeled "typical" language sites, and compared disruption in these areas with cognitive function. They found that patients with atypical language sites had significantly fewer years of education,

poorer verbal learning, and poorer fluency than patients with typical language sites. Furthermore, patients with IQ's lower than 80 were significantly more likely to have multiple sites and a wider spatial distribution where stimulation disrupted language function than patients with normal IQ's.

Functional Neuroimaging vs. Cortical Stimulation Language Maps

Although intraoperative cortical stimulation is considered the gold standard for purposes of localizing essential language sites on the cortical surface, there are several disadvantages associated with cortical stimulation. These disadvantages include the risk of inducing a seizure while applying electrical currents that are intense enough to disrupt language performance, the requirement of an awake and cooperative patient, and high time demands that increase the cost of the surgical procedure. Recently, PET and fMRI have been used as non-invasive pre-surgical mapping techniques in patients with intractable epilepsy or brain tumors as an alternative to more invasive cortical stimulation techniques (Benson et al., 1999; Cuenod et al., 1995; Binder, 1997; Fitzgerald et al., 1997; Modayur et al., 1997; Bookheimer et al., 1997; Herholz et al., 1997; Klein et al., 1997; Stapleton et al., 1997; Rutten et al., 1999; Schlosser et al., 1999; Beisteiner et al., 2000; Hirsch et al., 2000). Although PET and fMRI signals reflect secondary hemodynamic effects that are relatively slower than neuronal or glial changes that occur with cognitive processing (LeBihan and Karni, 1995), studies that have focused on language activation have indicated that there is a moderate to strong correspondence

between PET and fMRI language localizations and cortical stimulation mapping. These studies are reviewed below.

Regardless of the imaging technique, there is a fundamental difference in the way these language maps are derived compared to cortical stimulation: imaging is an activation method, yielding maps of all brain regions involved in a task where cerebral blood flow (CBF) or the blood oxygenation level dependent (BOLD) signal increases during task performance, while cortical stimulation, whether performed intraoperatively or extraoperatively (i.e., with grids) is a disruption method, yielding maps that show interference with a cognitive process when a current is applied to the cortical surface.

One of the earliest language studies that compared PET activations to extraoperative stimulation mapping (ESM) was done by Bookheimer et al. (1997) on seven epilepsy patients. PET tasks were visual object naming of color photos and auditory responsive naming of 3-word descriptions of concrete nouns, performed both overtly and covertly. The control task had patients resting with their eyes closed. Cortical stimulation tasks were overt visual object naming and auditory responsive naming tasks. Speech arrest, hesitation, and paraphasias were considered to be naming errors, and only those electrodes that showed errors for both auditory and visual tasks were taken into account. Similarly, only those PET activations that were common across all 4 tasks were considered. Using these criteria, all patients had at least one positive stimulation site in the posterior superior temporal gyrus (STG, also labeled Wernicke's area), but several regions in the lateral temporal lobe produced inconsistent results for auditory versus

visual object naming. All patients who had grids covering the inferior temporal/fusiform area (i.e., the basal temporal language area) showed significant language disruption in this area during stimulation. PET data showed between one and three activation foci in the inferior frontal gyrus (IFG) and the posterior superior temporal sulcus (STS), while five out of six patients showed activation in STG, three out of four patients showed activation in the basal temporal area, and three out of six patients showed activation in the temporal-parietal-occipital junction. One patient performed only auditory tasks, and showed temporal activation plus a small focus in the IFG, and one patient performed only visual tasks, showing comparatively less activation in the temporal lobe but additional activations in the occipital and posterior temporal-occipital regions, consistent with the imaging literature on visual object naming reviewed earlier. Comparing the two methods, all four patients who had language disturbances in the frontal lobe with cortical stimulation also showed increased CBF in the same region. Negative electrode points, that is, those electrodes that did not produce a language disturbance, showed either no CBF change or showed a decrease in the same region. Similarly, all patients showed increased CBF where electrodes produced a disturbance in the lateral temporal area, and four out of five subjects showed a CBF increase under positive electrodes in the basal temporal region. Overall, regions that were activated by both visual and auditory tasks were close (within 1cm) to electrode points that disrupted language during stimulation.

Herholz et al. (1997) used PET imaging to compare CBF activations to intraoperative cortical stimulation, but in glioma patients rather than epilepsy patients. Tasks in both the PET and intraoperative cortical mapping sessions were naming of line drawings and verb generation from a written noun. Control tasks in the PET scanner were a presentation of Japanese (Kana) letter strings for the picture naming task, and a uniform verbal response of a nonsense word for the verb generation task. Both language paradigms significantly activated the left IFG, including a deep portion of the opercular region, as well as the temporo-occipital cortex and inferior temporal gyri, especially the fusiform gyrus. Verb generation produced more lateralized and intense activity than picture naming in frontal and inferior temporal areas. Higher CBF increases were observed at positive stimulation sites most often during the verb generation task for five out of eight patients, but since tasks were not combined for sensitivity and specificity calculations, the authors reported a relatively high false-positive rate for this task, despite the fact that the sites sometimes produced errors in the picture-naming task. False-negative sites, that is, nonsignificant CBF changes where stimulation errors were found, were attributed either to overall poor activation or poor activation in the vicinity of the tumor. This study raised the issue of image signal in the presence of tumor pathology, but did not address it directly.

In a case study, Klein et al. (1997) used PET to observe activity in the left inferior frontal gyrus (IFG) in a tumor patient. Language tasks used during the PET session were overt auditory word repetition and overt synonym generation from aurally presented

words. Subtracting word repetition from synonym generation elicited strong left anterior IFG (BAs 45 & 47) activation, as well as bilateral activations in the orbito-frontal region (BA 11) and middle frontal gyrus (MFG) (BA 10). During cortical stimulation the patient counted and named visual objects, and was also required to repeat and generate a synonym to an aurally presented word within a single trial. When stimulation was applied to PET activation areas, the patient could repeat words and count but not produce synonyms or name objects, implying that word retrieval was being disrupted rather than speech abilities.

In short, the PET studies reviewed above have two points in common: 1) it appears that a combination of visual and auditory language paradigms are necessary to best delineate essential, or high-risk language sites, in both imaging and cortical stimulation settings, 2) activated areas that are common across several language tasks tend to correspond better to cortical stimulation language sites than areas active for specific tasks only. The studies above describe comparisons between PET and cortical stimulation qualitatively only, leaving several questions unanswered, including which parameters affect the spatial extent of activations and how cortical surfaces are co-registered across techniques.

Although PET is able to show regions of metabolic activation in response to language activity, there are several disadvantages of using PET as a pre-surgical language localization tool. Not only is PET costly, not readily available, and the injection of radioactive material required, but as a technique it is also limited by relatively low spatial

and temporal resolution. Functional MRI, on the other hand, is potentially a more valuable and useful tool for pre-surgical language localization because of its noninvasiveness, availability, and relatively better temporal and spatial resolution. It can also be used more easily with pediatric populations. It will be seen below that the points made with respect to PET paradigms and methodological approaches still apply to fMRI as a pre-surgical language mapping tool, but these points will be illustrated more quantitatively in some cases, while other studies raise additional issues concerning brain pathology and patient variability.

In an early study comparing fMRI and cortical stimulation, Mueller et al. (1996) examined the reliability of the fMRI signal in patients with raised intracranial pressure, cerebral edema, or neurological impairment. Four adult tumor patients underwent fMRI scanning, and two patients underwent both fMRI and cortical stimulation sessions. The language paradigms used in the fMRI setting consisted of the subject counting and generating as many words as possible from a given letter, both overtly and covertly. The control condition was not stated, but activation from this paradigm was found in the inferior frontal lobe, the sensorimotor cortex, and supplementary motor area (SMA) – activation in this last area was probably due to overt naming. During cortical stimulation, speech arrest was observed in the regions where fMRI showed activation in response to word generation or counting in both patients. In one patient, fMRI activation associated with word generation was within 0.5cm of the inferior border of the tumor, which was in a similar location to where counting was interrupted and speech was blocked. The

authors claimed that variances in medications and intracranial pressures did not prevent fMRI activations from being obtained, but it remains unclear with such a small number of subjects whether the fMRI signal is affected by certain types of brain pathology. Additionally, it is widely accepted that overt naming in fMRI produces severe motion artifact (Barch et al., 1999), but this issue was not raised by the authors. A similar study was done by Ruge et al. (1999) where five patients with lesions in the left superior temporal gyrus (STG) underwent both fMRI and cortical stimulation sessions. FMRI language paradigms included covert picture naming and listening to words in order to activate putative Broca's and Wernicke's areas respectively. By combining activated areas across the two tasks, Broca's area was activated for all patients, and Wernicke's area was activated in 3 out of the 5 patients. Cortical stimulation paradigms included counting forward and backward as well as picture naming. Stimulation of Broca's area resulted in speech arrest of all patients, while word-finding difficulties, such as literal and semantic paraphasic errors, were found with stimulation in Wernicke's area in the same 3 out of 5 patients that showed fMRI activation in this area. The remaining two patients did not demonstrate any language dysfunction during cortical stimulation in this area and their fMRI maps showed activation in the contralateral STG.

In an attempt to offer a task battery that encompassed a variety of functions, Hirsch et al. (2000) performed a study that examined motor, visual, tactile, and language matches between fMRI and cortical stimulation. With respect to the language portion of the study, paradigms included covert visual object naming of line drawings to activate

Broca's area/IFG, and listening to recordings of spoken words (object names) to activate Wernicke's area/STG. The control task for both conditions was fixation on a crosshair. Two runs of each task were performed, voxels were considered active only if common across both runs, and thresholds were set at three different levels ($p \leq 0.0001$, $p \leq 0.00025$, $p \leq 0.0005$) to evaluate the best matches with the cortical stimulation data. Paradigms were run both in healthy volunteers and in patients with various pathologies. In healthy volunteers, picture naming activated the STG in 73% and the IFG in 90% of subjects, while listening to spoken words activated the STG in all subjects and the IFG in 93% of subjects. These percentages reflect sensitivity. As expected, sensitivity was less robust in patients. Picture naming activated the STG in 65% and the IFG in 72% of patients, while listening to spoken words activated the STG in 88% and the IFG in 54% of patients. By combining the two tasks, sensitivity increases in these two language areas, but failures are still reported, especially in frontal areas. The authors variously attribute these failures to motion artifact, lack of compliance, neurological deficits, and pathology-related cognitive deficits, but no clear pattern emerges to explain these failures, and the reasons stated above remain speculative only.

To investigate the relationship between the magnitude and spatial extent of fMRI activations and cortical stimulation maps, Schlosser et al. (1999) performed a comparison study between fMRI and cortical stimulation, and found that stimulation delivered in proximity to regions with the most significant, i.e. the highest *t*-values, of fMRI activations produced significant and reproducible language deficits in twelve out of

fourteen patients. The relationship between the spatial extent of fMRI activations and cortical stimulation results was tenuous, however, finding that the extent of the regions that produced more subtle stimulation-induced language disruptions did not always correspond to the lower *t*-value fMRI activations that surrounded the centroid of activation. Several possibilities were given to explain this discrepancy. The first reason was that different language paradigms were used in the fMRI and cortical stimulation sessions. The fMRI session used one auditory task (English versus Turkish sentence comprehension), while the cortical stimulation session used several tasks, including visual object naming, sentence completion, reading, and following verbal commands. This explanation appears more likely to account for the two failures in matching fMRI activations with cortical stimulation sites, rather than accounting for spatial extent discrepancies. A more likely explanation for the spatial extent differences may concern statistical thresholds used to identify the centroid and surrounding activation, but it is also important to consider that stimulation disturbances can also be subtle, inconsistent, and subjective (Schaffler et al., 1996; Ojemann, 1989), perhaps rendering discrepancies of this sort unsurprising. The authors also considered current spread from the stimulation electrodes as a source of disagreement, noting the common finding that the stimulation level necessary to achieve language disruption was not uniform across sites within patients. However, the cortical stimulation results of Ojemann (1989), as well as the spatial-extent results of the intrinsic signal in the study of Haglund et al. (1992) both show that discrete areas of language disruption correspond with bipolar stimulation currents,

making it unlikely that the variability of current level necessary to produce language disturbances is due to unpredictability in current spread. The authors also had the concern that surface stimulation does not generate sufficient current density deep within the sulci, potentially becoming a source for apparent false-negative findings, i.e., where cortical stimulation does not produce deficits at the cortical surface above from where an area of fMRI activation is present. This is a legitimate concern, as a case study by Rutten et al. (1999) showed that an fMRI voxel activated across several language tasks and located 5-8mm below the cortical surface did not produce any errors when its projection to the cortical surface was stimulated, but when the area became accessible following tumor resection, the site repeatedly produced speech arrest during stimulation. This result is in contrast to the view that stimulation of the cortical surface can predict the effects of resections that include not only surface cortex, but buried cortex and white matter as well. Although essential areas of language are found on the crowns of the gyri rather than within the sulci during cortical stimulation (Ojemann, 1993), the implication of the Rutten et al. (1999) result challenges the view that essential language sites can be exclusively predicted from stimulations on the cortical surface.

Another study comparing fMRI activations with cortical stimulation mapping of language function was performed by Fitzgerald et al. (1997). They examined 11 patients, though there was a variable number of patients for each fMRI language paradigm, making generalizations difficult. FMRI language paradigms included visual word reading (3 patients) versus visual fixation on a cross hair, visual verb generation (10 patients), where

patients covertly generated a verb associated with a given noun, listening to single words (2 patients) or listening to text (4 patients) versus listening to scanner noise, and auditory verb generation (6 patients), akin to the visual verb generation task. It was unclear what combination of tasks was given to each patient. Although visual object naming is used extensively in cortical stimulation mapping, the authors did not use it in the fMRI battery, claiming that it produces poorly lateralized activity and a large amount of irrelevant visual cortex activity. Counting and other types of overlearned speech were also excluded from the fMRI battery because the authors claimed such abilities are frequently preserved in aphasic patients and therefore are not good indicators of high-risk functional cortex. Despite these concerns, cortical stimulation tasks consisted of visual object naming of line drawings, recitation of overlearned speech such as naming the days of the week or months of the year, counting from 1-20, reversals of overlearned speech, and reading words aloud. Errors included perseveration, hesitation, phonemic errors, semantic errors, or speech arrest for any of the four tasks on repetitive testing. Unlike previously described studies that used a fixed statistical threshold for fMRI analysis, the Fitzgerald et al. (1997) study adjusted the threshold on a task-by-task basis for each individual patient so that a 1cm (or larger) area of activation projected to the cortical surface. This spatial extent was chosen for its consistency with the observation of Steinmetz and Seitz (1991) that foci of language areas in cortical stimulation data is approximately 1-2cm^2 ; this spatial extent is also consistent with the observation that resections closer than 1-2cm to an essential language site results in a greater number of

deficits than resecting farther away (Ojemann, 1983; Haglund et al., 1994). A match between fMRI activations and cortical stimulation sites was deemed to have occurred if the activated area on the fMRI map contacted, overlapped, or surrounded a language tag. Matches between language areas and the centroid of cortical stimulation tags were also assessed as a function of distance, that is, the number of matches was recalculated as the borders of the fMRI activation areas were extended by 1 and 2 cm. Two standard measures were considered: 1) the sensitivity of fMRI, that is, the percentage of language stimulation tags that matched language fMRI activation areas (the true-positive rate), and 2) the specificity of fMRI, that is, the percentage of non-language tags (i.e. sensory or motor tags) not activated by the fMRI language paradigms (the true-negative rate). All tasks were combined for each patient and the overall sensitivity and specificity of fMRI was calculated.

As with other cortical stimulation studies (e.g. Ojemann, 1989), one of the most striking results in the Fitzgerald et al. (1997) study is the large amount of variability in the number of sites, specific location, and current level for a given language task. Between one and seven language sites were identified for this sample of patients, with current levels ranging from 1.5-11.5mA to cause a language disturbance; a between-site difference of up to 5mA was observed for any given patient. For the ten patients who performed visual verb generation, all showed fMRI activation in the inferior and middle frontal gyri, though the size and shape of activation differed across subjects, and all showed fMRI activation in temporal or parietal lobes, though these areas were smaller

and more variable in their exact location than frontal areas. For the four patients who listened to text, all had fMRI activation at or near the superior temporal gyrus (STG) as well as in the frontal lobe; frontal areas were smaller and more variable than in temporal areas. For the six patients who performed auditory verb generation, five showed fMRI activation at or near the superior temporal plane or STG. In short, the visual task appeared to produce more stable frontal activations plus more variable temporal activations, while the auditory tasks produced more stable temporal activations plus more variable frontal activations. The small number of patients who performed the tasks of reading and listening to words made any generalizations unreliable. Combined across patients, sensitivity increased when the match criterion was relaxed from contact to a 2cm radius: for the visual verb generation task sensitivity increased from 58% to 84%, for the auditory verb generation task it increased from 92% to 100%, and for the listening to text task it increased from 75% to 100%. Similarly, specificity decreased when the match criterion was relaxed from contact to a 2cm radius: for the visual verb generation task specificity decreased from 59% to 0%, for the auditory verb generation task it decreased from 40% to 0%, and for the listening to text task it decreased from 88% to 50%. The decreases in specificity may be misleading however, since the criterion that nonlanguage tags (i.e. sensory or motor) not be contacted by fMRI language activation areas is at odds with the well-established observation that sensory and motor centers are often in proximity to speech centers (Ojemann, 1992). Perhaps it can be anticipated, therefore, that extending the spatial extent of an fMRI area from contact with a language tag to a

2cm radius includes some of these sensory or motor tags near the speech areas, thereby decreasing specificity. Large increases in sensitivity between contact and a 1cm radius versus the relative lack of change in sensitivity between a 1 to 2cm radius is consistent with the findings of Ojemann (1993) and Haglund et al. (1994) that significantly fewer language deficits occur if resection margins from language sites are greater than 1-2cm.

Overall, the results from the fMRI and cortical stimulation language comparison studies have several points in common: 1) although generally consistent with frontal and temporal neuroanatomical areas identified during language processing in normals, a large amount of variability exists across subjects with respect to specific locations for a) motor-related disruptions such as speech arrest during cortical stimulation, as well as for b) distinct language tasks in specific sensory modalities, such as visual and auditory verb generation, in both fMRI and cortical stimulation environments (Ojemann, 1989; Davies et al., 1994; Schaffler et al., 1996; Malow et al., 1996; Bookheimer et al., 1997), 2) as seen in the PET studies reviewed earlier, it appears that more than one task is necessary to identify the maximum number of high-risk language areas in the fMRI session, and including both auditory and visual tasks appears to increase the likelihood of identifying these areas, 3) it appears that voxels which are active across language tasks provide the strongest correspondence to positive cortical stimulation sites, and 4) although the effect of brain pathology on the reliability of the fMRI signal is unclear, it is clear that changes in comparison methods or statistical criteria have large impacts on the sensitivity and specificity of fMRI activations when compared to sites of language disturbance.

Chapter 2 Pilot ERP Study

This study compares CSM to fMRI, PEPSI, and ERP techniques in two patients whose resection is planned in the dominant hemisphere as part of their clinical treatment for temporal lobe epilepsy. The purpose of this study is to identify anatomical areas activated by visual object naming across techniques within the same subjects in order to create a presurgical spatiotemporal profile that includes hemodynamic, metabolic, and electrophysiological information. This information will be compared to intraoperative cortical stimulation. The information from each technique will then be displayed on a 3D reconstruction of the individual's brain using Skandha4, a graphics program developed at the University of Washington, allowing direct comparisons of these techniques to be made.

This chapter describes a pilot ERP study that validates the use of a blocked-trial paradigm design over a randomized-trial design. ERP studies of visual object recognition or naming that use designs where subjects respond to target stimuli show strong habituation effects both on the P300 (Romero and Polich, 1996; Ravden and Polich, 1998, 1999) and N400 (Zhang et al., 1995; Penney et al., 2001), demonstrating that several repetitions of target stimuli produce a decrease in the amplitude of these waveforms over time. In order to avoid these habituation effects, a randomized design of target stimuli is often preferred over a blocked design when responses to a small number of target stimuli are required in the presence of a large number of non-target stimuli. However, it was unclear whether this habituation effect on the N400 applied to the

naming of visual object stimuli when compared to an equal number of scrambled objects. Therefore, a pilot study was performed to determine: a) whether a blocked design provided less robust N400 waveforms than a randomized design, and b) whether a blocked or randomized design introduced undesirable or interfering ERP component effects with visual object stimuli.

Pilot ERP study: Randomized vs. blocked design for visual object stimuli

Subjects

Six undergraduate students (3 females, 3 males) gave informed consent in accordance with the University of Washington's Internal Review Board and participated for small compensation ($20). Subjects ranged in age from 18-30 years. All subjects were native English speakers, right-handed, and reported no difficulty in seeing the stimuli.

Stimuli and Procedures

Over 175 intact color objects and their scrambled counterparts were developed in the Corina Neuropsychology laboratory (Corina, 2000) as described below in Chapter 3. Two conditions were compared: 1) Blocked design (n=3), where a block of 10 intact objects alternated with 10 scrambled objects for a total of 34 blocks, 2) Randomized design (n=3), where 10 items randomly (without replacement) appeared for a total of 34 blocks. In both conditions, a pause was randomly inserted after 4-6 trials to allow the

subject to rest. Varying rest periods between 4-6 trials allows the subject to rest momentarily without allowing them to predict when the rest period will occur. Preventing such a prediction eliminates the possibility of an "expectation" waveform from appearing that may contaminate the waveform of interest (i.e. N400).

Each session in both the block and randomized conditions consisted of subject instructions as follows: "Name the object silently when it appears. If you can't recognize the object, say the word 'scrambled' silently." A prompt appeared asking subjects to press a button when ready. When the subject pressed the button, a fixation cross appeared for 500ms, alternating with an object or scrambled object presented in the middle of the screen for 500ms. At rest periods and at the end of 10 trials, the prompt reappeared as before. Subjects were tested in one session that lasted approximately 1.5 hours, during which they were seated in a comfortable chair located in an isolated room.

Data acquisition and analysis.

Continuous EEG was recorded from 64 scalp sites using tin electrodes attached to an elastic cap (Electrocap International Inc., Eaton, OH). Impedance was maintained at less than 5 KΩs for each electrode. Electrode placement included and extended the International 10-20 system (Jasper, 1958) over occipital, temporal, parietal, and frontal lateral and midline sites. Vertical eye movements and blinks were monitored by two electrodes, one placed beneath the left eye and one placed to the right of the right eye. The 64 channels were referenced to an electrode placed over the left mastoid bone and

were amplified with a bandpass of 0.01 to 100Hz (3dB cutoff) by an S.A. Instrumentation Co. amplifier system. Activity over the right mastoid was actively recorded on an additional channel to determine if there were any effects of the experimental variables on the mastoid recordings. No such effects were observed.

Continuous analog-to-digital conversion of the EEG was performed by a Data Translation 2801-A board/Dell Pentium II computer and stimulus trigger codes were performed with a Dell Pentium III computer at a sampling frequency of 200Hz. Epochs were comprised of 100ms preceding and 800ms following presentation of individual objects or scrambled objects. Trials characterized by excessive eye movement, muscle activity, or amplifier blocking were removed prior to averaging. The rate of rejection was approximately equally distributed across the two conditions and remained under 5% of trials.

ERPs were quantified as the mean voltage with a latency range following presentation of objects/scrambled objects, relative to an averaged baseline of activity comprised of the 100ms prior to presentation of the object/scrambled object. Analyses of variance were performed on mean amplitudes between 300 and 500ms. This window was chosen because it roughly corresponds to the latency ranges of the P300 and N400 components often reported in cognitive ERP studies. Data acquired at 6 midline sites (Fz, FCz, Cz, CPz, Pz, and POz (from anterior to posterior)) were analyzed. Figure 10 below illustrates the approximate area of these sites:

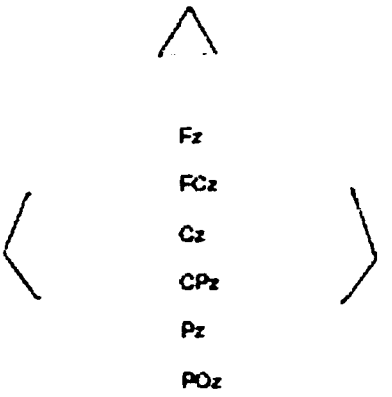

Figure 10. Layout of the location of the 6 midline scalp electrodes used for statistical analyses in the ERP recordings.

The ERP measures were averaged across subjects and subjected to ANOVAs with factors Block Type (2 levels, blocked and randomized), Condition (2 levels, normal and pixelated), Anterior-Posterior (2 levels, anterior and posterior), and Electrode Site (3 levels of electrode site within each of the 2 levels of Anterior-Posterior). Three analyses were performed: 1) an omnibus analysis including both Block Types, 2) simple effects analysis for the blocked Block Type, and 3) simple effects analysis for the random Block Type.

Results

Omnibus. A main effect of Condition was seen, indicating that waveform differences in the 300-500ms time range existed for normal compared to pixelated objects across blocked and randomized Block Types ($F(1,4) = 5.22$, $p = 0.08$). A two-way

interaction occurred between Condition and Anterior-Posterior ($F(1,4) = 5.01, p = 0.08$), indicating that differences between the normal and pixelated objects tend to change between anterior and posterior midline regions of the scalp. However, a three-way interaction between Block Type, Condition, and Anterior-Posterior ($F(1, 4) = 5.76, p = 0.07$), indicates that one can see more pronounced differences in waveforms between anterior and posterior regions in the blocked design than in the randomized design. The three-way interaction between Condition, Anterior-Posterior, and Electrode Site ($F(2, 8) = 9.34, p = 0.008$), indicates that the differences between normal and pixelated objects across electrode site are differently distributed for the 3 anterior electrode sites and for the 3 posterior electrode sites. Figures 11 and 12 show that differences between conditions generally become larger as one moves in an anterior to posterior direction within both of the larger anterior and posterior regions of the scalp.

Blocked design. A main effect of Condition occurred ($F(1,2) = 3.25, p = 0.22$), mainly reflecting the amplitude difference in the N400 between the normal and pixelated objects. The N400 effects are not statistically reliable due to the low power of the study. As can be seen in Figure 11 below, however, these effects are clearly present, particularly at posterior sites.

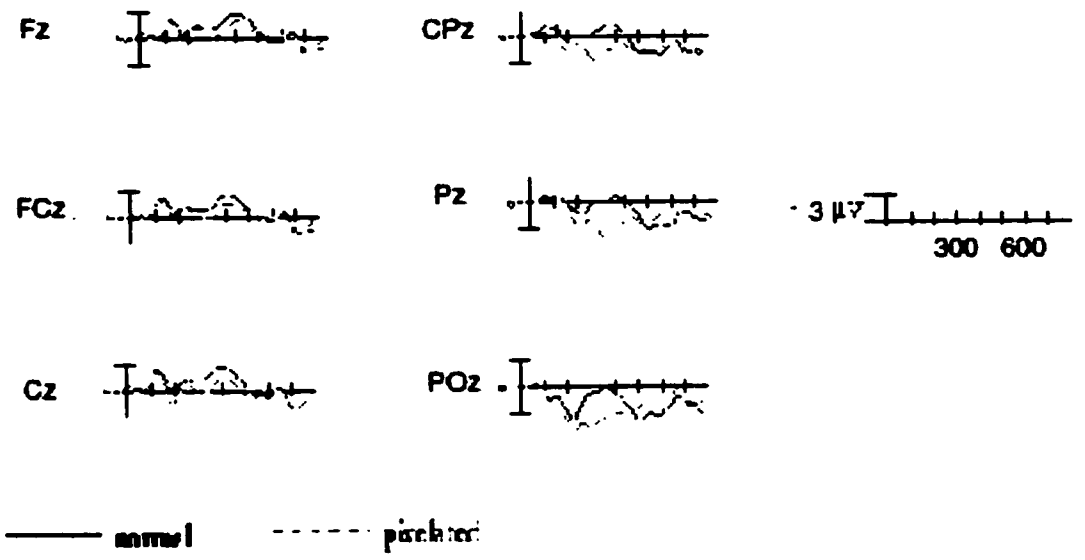

Figure 11. ERP waveforms averaged across subjects elicited by normal and pixelated objects in a blocked design. The waveforms are plotted for six electrodes in the anterior (Fz, FCz, Cz) and posterior (CPz, Pz, POz) midline regions. The N400 can be seen in response to normal objects particularly at posterior sites.

Randomized design. A main effect of Condition occurred ($F(1,2) = 7.93$, $p = 0.1$), reflecting amplitude differences between normal and pixelated objects. The interaction between Condition and Anterior-Posterior ($F(1,2) = 7.89$, $p = 0.1$), indicates that this difference alters when the anterior region is compared to the posterior region. Figure 12 shows that the difference in Condition is smaller in the posterior region than it is in the anterior region. The three-way interaction between Condition, Anterior-Posterior, and Electrode Site ($F(2,4) = 9.94$, $p = 0.02$), indicates that the differences

between normal and pixelated objects across electrode site are differently distributed for the 3 anterior electrode sites and for the 3 posterior electrode sites for the randomized design. Within the anterior region, the differences between normal and pixelated objects increase as one moves in an anterior to posterior direction, whereas in the posterior region, the differences between the normal and pixelated objects decrease. Despite a large difference in the waveforms between the normal and pixelated objects, it is clear from Figure 12 below that the N400 waveform becomes obscured due to the presence of a large P300 elicited by the pixelated objects.

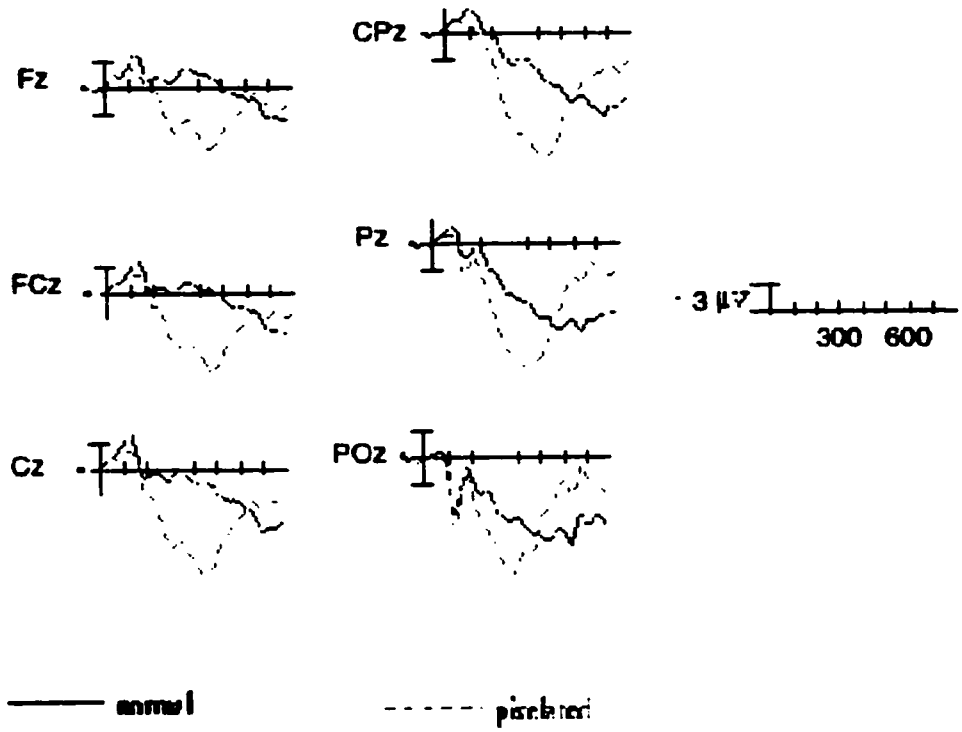

Figure 12. ERP waveforms averaged across subjects elicited by normal and pixelated objects in a randomized design. The waveforms are plotted for six electrodes in the anterior (Fz, FCz, Cz) and posterior (CPz, Pz, POz) midline regions. The N400 waveform to the normal objects is obscured by a large P300 waveform to the pixelated objects.

Discussion

These ERP results provide two lines of evidence for justifying the use of a blocked design for the proposed study. First, the blocked design shows N400 waveform differences between normal and pixelated objects. At posterior midline sites, the N400 can be seen clearly, and is elicited by normal objects. Although preliminary analyses were performed only on midline sites, a similar pattern can be seen for the N400 in lateral posterior sites as well (data not shown). These results show that the amplitude of the

N400 is not severely attenuated by habituation to the stimuli when trials are blocked. Second, the randomized design shows large waveform differences between the normal and pixelated objects, but this difference is dominated by a large P300 waveform elicited by pixelated objects that obscures the N400 response to normal objects. Again, although analyses were performed on midline sites only, this pattern is evident at lateral sites, in both anterior and posterior regions (data not shown). It appears that the dominance of the P300 waveform in the randomized design is due to the unexpected nature of the pixelated objects when they are randomly mixed with the normal objects. By blocking the stimuli, the surprise of the pixelated stimuli is reduced since it is no longer unexpected, and the amplitude of the P300 is therefore also reduced, allowing the N400 to be seen clearly.

Chapter 3 Methods

Please note that the terms "Scrambled" and "Pixelated" are used interchangeably to describe the Pixelated Objects condition throughout Chapters 3 and 4.

Subjects

Two female patients scheduled to undergo intraoperative (IO) and grid cortical stimulation mapping as part of their clinical treatment for intractable temporal-lobe epilepsy and one male control subject gave informed consent in accordance with the University of Washington's Internal Review Board and participated in fMRI, PEPSI, and ERP protocols for compensation. Language dominance of the two patients was determined preoperatively by intracarotid amobarbital perfusion (Wada) test. All participants were native English-speakers and reported no difficulty in seeing the stimuli. Profiles of each participant are given below in Table 3:

Table 3. Participant profiles.*Switched from right to left at age 3 after head trauma.

Subject	Age	Gender	Handedness	Lang. Dominance (by Wada)	Etiology	Mapping
P136	56	F	Right/Left*	Right	TLE	IO
P137	40	F	Right	Left	TLE	Grid
P138 (control)	38	M	Right	N/A	N/A	N/A

Stimuli

One hundred and sixty-eight (n=168) colored photographs of objects representing a variety of semantic categories were scanned with an AGFA Snapscan 1212 digital scanner onto a MacIntosh PowerMac G3 and pixelated in Adobe Photoshop (Version 5.0) using the filter/crystallize function so they retained their overall shape but could not be recognized (Corina Neuropsychology Laboratory; Corina, 2000). Examples of objects and their scrambled counterparts are given below in Figure 13; all stimuli are listed in Appendix A.

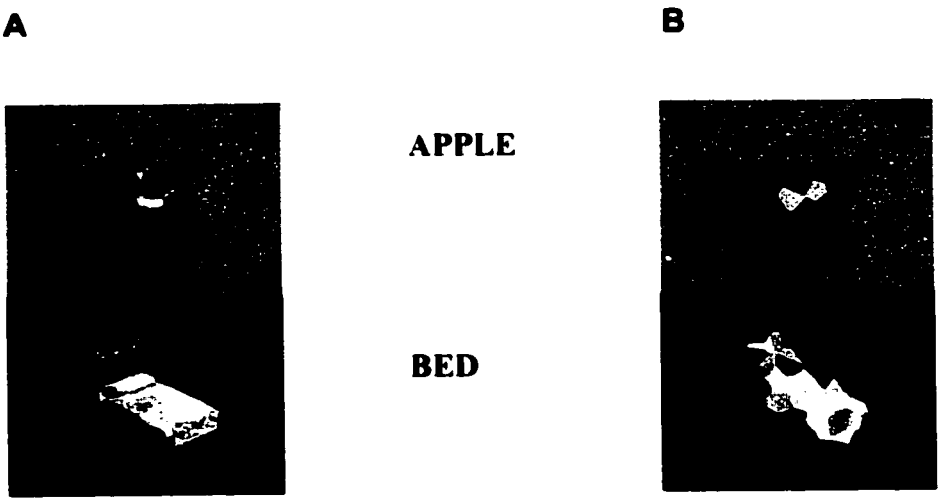

Figure 13. Examples of visual object stimuli (A) and pixelated counterparts (B). All object/pixelated object stimuli are listed in Appendix A.

All one hundred and sixty-eight (168) objects and their scrambled counterparts were utilized in the ERP protocol, while the fMRI and PEPSI protocols used different subsets of fifty (50) and sixty-eight (68) objects (and scrambled objects) respectively. Black-

and-white line drawings of common objects were used during the cortical stimulation mapping.

Data Collection

Cortical Stimulation Mapping

P136

For the awake intraoperative mapping session, the short-acting anesthesia diprovan (Propofol) was given. A field block using a combination of marcaine and lidocaine local anesthetic, and a craniotomy exposing the right frontal-temporoparietal area were performed. Following the craniotomy, the anesthesia was discontinued and the patient was allowed to waken. Stimulation currents below the threshold for evoking after-discharge potentials were determined and motor and sensory mapping performed. Mapping of speech cortex using object naming was then performed using slides of black-and-white line drawings of common objects presented once every 4 seconds. In the absence of stimulation there were a total of ninety-one (n=91) trials and eight (n=8) naming errors for this patient. During naming, cortical regions were sampled, stimulated, and tagged with sterile numbered tickets. Nineteen sites were sampled and the location of the sterile tags was photographed. Stimulation current was applied as the slide appeared and continued until the appearance of the next slide. Current between peaks of biphasic square-wave pulses with a total duration of 2.5ms (1.25ms for each pulse) ranged from 4mA for motor mapping to 10-12mA for language mapping for this

patient. Currents were delivered from a constant-current stimulator in 4-second trains at 60Hz across 1-mm bipolar electrodes separated by 5mm. One slide without stimulation separated each stimulation trial, and no site was stimulated twice in succession. Each site was stimulated at least three times with some sites stimulated as many as five times for sixty-nine (n=69) stimulated trials and nineteen (n=19) naming errors. In the absence of stimulation there were ninety-one (n=91) trials and eight (n=8) naming errors. The total number of stimulated and non-stimulated trials was one hundred and sixty (N=160). Feedback was immediately provided to the surgeon. The patient's responses and markers indicating when and where stimulation had occurred were recorded manually and on audiotape and used for off-line error analysis.

P137

This subject underwent placement of a grid (8 x 8 electrical stimulation grid, electrodes 5mm apart) over the left lateral temporal lobe. This subject was tested for object naming at bedside in two separate sessions on different days, with thirty-six electrode pairs sampled. The number of stimulation trials for each electrode pair ranged from one to twelve for two hundred and eight (n=208) stimulated trials and thirty-one (n=31) naming errors. In the absence of stimulation there were two hundred and nine (n=209) trials and one (n=1) naming error. The total number of stimulated and non-stimulated trials was four hundred and seventeen (N=417). The patient's responses and markers indicating when and where stimulation occurred were recorded manually and

used for off-line error analysis. The patient was taken back to the operating room to have the grid removed, and sites significant for language and memory retrieval were tagged and photographed on the exposed cortex.

Language Analysis

Subjects' responses were recorded for off-line error analysis. The errors included speech arrest, anomic responses, semantic/phonological paraphasias, and hesitations. The reliability of errors for each site was calculated relative to the unstimulated baseline error rate by Fisher's Exact Tests ($p < 0.05$). Although hesitations receive less emphasis as an error type in clinical settings, they are included here because they are markedly different from error-free trials when heard on audio-tape (e.g. P136). Patients are trained-to-ceiling in naming these items before their language-testing sessions, and error-free trials are distinguished by the ability of these patients to name the objects quickly and clearly. When hesitations do occur, it is readily apparent that they occur infrequently and not as a matter of course throughout the testing session.

FMRI and PEPSI Imaging and acquisition parameters

All fMRI and PEPSI images were acquired on a GE Signa 1.5 Tesla system using a radio-frequency (RF) custom head coil (Hayes and Mathis, 1996). Structural MRI images included coronal and sagittal T1-weighted localizers, 3-D Spoiled Grass (SPGR) sagittal series (124 slices, 1.4mm thick (0mm gap), flip angle = 45°, TR/TE 29/4.2ms, 256x192 matrix, FOV = 22cm, NEX = 1), and 2-D SPGR high-resolution axial slices (20

slices, 5mm thick (1mm gap), flip angle = 70°, TR/TE 200/2.1ms, 256x192 matrix, FOV = 24cm, NEX = 2). Subjects were fitted with custom-made fiber optic goggles and headphones to view the items and provide sound protection from gradient noise.

The PEPSI pulse sequence (Posse et al., 1997) (TR/TE 4000/272ms, 256x32x32 matrix, FOV = 22cm, NEX = 1) acquired a 20mm axial slice along the Sylvian fissure, with a voxel size of 6.8x6.8x20mm. The center of the 20mm axial slice used in the PEPSI protocol was based on an image within the 20 axial slices that was closest to the Sylvian fissure (image 9/20 for P136 and P137, image 10/20 for P138). An example of this slice location is shown below in Figure 14.

Figure 14. Approximate location of 20mm axial slice along the Sylvian fissure during the PEPSI session.

One slice was acquired during the 4min, 32sec PEPSI acquisition for each condition: 1) the object condition, and 2) the scrambled object condition. Within each TR of 4 seconds, 700ms of lag time was introduced so that the item was viewed during a silent gap between pulses; the duration of each item was 2500ms. Subjects were instructed to name objects covertly, to covertly say the word "scrambled" for scrambled objects, and to press a button at each trial using alternate thumbs. Button presses were used to monitor engagement with the task.

The fMRI pulse sequence is an EPI-BOLD, 2-D single-shot gradient-echo sequence (20 slices per volume, 128 volumes, 5mm thick axial slices (1mm gap), flip angle = 90°, TR/TE 2500/50ms, 64x64 matrix, FOV = 24cm, NEX = 1), and a voxel size of 3.75x3.75x5mm. One time point was acquired every 2.5 seconds for each volume of twenty slices. A 20 second delay (8 volumes) was inserted at the beginning of the run to allow for hemodynamic delay and to achieve a steady-state environment. No pictures were presented during this time. Using a box-car design, 10 objects ("on" condition) alternated with 10 scrambled objects ("off" condition) for five on/off cycles. Subjects were instructed to name objects covertly, to covertly say the word "scrambled" for scrambled objects, and to press a button with alternate thumbs for each trial. Button presses were used to monitor engagement with the task. Instructions ("Name the Picture" for objects, "Just Look" for scrambled objects) were shown for 5 seconds (i.e., 2TR) at the beginning of each block, resulting in ten cycles of 30 seconds each, 120 time points for each volume in 5min, 20sec of scan time. The two time points corresponding to the

instructions at the beginning of each block were later discarded during statistical analysis (see later text). The box-car design is illustrated below in Figure 15.

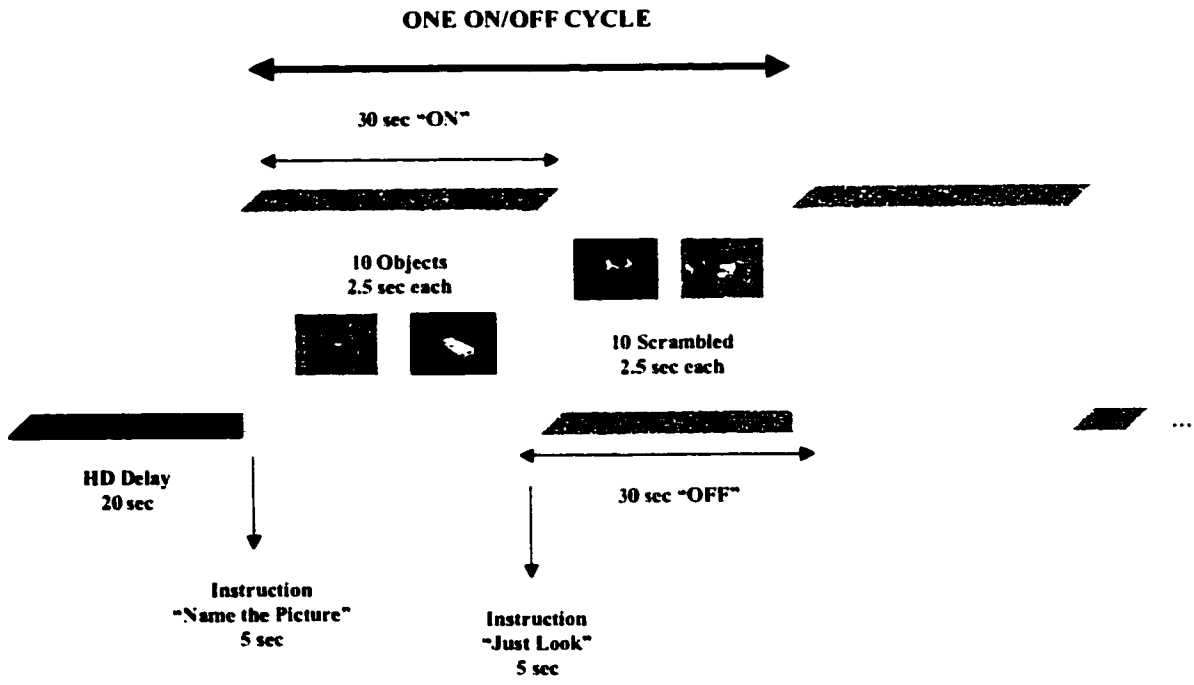

Figure 15. Boxcar design for fMRI protocol of objects vs. scrambled objects.

E-Prime software (version 1.0; Beta 5.0, 1.0.15.17) (Psychology Software Tools Inc., Pittsburgh, PA) was run on a Dell PC and used to present stimuli during fMRI scans, to time the stimulus presentations during PEPSI scans (stimuli were presented during gaps of silence in between PEPSI pulse sequences), and to record button-press responses. An audiovisual system developed at the University of Washington's Human Interface Technology (HIT) Laboratory was used in conjunction with an Infocus Projector (Model 435-Z). The headphone portion of the audiovisual system was used to attenuate the scanner noise to within OSHA safety limits. The goggles portion consisted of high-resolution fiber optics connecting the projector to the system, providing high-resolution images to the subjects.

ERP procedures and acquisition parameters

As per the findings of the ERP pilot study (see Chapter 2), a blocked design was used for ERP data collection. Each run consisted of a block of 10 objects ("on" condition) alternated with 10 scrambled objects ("off" condition) for a total of 17 on/off cycles (34 half-cycles). Items within blocks were randomly selected without replacement. Each subject performed two runs for a total of 340 object trials and 340 scrambled object trials; the order of items of the first run was different from the second run. A pause was randomly inserted every 3-4 trials to allow the subject to blink and/or rest. Varying rest periods between 3-4 trials allows the subject to rest momentarily without allowing them to predict when the rest period will occur. Preventing such a

prediction eliminates the possibility of an "expectation" waveform from appearing that may contaminate the waveform of interest (i.e. N400).

Subjects were tested in one session that lasted approximately 1.5-2 hours, during which they were seated in a comfortable chair located in an isolated room. Subjects were instructed to covertly name objects and to covertly say the word "scrambled" for scrambled objects. A prompt appeared for subjects to press a button when ready. During the same prompt, they were given instructions specific to the next set of items, i.e. either "Ready? Name the Picture" (Objects) or "Ready? Just Look" (Scrambled Objects). When the subject pressed the button, a fixation cross appeared in the middle of the screen for 250ms, and alternated with an object (during object blocks) or a scrambled object (during scrambled object blocks), also in the middle of the screen, for 1500ms. At rest periods and at the end of 10 trials, the prompt reappeared as before. Figure 16 below illustrates the blocked design used.

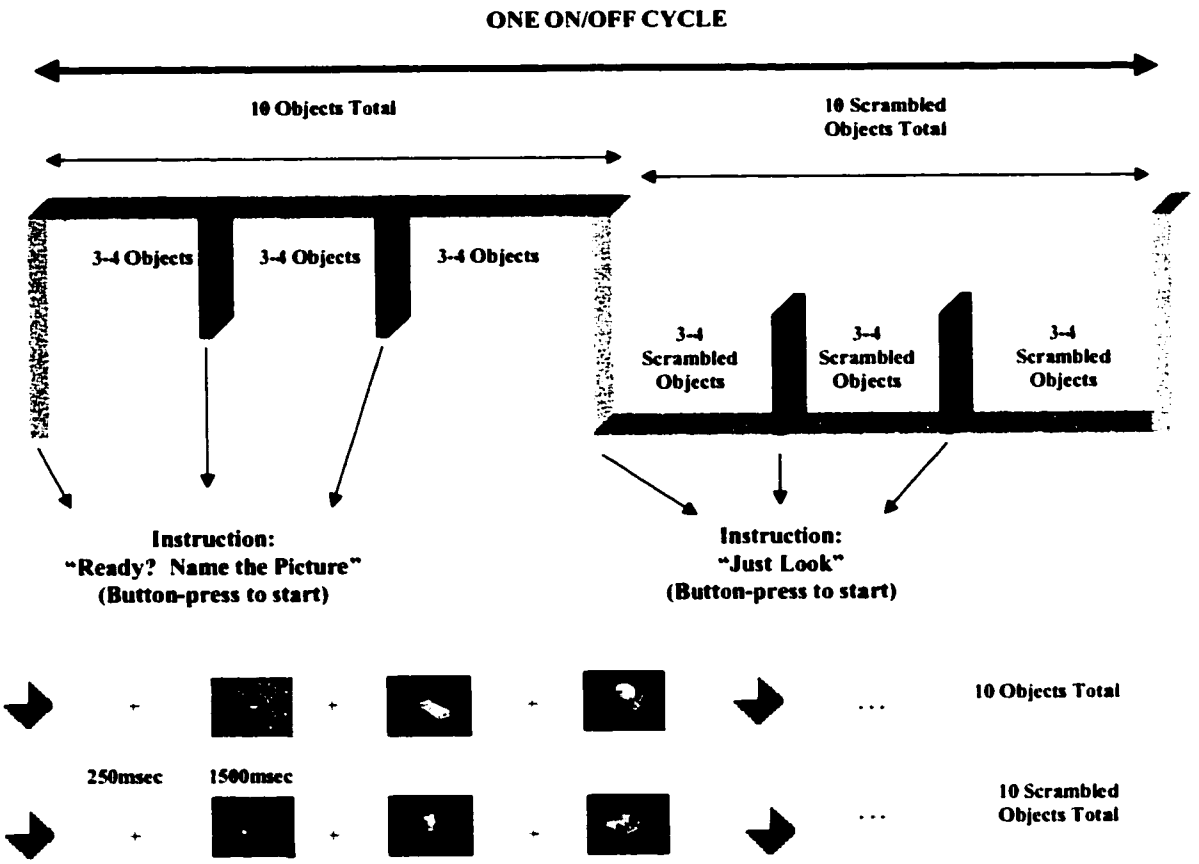

Figure 16. Blocked design for ERP protocol of objects vs. scrambled objects (one on/off cycle).

Continuous EEG was recorded from 64 scalp sites using tin electrodes attached to an elastic cap (Electrocap International Inc., Eaton, OH). Figure 17 below illustrates the location of these sites on the scalp.

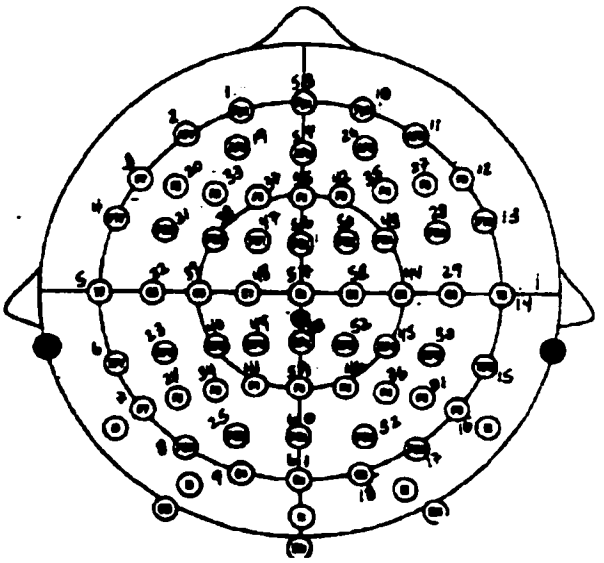

Figure 17. Scalp-electrode site locations for ERP data collection.

Impedance was maintained at less than 5 KΩs for each electrode. Electrode placement included and extended the International 10-20 system (Jasper, 1958) over occipital, temporal, parietal, and frontal lateral and midline sites. Vertical eye movements and blinks were monitored by two electrodes, one placed beneath the left eye and one placed to the right of the right eye. The 64 channels were referenced to an electrode placed over the left mastoid bone and were amplified with a bandpass of 0.01 to 100 Hz (3dB cutoff) by an S.A. Instrumentation Co. amplifier system. Activity over the right mastoid was actively recorded on an additional channel to determine if there were any effects of the experimental variables on the mastoid recordings. No such effects were observed.

Continuous analog-to-digital conversion of the EEG was performed by a Data Translation 2801-A board/Dell Pentium II computer and stimulus trigger codes were performed with a Dell Pentium III computer at a sampling frequency of 200Hz. Epochs were comprised of 100ms preceding and 800ms following presentation of individual objects or scrambled objects. Trials characterized by excessive eye movement, muscle activity, or amplifier blocking were removed prior to averaging. The rate of rejection was approximately equally distributed across the two conditions and remained under 5% of trials. ERPs were quantified as the mean voltage with a latency range following presentation of objects/scrambled objects, relative to an averaged baseline of activity comprised of the 100ms prior to presentation of the object/scrambled object.

Analysis methods

Cortical Stimulation Error Rates

Using the error criteria described above, each trial was coded according to site location, whether the trial was stimulated or not stimulated, the current level during stimulated trials, the object shown, and the patient's response. The reliability of errors for each site was calculated relative to the unstimulated baseline error rate by Fisher's Exact Tests ($p < 0.05$). The Fisher's Exact Test tests for independence between error and trial type when sample sizes are small (<20) (the number of stimulated trials at a given site is usually below 20). Non-significant p-values ($p > 0.05$) imply that the error rate is independent of

the trial type (stimulated vs. non-stimulated), whereas significant p-values ($p < 0.05$) imply that the error rate is not independent of the trial type.

PEPSI

The peaks in the proton spectra of the brain come from different chemicals, called metabolites. The amplitude (area under the curve) of the peak depends on several factors, including metabolite concentration, the pulse sequence used to acquire the spectrum, and acquisition parameters such as echo time and repetition time. The two metabolites of interest in the data collected here are N-Acetyl aspartate (NAA) and lactate. NAA is thought to be a neuronal marker, though it may reflect contributions from other compounds containing N-Acetyl residues. Lactate is widely thought to be an end product of anaerobic glycolysis, but recent evidence shows that it can also be produced aerobically and used as a neuronal energy substrate (Magistretti and Pellerin, 2000). Figure 18 below shows metabolite spectrums of interest:

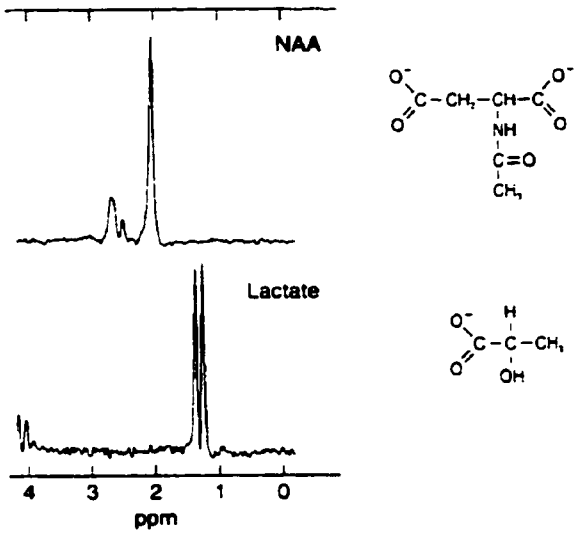

Figure 18. Spectra and chemical structure for N-Acetyl Aspartate (NAA) and Lactate. PPM = Parts per million. Adapted from Richards et al., 1996.

There are several steps involved in processing PEPSI data to produce the *Z*-score images of lactate seen in Chapter 4 (Results), including reading in the raw data, sorting the data into real and imaginary components, 3D Fourier Transforms, locating and fixing NAA peaks, and determining the *Z*-scores. These steps are described in more detail in the flow chart below (Figure 19):

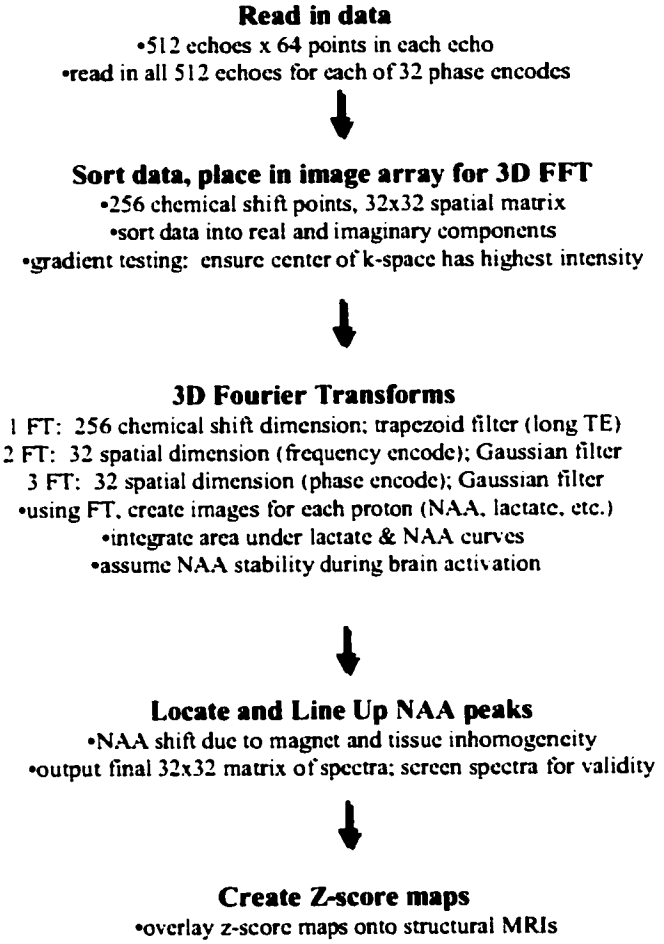

Figure 19. Flow chart of steps for PEPSI analysis.

An acquisition time of 4:32 for each condition (objects and scrambled objects) is used in the PEPSI session. Functional *Z*-score maps are calculated for PEPSI from lactate/N-Acetyl Aspartate (NAA) ratios based on Eq. [1]:

$$Z = \frac{\text{lactate/NAA (objects)} - \text{lactate/NAA (scrambled objects)}}{\text{standard deviation of lactate/NAA (scrambled objects)}} \quad [1]$$

Z-scores are calculated for all voxels with valid spectra using custom software. Spectra are screened for validity based on the following criteria: 1) line width of NAA, 2) lipid contamination from scalp, 3) deepness of the valley between the creatine and choline peaks, and 4) frequency distance between the creatine and choline peaks. Figure 20 below gives examples of both a valid PEPSI spectrum that meets the above criteria, and an invalid PEPSI spectrum that does not.

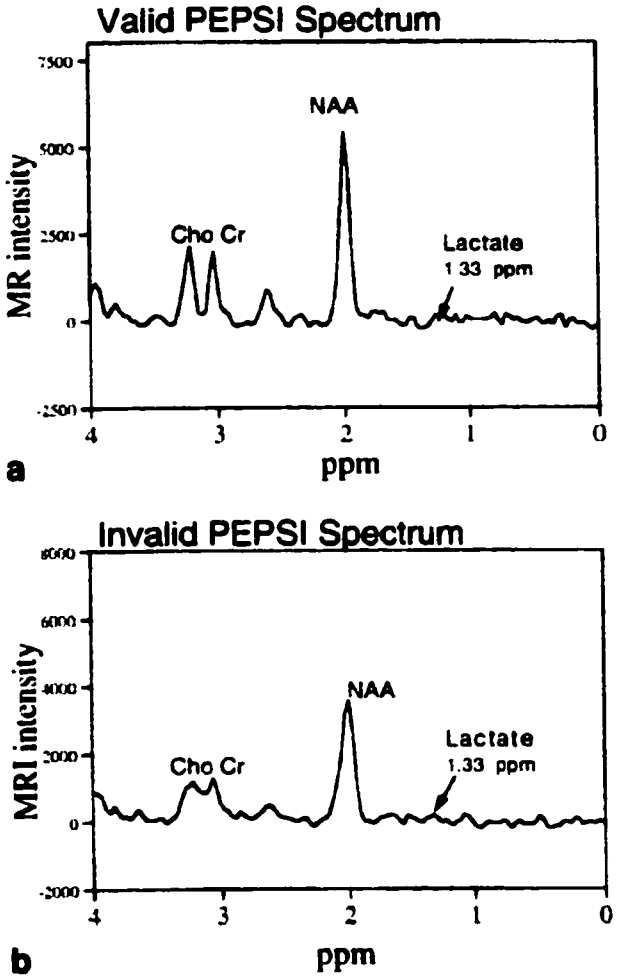

Figure 20. Proton MR spectra extracted from subject CP (from Serafini et al., 2001) showing a valid PEPSI spectrum (a) that meets spectrum validity criteria and an invalid spectrum (b) that does not. Proton metabolites are abbreviated as follows: Choline (Cho), Creatine (Cr), N-Acetyl-Aspartate (NAA).

It has been seen previously (Serafini et al., 2001) that screening for spectra validity at this slice location excludes most voxels from frontal areas. The difficulty of obtaining valid MR spectra (as defined above) from air-tissue interfaces in frontal brain regions at this

particular axial level is well known, and is due to the magnetic susceptibility of the sinuses causing a severe signal drop-out below the inferior frontal gyrus. Rather than attempt to improve homogeneity via shimming throughout areas of the slice that have large magnetic susceptibility effects, the area of shimming and analysis was restricted to the posterior 2/3 of the brain, providing more external field homogeneity and less variability in the signal.

The data are expressed in relation to the center of the fixed magnet once the analysis is complete in order to be displayed on the 3-D reconstruction and compared to the cortical stimulation data.

fMRI

Similar to the PEPSI data, fMRI images need to be expressed in relation to the center of the fixed magnet for proper display and comparison to the cortical stimulation data on the 3-D reconstruction (described in later text). A custom script GE2SPM 3.2 (Inati, 2002) that uses header information to transform images into magnet space is applied to both structural and EPI-BOLD (functional) data before further analysis using SPM99 (Wellcome Department of Cognitive Neurology, University College London). Analysis using SPM for single-subject data involves 3 major stages: 1) spatial preprocessing, 2) model specification and parameter estimation, and 3) statistical inference. Each of these stages requires several steps. The first step in spatial preprocessing is the co-registration of functional data to T1-weighted structural images. Image segmentation is performed to partition the structural and functional images into

CSF, white, and gray matter, which are then used in the coregistration. Coregistration determines the parameters used to realign subsequent functional images to the first image in the functional series, and the transformation parameters are later used as a set of 6 covariates to regress out movement-related activations. Three movement parameters relate to translation (x, y, z directions in mm), while the remaining three parameters relate to rotation (pitch, roll, yaw directions in degrees). The next step in spatial preprocessing is smoothing. Smoothing is a three-dimensional convolution of the image volume with a Gaussian kernel, which increases the signal-to-noise ratio and allows statistical inferences to be made about regionally specific effects. The next stage is model specification (based on the General Linear Model (GLM)) and parameter estimation. Specifying the model inputs the parameters used in the fMRI protocol, such as TR, number of conditions, condition onset, epoch length, etc. Movement parameters determined above are specified as regressors, proportional scaling is applied to remove global effects, and default F-contrasts are made for each condition. The default effects-of-interest F-contrast was set at $p < 0.01$ for these analyses. The final stage is statistical inference, which analyzes and displays regional effects using t-contrasts or F-contrasts. Main effects for the Object > Pixelated Object condition was specified as a one-sided 1 -1 t-contrast, which displays voxels when the signal for Objects > Pixelated Objects. All p-values shown in these analyses are uncorrected for multiple comparisons. It was deemed unnecessary to correct for multiple comparisons for two reasons: 1) the null-hypothesis Objects = Pixelated Objects was not being tested, but rather Objects > Pixelated Objects, and 2) activation

was expected in certain regions of interest, specifically those in the object-naming network described in Chapter 1 (e.g. occipital, temporal, and frontal areas). Cluster size was also unrestricted, meaning single voxels of activation were included in the display. Three conditions were analyzed for each subject: 1) Objects > Pixelated Objects (*t*-contrast), 2) Objects > implicit Baseline[3] (*t*-contrast, *F*-contrast) 3) Pixelated Objects > implicit Baseline (*t*-contrast, *F*-contrast). Each condition was analyzed at $p < 0.001$, 0.005, 0.01, and 0.05 thresholds to determine which threshold corresponded best with expected regions of interest from the object-naming network. These thresholded data were used in later comparison analyses with CSM sites, PEPSI, and ERP source maps.

ERP

Single-subject ERP data, by their very nature, are ill-suited to ANOVA-type analyses because of the lack of variance in amplitude at a given time point on a specific electrode. In addition, the motivation of including ERPs in this study is not to make inferences about a specific population or between populations, but rather to compare the information available from ERPs with imaging methods within the same subject. This motivation also makes ANOVA analyses of waveform components or effects inappropriate. For the purposes of functional brain mapping, the scalp distribution of an ERP component or effect gives limited information about where in the brain an effect is taking place (Kutas et al., 1999). The temporal information of ERP data can contribute to

[3] The implicit baseline refers to the case where there is no correlation between the signal and the reference function.

localization by distinguishing spatially contiguous, but functionally distinct processes that are difficult to differentiate temporally using fMRI (Kutas et al., 1999). Ultimately, however, the a determination of the most probable current distribution throughout the brain volume that could give rise to a given ERP component is needed to make a meaningful comparison with imaging methods.

Calculating current distributions inside the brain given field or scalp measurements is known as the inverse problem. The inverse problem is considered mathematically ill-posed; the general, unconstrained case has no unique solution. An infinite number of source distributions may account equally well for the same scalp potential (or magnetic field) distributions, because there are an infinite number of mathematically correct solutions. The LORETA (Low Resolution Electromagnetic Tomography) algorithm (Pascual-Marqui et al., 1994) is used to estimate source location, orientation, and amplitude from the measured scalp signal. It assumes that measured signals from the scalp may be accounted for by a set of dipoles uniformly distributed throughout a source region within the head. The algorithm computes distributed activity throughout the brain volume by forming a 3-D grid where sources are located on each grid point, and selects the smoothest of all possible 3-D current distributions. It assumes that neighboring neurons are simultaneously and synchronously activated, and therefore neighboring grid points will be more likely to be synchronized (i.e. a similar orientation and strength), than grid points that are distant from each other. The ability to calculate a source distribution image, however, rests on choosing an appropriate head model to restrict the solution space to within the brain. To this end, an inverse operator is

constructed using a realistic boundary element model (BEM), which considers the compartments of scalp, skull, cerebro-spinal fluid (CSF), and cortex using values of conductance from available literature.[4] Meshes created from the segmentation of the brain (gray/white matter), scalp, and skull provide a fairly accurate representation of the selected surface.

These linear source estimation techniques result in 3-D current density distributions that can be viewed as a sequence of slices through a reconstructed region at a specific time point. Since a sampling frequency of 200Hz was used during this study, the sources for these slices can be viewed every 5ms for the entire 800ms waveform.

3-D Model for Data Integration

A three-dimensional model of each participant's brain was created by combining a T1-weighted 3-D MR volume of a patient-specific brain with a 2-D Time of Flight (TOF) MR Venogram (MRV) (1.5mm thick slices (number of slices variable), flip angle = 60°, TR/TE 45/9msec, 256x128 matrix, FOV = 22cm, NEX = 1). The primary method of integration constructs a patient-specific model of the brain, obtained from the structural MR scans. The other MR image volumes (veins, fMRI, PEPSI) are registered to the anatomy MR volume and subsequently to the extracted anatomical model by expressing the voxels in relation to the center of the fixed magnet. ERP sources are not compared with CSM sites. The cortical stimulation data is integrated using a

[4] Ratio of skull/csf conductance is fixed at 0.0125, with tissue conductivity assumed to be $0.33(\Omega m)^{-1}$ (Geddes and Baker, 1967). Ratio of [inner skull radius]/[outer skull radius]/[head radius] is fixed at 0.87/0.92/1.0 (Rush and Driscoll, 1986). Head shape is taken into account explicitly from the MRI.

visualization-based approach as described in Modayer et al. (1997). Briefly, the cortical surface model is combined with the MR-based models of the cortical veins and rendered to visually match a photograph of the cortical surface when it is exposed during the neurosurgical procedure. The veins provide landmarks that are used to match the cortical anatomy seen in the photograph with the MR-based images, and an interactive tool is then used to map the location of the stimulation sites onto the reconstructed cortical surface.

Chapter 4 Results

Results are presented for one control subject (P138) and two patients (P136, P137) for cortical stimulation mapping (CSM) (patients only), PEPSI, fMRI, and ERP protocols. PEPSI and ERP sources overlayed onto structural MRI images are in radiological convention (Left (L) side of image = Right (R) side of hemisphere, R side of image = L side of hemisphere). FMRI and ERP original source maps are in neurological convention (L side of image = L hemisphere, R side of image = R hemisphere). Indicators (L, R) are shown above figures throughout the chapter.

P138 (control subject)

No cortical stimulation was performed on this subject. PEPSI, fMRI, and ERP data are presented and compared using neuroanatomical landmarks.

PEPSI

The figure below (Figure 21) shows two lactate images: 1) the image on the left shows voxels with *Z*-scores of 2 or greater overlayed onto the structural MRI represented in red, 2) the image on the right shows voxels with *Z*-scores between 1 and 2 in grey (red voxels are included as reference points).

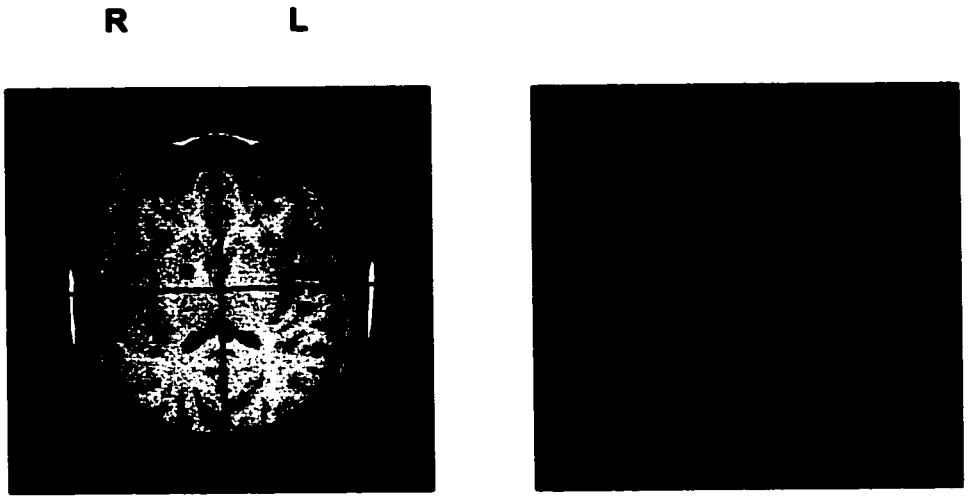

Figure 21. PEPSI activations for P138 showing increases in lactate during visual object naming. Voxels with *Z*-scores of 2 or greater are represented in red (left image), and voxels with *Z*-scores between 1 and 2 are represented in grey (right image).

As noted previously, only the posterior two-thirds of the slice are examined for activations due to the magnetic susceptibility of the air-tissue interface at the sinuses. This subject was right-handed, and presumably left-dominant for language. Activation is seen in the left inferior frontal gyrus (operculum), and the left superior temporal gyrus (red voxels, left image). Some weaker left-sided activations (grey voxels, right image) are in the inferior temporal gyrus and occipital gyrus. Right-sided activations are in the middle temporal gyrus and putamen. Weaker bilateral cingulate, precuneus, and striate activations are also present, probably reflecting attentional and early visual processing.

Frontal, temporal, and occipital activations seen here are consistent with areas described earlier in the visual object naming network.

FMRI

Three fMRI datasets analyzed with SPM are shown here: 1) Objects vs. Pixelated Objects (t-contrast), 2) Objects vs. Baseline (t-contrast and F-contrast), 3) Pixelated Objects vs. Baseline (F-contrast). The two types of contrasts are shown to reveal signal increases (t-contrast) versus signal decreases (F-contrast) in activation, when activations localize to different areas, though not necessarily to different neuroanatomical structures (activations common to t- and F-contrasts show signal increases). It will be seen that matches across fMRI, PEPSI, and ERP techniques occur with both signal increases and decreases. The first dataset below (Figure 22) shows t-test results from the Objects vs. Pixelated Objects comparison at a threshold of $p < 0.001$. Slices are shown so that changes in activation patterns are shown in the most inferior slice, i.e. slice –25 demonstrates the activation pattern in subsequent 1mm slices ascending superiorly until slice –19, which displays the activation pattern in subsequent superior slices until –13, and so on.

1) Objects vs. Pixelated Objects

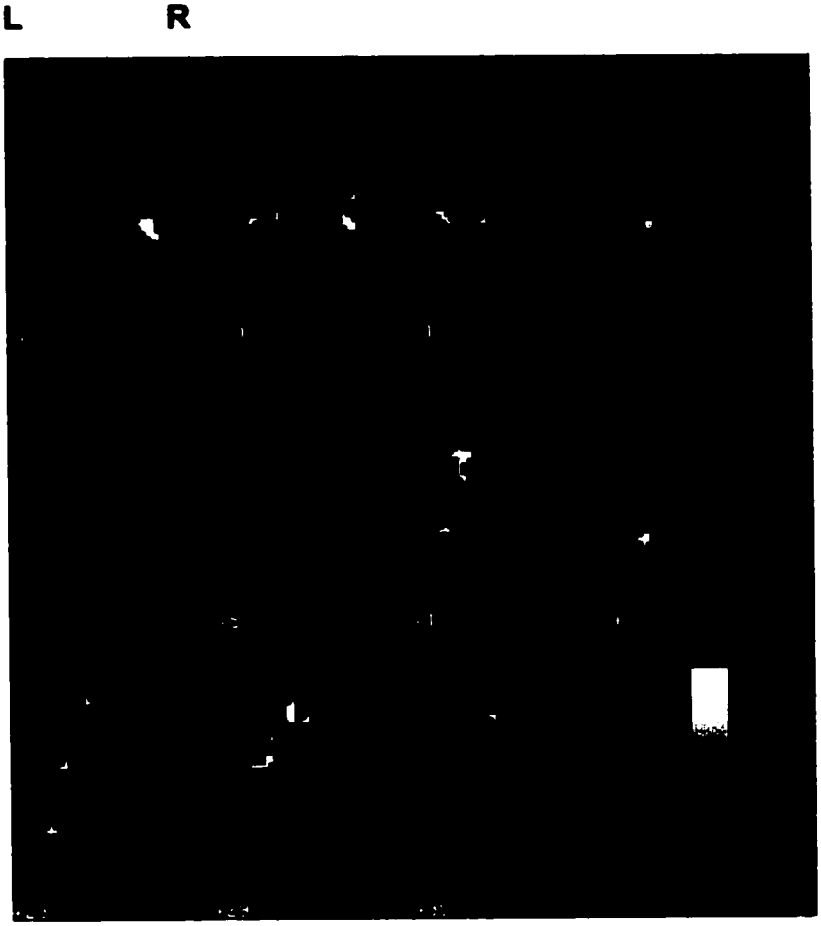

Figure 22. FMRI Objects vs. Pixelated Objects ($p < 0.001$) *t*-contrast.

Although fusiform gyri are activated bilaterally, activation patterns in general are mainly left-lateralized. Areas in the left hemisphere include occipital gyrus, middle and superior temporal gyri, supramarginal gyrus, inferior and middle frontal gyri, insula, and cingulate. Table 4 below shows local maxima for this volume in SPM coordinates, associated *t*-values, and anatomical location.

Table 4. FMRI Objects vs. Pixelated Objects ($p < 0.001$) *t*-contrast.

(X,Y,Z)	*t*-value	Location
(30, -17, -18)	4.56	Right fusiform
(-49, -36, 17)	4.25	Left SMG
(-45, -17, -6)	4.05	Left MTG/STG
(-18, 47, 30)	3.90	Left IFG/MFG
(-19, -17, -12)	3.84	Left OcG
(-34, 13, 30)	3.76	Left IFG
(-34, 24, 12)	3.74	Left insula/IFG Op
(-3, 43, 30)	3.70	Left (midline) cingulate
(38, -28, -48)	3.62	Right cerebellum
(34, 2, -18)	3.57	Right fusiform
(23, -28, 6)	3.56	White mtr (~right lat ven)
(-41, 5, 42)	3.48	Left MFG
(-30, 32, 30)	3.40	Left MFG/IFG
(15, -10, 18)	3.37	White mtr (~right lat ven)
(-34, 9, -12)	3.29	Left fusiform
(-7, 17, 30)	3.28	Left cingulate

2) Objects vs. Baseline

The second dataset shows *t*-test and *F*-test results for Objects vs. (implicit) Baseline at a threshold of $p < 0.05$ and $p < 0.001$ respectively (Figure 23).

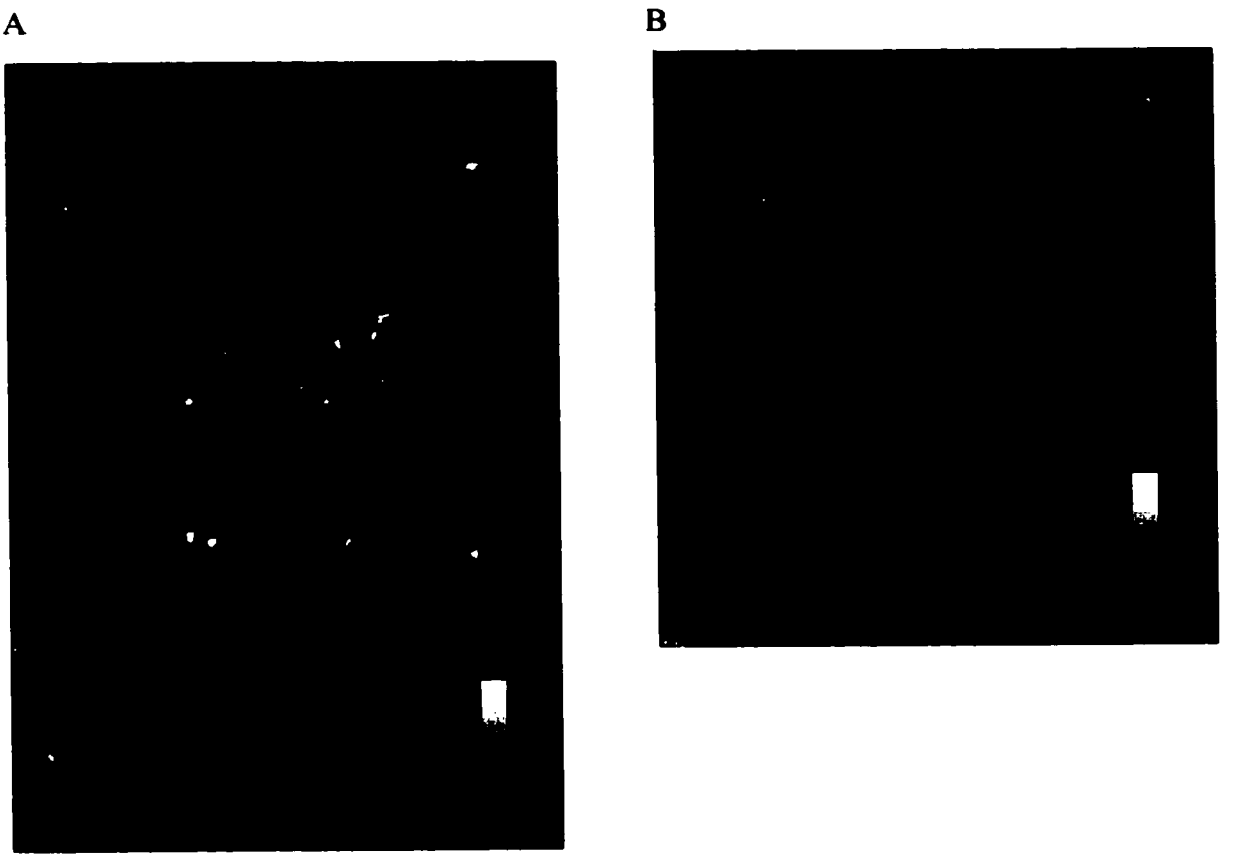

Figure 23. FMRI (A) Objects vs. Baseline *t*-contrast ($p < 0.05$) (signal increases) (B) Objects vs. Baseline *F*-contrast ($p < 0.001$) (signal decreases).

Activated areas in the *t*-contrast are seen bilaterally. Left-lateralized activations include the inferior, middle, and superior frontal gyri, superior temporal/supramarginal gyrus, and angular gyrus. Right-lateralized activations include the insula/inferior frontal gyrus operculum, transverse temporal gyrus, cuneus, and various basal ganglia structures. Activated areas in the *F*-contrast are also seen bilaterally. Left-lateralized activations

include superior and middle frontal gyri, and middle temporal gyrus. Right-lateralized activations include the cingulate, occipital, post-central, and superior frontal gyri. Table 5 below shows local maxima in each volume in SPM coordinates, associated *t*-contrast and *F*-contrast values, and anatomical location.

Table 5. FMRI Objects vs. Baseline $p < 0.05$ (*t*-contrast) and $p < 0.001$ (*F*-contrast).

(X,Y,Z)	*t*-value	Location
(-7, 17, 30)	2.79	Left cingulate
(-19, -6, -12)	2.78	Left subicullum/hippocam
(-19, 13, 12)	2.53	Left (putamen, glob pall)
(27, 43, 6)	2.43	Right insula/IFG Op
(-30, -47, -1)	2.37	Left angular gyrus
(-30, 24, 30)	2.36	Left IFG/MFG (border)
(-56, -32, 5)	2.27	Left STG/SMG (border)
(30, -25, 6)	2.20	Right transverse TG
(-49, 17, 12)	2.16	Left IFG
(26, -24, -48)	2.10	Right cerebellum
(23, -2, 36)	2.08	Right SFG/MFG (border)
(8, 9, 0)	2.02	Right thalamus
(45, -21, 18)	1.92	Right PoG (near SMG)
(-11, 5, 60)	1.91	Left SFG
(-26, 47, 12)	1.90	Left OFG (orbitofrontal)
(19, -2, 6)	1.85	Right thalamus, int cap
(19, -51, -13)	1.80	Right cuneus
(26, -47, -1)	1.75	Right angular gyrus
(15, -58, -1)	1.73	Right cuneus
(-56, 24, 0)	1.71	Left STG
(X,Y,Z)	***F*-value**	**Location**
(-15, 39, 54)	19.05	Left SFG
(8, 54, 12)	16.49	Right cingulate
(0, -47, -43)	16.26	Midline OcG
(-45, -47, -19)	15.40	Left MTG
(0, -29, 42)	*14.99*	*Artifact from vein*
(41, -55, -31)	14.78	Right OcG
(-4, 35, 48)	13.99	Left SFG
(15, -36, 35)	13.80	Right PoG

Table 5. Continued.

(15, -77, 5)	13.78	Right OcG
(8, 69, 18)	13.75	Right superior rostral gyrus
(8, 43, 38)	13.30	Right SFG
(60, -21, 18)	13.02	Right PoG
(-3, 69, 18)	12.68	Left SFG
(-22, 69, 30)	12.36	Left MFG

3) Pixelated Objects vs. Baseline

The third dataset shows *F*-test results from Pixelated Objects vs. Baseline at a threshold of $p < 0.001$ (Figure 24).

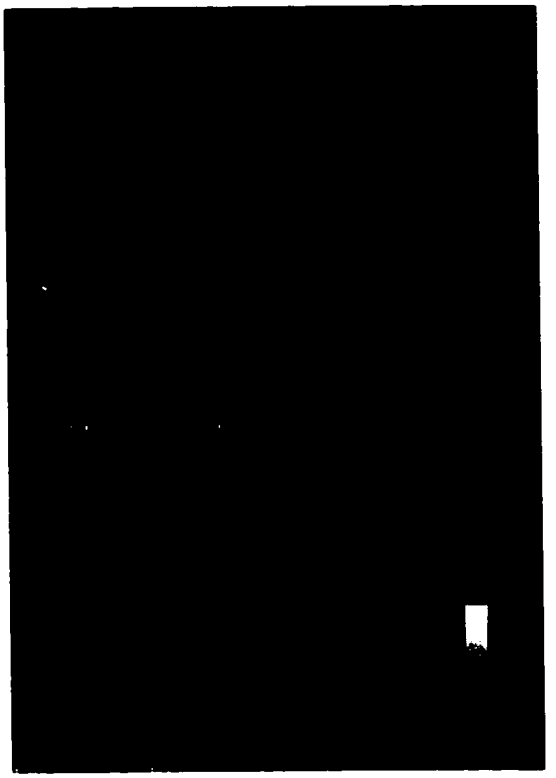

Figure 24. FMRI Pixelated Objects vs. Baseline $p < 0.001$ F-contrast.

Activations are found predominantly on the left side, but some bilateral and right-sided activation occur as well. Bilateral activation is found in the cingulate, occipital, and superior rostral/superior frontal gyri. Left-lateralized activations include the fusiform, middle frontal, inferior and transverse temporal gyri, pre-central gyrus, and the insula. Right-lateralized activations occur in the supramarginal gyrus. Table 6 below shows local maxima for this volume in SPM coordinates, associated F-values, and anatomical location.

Table 6. FMRI Pixelated Objects vs. Baseline $p < 0.001$ *F*-contrast.

(X,Y,Z)	*F*-value	Location
(12, 69, 18)	23.95	Right SRoG/SFG
(60, -32, 18)	20.83	Right SMG
(-30, 9, -18)	19.30	Left fusiform
(-7, 69, 18)	18.22	Left SroG/SFG
(-19, -32, 53)	16.59	Left SFG
(-4, 35, 48)	16.45	Left SFG
(-15, 35, 48)	15.77	Left MFG
(26, -24, -30)	15.85	Right OcG
(-26, -21, -24)	15.28	Left OcG
(-45, -13, 6)	15.27	Left TTG
(-49, 9, 30)	15.20	Left PrG
(-45, -47, -19)	13.91	Left ITG
(8, 50, 12)	13.78	Right cingulate
(-4, -25, 24)	13.30	Left cingulate
(37, -51, -31)	13.30	Right OcG
(-30, -13, 6)	13.16	Left insula
(-52, -2, 24)	13.05	Left PrG
(-34, 9, 12)	12.96	Left insula
(-4, -29, 42)	12.87	Left cingulate
(49, 43, 24)	12.70	Right IFG
(-34, -58, -13)	12.36	Left OcG
(11, -28, -42)	12.35	Right cerebellum

Overall, activated areas are consistent with visual object naming areas described in Chapter 1, including occipital, inferior and middle temporal, fusiform, and inferior frontal activation. Superior temporal, supramarginal, and angular gyri were also seen, though these areas are more often associated with picture versus word paradigms (eg. Menard et al., 1996; Moore and Price, 1999b).

ERP

The figure below (Figure 25) shows Grand Mean waveforms for each of the 64 electrodes for the Objects (solid lines) and Pixelated Objects (dashed lines) conditions. Components of interest are the N100, which is associated with early sensory processing (in this case visual processing) and the N400, which is associated with semantic processing (see Chapter 1 review).

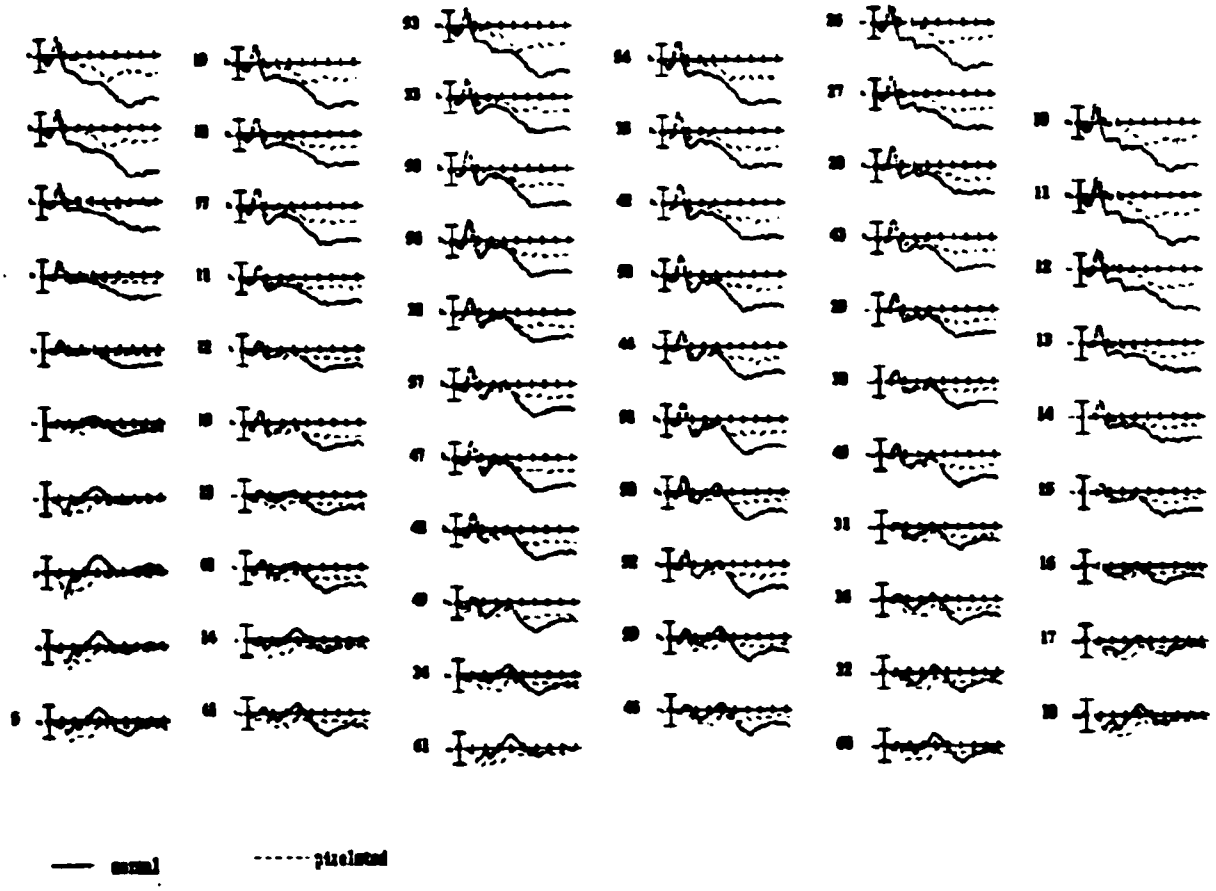

Figure 25. Grand mean for Objects (solid lines) and Pixelated Objects (dashed lines) for all channels. X-axis is in 100msec increments, y-axis is in microvolts.

An early negative-going peak corresponding to the visual perceptual N100 can be seen at 130msec in both conditions, which is distributed anteriorly, both laterally and along the midline. A later negative-going peak corresponding to the N400 occurs at 400msec in the Objects condition and at 390msec in the Pixelated Objects condition. For the purposes of source-localization and comparison to fMRI and PEPSI techniques, Objects and Pixelated Objects conditions are examined separately.

Objects

The two negative-going peaks expected in this condition are seen: 1) an early sensory peak (N100) corresponding to visual perceptual processing of the stimuli, and 2) a later peak (N400) corresponding to the semantic processing stage that occurs when naming the object, consistent with models of object naming and ERP studies (Barrett and Rugg, 1990; Ganis et al. 1996; Holcomb and McPherson, 1994; Kutas and Van Petten, 1990; Nigam et al., 1992). The spatial distribution of these peaks across the scalp are seen in Figure 26 (A) below. The N100 component occurs between 90-180msec with a peak amplitude at 130msec and is most prominent at central and bilateral (slightly right-lateralized) anterior sites; amplitudes are reduced at lateral sites and absent at posterior sites. The N400 component occurs between 280-540msec with a peak amplitude at 400msec and is most prominent at left posterior sites and midline/right centro-temporal sites. Amplitudes are reduced at mesial lateral sites and absent at anterior sites

bilaterally. These distributions are also illustrated in the field and current source density (CSD)/Laplacian[5] maps in Figure 26 (B) below.

A

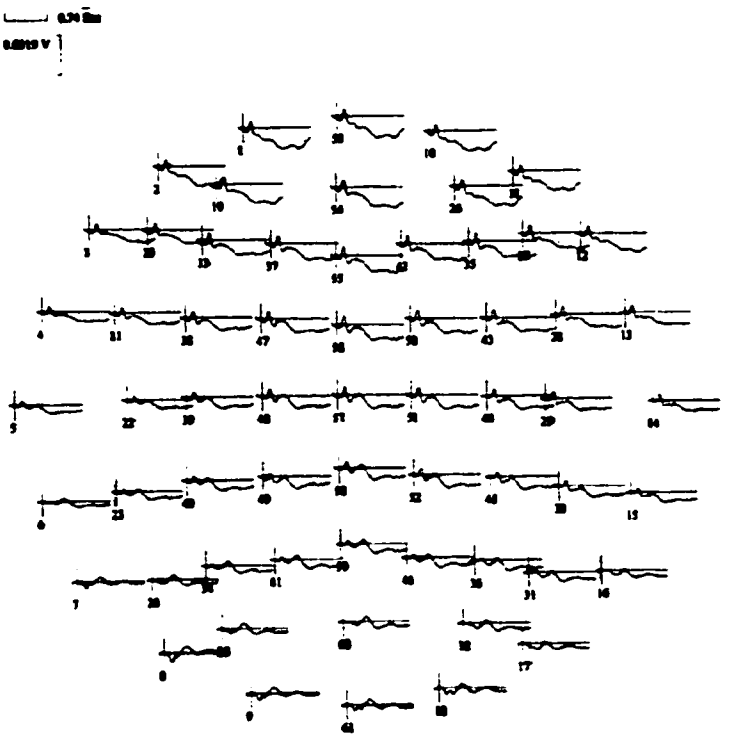

Figure 26. (A) 64-channel orientation of ERP waveforms for the Object condition. Frontal areas are at the top, occipital areas at the bottom, time and voltage scale bars are in the top left corner. (B) Top views of field and Laplacian (current source density) maps at 130msec and 400msec for objects. Areas of interest are in blue for the field map and in red for the Laplacian map.

[5] The Laplacian operator is a common spatial enhancement technique which takes the second spatial derivative of the potential field at each electrode site, and is proportional to the current entering and exiting the scalp at each electrode site (Kutas et al., 1999).

B

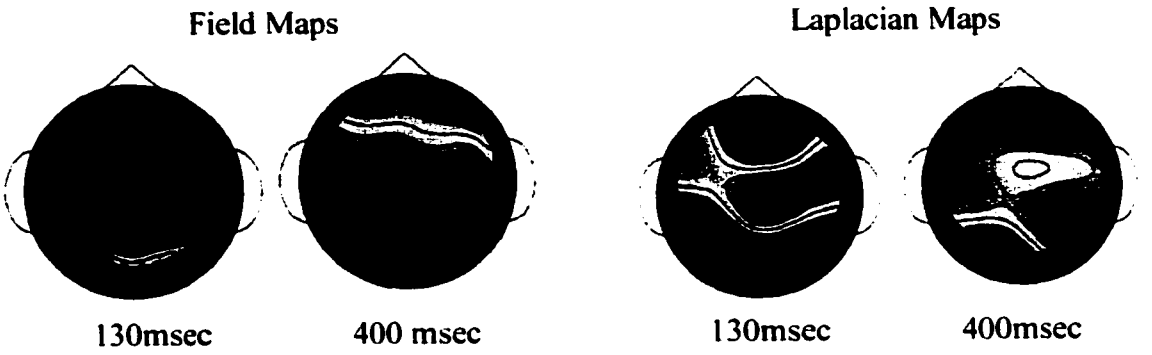

Figure 26. Continued.

Although it is important to note the scalp distributions and amplitudes of these components, components do not necessarily represent the activity of a single source or neural generator within the brain, and larger amplitudes over certain scalp locations do not necessarily reveal the source of the underlying generator(s). Multiple generators, for example, result in scalp distributions that are the sum of the scalp distribution of each generator alone. Therefore, the distribution of activity at the scalp at any given time may be misleading when attempting to determine a source, especially if more than one generator is active. To determine the number and location of neural generator(s) for the components of interest, tomographic estimation techniques with the LORETA algorithm are used (see Chapter 3). Waveforms across electrode sites are superimposed below in Figure 27 to better visualize peak amplitudes of components.

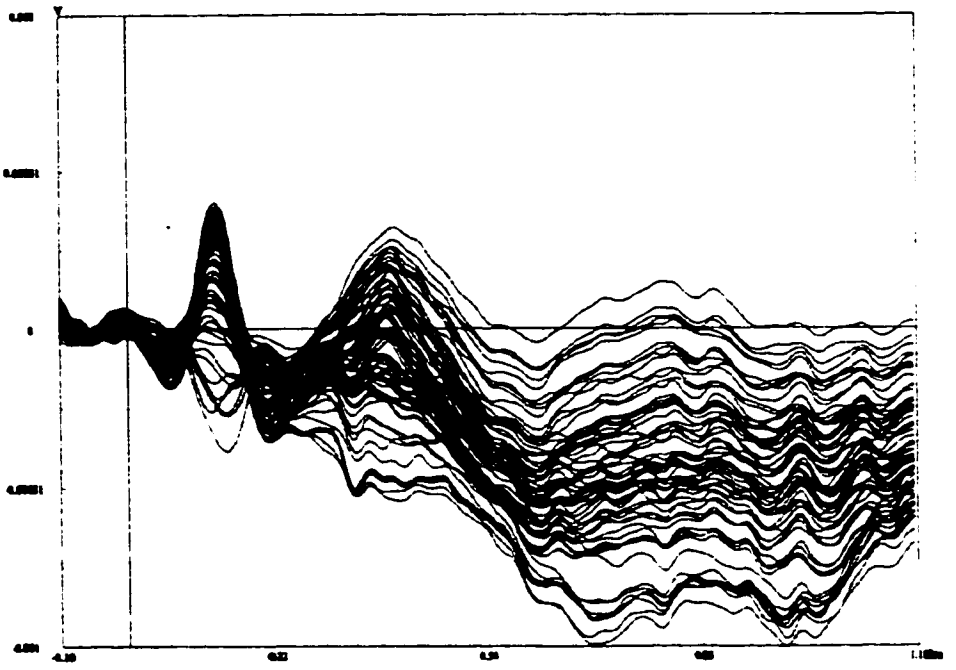

Figure 27. Superimposed 64-channel waveforms for the Object condition. Negative voltages are plotted upwards, positive voltages are plotted downwards; negative-going peaks occur at 130 and 400msec.

Before examining the sources for each component of interest (N100, N400) in more detail, it is important to ensure that sources vary across the timecourse of the waveform in such a way that they are temporally bound by the components. In other words, the sources should change with the timecourse of the waveform components. It can be seen in Figure 28 below that sources not only change across the timecourse of the waveform but are temporally bound by the components in the waveform, implying that such components have distinctive neural generators. Sources are seen in the left posterior area from 90-180msec, in bilateral frontal areas from 210-260msec, then in right frontal

areas from 280-500msec, when a second source starts to emerge in the left posterior area, remaining until 630msec.

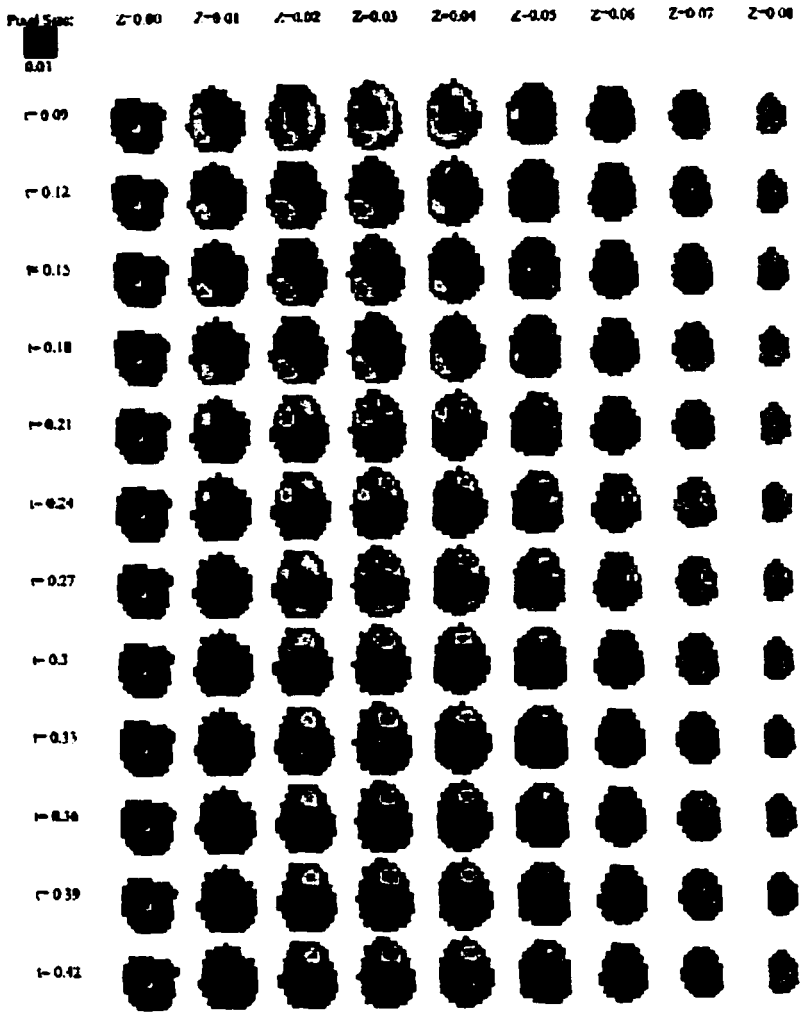

Figure 28. Source maps for the object condition from 90-630msec in 30msec increments. Sources are differentiated for the N100 (90-180msec) and N400 (280-540msec) components.

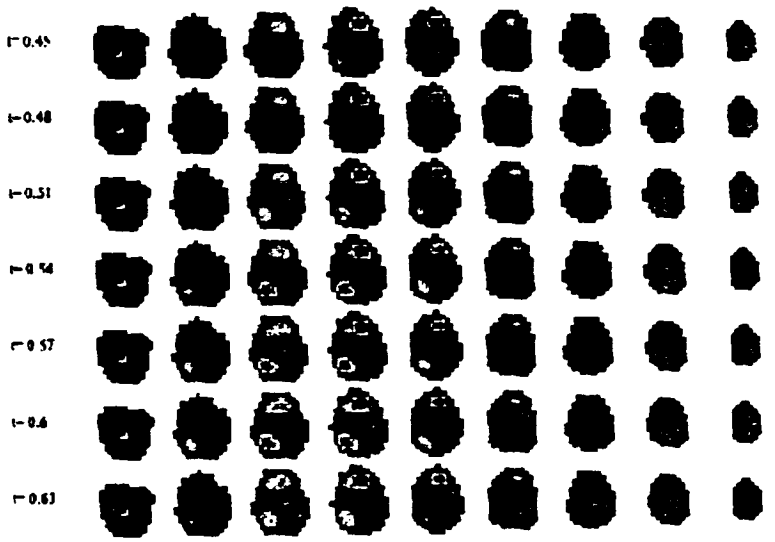

Figure 28. Continued.

The peak amplitude for the N100 component occurs at 130msec. The LORETA algorithm is applied to this timepoint and a source in the posterior left hemisphere is seen (Figure 29 (A)), specifically in the left occipital gyrus, extending superiorly into the inferior and middle temporal gyri (Figure 29 (B)). The occipital source is consistent with attributing the N100 component to visual perceptual processing of these stimuli.

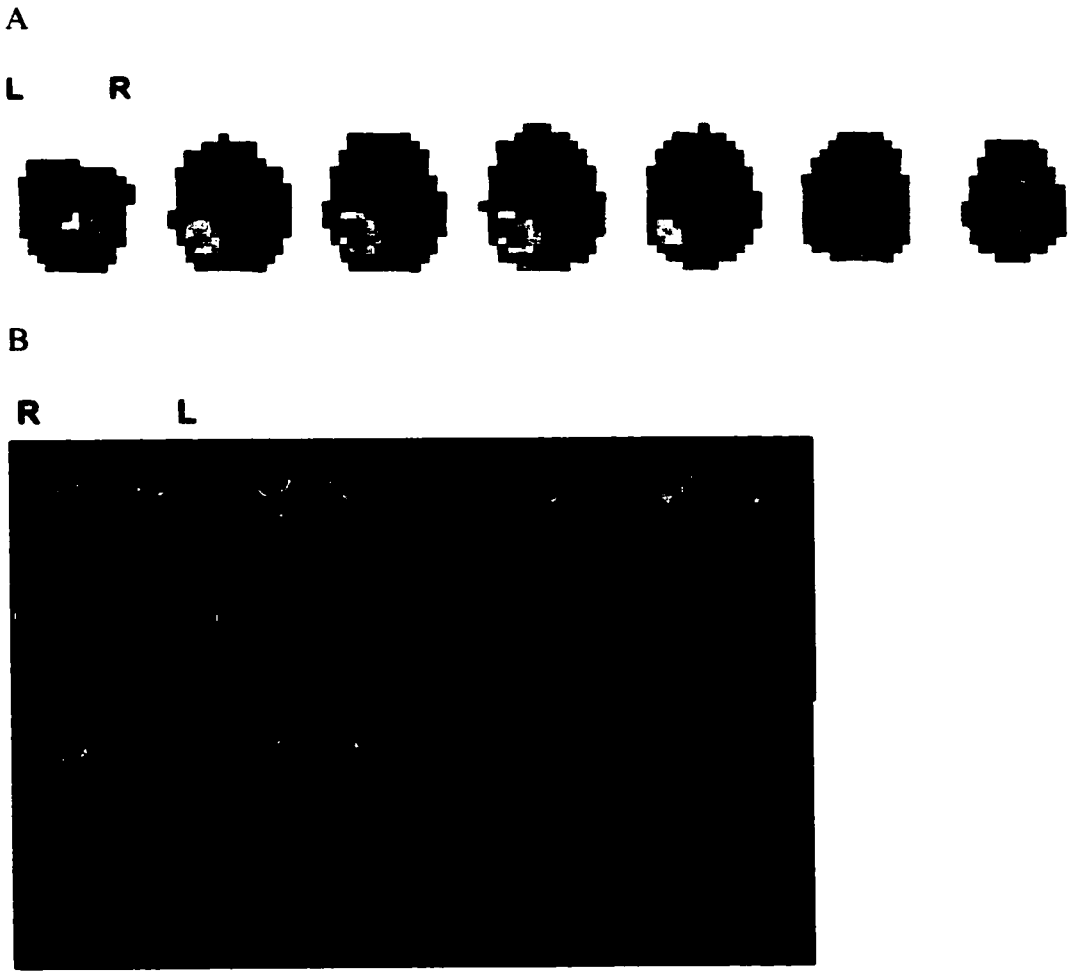

Figure 29. (A) Source maps at 130msec for objects. Pixels = $1cm^3$, direction is inferior to superior (L-R), axial views. (B) The source is seen mainly in the left occipital gyrus when overlayed onto structural MRI scans.

The peak amplitude for the N400 component occurs at 400msec. The source is seen in the anterior right hemisphere (Figure 30 (A)), specifically in the right cingulate and middle frontal gyrus, extending superiorly into the superior frontal gyrus (Figure 30 (B)). The middle frontal gyrus is consistent with visual object naming areas identified in

Chapter 1. Cingulate activity likely reflects attentional processing; a lateralization to the nondominant hemisphere is also seen.

A

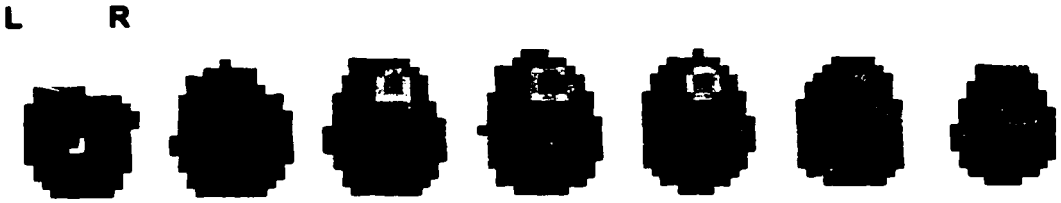

B

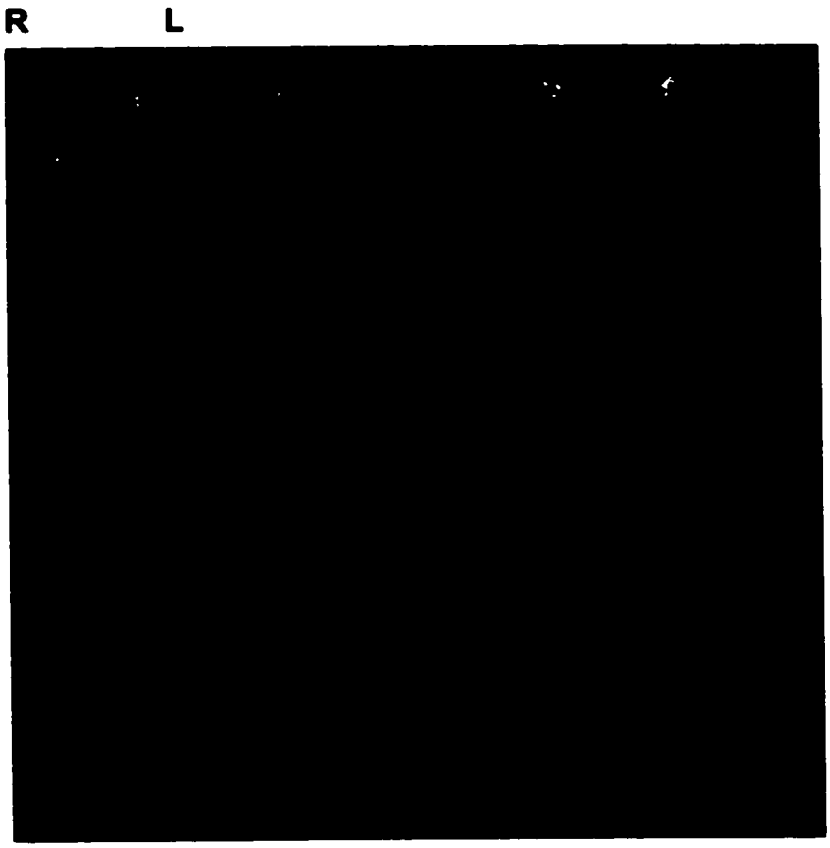

Figure 30. (A) Source maps at 400msec for objects. (B) The source is seen in the right cingulate, MFG, and SFG when overlayed onto structural MRI scans.

Overall, the N100 source appearing in posterior areas such as occipital gyrus is consistent with its interpretation as an early sensory processing component, in this case visual processing. The N400 source in anterior areas, particularly middle frontal gyrus, is consistent with the semantic processing and visual object naming areas described in Chapter 1.

Pixelated Objects

The spatial distribution of the N100 and N400 components across the scalp are seen below in Figure 31 (A). The N100 component occurs between 90-190msec with a peak amplitude at 130msec and is most prominent at anterior sites bilaterally; amplitudes are slightly reduced at anterior left lateral sites and severely reduced or absent at posterior sites bilaterally. Overall, the pattern is very similar to the Objects condition. An N400 component occurs between 300-540msec with a peak amplitude at 390msec and is most prominent at midline/right centro-frontal sites. Amplitudes are reduced at posterior left lateral sites. Overall, this pattern is different from the Objects condition, which showed more prominent amplitudes at left posterior and midline/right centro-temporal sites. These distributions are illustrated in the field and Laplacian maps in Figure 31 (B) below.

A

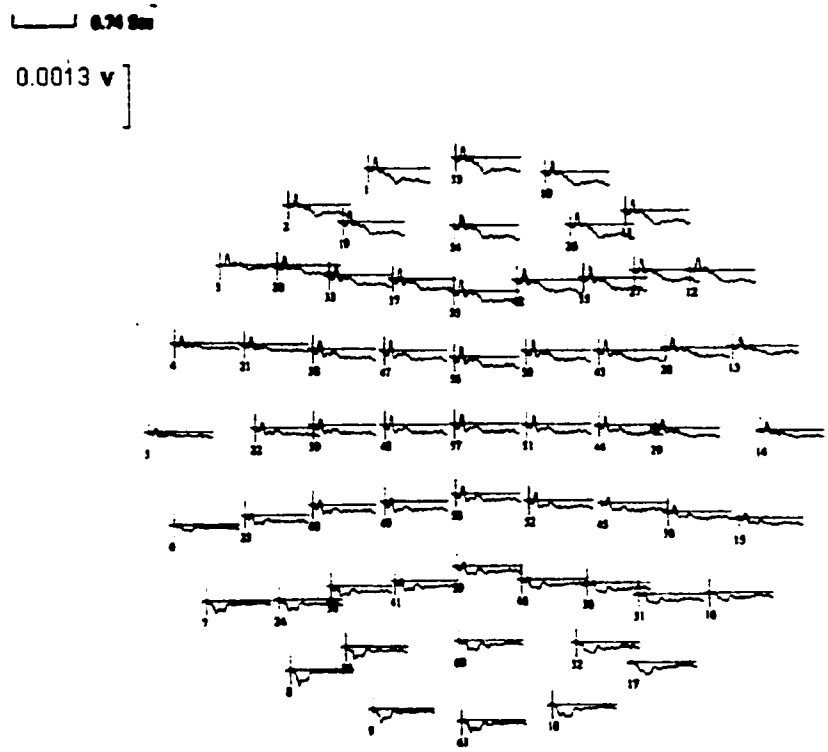

B

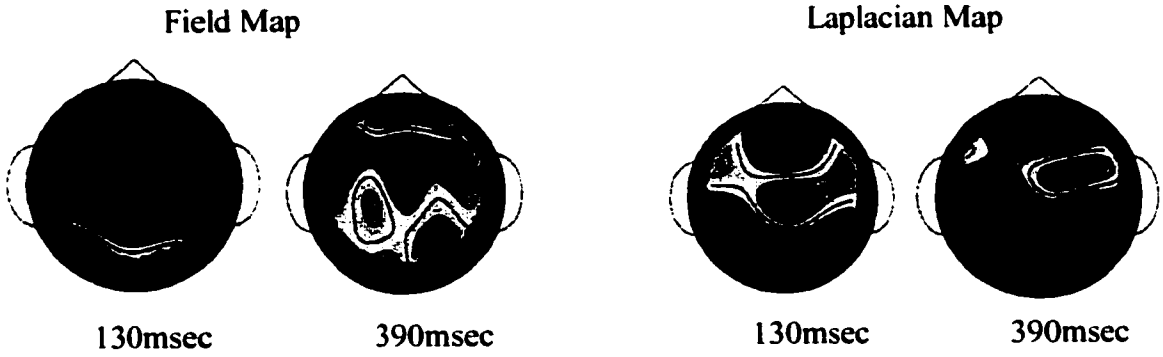

Figure 31. (A) 64-channel orientation of ERP waveforms for the Pixelated Object condition. (B) Top views of field and Laplacian (current source density) maps at 130msec and 390msec for pixelated objects. Areas of interest are in blue for the field map and in red for the Laplacian map.

Waveforms across electrode sites are superimposed and shown below in Figure 32 to better visualize peak amplitudes prior to source estimation.

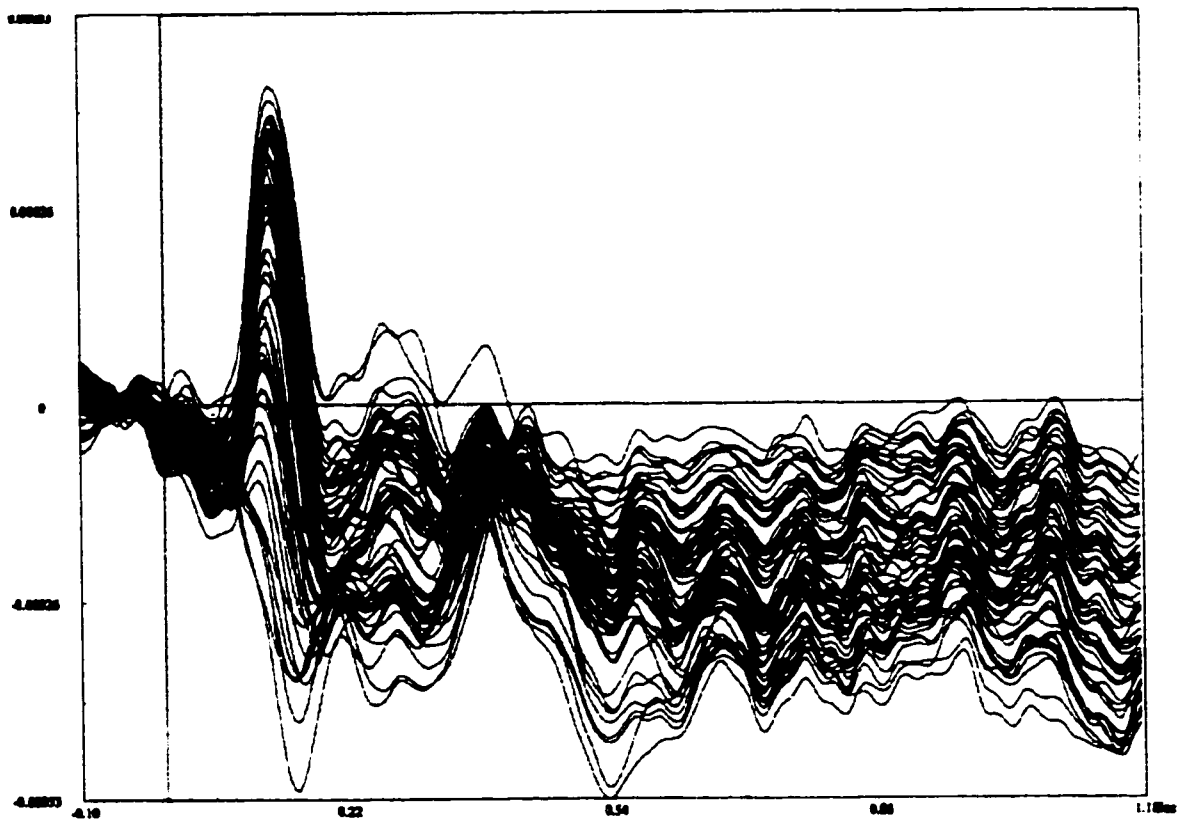

Figure 32. Superimposed 64-channel waveforms for the Pixelated Object condition. Negative voltages are plotted upwards, positive voltages downwards; negative peaks occur at 130 and 390 msec.

Again, it can be seen below (Figure 33) that sources vary across the timecourse of the waveform and are temporally bound by the components of interest. Unlike the object

condition, multiple sources are seen at several time blocks including bilateral posterior sources at 90-190msec and bilateral frontal sources and right posterior sources at 300-540msec, corresponding to the N100 and N400 components respectively.

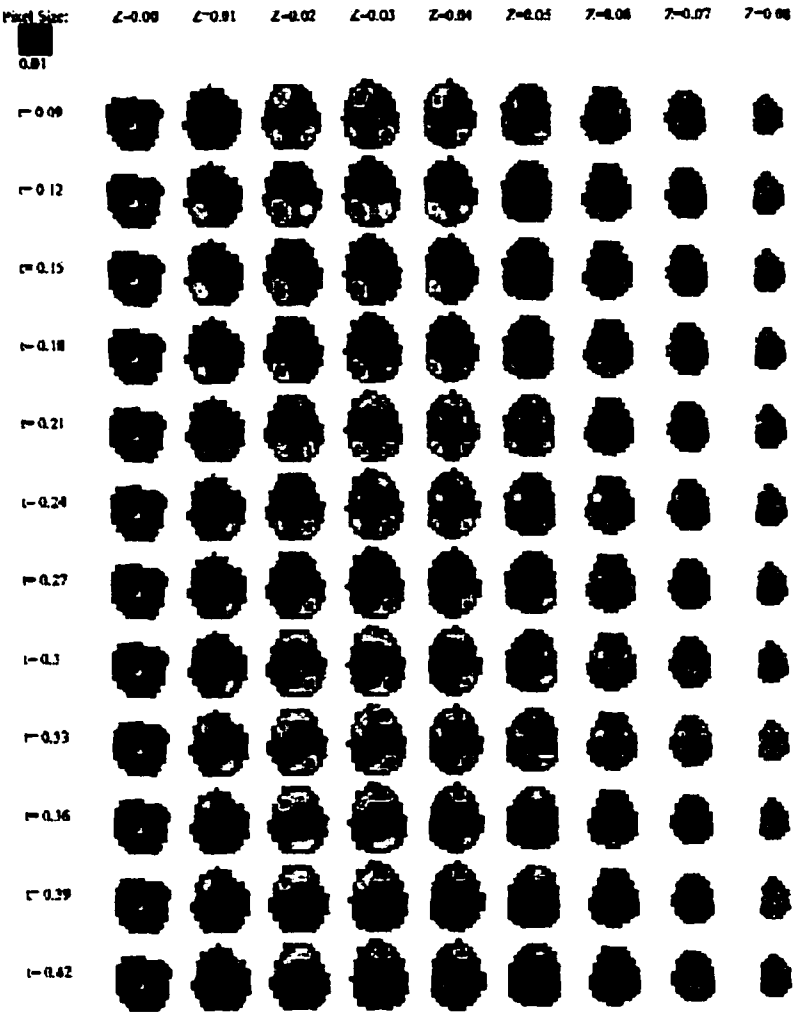

Figure 33. Source maps for the pixelated object condition from 90-630msec in 30msec increments. Sources are differentiated for the N100 (90-190msec) and N400 (300-540msec) components.

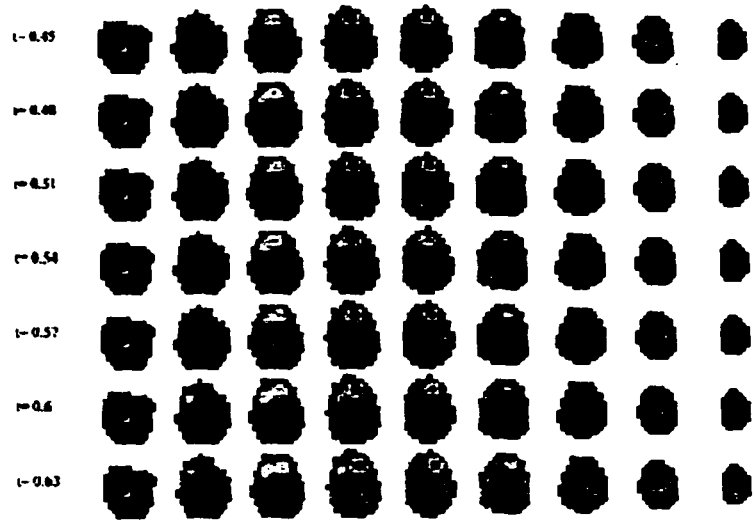

Figure 33. Continued.

The peak amplitude for the N100 component occurs at 130msec. The algorithm is applied to this timepoint and two sources are seen (Figure 34 (A)). The main source extends superiorly from the left occipital gyrus and inferior temporal gyrus to the middle temporal gyrus and into the angular gyrus. A smaller secondary source extends superiorly from the right occipital gyrus and inferior temporal gyrus to the middle temporal gyrus (Figure 34 (B)). This condition is less lateralized than the N100 sources for the Objects condition.

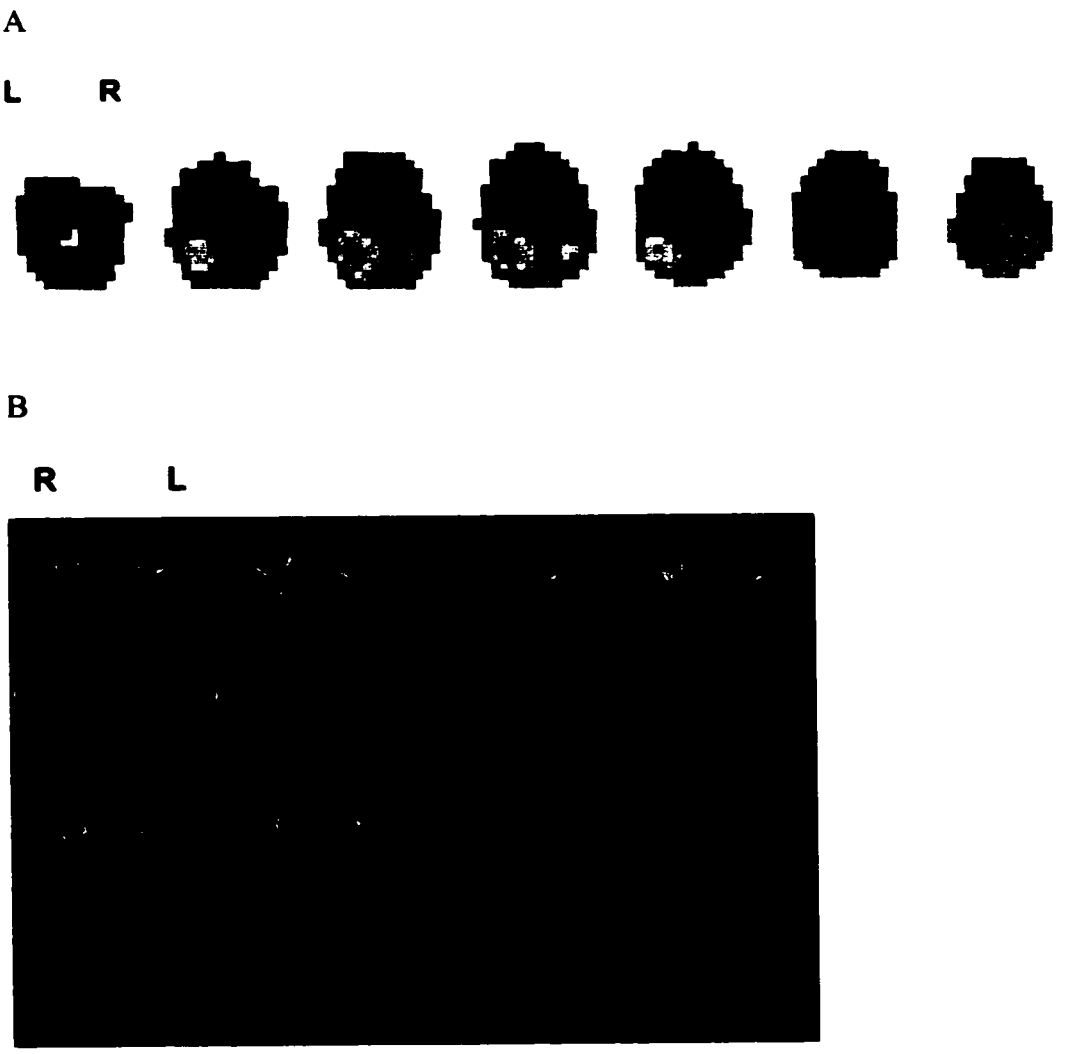

Figure 34. (A) Source maps at 130msec for Pixelated Objects. (B) The main source is seen in the left occipital gyrus and inferior/middle temporal gyri. A second source is seen in the same areas on the right.

The peak amplitude for the N400 component occurs at 390msec. As with the early sensory component, sources are seen bilaterally, but in anterior areas rather than posterior

areas (Figure 35 (A)). One source is in the left hemisphere, extending from the inferior frontal gyrus to the middle frontal gyrus. The second source is in the right cingulate/superior frontal gyrus (Figure 35 (B)).

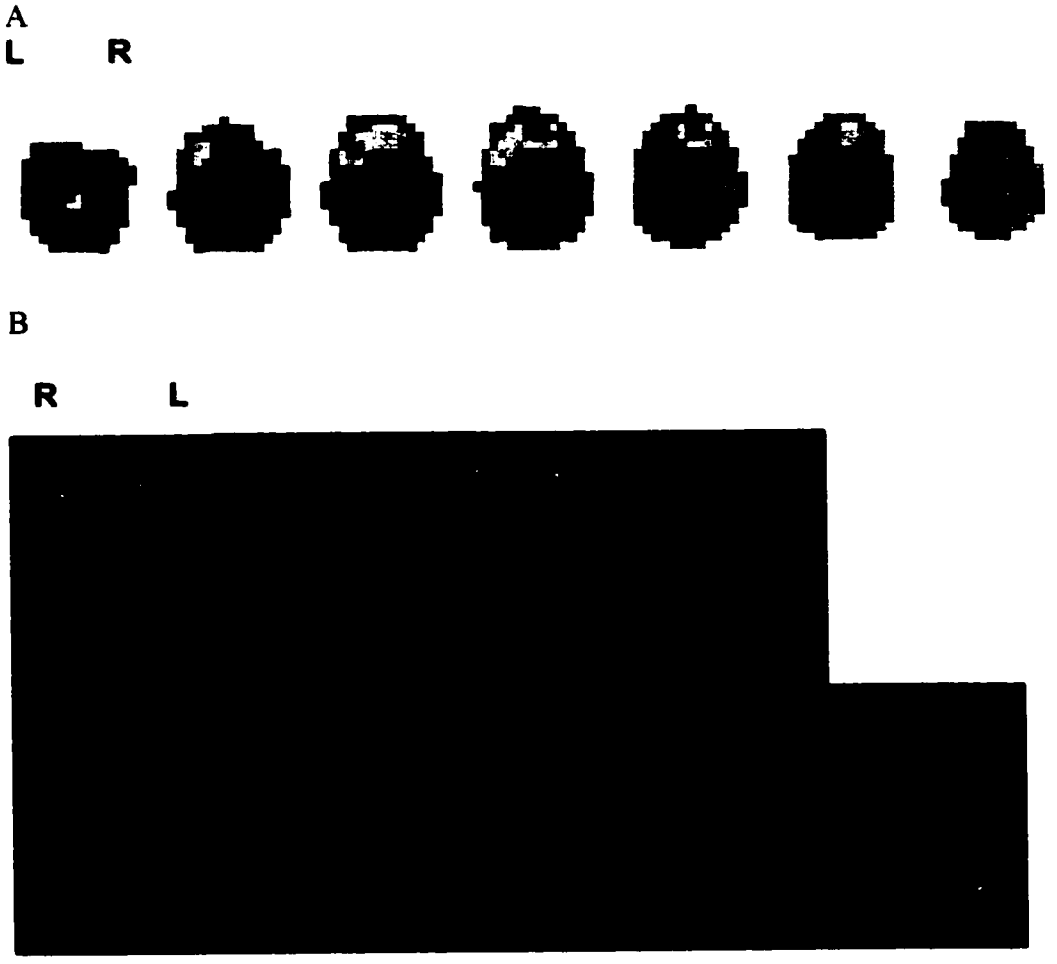

Figure 35. (A) Source maps at 390msec for Pixelated Objects. (B) Sources are seen bilaterally, in the inferior/middle frontal gyri on the left side and in the superior frontal gyrus on the right side.

A summary of sources for the Object and Pixelated Object conditions are listed in the table below (Table 7). Common sources for the N100 component across conditions include the left occipital gyrus and left inferior and middle temporal gyri; common sources for the N400 component include the right cingulate and superior frontal gyrus. Sources are posterior for the N100 component and anterior for the N400 component across conditions. The Objects condition shows left-lateralized sources for the early sensory N100 component and right-lateralized sources for the later semantic N400 component, while the Pixelated Objects condition shows bilateral sources for both components. Overall, sources are more lateralized for the Objects condition and less lateralized for the Pixelated Objects condition.

Table 7. Summary of ERP sources across conditions.

Objects	**Pixelated Objects**
N100	*N100*
Left OcG	Left OcG
Left ITG, MTG	Left ITG, MTG
	Left angular gyrus
	Right OcG
	Right ITG
	Right MTG
N400	*N400*
Right cingulate	Right cingulate
Right SFG	Right SFG
Right MFG	Left MFG
	Left IFG

Comparisons across modalities

Three comparisons across modalities are made: 1) Objects vs. Pixelated Objects, 2) Objects vs. Baseline, 3) Pixelated Objects vs. Baseline. Figure 36 shows matching slices across techniques that have been described above.

1) Objects vs. Pixelated Objects

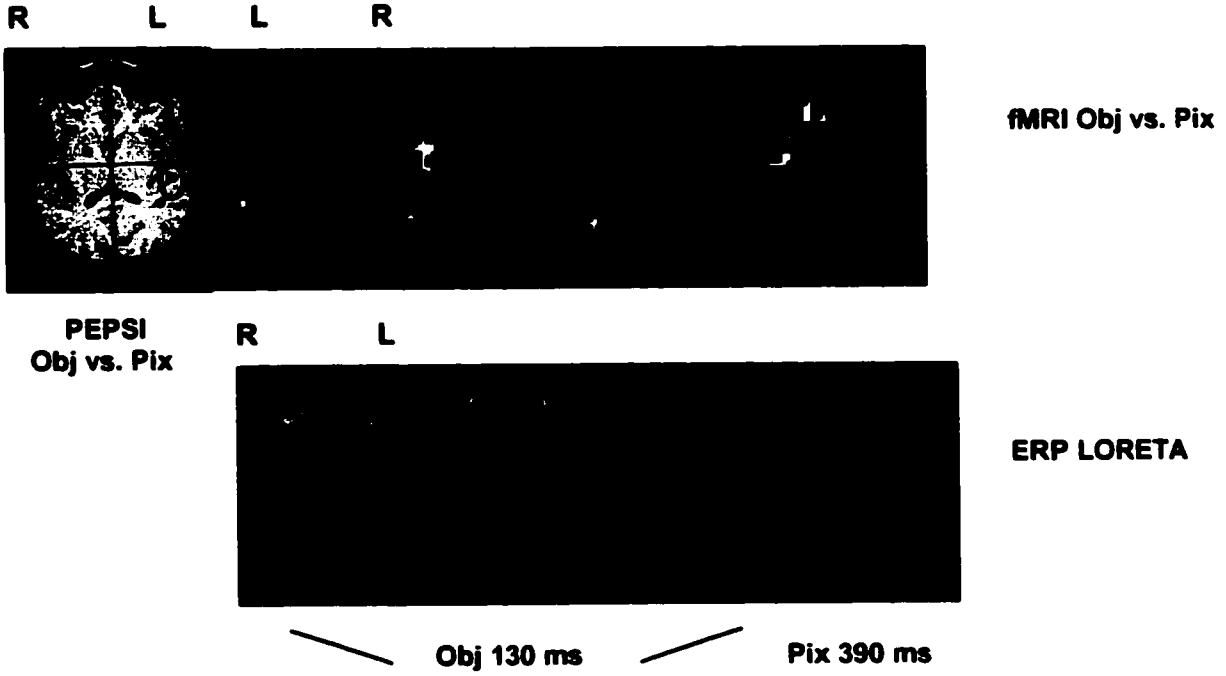

Figure 36. Comparison across modalities between Objects vs. Pixelated Objects (fMRI/PEPSI/ERP).

In this condition, the following matches occur between fMRI activations, PEPSI, and ERP sources: 1) left superior/middle temporal gyri for PEPSI, fMRI, and ERP Objects

N100 (blue circles), 2) left superior/middle temporal gyri for fMRI and ERP Objects N100 (green circles), 3) left middle temporal gyrus for fMRI and ERP Objects N100 (orange circles) and 4) left superior frontal gyrus for fMRI and ERP Pixelated Objects N400 (lavender circles). Both early and late ERP sources are reflected in this fMRI volume, and sources from both the Objects and Pixelated Objects conditions are reflected.

2) Objects vs. Baseline

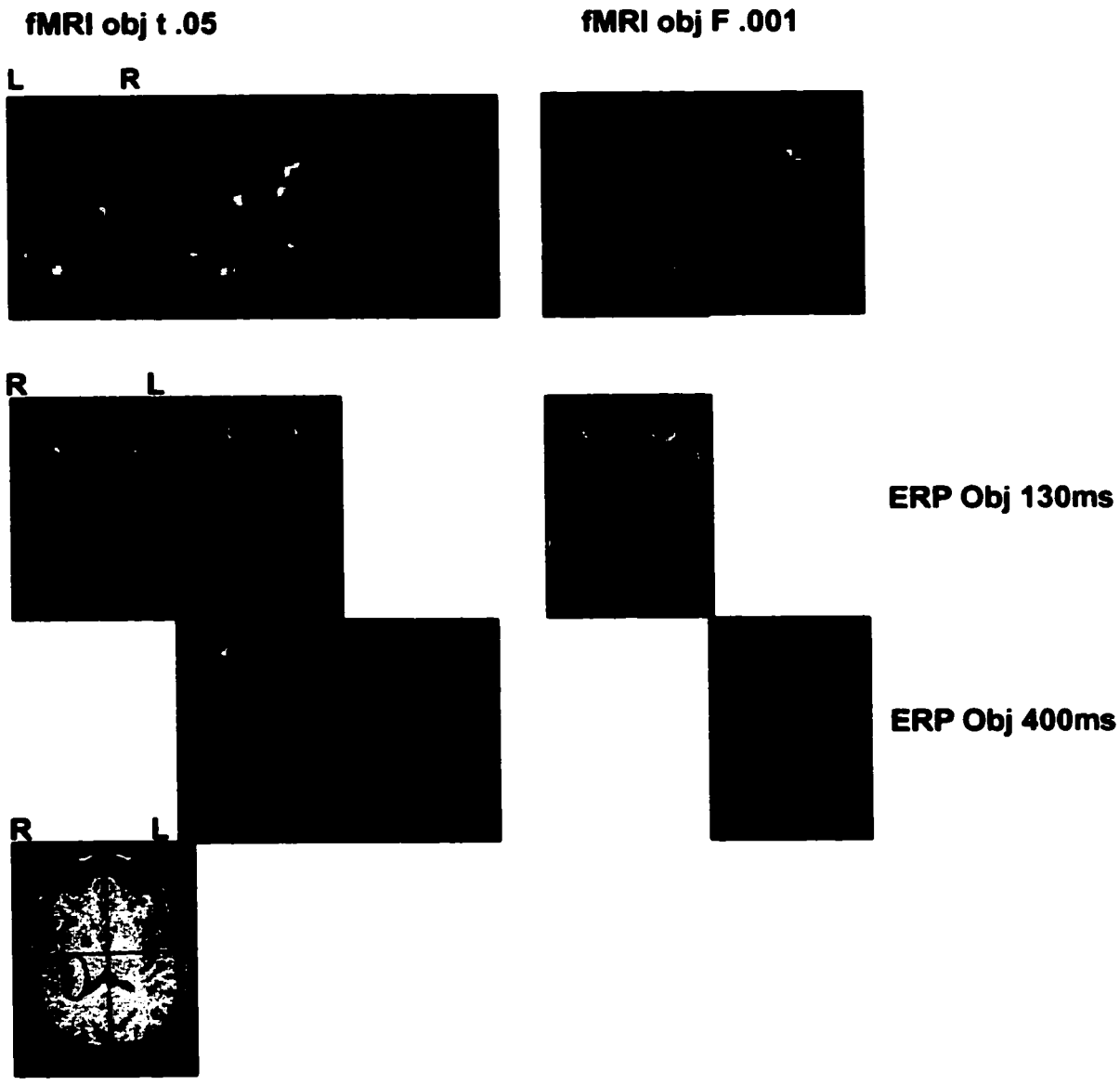

Figure 37. Comparisons across modalities for Objects vs. Baseline for fMRI, PEPSI, and ERP sources.

Several matches occur across modalities in this condition: 1) right insula for fMRI (*t*) and PEPSI (plum circles), 2) left middle temporal gyrus (dark blue) and occipital gyrus (pale blue) for fMRI (*t*) and ERP Objects N100, 3) right inferior frontal gyrus for fMRI and ERP Objects N400 (green), 4) right middle frontal gyrus for fMRI (*t*) and ERP Objects N400 (orange). Matches also occur with the fMRI *F*-contrast. These matches are in left middle temporal gyrus for fMRI (*F*) and ERP Objects N100 and in right superior frontal gyrus for fMRI (*F*) and ERP Objects N400. Overall for the Objects condition, posterior activations in fMRI correspond to N100 ERP sources while anterior activations in fMRI correspond to N400 ERP sources. Mesial fMRI activations tend to correspond with PEPSI activations.

3) Pixelated Objects vs. Baseline

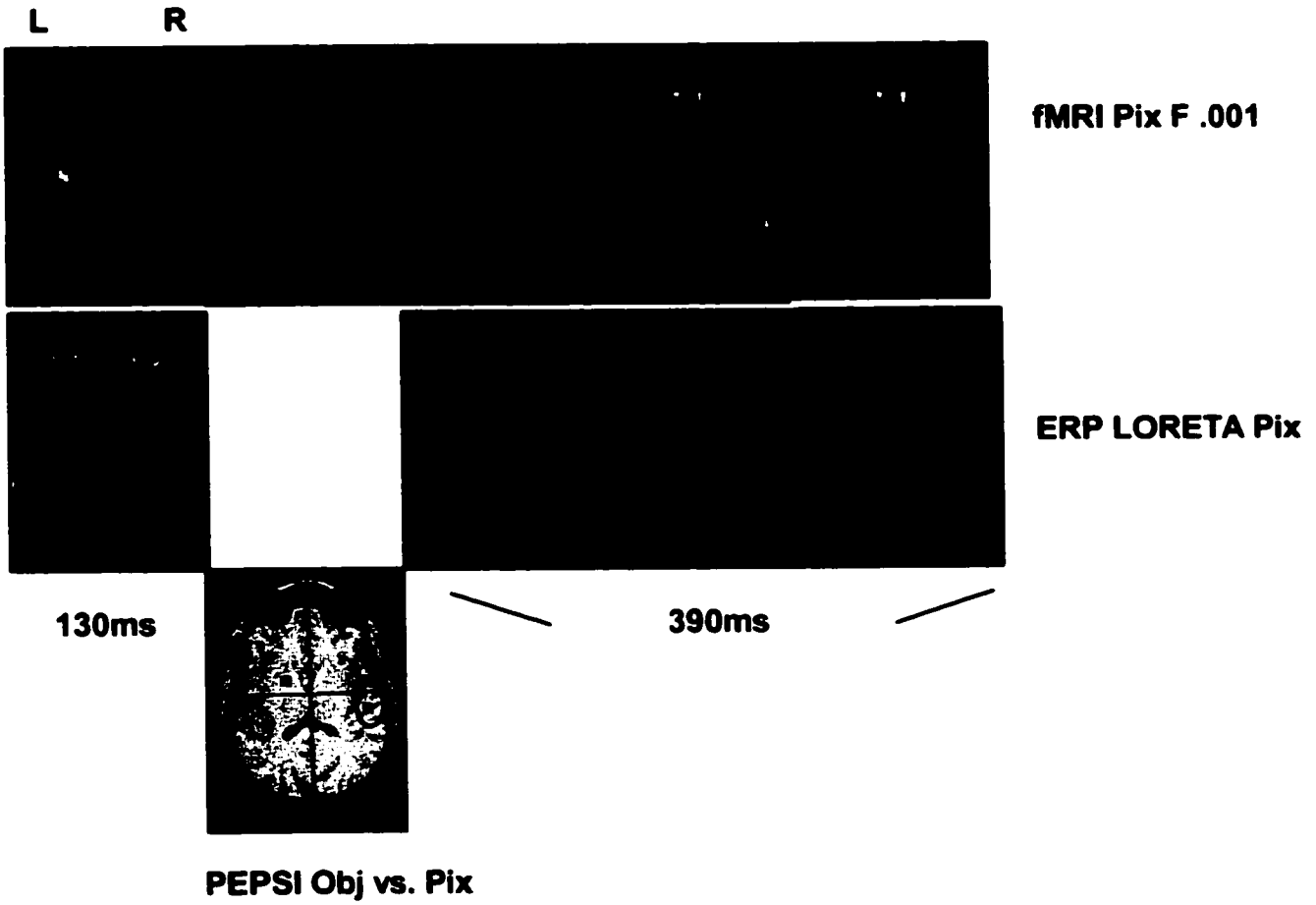

Figure 38. Comparisons across modalities for Pixelated Objects vs. Baseline for fMRI, ERP, and PEPSI.

Matches occur across modalities for the following: 1) left middle temporal gyrus for fMRI and ERP Pixelated Objects N100 (blue circles), 2) left superior temporal gyrus for fMRI and PEPSI (green circles), 3) right superior frontal gyrus/cingulate for fMRI and ERP Pixelated Objects N400 (this becomes a bilateral match with more superior slices).

Similar to the Objects condition, posterior fMRI activations for Pixelated Objects correspond to ERP Pixelated Objects N100 sources and anterior fMRI activations correspond to ERP Pixelated Objects N400 sources. Again, mesial fMRI activations tend to correspond with PEPSI activations.

P136

CSM Mapping

This patient showed right hemisphere language dominance with the Wada test. A large right frontal temporoparietal exposure allowed stimulation of sites in a region bounded by the ventral portions of pre- and post-central gyri superiorly, the middle temporal gyrus inferiorly, the inferior frontal gyrus (operculum) anteriorly, and the angular gyrus posteriorly. Significant language disruption was found in the ventral postcentral gyrus (tag 36), the posterior middle temporal gyrus (tag 29); a near-significant language disruption was found in a relatively anterior portion of the superior temporal gyrus (tag 24). The tagged cortical surface is shown below in Figure 39. Areas considered significant for language disruption are boxed in blue (A) and indicated with orange markers (B) on the 3-D reconstruction.

A B

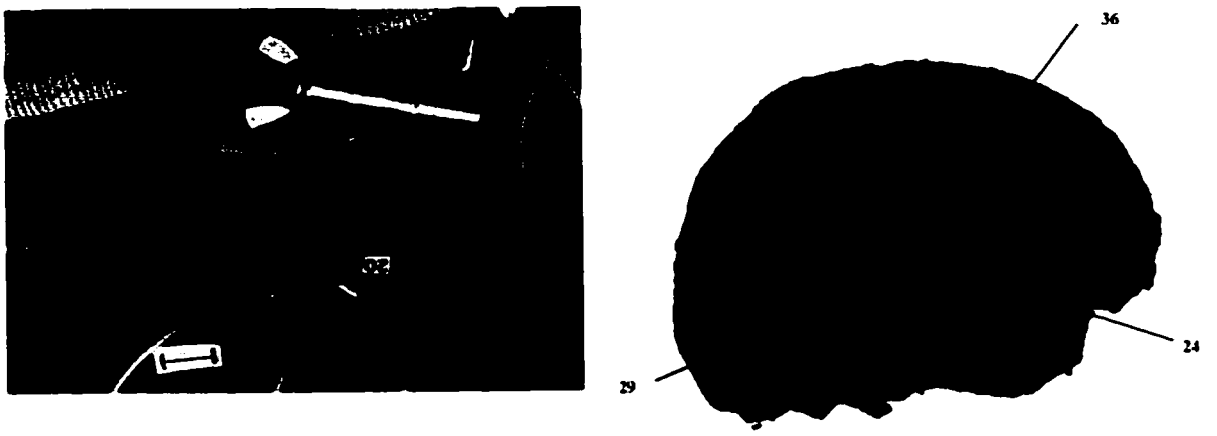

Figure 39. Stimulation sites for P136. Tags boxed in blue (A) and orange sites (B) signify language disruption.

Semantic Category and Error Types

Table 8 below lists the sites stimulated for language testing, the Error:Trial ratio, *p*-values from the Fisher's Exact Test, the location of each site, error items, and error types. The coding scheme was developed in the Corina Cognitive Neuropsychology Laboratory (Corina, 2001), and is shown in Appendix B.

Table 8. Naming errors in stimulated sites for P136. Shaded areas indicate sites significant ($p < 0.05$) for language disruption.

P136 (IO) Site	Errors/ Trials	Fisher's *p*-value	Location	Item	Error type
1	Motor	N/A	Ventral PoG	N/A	N/A
22	1/3	0.41	Ant MTG	Paintbrush	Filler (target)
23	1/5	0.581	Ant STG	Motorcycle	No target
24	3/6	0.065	Ant STG	Television Lamp Paintbrush	Repeated successive attempts/approx. No target Short delay (target)
25	1/3	0.41	Med MTG	Bear	Filler (no target)
26	1/6	0.646	Med STG	Horse	Perseveration on "Elephant" (self-corrects to target)
27	1/3	0.41	Med STG	Lion	Filler (off target)
28	0/4	0.523	Pos STG		
28S	0/1	0.848	Pos STG		
28I	0/4	0.523	Pos MTG		
29	5/6	0.001	Pos MTG	Pants Eye Bicycle Window Mouse	Off target Short delay (target) No target Filler, Long delay (target) Filler (no target)
30	0/3	0.613	Pos STG		
30S	1/3	0.41	SMG	Squirrel	Short delay, filler (no target)
31	0/4	0.523	Angular G		
31S	0/1	0.848	SMG		
32	1/6	0.646	Pos STG	Desk/Table	Off target
33	1/3	0.41	Ventral PoC	Moon	Semantic paraphasia ("Sun")
34	0/3	0.613	Ventral PreC		
35	1/3	0.41	IFG (Op)	Screwdriver	Short delay (target)
36	2/2	0.028	Ventral PoC	Eye Doll/Baby	No target Long delay (target)

Items were categorized in one of two semantic categories: 1) artifact, or 2) natural/animal. The reliability of errors in a specific semantic category was calculated relative to the semantic category of the baseline error rate during a) all stimulated trials and b) stimulated trials at significant sites only. Errors that are made following a stimulation error, but in the absence of stimulation, are termed FSE-type errors. The semantic category of FSE's and non-FSE's were calculated relative to the semantic category of the trial which followed a stimulated trial. This calculation was done for all stimulated sites and for significant sites only.

A total of 19 errors occurred during the 69 stimulated trials. Eleven of the nineteen items were artifacts; 6 of these 11 items were either off-target or missed (no target), while the remaining 5 items were named with hesitations. Of the 19 total errors, 8 items were natural/animal. Five items were animals; 4 out of these 5 errors were missed or off-target, while 1 item was named as an animal shown earlier (perseveration) but the patient self-corrected to the appropriate name. The remaining 3 errors were on natural objects; the item "eye" was missed once and named once with a hesitation. The only semantic paraphasia from all the errors occurred with the natural item "moon". The occurrence of an error was not dependent on the semantic category of the item, (artifact, natural/animal; Pearson chi-square $X^2 = 0.532$, Fisher's Exact Test $p = 0.361$).

Of the 10 errors at sites significant for language, 7 items were artifacts; 4 of these items were missed and 3 were named with hesitations. One natural item occurred twice ("eye"), which was missed once and named once after a delay. The one animal item was

missed. The occurrence of an error was not dependent on the semantic category of the item (artifact, natural/animal; Pearson chi-square $X^2 = 0.852$, Fisher's Exact Test $p = 0.689$).

Errors during non-stimulated trials are described below. Errors that are made following a stimulation error, but in the absence of stimulation, are termed FSE-type errors; these are considered separately from other non-stimulation errors because of their close proximity to a stimulation trial. Table 9 below describes these errors for P136.

Table 9. Naming errors during non-stimulated trials for P136. FSEs are shaded.

Trial #	After Stimulation of Site #	Item	Error type
22	30S	Ruler	Short delay (target)
32		Stove	Filler (target)
50	24	Lamp	Semantic Paraphasia ("Light")
62	33	Truck	Filler, Semantic Paraphasia ("Train, Boat")
83	29	Table	Filler (no target)
88		Squirrel	Semantic paraphasia ("Mouse")
98	29	Candle	Long delay (target)
99		Stove	Long delay (target)
100		Brush	Long delay (target)
121	23	Chair	No target
137	33	Train	Semantic paraphasia ("Bus, Semi")
140	29	Coat	Long delay (target)
152		Airplane	Filler (target)
153		Ball	Filler (target)

Eight FSE's were made; 3 of these items showed semantic paraphasias, 2 items were missed (no target), and 3 items were named correctly after hesitations. All errors were made on artifact items, but the occurrence of an error was independent of the semantic category of the item (artifact, natural/animal; Pearson chi-square $X^2 = 0.085$, Fisher's Exact Test $p = 0.093$). Four FSE's occurred after trials at significant language sites (24, 29); 1 item showed a semantic paraphasia, 1 item was missed, and 2 items were named after hesitations. The occurrence of an error was not dependent on the semantic category of the item (artifact, natural/animal; Pearson chi-square $X^2 = 0.134$, Fisher's Exact Test $p = 0.21$).

Six non-FSE errors occurred; 1 item showed a semantic paraphasia, and the remaining 5 items were named after hesitations. The semantic paraphasia was on a natural/animal item while the hesitation errors occurred with artifacts. The occurrence of an error was not dependent on the semantic category of the item (artifact, natural/animal; Pearson chi-square $X^2 = 0.533$, Fisher's Exact Test $p = 0.468$). Figure 40 below summarizes the above errors.

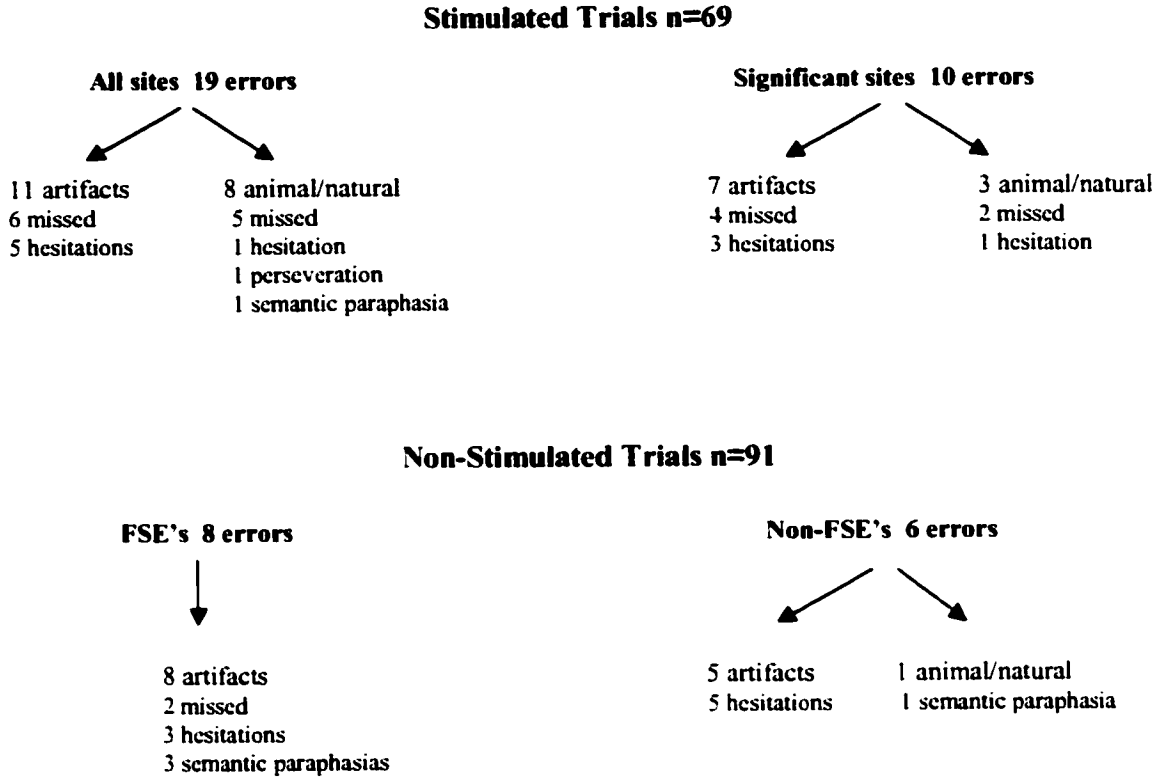

Figure 40. Semantic category and error types for stimulated and non-stimulated trials for P136. In all cases, the occurrence of an error was not dependent on the semantic category of the item (Fisher's Exact Tests, $p > 0.2$).

PEPSI

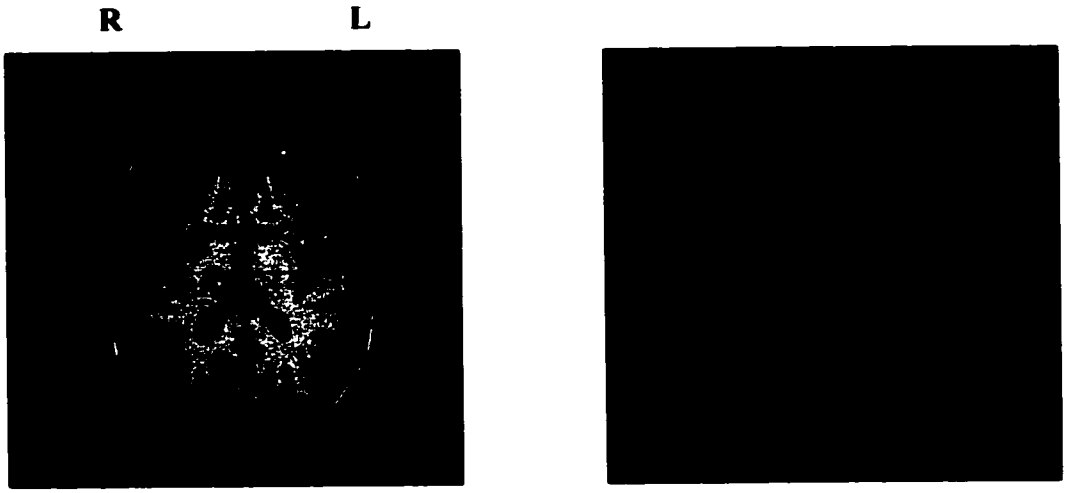

Figure 41. PEPSI activations showing increases in lactate during visual object naming.

The largest activation cluster is seen in the posterior right middle and inferior temporal gyri, with weaker activations in the left middle and inferior temporal gyri, and the occipital gyrus (grey voxels, right image). Activations are also seen in the basal ganglia (right putamen, claustrum, left thalamus) as well as the left insula.

fMRI

Three fMRI datasets are shown here: 1) Objects vs. Pixelated Objects, 2) Objects vs. Baseline, 3) Pixelated Objects vs. Baseline.

1) Objects vs. Pixelated Objects ($p < 0.005$) *t*-contrast

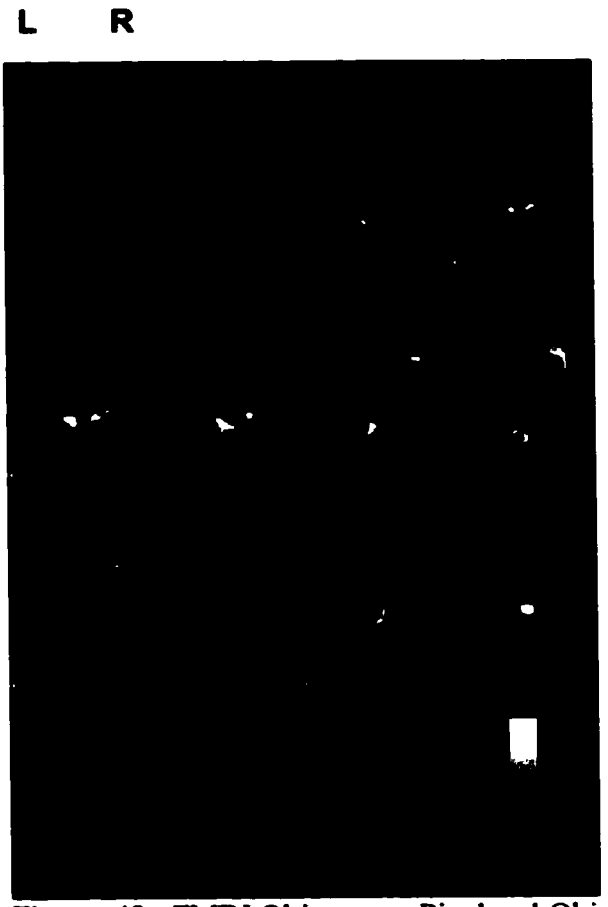

Figure 42. FMRI Objects vs. Pixelated Objects ($p < 0.005$) *t*-contrast.

Although some activations occur bilaterally in the cerebellum and occipital gyrus, this subject shows relatively strong lateralization to the right hemisphere, which was determined preoperatively to be dominant for language. Right-lateralized activations include the cuneus, cingulate, superior temporal gyrus, insula, and orbitofrontal gyrus. Occipital and cuneus areas are likely attributable to early visual processing while the

STG is consistent with the visual object naming network of regions. Table 10 below shows local maxima for this volume in SPM coordinates, associated *t*-values, and anatomical location.

Table 10. FMRI Objects vs. Pixelated Objects ($p < 0.005$) *t*-contrast.

(X,Y,Z)	*t*-value	Location
(-6, 50, 11)	4.22	Left OcG (cuneus border)
(9, -28, 53)	3.78	Right cingulate
(16, -43, 11)	3.67	Right OcG
(5, -73, 29)	3.66	Right (midline) cuneus
(47, 17, 22)	3.52	Right STG/TTG
(35, 21, 34)	3.32	Right insula
(17, 40, 34)	2.97	Right OFG
(20, -21, -7)	2.94	Right cerebellum
(-6, -43, -13)	2.87	Left cerebellum
(54, -36, 17)	2.82	Right MTG/STG border
(-21, 14, 41)	2.81	Left putamen
(-6, -39, -1)	2.75	Left cerebellum
(13, -13, -1)	2.75	Right pons

2) Objects vs. Baseline ($p < 0.01$) *F*-contrast.

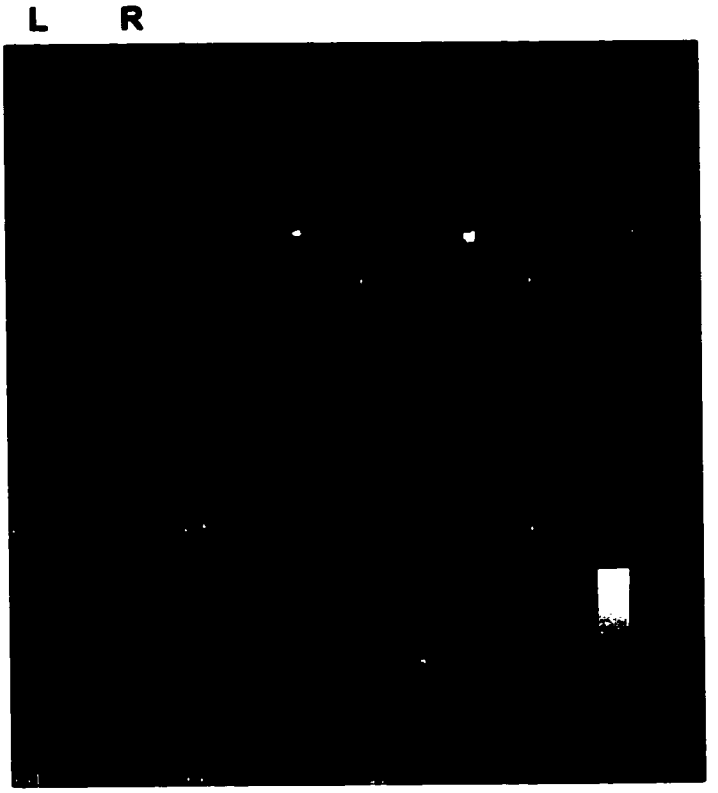

Figure 43. FMRI Objects vs. Baseline ($p < 0.01$) *F*-contrast.

Inferior and posterior activations are predominantly right-lateralized, occurring in the striate and occipital gyrus. The right insula is also active. Left-sided activations are seen in the fusiform, inferior temporal, orbitofrontal, and cingulate gyri. A fair amount of basal ganglia activation is also seen, which could be due to a low signal-to-noise ratio for

this subject.[6] Table 11 below shows local maxima for this volume in SPM coordinates, associated *F*-values, and anatomical location.

Table 11. FMRI Objects vs. Baseline ($p < 0.01$) *F*-contrast.

(X,Y,Z)	*F*-value	Location
(31, -62, -1)	18.59	Right OcG
(20, -62, 11)	14.92	Right OcG
(-17, -1, 53)	13.93	Left basal gang (thalamus)
(-29, -31, 23)	13.15	Left fusiform/OcG
(-2, 14, 47)	*12.94*	*Artifact--ventricle*
(20, -13, 53)	*10.27*	*Artifact -- ventricle*
(16, -73, 17)	9.38	Right OcG
(-6, -39, 35)	8.78	Left cingulate
(35, 2, 34)	8.50	Right insula
(-51, -28, 5)	8.49	Left ITG
(9, -28, 29)	8.27	Right cingulate
(-29, -58, 29)	8.10	Left angular gyrus
(2, 40, 22)	8.07	Midline cingulate
(-13, 40, 35)	8.01	Left OFG
(17, 10, 53)	7.85	Right basal gang (caudate)
(24, -65, 29)	7.49	Right OcG
(20, -77, 11)	7.46	Right striate/OcG
(24, -2, 41)	7.42	Right basal gang (putam)
(-10, -13, 35)	7.41	Left basal gang (thalamus)
(1, -65, 5)	7.34	Midline striate

[6] A malfunction started to occur in the RF amplifier while collecting fMRI data for this subject. The 90 degree pulses which are necessary for gradient spin-echo techniques were slightly compromised. This malfunction did not affect PEPSI data because increased pulse widths can be used to compensate. The result is a somewhat lower signal-to-noise ratio.

3) Pixelated Objects vs. Baseline ($p < 0.005$) F-contrast.

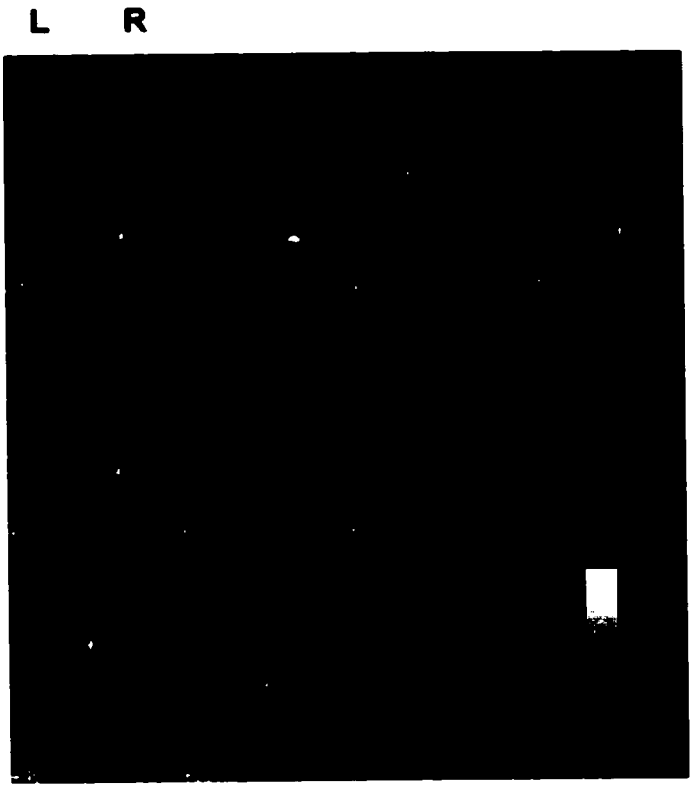

Figure 44. FMRI Pixelated Objects vs. Baseline ($p < 0.005$) F-contrast.

Activations predominantly right-lateralized include occipital and cuneus areas, fusiform gyri (though some left-sided activation occurs as well), and transverse (superior) temporal gyrus. Bilateral activations occur in the orbitofrontal gyrus, insula, and cingulate. Table 12 below shows local maxima for this volume in SPM coordinates, associated F-values, and anatomical location.

Table 12. FMRI Pixelated Objects vs. Baseline ($p < 0.005$) *F*-contrast.

(X,Y,Z)	*F*-value	Location
(31, -58, -1)	18.12	Right OcG
(-2, 14, 47)	16.60	Left bas gang (caudate)
(24, -47, 17)	14.80	Right cuneus
(17, 40, 34)	14.44	Right gyrus rectus/OFG
(-51, -28, 5)	14.04	Left ITG
(1, -24, 53)	13.84	Midline/right cingulate
(35, 28, 28)	13.65	Right insula
(-17, -2, 5)	13.64	Left pons
(-29, -31, 23)	13.11	Left fusiform
(9, -28, 29)	12.94	Midline/right cingulate
(-10, -47, -1)	12.35	Left cerebellum
(46, 2, 28)	12.22	Right TTG
(-13, 40, 35)	12.16	Left OFG
(31, -32, 17)	12.09	Right fusiform
(28, -2, 41)	11.66	Right insula (border claus)
(-6, -43, 47)	10.78	Left cingulate
(-32, 2, 35)	10.70	Left insula
(-21, 25, 41)	10.25	Left bas gang (claustrum)
(2, 40, 28)	9.25	Midline gyrus rectus
(35, -6, 17)	8.91	Right fusiform
(35, 13, 16)	8.90	Right fusiform
(-17, 2, 53)	8.89	Basal ganglia (caud/putam)

ERP

The ERP pilot study described in Chapter 2 demonstrated in normal subjects that blocking the stimuli prevented P300 effects due to novelty or surprise from occurring with pixelated objects. These results were replicated with the control subject P138. This subject, however, was not consistent with this pattern and shows a P300 effect for pixelated objects which obscures the N400 component. It will be shown below that a clear N400 component is absent for this subject in the Pixelated Objects condition. The

figure below (Figure 45) shows grand mean waveforms for each of the 64 electrodes for the Objects (solid lines) and Pixelated Objects (dashed lines) conditions.

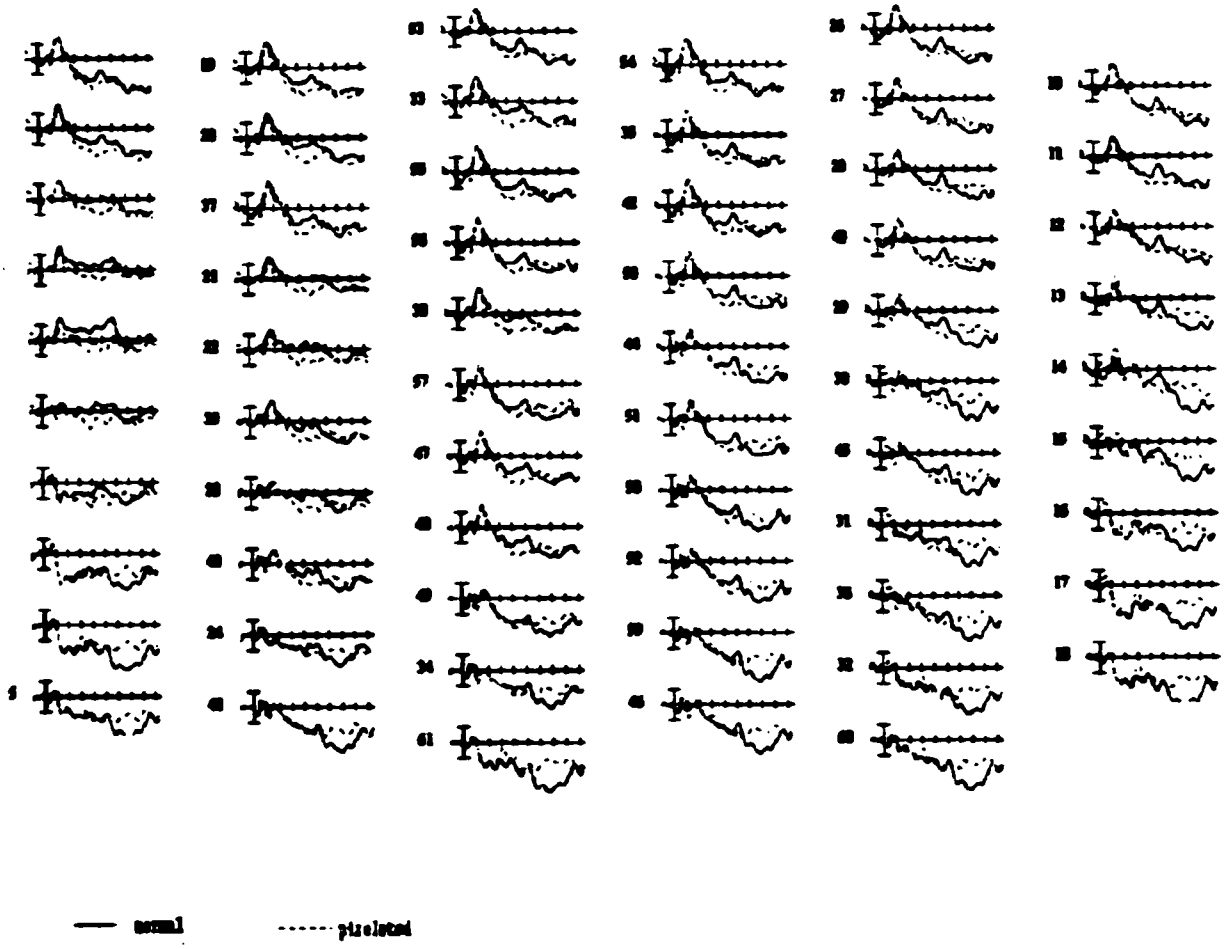

Figure 45. Grand mean for Objects (solid lines) and Pixelated Objects (dashed lines) for all channels for P136. X-axis is in 100msec increments, y-axis is in microvolts.

An early negative-going peak corresponding to the N100 can be seen at 160msec in both conditions, which is most prominent at anterior sites, both laterally and along the midline.

A later negative-going peak corresponding to the N400 occurs at 515msec in the Objects condition and is seen at midline and right lateral sites, particularly at anterior sites. The Pixelated Objects condition shows no obvious N400 component.

Objects

Both the N100 and N400 components are seen in this condition. The spatial distribution of these components across the scalp are seen in Figure 46 (A) below. The N100 component occurs between 100-260msec with a peak amplitude at 160msec and is most prominent at midline and bilateral anterior sites; amplitudes are reduced at extreme lateral sites and are absent at posterior sites. The N400 component occurs between 450-560msec with a peak amplitude at 515msec and is most prominent at mesial and left anterior sites. Amplitudes are reduced or absent at posterior sites bilaterally. These distributions are also illustrated in the field and CSD/Laplacian maps in Figure 46 (B) below.

A

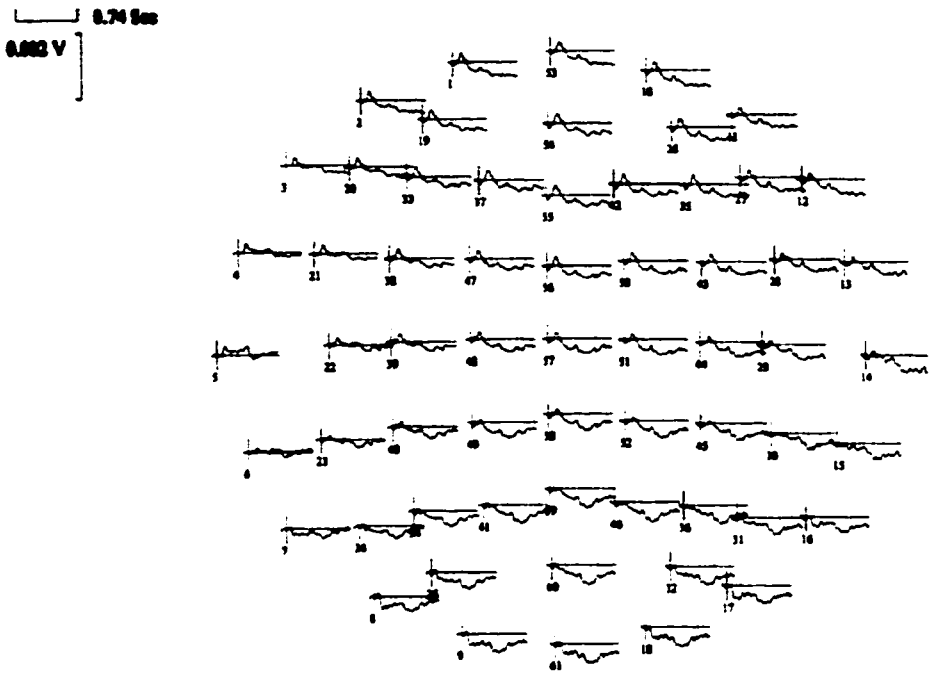

B

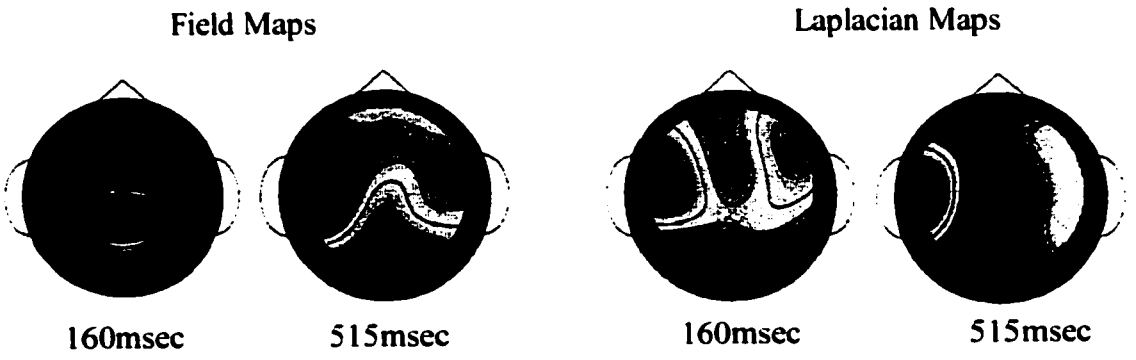

Figure 46. (A) 64-channel orientation of ERP waveforms for the Object condition. Frontal areas are at the top, occipital areas at the bottom, time and voltage scale bars are in the top left corner. (B) Top views of field and Laplacian (current source density) maps at 160msec and 515msec for objects. Areas of interest are in blue for the field map and in red for the Laplacian map.

Waveforms across electrode sites are superimposed and shown below in Figure 47 to better visualize the peak amplitudes of the N100 and N400 components which were subjected to LORETA analysis.

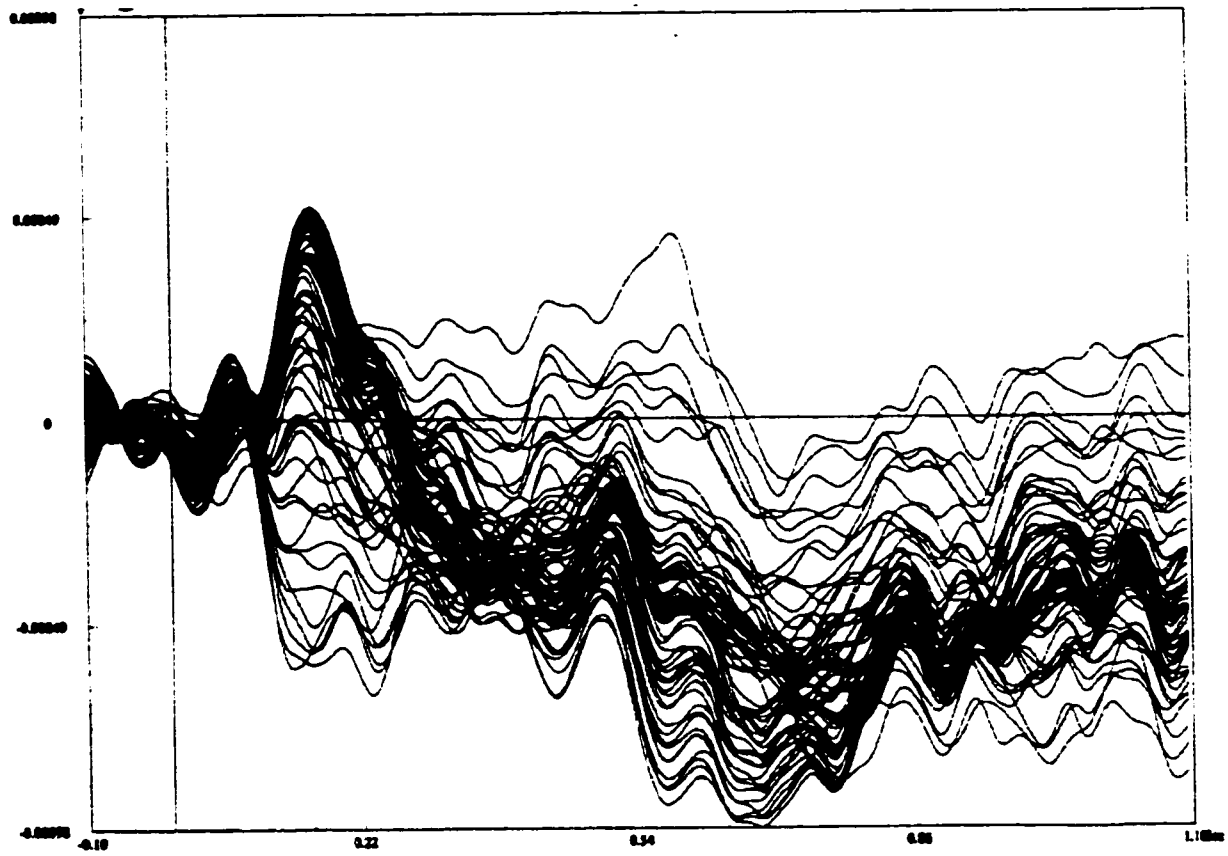

Figure 47. Superimposed 64-channel waveforms for the Object condition. Negative voltages are plotted upwards, positive voltages are plotted downwards. Negative peaks corresponding to N100 and N400 components occur at 160 and 515msec respectively.

It can be seen in Figure 48 below that sources vary across the timecourse of the waveform and are temporally bound by the N100 and N400 components, implying that

each component has distinct neural generators. Sources are seen in bilateral posterior (occipital) areas from 100-260msec, mainly in left temporal areas but occasionally extending superiorly and with a second, weaker right posterior source from 280-460msec. Left temporal sources are seen consistently from 470msec until 610msec.

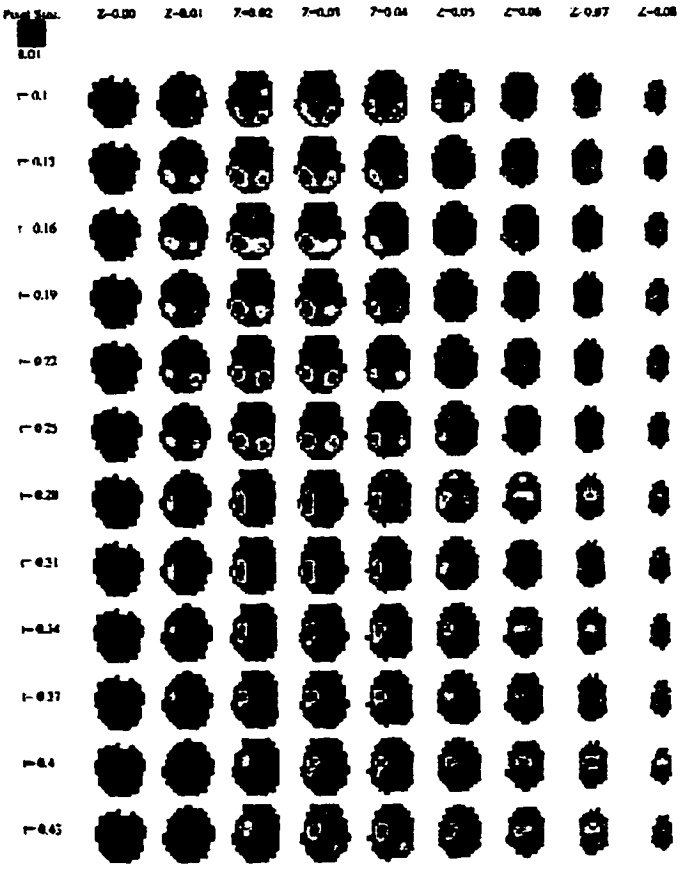

Figure 48. Source maps for the object condition from 100-610msec in 30msec increments. Sources are differentiated for the N100 (100-260msec) and N400 components (470-560msec).

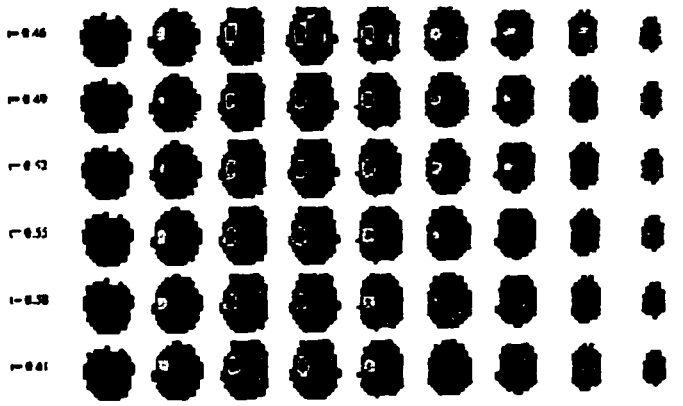

Figure 48. Continued.

The peak amplitude for the N100 component occurs at 160msec. The algorithm is applied to this timepoint and a primary source is seen in the posterior left hemisphere with a secondary source in the posterior right hemisphere (Figure 49 (A)), specifically in the left middle and superior temporal gyri, extending posteriorly and superiorly out of the left occipital gyrus into the inferior temporal gyrus and cuneus. The second source sits on the border of the right inferior and middle temporal gyri (Figure 49 (B)).

A

B

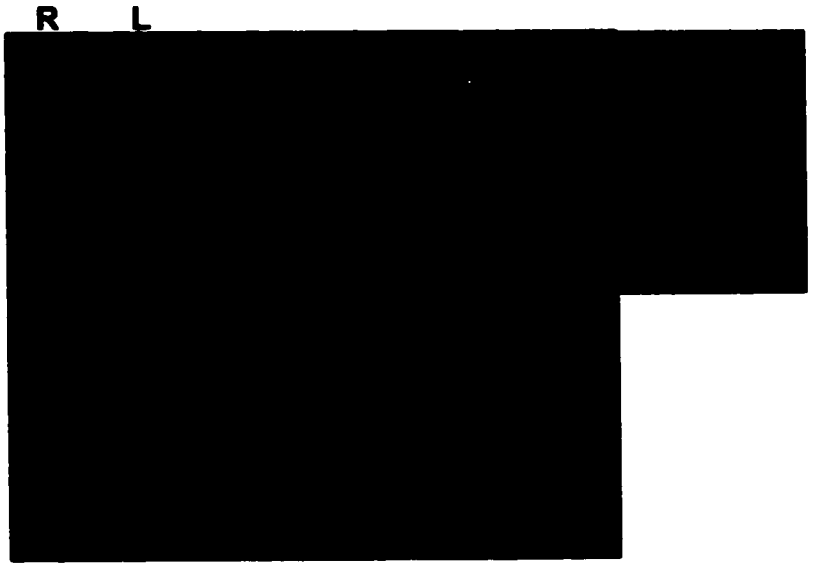

Figure 49. (A) Source maps at 160msec for objects. Pixels = $1cm^3$, direction is inferior to superior (L-R), axial views (B) The main source is seen in the left inferior, middle, and superior temporal, and occipital gyrus. A secondary source is in the right inferior and middle temporal gyri when overlayed onto structural MRI scans.

The peak amplitude for the N400 component occurs at 515msec. The source is seen in left mesial and superior areas (Figure 50 (A)), specifically in the left superior temporal

gyrus and insula, and extends superiorly to the frontal operculum and pre/post-central gyri (Figure 50 (B)).

A

B

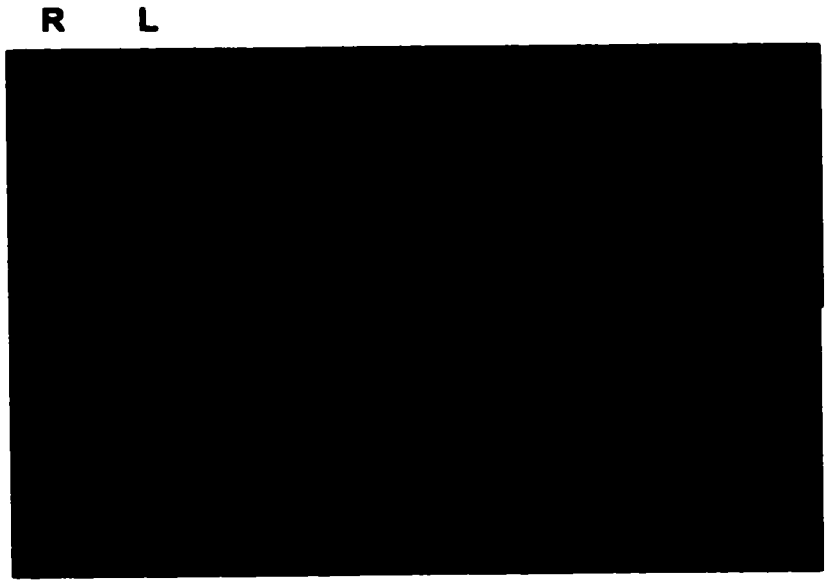

Figure 50. (A) Source maps at 515msec for objects (B) The source is seen in the left insula, frontal operculum, and pre/post-central gyri when overlayed onto structural MRI scans.

For the Objects condition overall, sources for the N100 component are seen in posterior areas consistent with visual processing while the N400 component occurs in relatively more anterior and superior areas, consistent with semantic processing in the object naming network described earlier.

Pixelated Objects

The spatial distribution of the N100 and N400 components across the scalp are seen below in Figure 51 (A). The N100 component occurs between 100-230msec with a peak amplitude at 160msec and is most prominent at anterior midline and right lateral sites; amplitudes are reduced at anterior left lateral sites and severely reduced or absent across posterior sites. The N400 component is essentially absent in this condition. The distribution for the N100 component is illustrated in field and Laplacian maps in Figure 51 (B) below.

A

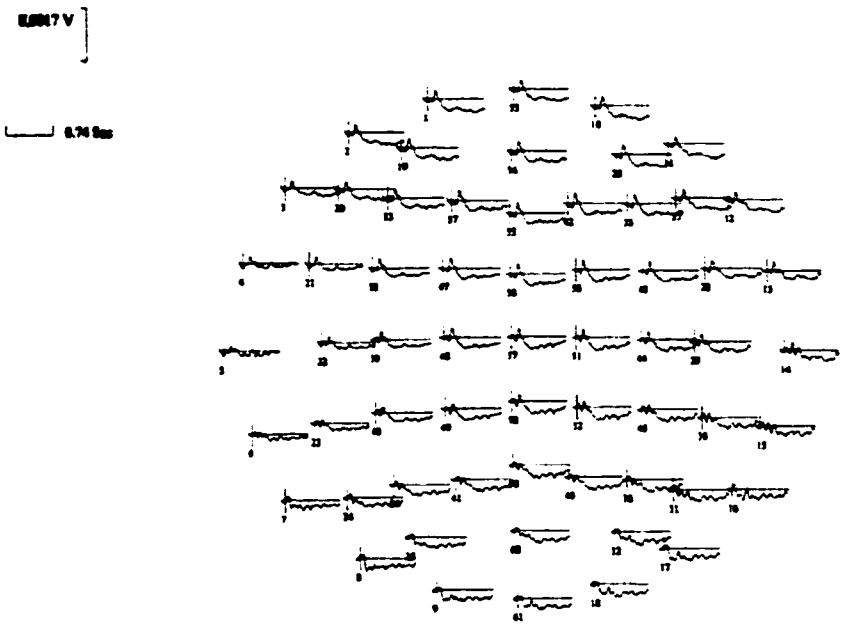

B

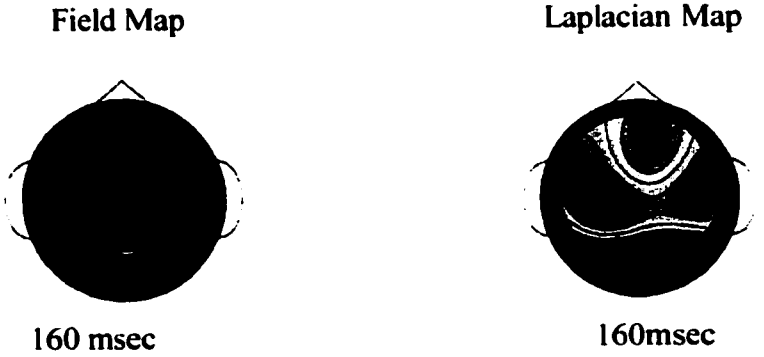

Figure 51. (A) 64-channel orientation of ERP waveforms for the Pixelated Object condition. (B) Top views of field and Laplacian (current source density) maps at 160msec for pixelated objects. Areas of interest are in blue for the field map and in red for the Laplacian map.

Waveforms across electrode sites are superimposed and shown below prior to source estimation in Figure 52. Note that there are several negative-going peaks after 340msec, but no clear N400 component is present.

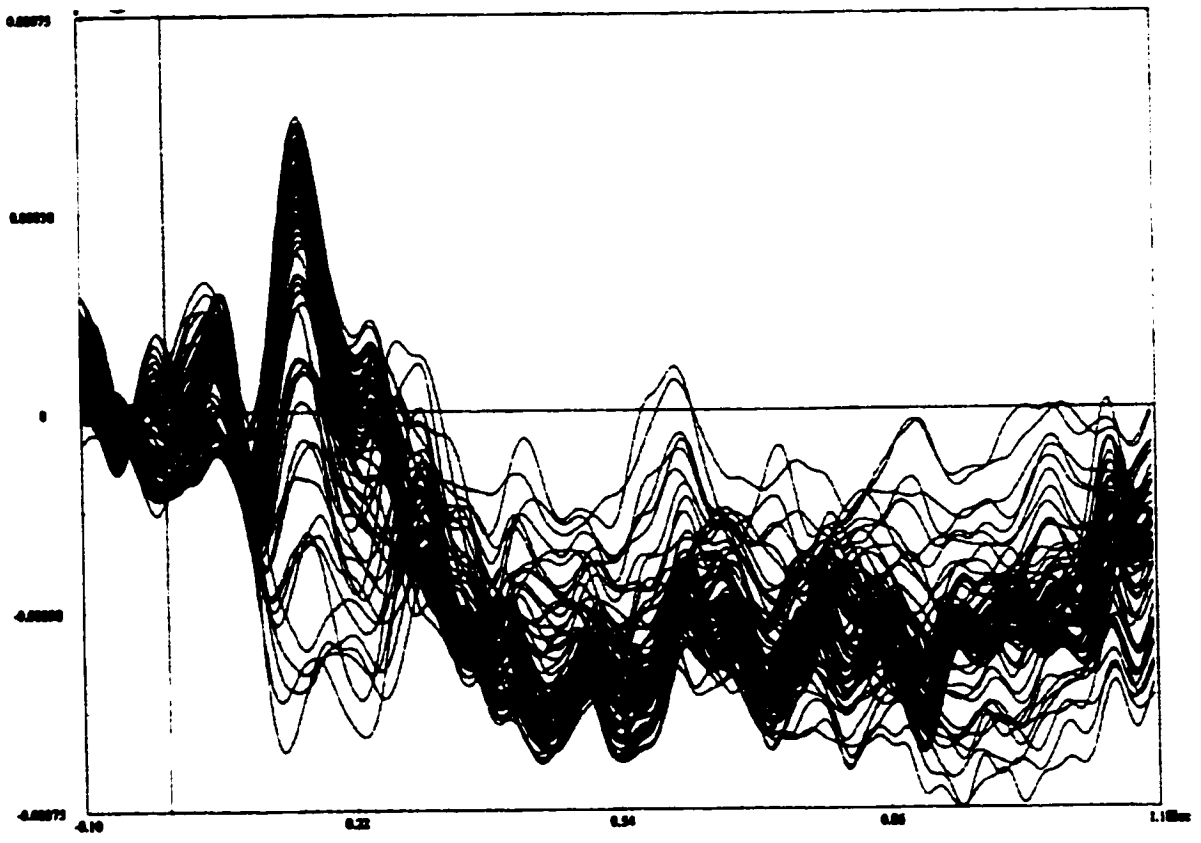

Figure 52. Superimposed 64-channel waveforms for the Pixelated Object condition. Negative voltages are plotted upwards, positive voltages are plotted downwards. A negative peak occurs at 160msec, but a prominent N400 component is not seen.

It can be seen below (Figure 53) that sources vary across the timecourse of the waveform. The N100 component shows a consistent source between 100-230msec and sources vary from bilateral temporal to right temporal, bilateral frontal, and left temporal areas with the negative-going peaks that appear across the waveform after 300msec.

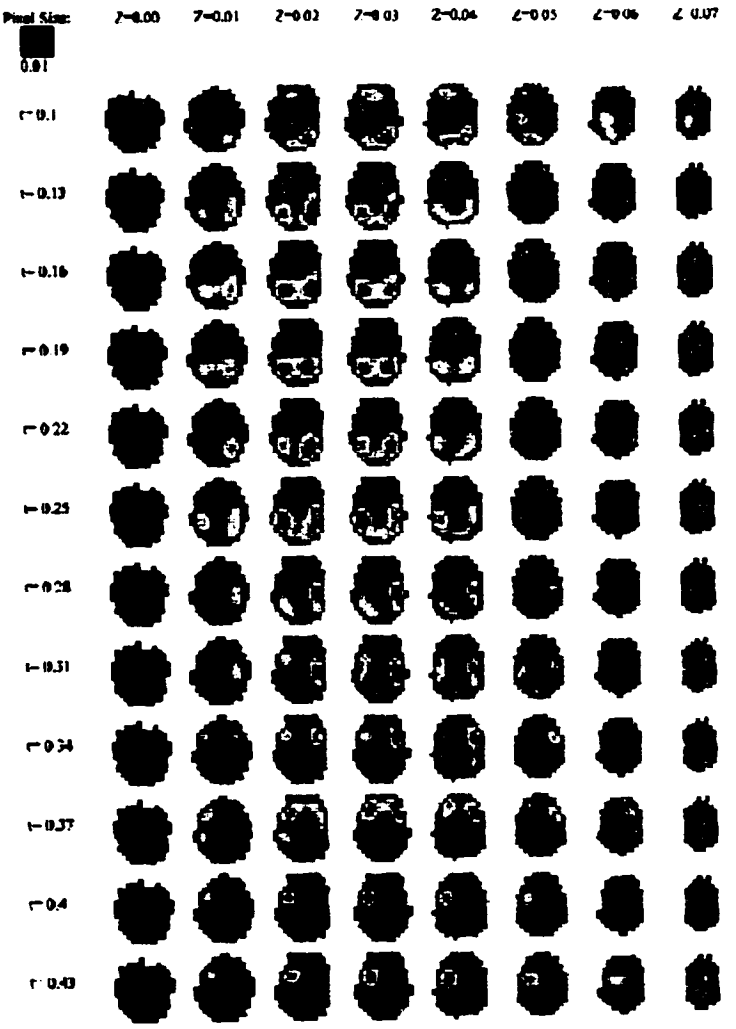

Figure 53. Source maps for the pixelated object condition from 100-700msec in 30msec increments. Sources are differentiated for the N100 (100-230msec) and the remainder of the waveform. [Additional negative peaks and associated sources are seen at 340, 400, 505, 620, and 685msec.]

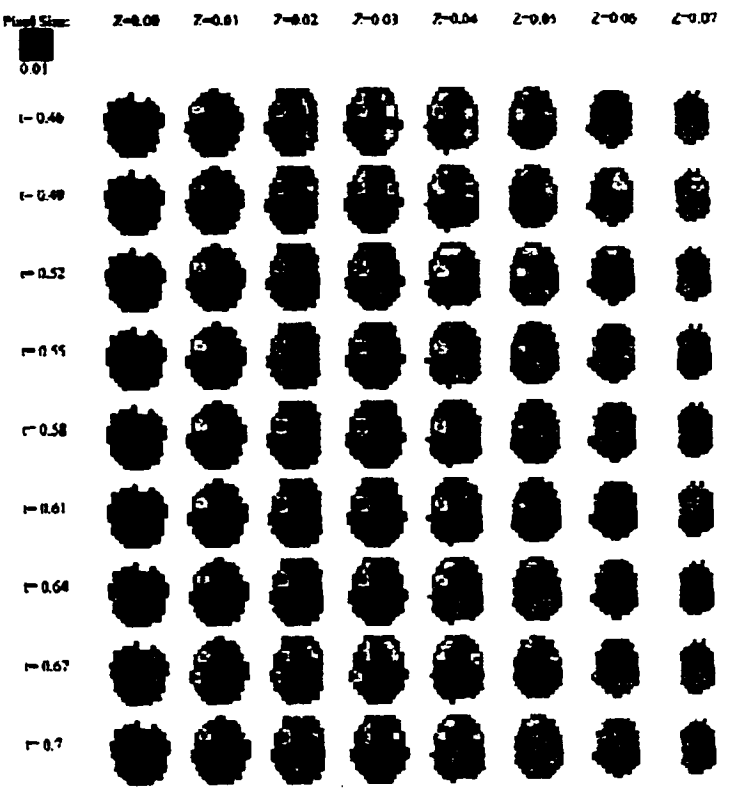

Figure 53. Continued.

The peak amplitude for the N100 component occurs at 160msec. The algorithm is applied to this timepoint and two sources are seen (Figure 54 (A)). Sources are bilateral, involving the inferior and middle temporal gyri and extending posteriorly and superiorly into the occipital gyrus and superior temporal gyrus (Figure 54 (B)).

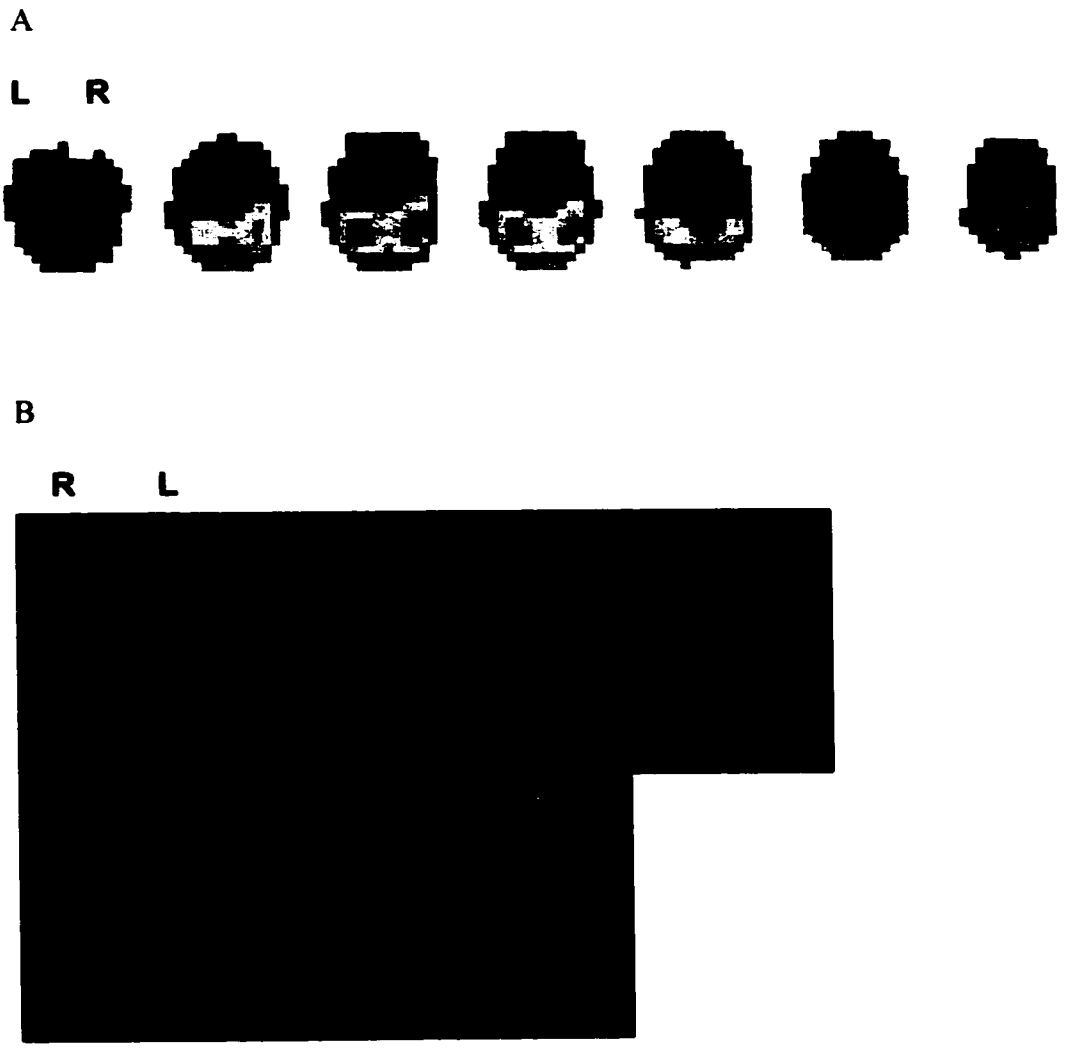

Figure 54. (A) Source maps at 160msec for Pixelated Objects (B) Bilateral sources are seen in the left and right inferior and middle temporal gyri extending posteriorly/superiorly into the occipital gyrus and superior temporal gyrus.

Compared to the object condition, where the main source was left lateralized and a weaker source was right lateralized, the pixelated object condition shows two equally strong sources for the N100 component in posterior left and right hemispheres. A summary of sources for the Object and Pixelated Object conditions are listed in the table below (Table 13). Common sources for the N100 component across conditions are limited to bilateral middle temporal gyri. The Objects condition shows mainly left-lateralized sources (with weak right-lateralized sources in ITG/MTG), while the Pixelated Objects condition shows bilateral sources throughout posterior occipital and temporal areas. Posterior sources for the N100 component in both conditions are consistent with early sensory (visual) processing, while the N400 component for Objects is more anterior and superior, in areas consistent with semantic processing.

Table 13. Summary of ERP sources across conditions.

Objects	**Pixelated Objects**
N100	*N100*
Left MTG/STG	Bilateral ITG/MTG
Left OcG	Bilateral OcG
Left ITG	Bilateral STG
Left cuneus	
Right ITG/MTG	
N400	*N400 N/A*
Left insula	
Left TTG	
Left frontal operculum	
Left PrG/PoG	

Comparison across modalities

Two sets of comparisons are made below. These comparisons are between: 1) CSM sites and MR volumes (fMRI and PEPSI), and 2) fMRI, PEPSI, and ERP sources, which is further divided into comparisons for the Objects vs. Baseline and Pixelated Objects vs. Baseline conditions. Comparison 1 is made between CSM sites and PEPSI volume as well as between CSM sites and the MR volumes considered in the fMRI section for this subject: a) Objects (F-contrast) b) Pixelated Objects (F-contrast) c) Objects vs. Pixelated Objects (t-contrast). These volumes are displayed below (Figure 55) on the 3-D reconstructions of this subject's brain as per the method described in Poliakov et al. (1999). CSM sites and MR volumes are both displayed on the surface; activations with high intensities are displayed as brighter areas.

1) CSM and MR volumes

A

PEPSI Objects vs. Pixelated Objects

B

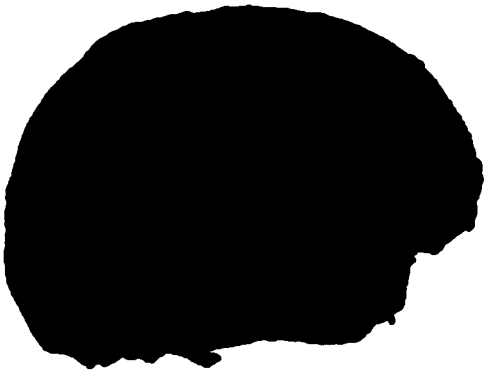

Objects vs. Baseline F-contrast

C

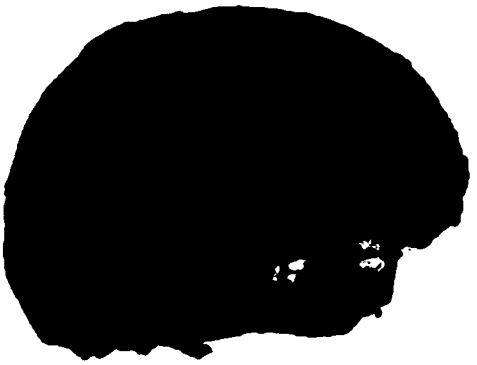

Pixelated Objects vs. Baseline F-contrast

D

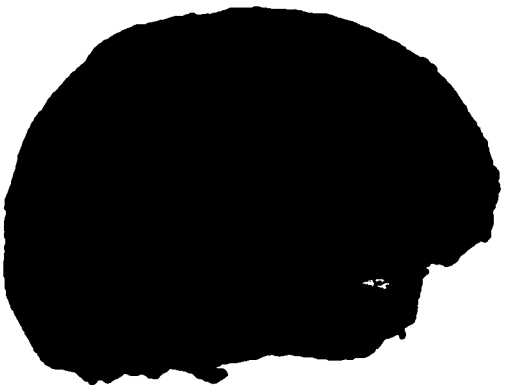

Objects vs. Pixelated Objects

Figure 55. CSM sites and MR volume activations displayed on 3-D reconstructed surfaces.

CSM sites are tested on the surface of the cortex. However, PEPSI and fMRI activations are rarely observed at the surface and are typically observed in deeper structures of the brain. The 3-D reconstruction of a subject-specific brain allows a quantitative comparison to be made between CSM sites and each volume of activation (Poliakov, 2002). PEPSI volumes are thresholded as described above, where voxels with *Z*-scores of 1 or higher are considered. FMRI volumes of activation are examined as thresholded data. Thresholded data is used because the comparison of interest is between the CSM sites and the peak fMRI activations identified through thresholds chosen during SPM analysis. This comparison analysis is a modification of the method used by Corina et al. (personal communication, 2001), who used values based on the log transform of the weighted average *t*-scores sampled in a 5mm radius at a given depth as the statisitic of interest. Here, the statistic of interest is a sum of voxel intensities that are weighted according to lateral displacement (*radius* parameter) and distance from the surface of the brain (*depth* parameter). Depth from a CSM site is rendered by an imaginary line that is drawn from the site to the center of the anterior and posterior commisure (AC-PC). Setting these parameters forms a "cone" shape where the weighting for a significant voxel declines as a) the distance from the surface increases, and b) as significant voxels are laterally displaced from the transect between the surface and the center of the AC-PC based on the function of the normal distribution. These weights are multiplied by the intensity of the voxel then summed together to give a final output value as in Eq. [2]:

$$\textbf{Value} = \sum I * W \qquad [2]$$

I = voxel intensity (t or F value from SPM volume)
W = w1 * w2
w1 = depth parameter d and is weighted according to a declining exponential function; higher weight is given to smaller depths, lower weight is given to larger depths
w2 = radius parameter r and is weighted according to the lateral displacement of the voxel from the AC-PC transect line at a given depth below a CSM site using the normal distribution function; higher weight is given to smaller lateral displacements, lower weight is given to larger lateral displacements

Values that are relatively high correspond to activations that are generally closer to the surface and less laterally displaced from a specific CSM site, while values that are relatively low correspond to activations that are generally farther from the surface and more laterally displaced from the site. In the final step, these values are correlated with CSM sites that have been classified as significant or non-significant for language disruption by the Fisher's Exact Test ($p < 0.05$). MR volume samples are examined with a surface radius of 1mm and depths of 5, 10, and 15mm as well as a radius of 5mm and a depth of 1mm to examine activations that are displaced laterally but are close to the surface. The results of these analyses are shown below in Table 14 for this subject. CSM sites significant for language disruption are shaded. Additional columns show the MR volumes of interest examined earlier for this subject. Only those CSM sites that fall within the PEPSI slice location are considered for that volume.

Table 14. Weighted sums of voxel intensities for MR volumes of interest. CSM sites significant for language disruption are shaded. No significant correlations are found.

CSM sites	PEPSI	F-Obj	F-Pix	T-Obj vs. Pix
Radius = 1 Depth = 5				
26	0.000	0.000	0.000	0.000
27		0.000	0.000	0.000
28	0.000	0.000	0.000	0.000
32	0.611	0.000	0.000	0.000
30		0.000	0.000	0.000
31	0.000	0.000	0.000	0.000
29		0.000	0.000	0.000
36		0.000	0.000	0.000
35	0.171	0.000	0.000	0.000
23	0.315	0.000	0.000	0.000
22		0.000	0.000	0.011
25		0.000	0.000	0.000
24	0.000	0.000	0.000	0.000
33		0.000	0.000	0.000
34		0.000	0.000	0.000
CSM sites	**PEPSI**	**F-Obj**	**F-Pix**	**T-Obj vs. Pix**
Radius = 1 Depth = 10				
26	0.000	0.000	0.000	0.000
27		0.000	0.014	0.000
28	0.035	0.000	0.000	0.000
32	2.434	0.000	0.000	0.000
30		0.000	0.000	0.000
31	1.832	0.000	0.000	0.000
29		0.000	0.000	0.000
36		0.000	0.000	0.000
35	0.692	0.000	0.000	0.001
23	0.706	0.000	0.015	0.057
22		0.000	0.028	0.092
25		0.000	0.231	0.040
24	0.000	0.000	0.021	0.000
33		0.000	0.000	0.000
34		0.000	0.000	0.000

Table 14. Continued.

CSM sites	PEPSI	F-Obj	F-Pix	T-Obj vs. Pix
Radius = 1 Depth = 15				
26	0.000	0.005	0.008	0.000
27		0.005	0.024	0.000
28	0.104	0.000	0.000	0.000
32	4.042	0.000	0.000	0.000
30		0.000	0.000	0.000
31	4.538	0.000	0.000	0.000
29		0.000	0.000	0.000
36		0.000	0.003	0.000
35	1.346	0.001	0.069	0.002
23	1.562	0.003	0.245	0.078
22		0.020	0.428	0.112
25		0.075	0.469	0.046
24	0.054	0.023	0.319	0.000
33		0.000	0.033	0.000
34		0.000	0.015	0.000
CSM sites	**PEPSI**	**F-Obj**	**F-Pix**	**T-Obj vs. Pix**
Radius = 5 Depth = 1				
26	0.000	0.000	0.000	0.000
27		0.000	0.000	0.000
28	0.010	0.000	0.000	0.000
32	0.030	0.000	0.000	0.000
30		0.000	0.000	0.000
31	0.000	0.000	0.000	0.000
29		0.000	0.000	0.000
36		0.000	0.000	0.000
35	0.006	0.000	0.000	0.000
23	0.017	0.000	0.000	0.002
22		0.000	0.000	0.001
25		0.000	0.000	0.000
24	0.002	0.000	0.000	0.000
33		0.000	0.000	0.000
34		0.000	0.000	0.000

No significant correlations were found between CSM sites and PEPSI or fMRI peak activations at the depths and radii tested. Qualitative comparisons show that language site 29, which is slightly inferior to the lower boundary of the PEPSI slice, is closest to the largest cluster of PEPSI activation in the posterior middle temporal gyrus, though non-significant sites 28 and 32 are also in close proximity to this cluster. Right putamen and claustrum PEPSI activation is below language site 24 in the anterior superior temporal gyrus, but at such a considerable depth that the relationship between the surface site and this deep activation is unclear. Figure 56 below displays these qualitative relationships.

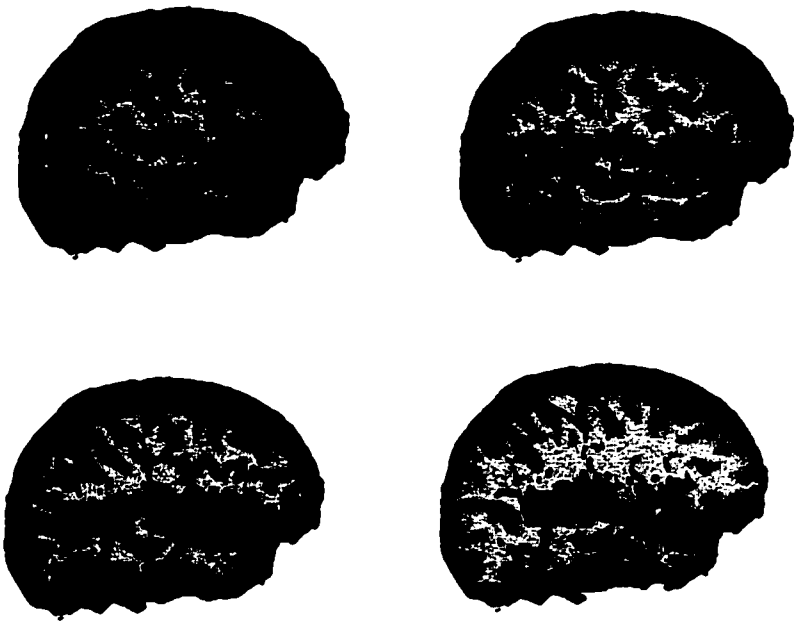

Figure 56. PEPSI activations and CSM sites at progressively greater depths from the surface of the cortex. Higher intensity PEPSI activations are in yellow, lower intensities are in orange; significant CSM sites are represented by orange dots, non-significant sites are shown with blue dots.

For fMRI activations in the Objects vs. Pixelated Objects condition, non-significant sites 22 (anterior middle temporal gyrus) and 25 (medial middle temporal gyrus) are closest to fMRI activations in the right insula and middle temporal gyrus respectively. For the Objects vs. Baseline condition, non-significant site 26 (medial superior temporal gyrus) is closest to the activation in the right insula, while non-significant site 33 and significant site 36 (ventral post-central gyrus) are in line with deep activation in the thalamus. For the Pixelated vs. Baseline condition, right insular activation is seen below non-significant

sites 25 (medial middle temporal gyrus) and 23 (anterior superior temporal gyrus). These qualitative comparisons are shown below in Figure 57.

A Objects vs. Pixelated Objects

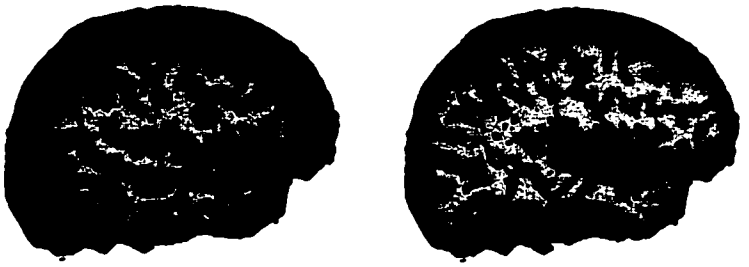

B Objects vs. Baseline

C Pixelated Objects vs. Baseline

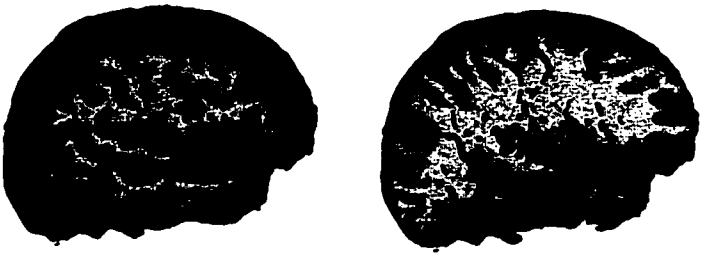

Figure 57. CSM sites and fMRI activation for Objects vs. Pixelated Objects (A), Objects vs. Baseline (B), and Pixelated Objects vs. Baseline (C).

ERP sources for the N100 component for Objects and Pixelated Objects in the right hemisphere were found in the inferior and middle temporal gyri for both conditions, plus the superior temporal gyrus for the Pixelated Objects condition. These sources sit anterior and at a considerable depth only to non-significant site 30 in the posterior superior temporal gyrus. No right-sided sources were found for the N400 component for Objects.

2) Comparisons between PEPSI, fMRI, and ERP sources

Two comparisons are made across these techniques: A) Objects and B) Pixelated Objects. No matches were found between fMRI Objects vs. Pixelated Objects and PEPSI or ERP sources.

A Objects

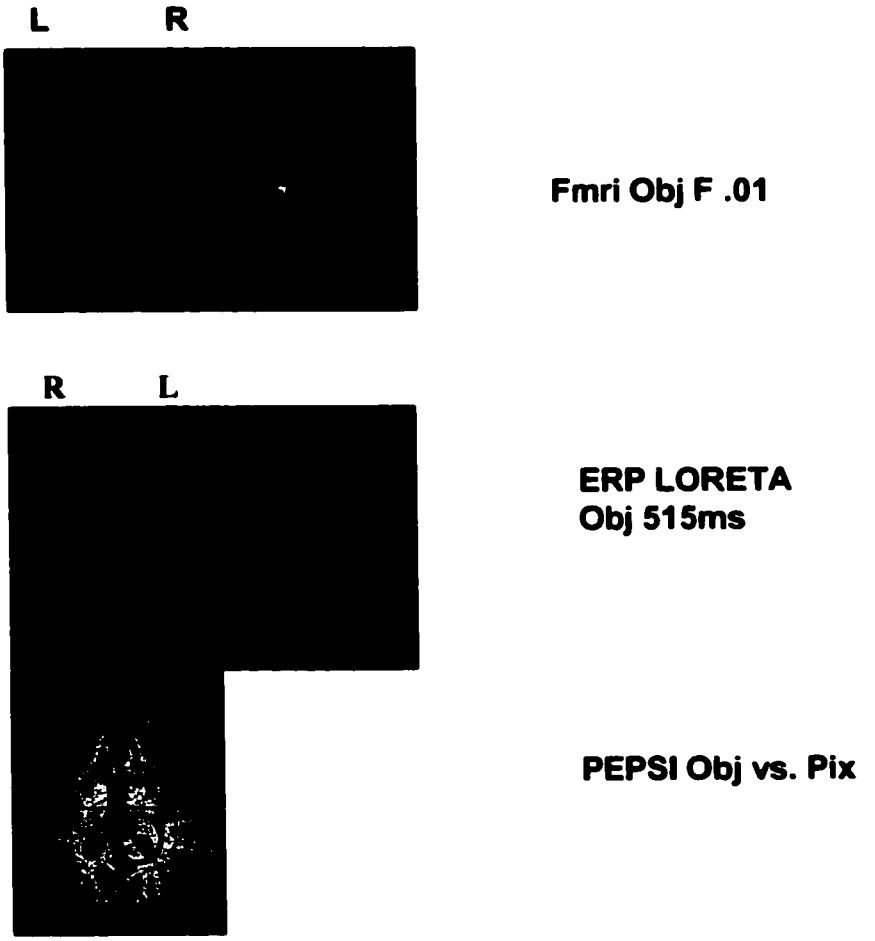

Figure 58. Comparison across imaging modalities for Objects.

No matches are seen between fMRI, PEPSI, and left posterior ERP Objects N100 sources. Matches do occur in the left thalamus between fMRI and PEPSI (blue circles), in the left posterior insula (orange) and left thalamus (lavender, superior slice) between fMRI and ERP Objects N400, and the right insula between fMRI, PEPSI, and ERP Objects N400 (green). Overall for Objects, no N100 source match is seen in left

postererior areas with fMRI or PEPSI. FMRI activations in bilateral insula and basal ganglia do match sources for the N400 component and PEPSI.

B Pixelated Objects

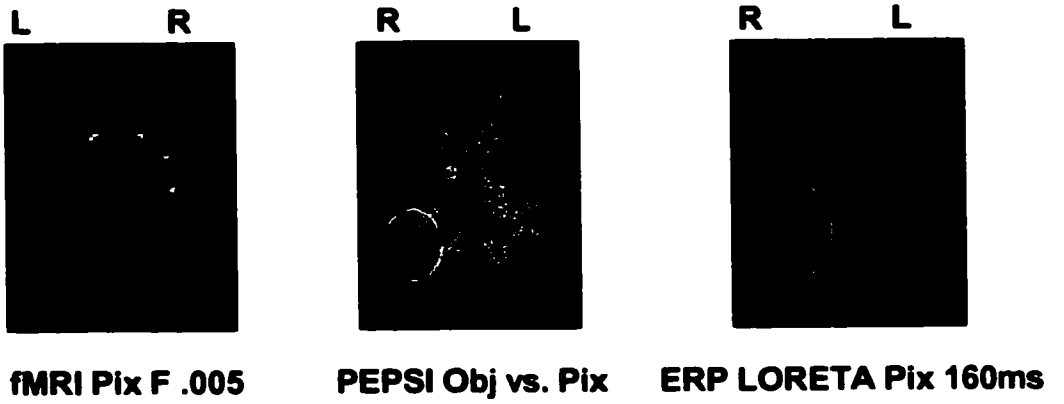

Figure 59. Comparison across imaging modalities for Pixelated Objects.

For Pixelated Objects, matches occur between fMRI, PEPSI, and ERP Pixelated Objects N100 sources. Matches are seen in the right insula/putamen (green circles) and left insula (blue) between fMRI and PEPSI (including the adjacent grey voxels shown earlier), and in right posterior MTG/ITG between PEPSI and ERP Pixelated Objects N100 (right source only). Again, posterior activations in fMRI and PEPSI correspond best with N100 sources. Since there was no clear N400 component for Pixelated Objects, it is unknown whether anterior activations for these stimuli would have corresponded with anterior N400 sources.

The right insula was identified as a common area of activation in both fMRI and PEPSI and this area sits reasonably in line with language site 24 in the anterior superior temporal gyrus, while the right posterior middle temporal gyrus, common to PEPSI and an N100 ERP source sits just inferior to language site 29 in the posterior middle temporal gyrus.

P137

CSM Mapping

This patient showed left hemisphere language dominance. A left temporoparietal exposure allowed stimulation of sites in a region bounded by the mesial middle frontal gyrus anteriorly and superiorly, the inferior temporal gyrus inferiorly, and the anterior supramarginal gyrus posteriorly. The grid is shown below in Figure 60. See figure caption for electrode numbering scheme.

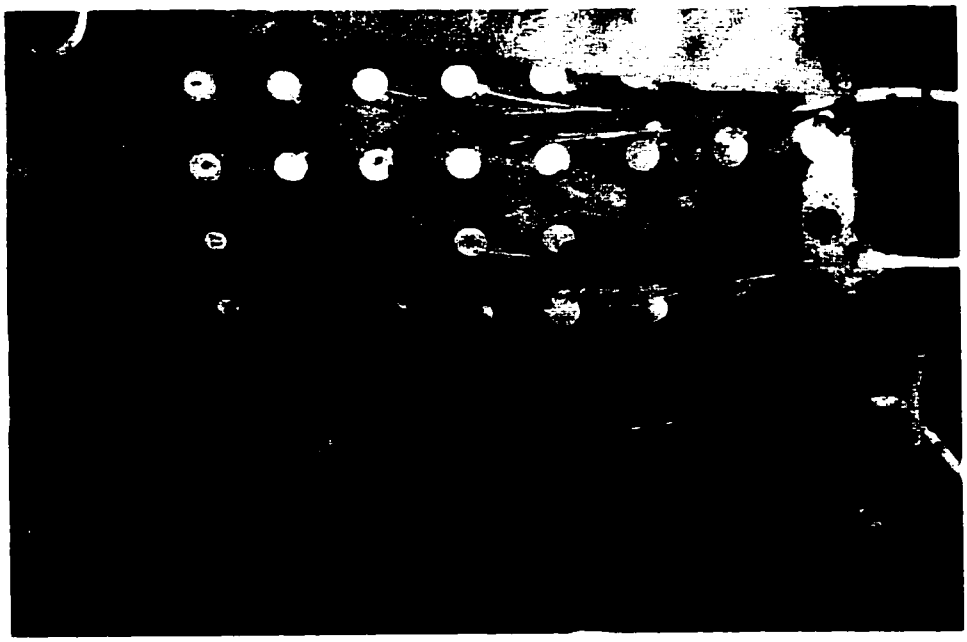

Figure 60. Eight-by-eight electrode array for P137. Electrodes are numbered left to right. The first number of each row is shown in the left column of electrodes (1, 9, 17, 25, 33, 41, 49, 57).

Because of the large number of electrode pairs that are stimulated for language testing, not all stimulated sites are tagged. In addition, only a subset of electrode pairs which are significant for language disruption (Fisher's Exact Test, $p < 0.05$) are tagged for clinical use. In all, there are four types of stimulation results: 1) stimulated sites (i.e. electrode pairs) that are not language-related (motor, memory) but are tagged, 2) stimulated sites that are significant for language disruption and are tagged, 3) stimulated sites that are significant for language disruption and are not tagged, and 4) stimulated sites that are not

significant for language disruption and are not tagged. As such, the original surgical photograph was modified[7] to include these four types of stimulation results and is shown below in Figure 61 (A). Sites are overlayed on the 3-D reconstruction in B, where markers in orange represent significant sites and markers in blue represent non-significant sites.

[7] The location of additional tags was determined by the visualization method described in Modayer et al., 1997. Tags from the surgical photograph were relabeled in order to satisfy the requirements of the Skandha4 graphics program, which limits the number of sites that can be displayed to 50. Letters represent the boundaries of the grid.

A

B

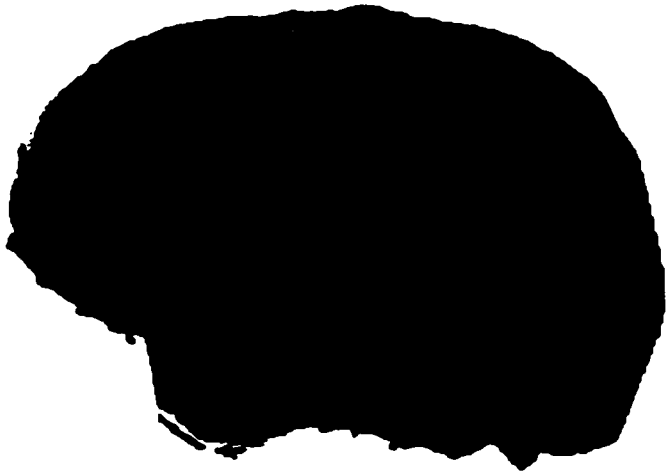

Figure 61. CSM sites for P137. Sites significant for language disruption are represented by tags 5-17 (A) and orange markers (B). See text for additional coding information.

The coding scheme for the different types of stimulation results as described above is as follows: 1) non-language (motor, memory) sites are represented by light grey numbers on white tags (tags 1-3), 2) sites significant for language disruption are represented by black numbers on white tags (tags 5-10), 3) additional sites significant for language disruption are represented by black numbers on blue tags (tags 11-17), and 4) stimulated sites not significant for language disruption are represented by dark gray numbers on light grey tags (tags 30-50). All categories are described below in Table 15.

Table 15. Naming errors in stimulated sites for P137. *Sites 55-56 and 14-15 are excluded; language testing was discontinued at these sites after one stimulation trial due to pain.

P137 (Grid) Site*	Errors/ Trials	Tag	Fisher's *p*-value	Location	Item	Error type
14	Motor/ Sensory	1	N/A	Mid PoG	N/A	N/A
27-28	Motor/ Sensory	2	N/A	Ven PoG	N/A	N/A
61-62	Memory Retrieval	3	N/A	Mes MTG	N/A	N/A
11-12	4/6	5	0.0001	Ven PrG	Moon Pig Bus Candle	Filler (target) Filler (target) Filler (target) Filler (target)
19-20	3/4	6	0.0001	Ven PrG	Nose Fish Doll/ Baby	Apraxic (slur) Filler (no target) Filler (target)
21-22	3/5	7	0.0001	Ven PoG	Coat Glasses Sock	Filler (no target) Filler (target) Filler (target)
40-48	1/5	8	0.046	Post SMG	Cat	Off target ("Cake")

Table 15. Continued.

47-48	3/9	9	0.0001	Post STG	Saw Corn Dog	Filler (target) Off target ("Cow") Filler (target)
39-40	3/18	10	0.002	Post SMG	Belt Dress Book	Filler (target) Slow (target) Slow (target)
26-27	2/5	11	0.001	Ven PrG	Leg Nose	Filler (target) Decreased volume (target)
49-50	1/3	12	0.028	Ant MTG	Dresser	Slow (target)
27-28	1/4	13	0.037	Ven PoG	Bowl	Filler (target)
29-30	1/3	14	0.028	Ant SMG	Eye	Filler (no target)
37-38	2/11	15	0.007	Mes STG	Star Pig	Slow (target) Phonological paraphasia ("Peg")
38-39	5/12	16	0.0001	Post STG	Truck Train Violin Tiger Glasses	Slow (target) Filler (target) Filler (target) Slow (target) Filler (target)
15-16	1/3	17	0.028	Post SMG	Hammer	Slow (target)
9-10	0/3	30		Post MFG		
17-18	0/4	31		IFG Op		
25-26	0/3	32		IFG Op		
41-42	0/4	33		Ant STG		
57-58	0/7	34		Ant ITG		
10-11	0/4	35		IFG Op		
18-19	0/3	36		IFG Op		
50-51	0/5	37		Ant MTG		
35-36	0/3	38		Mes STG		
43-44	0/8	39		Mes MTG		
51-52	0/4	40		Mes MTG		
59-60	0/8	41		Mes ITG		
52-53	1/11	42	0.098	Mes MTG	Leg	Semantic paraphasia ("Foot")
45-46	0/12	43		Mes MTG		
61-62	0/6	44		Mes ITG		
22-23	0/5	45		Ant SMG		
46-47	0/4	46		Post MTG		
54-55	0/5	47		Post MTG		
23-24	0/3	48		Post SMG		
31-32	0/5	49		Post SMG		
63-64	0/11	50		Post ITG		

Semantic Category and Error Types

A total of 31 errors occurred during the 208 stimulated trials. Seventeen items were artifacts; 16 of these 17 items were hesitations while the remaining item was off-target. Of the 31 total errors, 9 items were natural objects; 5 out of these 9 errors were hesitations, 2 were missed or off-target, 1 was a semantic paraphasia, and 1 was a phonological paraphasia. The remaining 5 errors were on animals; 3 out of these 5 errors were hesitations, and 2 were missed or off-target. The occurrence of an error was more likely if the semantic category of the item was natural/animal, but did not reach significance (artifact, natural/animal; Pearson chi-square $X^2 = 0.073$, Fisher's Exact Test $p = 0.074$).

Only one error was made at a site non-significant for language disruption. This was a semantic paraphasia made on the natural item "leg". In the 30 remaining errors at sites significant for language, the occurrence of an error was again more likely if the semantic category of the item was natural/animal, but did not reach significance (artifact, natural/animal; Pearson chi-square $X^2 = 0.077$, Fisher's Exact Test $p = 0.064$). The only individual site where the occurrence of an error tended to be dependent on the category of the item was site 15 (mesial STG) (Pearson chi-square $X^2 = 0.011$, Fisher's Exact Test $p = 0.055$), where more errors occurred with natural/animal items than expected. Only one error was made out of 209 non-stimulated trials, a delayed naming of the artifact "book". Figure 62 below summarizes the errors during stimulated trials.

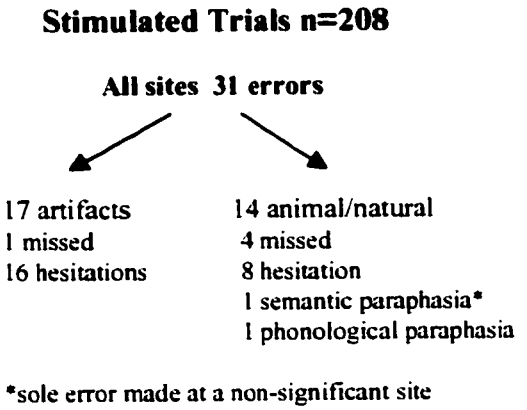

Figure 62. Semantic category and error types for stimulated trials for P137. The occurrence of an error at a significant site was more likely if the semantic category of the item was natural/animal (Fisher's Exact Tests, $p = 0.064$).

PEPSI

This patient is left-dominant for language as determined by Wada testing. PEPSI activations are shown below in Figure 63.

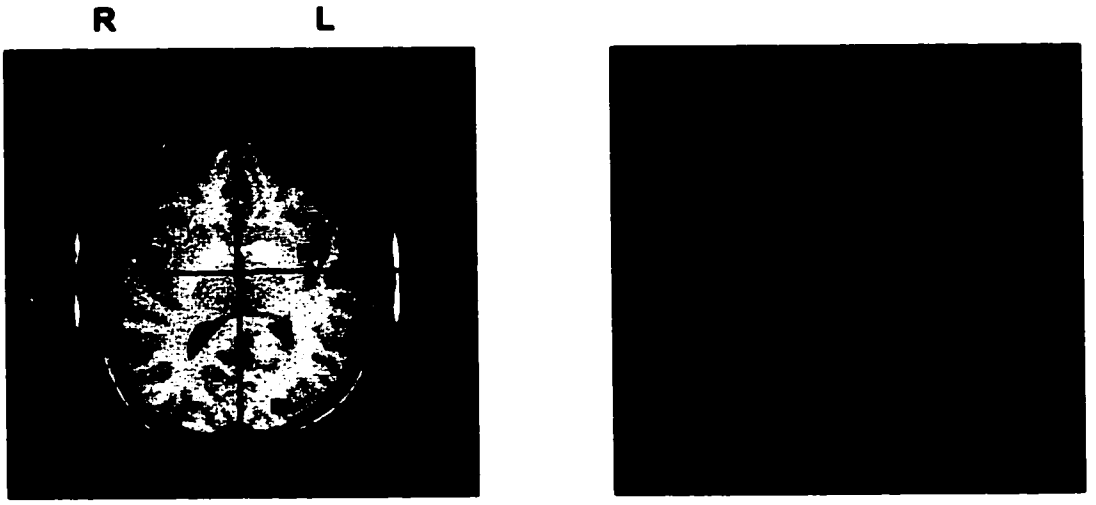

Figure 63. PEPSI activations showing increases in lactate during visual object naming.

Left-lateralized activation is seen anteriorly in the insula and inferior frontal gyrus and posteriorly in the occipital gyrus. Weaker activations occur in the superior temporal gyrus (grey voxels in right image) Right-lateralized activation is seen in the middle temporal gyrus. Weaker activation is seen in the right insula and basal ganglia (putamen and thalamus).

FMRI

Three fMRI datasets are shown below: 1) Objects vs. Pixelated Objects, 2) Objects vs. Baseline (t and F-contrasts), 3) Pixelated Objects vs. Baseline (F-contrast).

1) Objects vs. Pixelated Objects

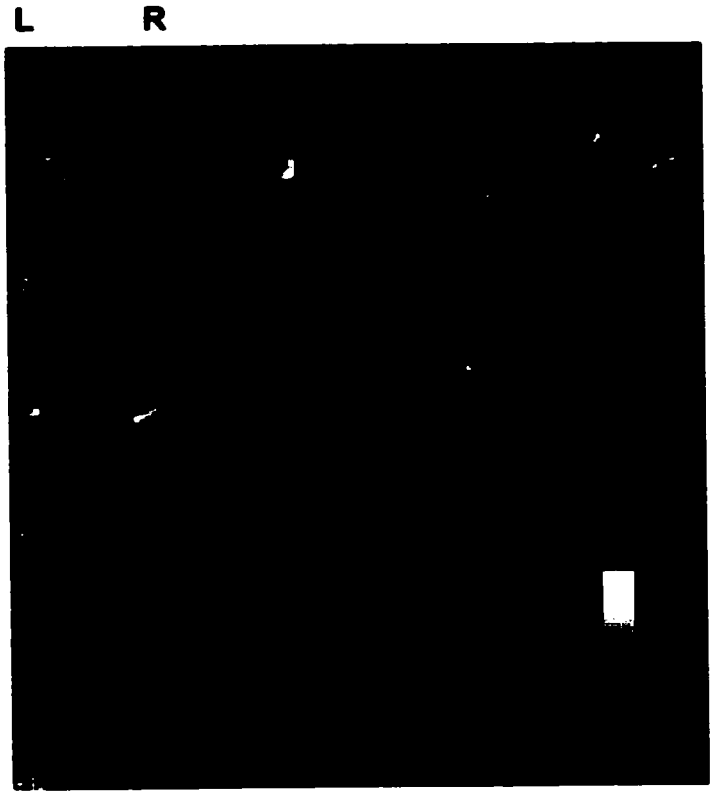

Figure 64. FMRI Objects vs. Pixelated Objects ($p < 0.001$) *t*-contrast.

Activation is bilateral in the cerebellum, fusiform, superior temporal, inferior frontal opeculum, and post-central gyri. Lateralized activations occur in the left precuneus and middle frontal gyrus and right middle temporal gyrus. Table 16 below shows local maxima for this volume in SPM coordinates, associated *t*-values, and anatomical location.

Table 16. FMRI Objects vs. Pixelated Objects ($p < 0.001$) *t*-contrast.

(X,Y,Z)	*t*-value	Location
(-56, -4, 3)	4.98	Left STG (TTG border)
(-22, -35, -38)	4.80	Left cerebellum
(12, -13, -14)	4.52	Right subicullum
(-7, -42, -50)	3.93	Midline cerebellum
(34, -9, 5)	3.86	Right insula
(-18, 18, -2)	3.84	Left putamen
(-41, 3, -20)	3.71	Left fusiform
(19, 32, 17)	3.69	Right insula/IFG Op
(-15, -8, -20)	3.67	Left entorhinal cortex
(-19, 3, 40)	3.62	Left MFG
(30, -24, -19)	3.55	Right fusiform
(-19, -42, -2)	3.54	Left precuneus
(-30, -16, -20)	3.54	Left fusiform
(37, -32, -7)	3.53	Right STG
(-41, -4, 10)	3.42	Left PoG
(37, -32, 41)	3.38	Right PrG
(48, -32, 35)	3.35	Right PoG
(57, -17, -13)	3.30	Right MTG
(-30, 18, 16)	3.30	Left IFG Op

2) Objects vs. Baseline

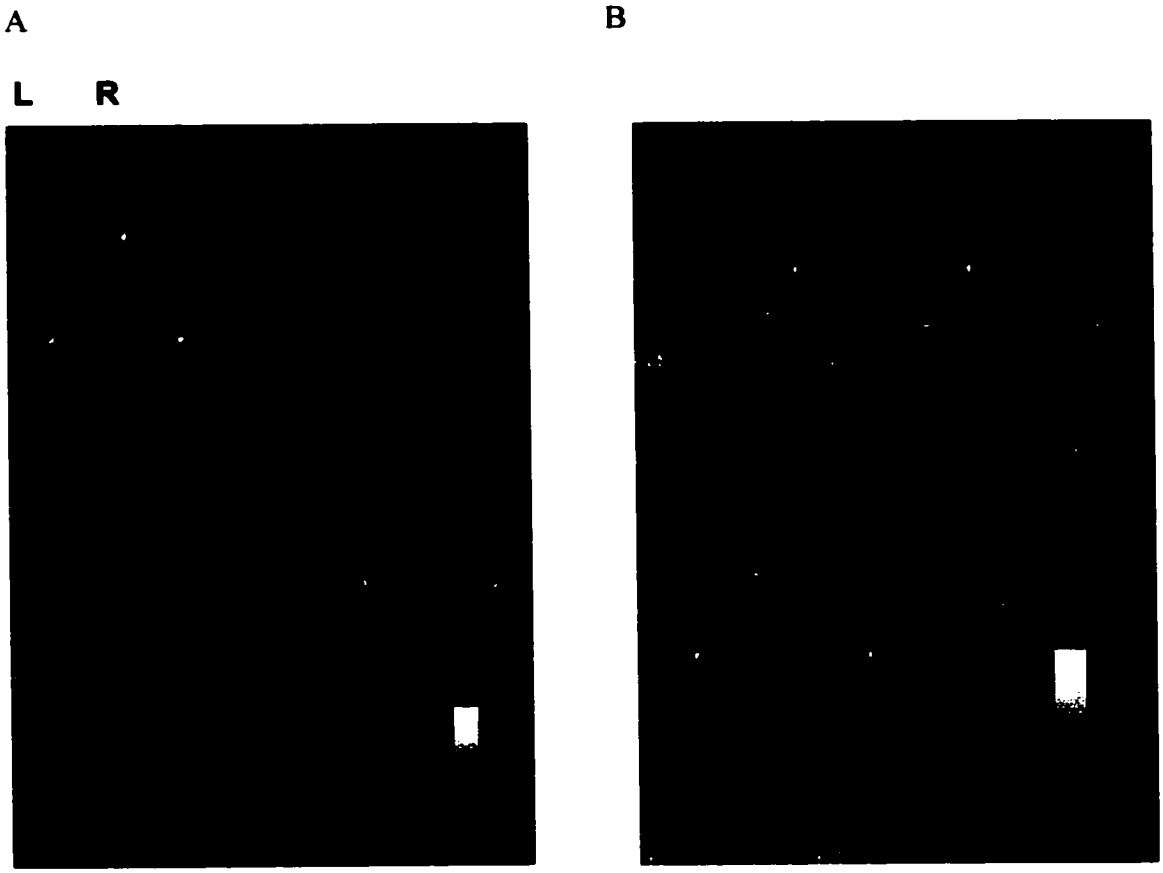

Figure 65. FMRI Objects vs. Baseline (A) $p < 0.01$ *t*-contrast (B) $p < 0.001$ *F*-contrast.

An artifact is seen in the fat pads behind both eyes. Activations in the *t*-contrast are seen bilaterally in the middle temporal, middle frontal, and superior frontal gyri, though many of these activations are more intense on the left side. Lateralized activations occur in the left inferior frontal gyrus and right pre-central gyrus. Activations in the *F*-contrast emphasize visual processing areas, particularly in the right occipital gyrus. Bilateral

activation occurs in the middle temporal gyrus, while lateralized activations are seen in the right middle frontal gyrus and left post-central gyrus. Table 17 below shows local maxima in each volume in SPM coordinates, associated *t*-contrast and *F*-contrast values, and anatomical location.

Table 17. FMRI Objects vs. Baseline *t*-contrast ($p < 0.01$) and *F*-contrast ($p < 0.001$).

(X,Y,Z)	***t*-value**	**Location**
(60, -28, -25)	4.48	Right MTG
(-25, 70, 10)	*4.06*	*Artifact—fat pad/left eye*
(30, 2, 41)	3.54	Right MFG
(-41, 44, 34)	3.23	Left IFG
(-45, 11, 34)	3.12	Left MFG
(-38, 3, 46)	2.99	Left MFG
(-60, -27, -15)	2.97	Left MTG
(29, -84, 11)	2.96	*Artifact*
(29, -28, 47)	2.92	Right PrG
(-15, -1, 52)	2.89	Left SFG
(-14, 3, -14)	2.86	Left subicullum
(-18, 10, 4)	2.81	Left basal ganglia gl pall
(35, 62, 5)	*2.80*	*Artifact – fat pad/right eye*
(14, -54, 46)	2.70	Right PrG
(3, -13, 58)	2.69	Right/midline SFG
(3, -72, 16)	2.69	Right/midline precuneus
(X,Y,Z)	***F*-value**	**Location**
(60, -28, -25)	20.08	Right MTG
(-25, 70, 10)	*16.5*	*Artifact – fat pad/left eye*
(4, 29, 4)	15.1	Right cingulate
(-45, -34, -44)	14.39	Left cerebellum
(22, -80, -19)	14.07	Right OcG
(37, -69, -25)	13.92	Right OcG
(8, 32, 10)	13.63	Right cingulate (border cc)
(-49, -61, -20)	12.89	Left MTG
(30, 2, 41)	12.56	Right MFG
(-20, -46, 52)	12.41	Left PoG

3) Pixelated Objects vs. Baseline

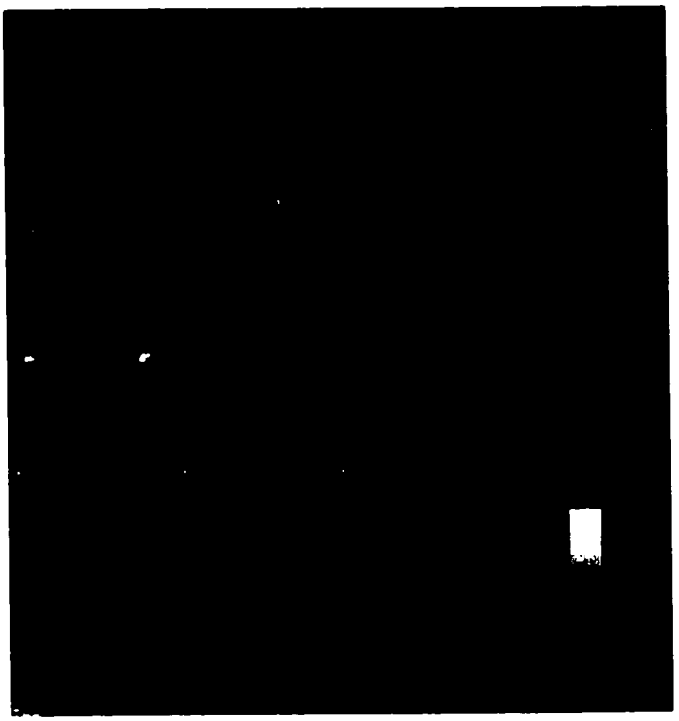

Figure 66. FMRI Pixelated Objects vs. Baseline ($p < 0.005$) *F*-contrast.

Bilateral activations are seen in several areas, including occipital, inferior frontal, superior frontal, and superior parietal gyri. Left-lateralized activations include the fusiform gyrus, insula, and cerebellum, while right-lateralized activations include the middle frontal and temporal gyri. Table 18 below shows local maxima in each volume in SPM coordinates, associated *F*-contrast values, and anatomical location.

Table 18. FMRI Pixelated Objects vs. Baseline *F*-contrast ($p < 0.005$).

(X,Y,Z)	*F*-value	Location
(-60, -4, 3)	22.95	Left IFG
(45, -2, -1)	21.11	Right IFG Op
(30, -9, 47)	20.80	Right SFG/MFG
(22, -80, -19)	17.36	Right OcG
(-30, -42, -8)	16.66	Left fusiform
(-45, -34, -44)	15.91	Left cerebellum
(16, 2, -14)	15.65	Right white matter
(-18, -8, -20)	15.24	Left entorhinal cortex
(19, 25, 17)	*13.58*	*Artifact – lat ventricle*
(25, -84, 11)	13.09	Right OcG
(-35, -68, 34)	13.03	Left SPL
(-25, 70, 10)	*12.45*	*Artifact—fat pad left eye*
(-7, -20, -50)	11.85	Midline/left cerebellum
(27, -20, -19)	11.82	Right hippocampus
(-15, 51, 40)	11.67	Left SFG
(-1, -72, 10)	11.41	Midline precuneus
(-14, 7, -14)	10.98	Left uncus
(0, -24, -38)	10.78	Midline cerebellum
(-16, -1, 58)	10.43	Left SFG
(-37, 7, -8)	10.26	Left insula
(-19, -68, -32)	9.95	Left OcG
(34, 47, 41)	9.87	Right MFG
(-38, -12, 46)	9.83	Left PrG
(-11, -16, -8)	9.60	Left thalamus
(12, -5, -32)	9.51	Right pons
(10, -76, 22)	9.40	Right SPL
(30, -35, -13)	9.25	Right MTG/STG border
(-49, -61, -20)	8.96	Left OcG
(11, -46, -26)	8.82	Right OcG

ERP

This subject was also inconsistent with the pattern seen in the ERP pilot study, which demonstrated in normal subjects that blocking the stimuli prevented P300 effects due to novelty or surprise from occurring with pixelated objects. Like P136, this subject

shows a large P300 effect to pixelated objects, but this effect is limited to right lateral posterior electrode sites, and an N400 component is still found at other electrode sites. The figure below (Figure 67) shows grand mean waveforms for each of the 64 electrodes for the Objects (solid lines) and Pixelated Objects (dashed lines) conditions.

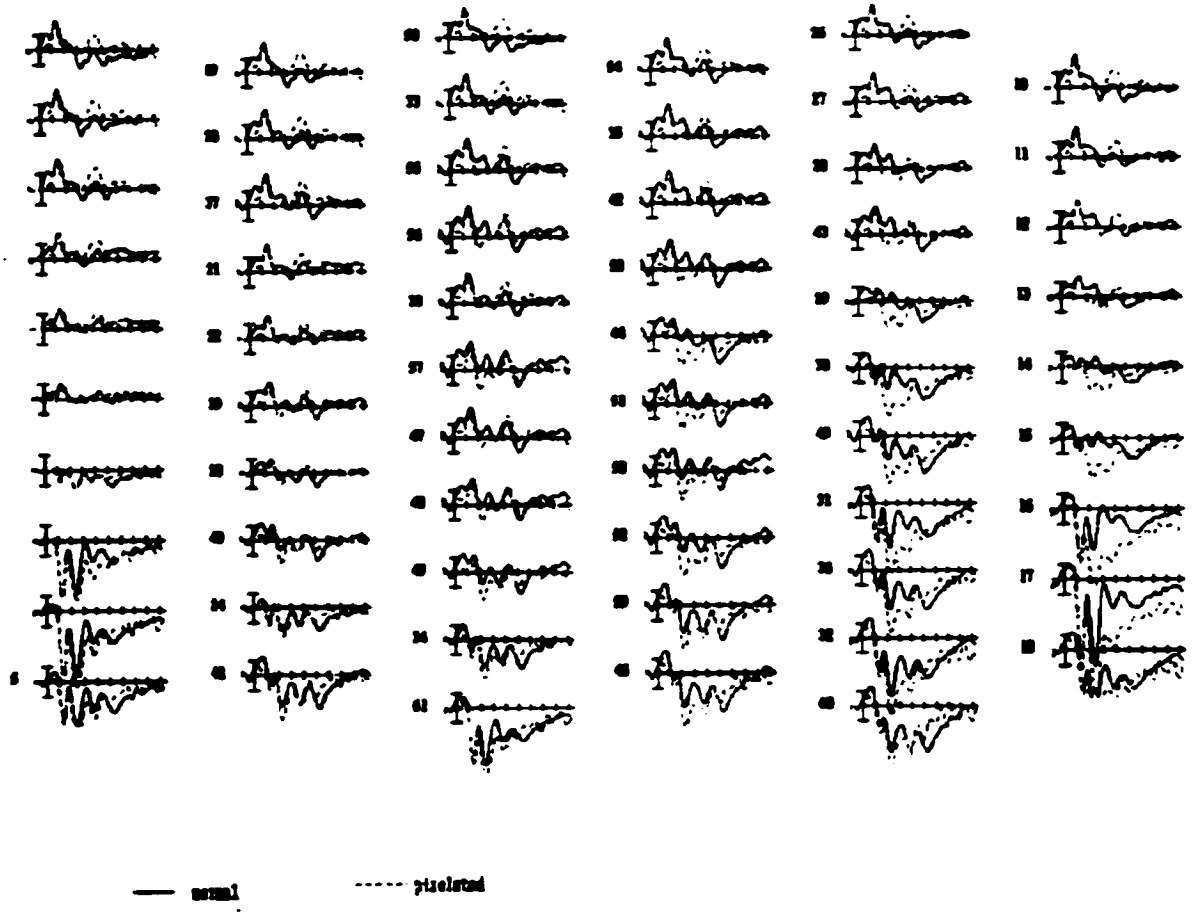

Figure 67. Grand mean for Objects (solid lines) and Pixelated Objects (dashed lines) for all channels for P137. X-axis is in 100msec increments, y-axis is in microvolts.

An early negative-going peak corresponding to the N100 can be seen at 140msec for the object condition and 135msec in the pixelated object condition. This component is most prominent for objects at anterior midline and lateral sites; amplitudes are reduced or absent at posterior sites laterally and at midline. The N400 component is seen for objects at 430msec and at 445msec for pixelated objects in midline/right anterior sites, but is not seen for pixelated objects in right posterior sites due to a large P300 effect.

Objects

Again, the N100 and N400 components are clearly seen in this condition. The spatial distribution of these components across the scalp is seen in Figure 68 (A) below. The N100 component occurs between 90-170msec with a peak amplitude at 140msec and is most prominent at midline and bilateral anterior sites; amplitudes are reduced at extreme lateral sites and are severely reduced or absent at midline and lateral posterior sites respectively. The N400 component occurs between 360-540msec with a peak amplitude at 430msec and is most prominent at mesial midline sites. Amplitudes are reduced at anterior sites, both midline and laterally, and absent in posterior sites across the scalp. These distributions are illustrated in the field and CSD/Laplacian maps in Figure 68 (B) below.

A

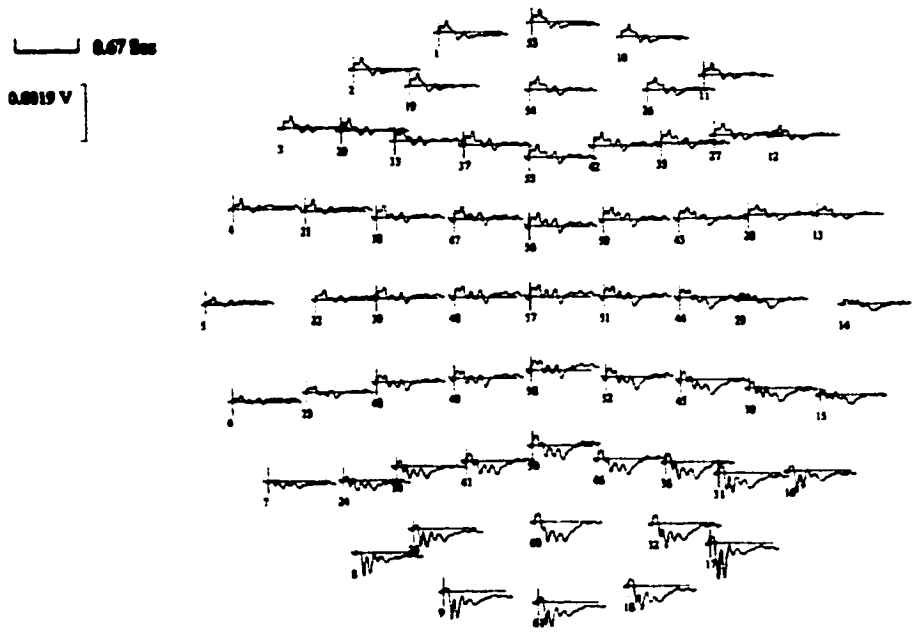

B

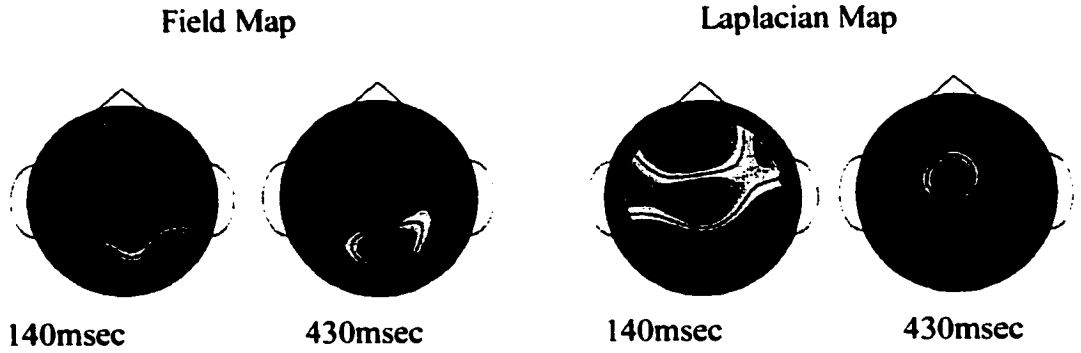

Figure 68. (A) 64-channel orientation of ERP waveforms for the Object condition. Frontal areas are at the top, occipital areas at the bottom, time and voltage scale bars are in the top left corner. (B) Top views of field and Laplacian (current source density) maps at 140msec and 430msec for objects. Areas of interest are in blue for the field map and in red for the Laplacian map.

Waveforms across electrode sites are superimposed and shown below in Figure 69 to better visualize the peak amplitudes of the N100 and N400 components subjected to LORETA analysis.

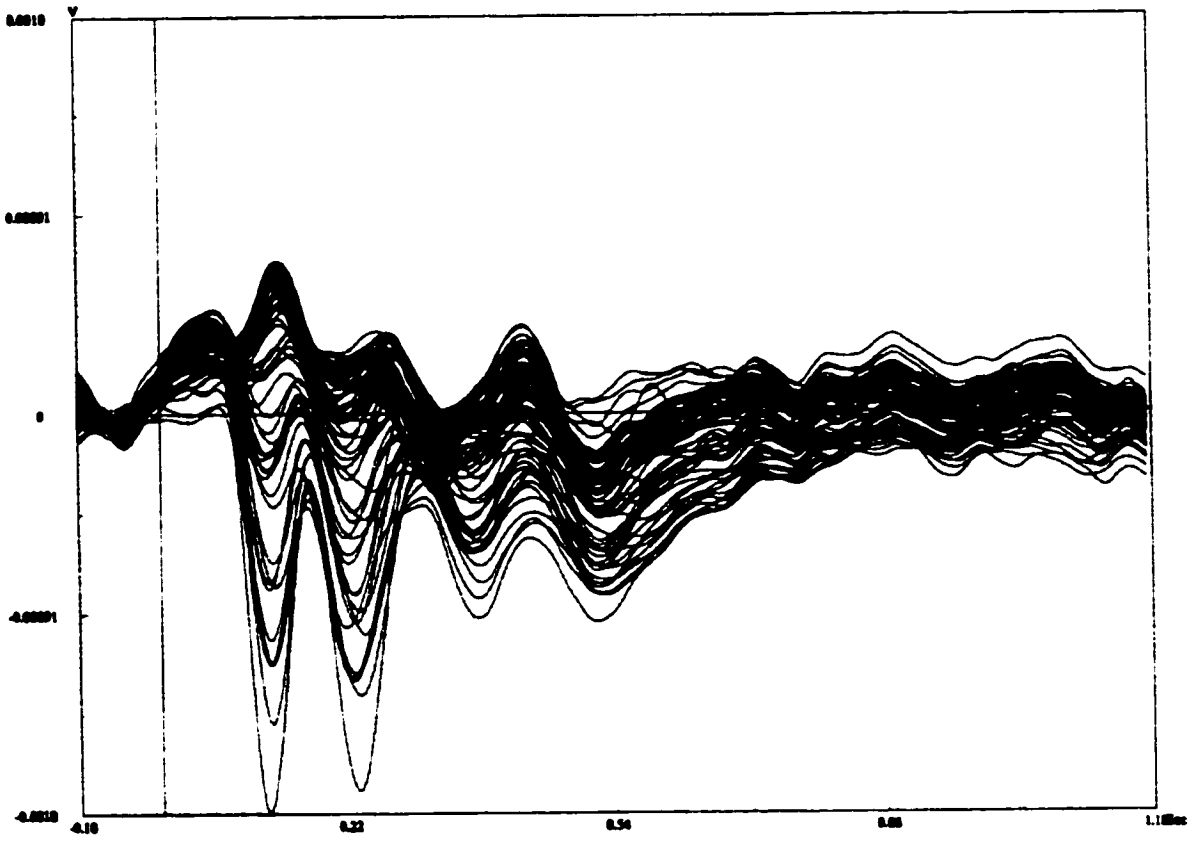

Figure 69. Superimposed 64-channel waveforms for the Object condition. Negative voltages are plotted upwards, positive voltages are plotted downwards. Negative peaks corresponding to the N100 and N400 components occur at 140 and 430 msec.

It can be seen below in Figure 70 that sources vary across the timecourse of the waveform and are temporally bound by the N100 and N400 components. Sources are seen in bilateral, but mainly right, posterior (occipital) areas from 90-170msec, extending superiorly and with a secondary frontal source from 210-330msec. Posterior and superior sources appear through 510msec.

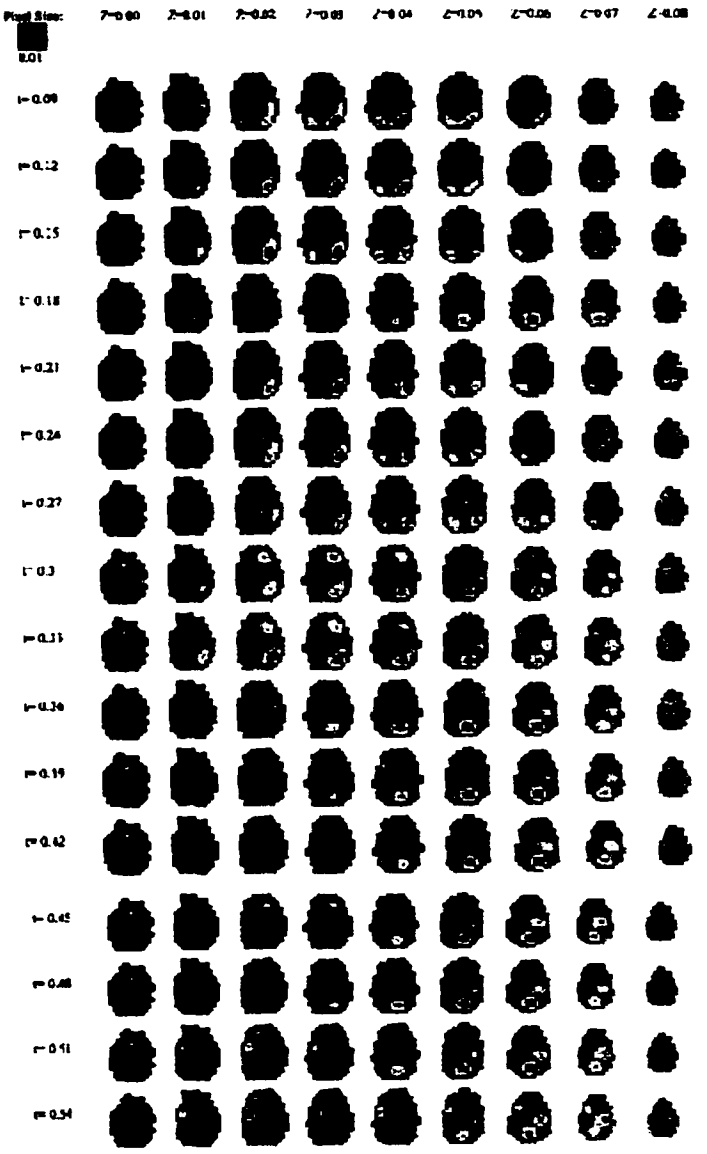

Figure 70. Source maps for the object condition from 90-540msec in 30msec increments. Sources are differentiated for the N100 (90-170msec) and N400 (360-540msec components.

The peak amplitude for the N100 component occurs at 140msec. The algorithm is applied to this timepoint and a primary source is seen in the posterior right hemisphere with a secondary source in the posterior left hemisphere (Figure 71 (A)), specifically in the right inferior and middle temporal gyri, extending superiorly and posteriorly into the occipital gyrus. The second source is in the left hemisphere and stays mainly in the occipital gyrus, but extends superiorly into the cuneus (Figure 71 (B)).

A

L R

B

R L

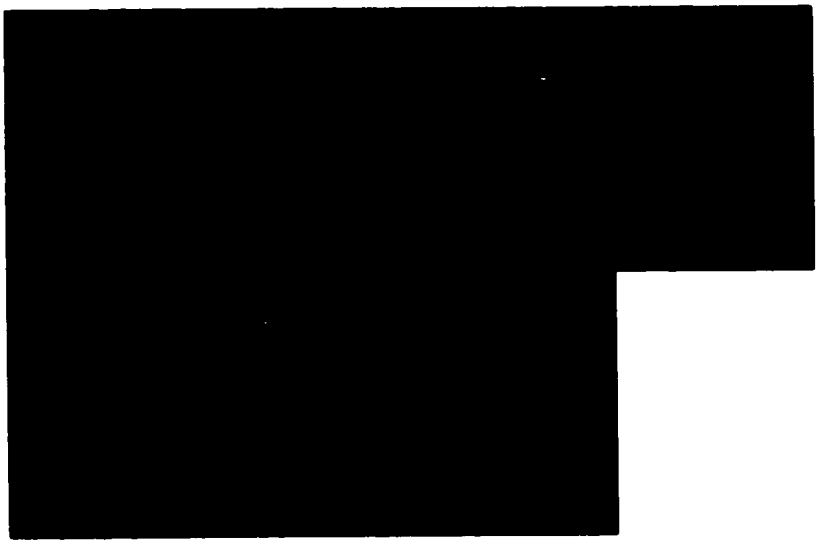

Figure 71. (A) Source maps at 140msec for objects. Pixels = $1cm^3$, direction is inferior to superior (L-R), axial views (B) Sources are in the right ITG/MTG and OcG and left OcG/cuneus.

The peak amplitude for the N400 component occurs at 430msec. The main source is seen in posterior midline areas and a secondary source occurs superiorly in right mesial areas (Figure 72 (A)), specifically in the left/midline occipital gyrus (striate) area and right supramarginal gyrus and superior parietal lobe (Figure 72 (B)).

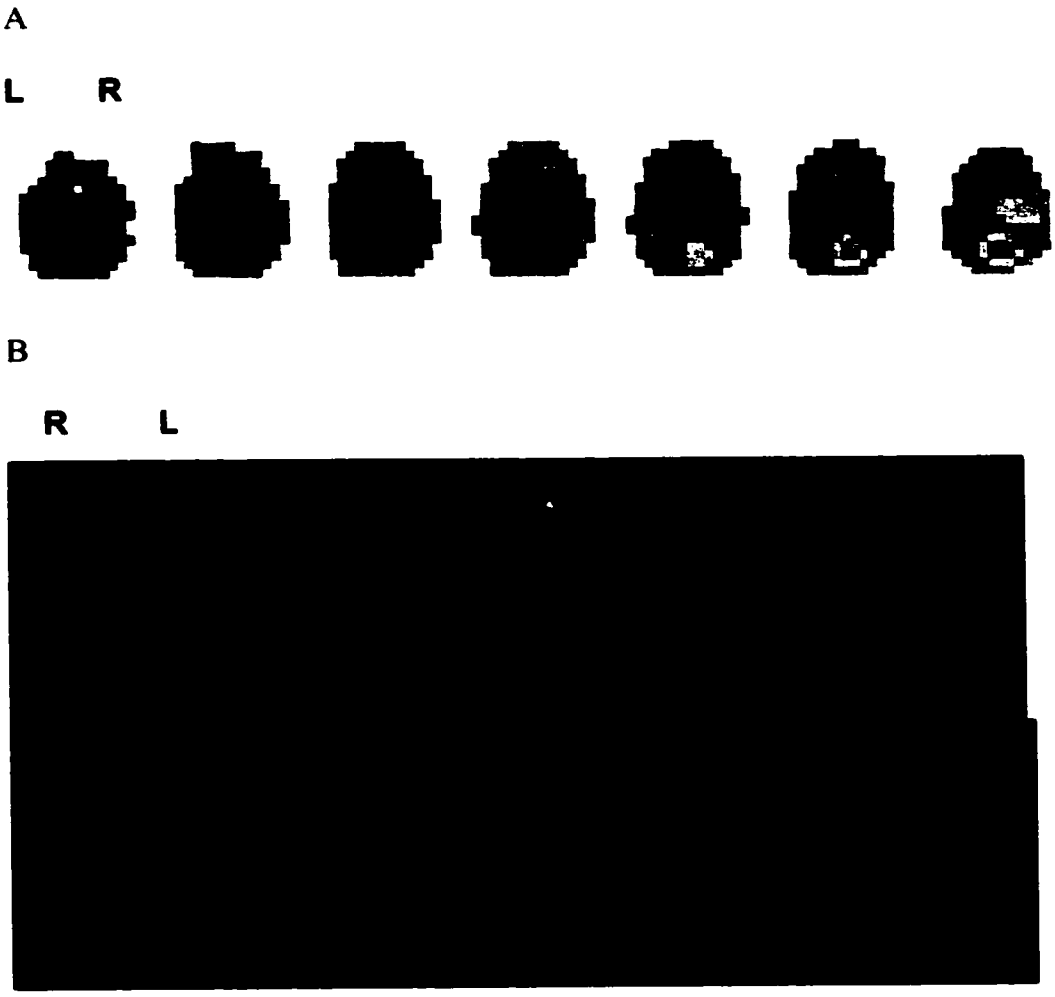

Figure 72. (A) Source maps at 430msec for objects (B) The source is seen in the left/midline OcG/striate area and right SMG/superior parietal lobe when overlayed onto structural MRI scans.

Sources for the N100 component in posterior areas are consistent with early sensory (visual) processing. Sources for the N400 component occur in both midline occipital areas, which is inconsistent with semantic processing areas, and in more superior areas such as supramarginal gyrus, which is consistent with areas involved in word versus picture naming.

Pixelated Objects

The spatial distribution of the N100 and N400 components across the scalp are seen below in Figure 73 (A). The N100 component occurs between 90-200msec with a peak amplitude at 135msec and is most prominent at anterior midline and lateral sites; amplitudes are reduced or absent at all posterior sites. The N400 component occurs between 355-500msec with a peak amplitude at 445msec and is most prominent at anterior midline and left lateral sites; amplitudes are reduced at anterior right lateral and absent across posterior sites. Note that a large P300 effect is seen in right posterior areas in electrodes 15, 16, 17, 18, 30, 31, 32, 36. The distribution for these components is illustrated in field and Laplacian maps in Figure 73 (B) below.

A

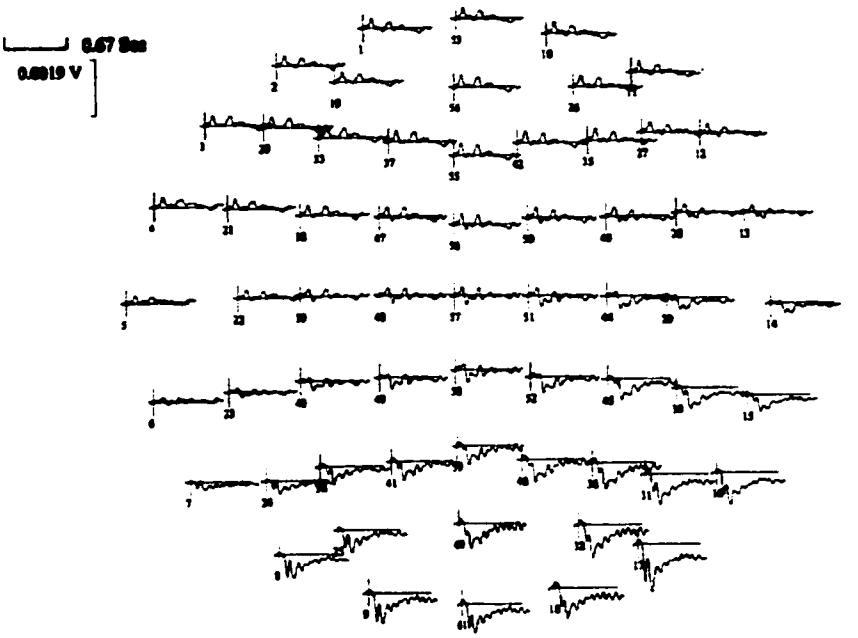

B

Figure 73. (A) 64-channel orientation of ERP waveforms for the Pixelated Object condition. Frontal areas are at the top, occipital areas at the bottom, time and voltage scale bars are in the top left corner. (B) Top views of field and Laplacian (current source density) maps at 135msec and 445msec for pixelated objects. Areas of interest are in blue for the field map and in red for the Laplacian map.

Waveforms across electrode sites are superimposed and shown below in Figure 74 to better visualize the peak amplitudes of the N100 and N400 components subjected to LORETA analysis.

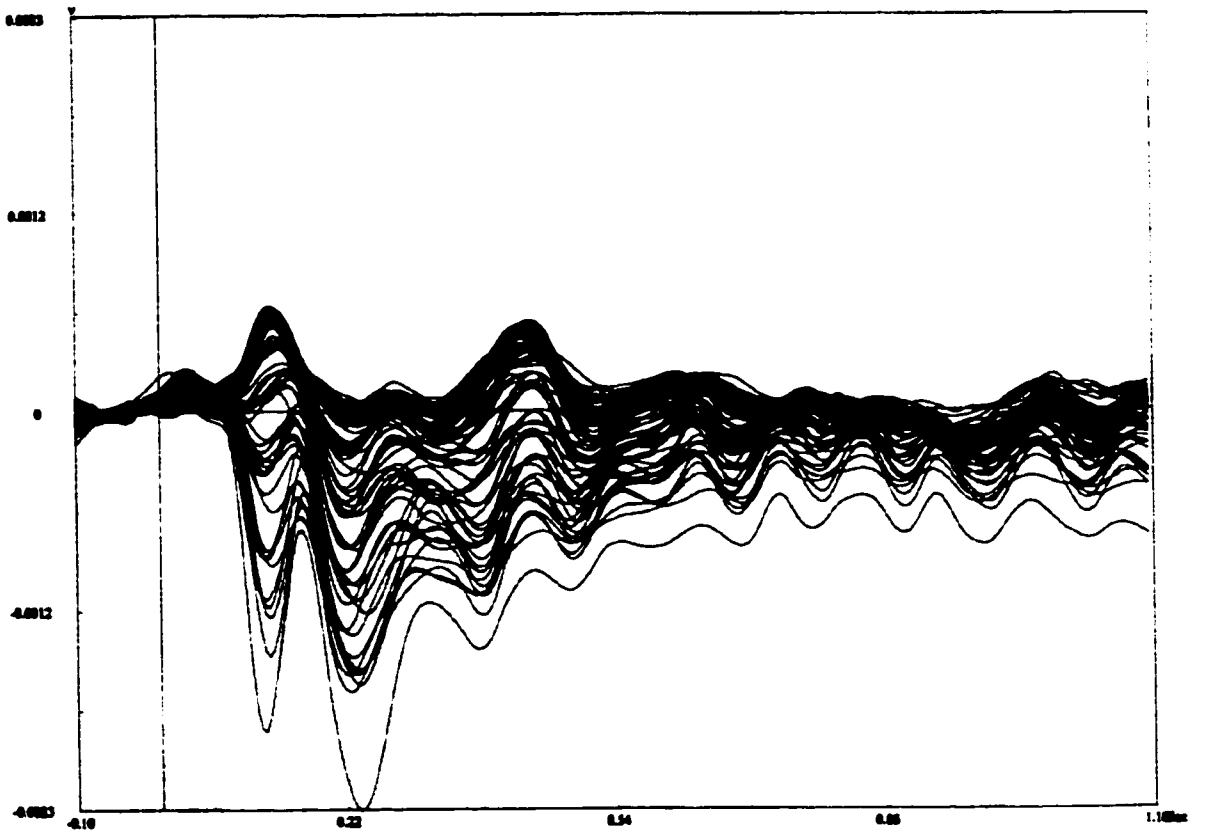

Figure 74. Superimposed 64-channel waveforms for the Pixelated Object condition. Negative voltages are plotted upwards, positive voltages are plotted downwards. Negative peaks corresponding to N100 and N400 components occur at 135 and 445msec.

It can be seen below (Figure 75) that posterior sources are relatively consistent across the waveform for both components. Sources for the N100 component are bilateral, however, compared to the right-lateralized source seen with the N400 component. It is unclear what kind of influence the P300 effect in posterior sites has upon the source localization. Sources are localized to very similar areas as the object condition for the N100 component, but are more inferior for the N400 component compared to the object condition.

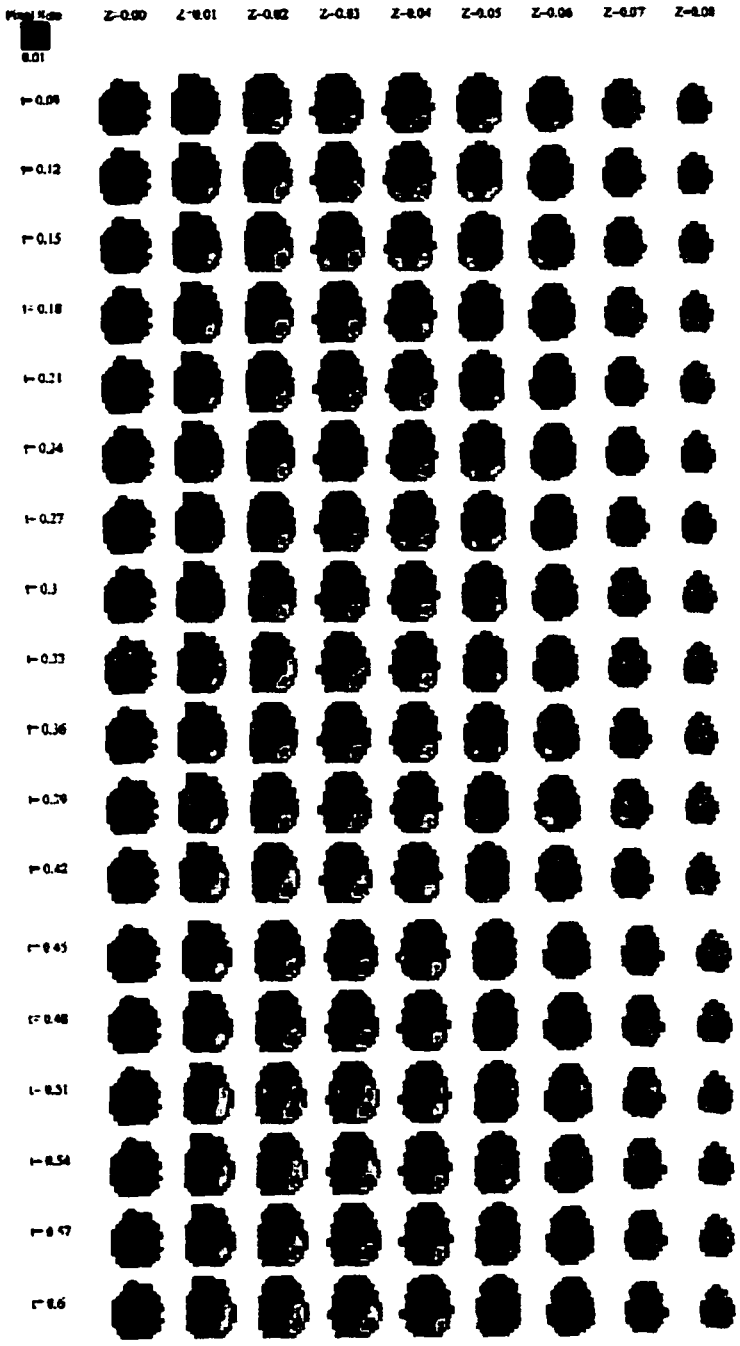

Figure 75. Source maps for the Pixelated Objects condition from 90-600msec in 30msec increments. Sources are more consistent for the N100 (90-200msec) and N400 (355-500msec) components than in the Objects condition.

The peak amplitude for the N100 component occurs at 135msec. The algorithm is applied to this timepoint and two sources are seen (Figure 76 (A)). The main source is in the posterior right hemisphere, specifically in the right occipital gyrus, bordering with the fusiform gyrus and extending superiorly to the middle temporal gyrus (Figure 76 (B)). At lower thresholds a weaker source is seen in the posterior left hemisphere, also in the middle temporal gyrus (not shown on overlay).

A

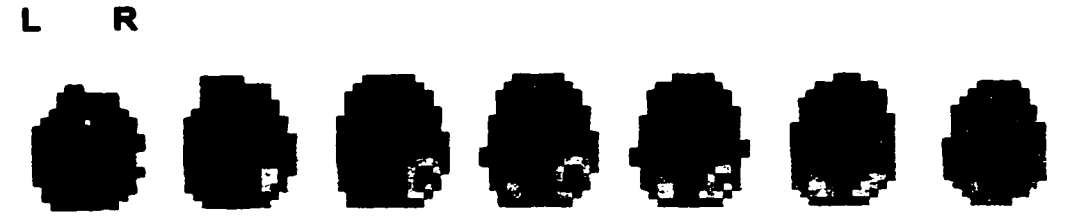

B

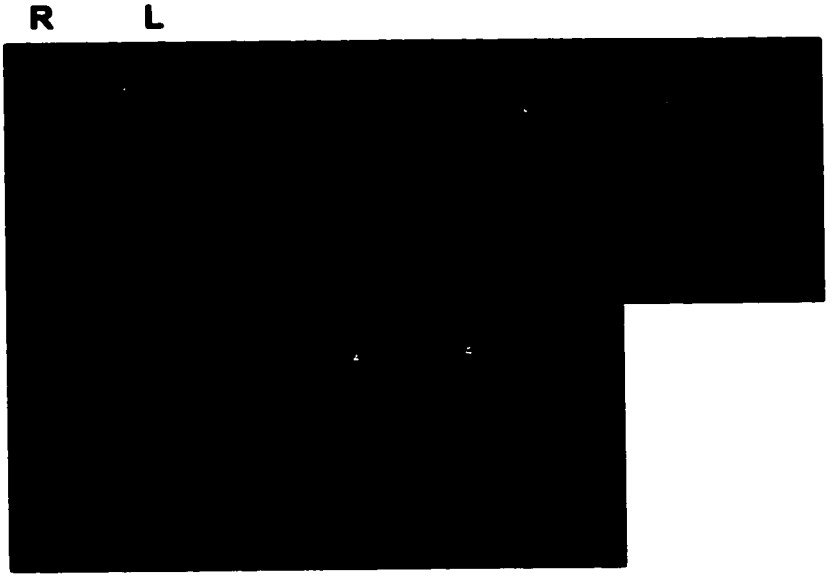

Figure 76. (A) Source maps at 135msec for Pixelated Objects (B) The source is seen in the right OcG, bordering the fusiform gyrus, extending superiorly to the MTG when overlayed onto structural MRI scans.

The peak amplitude for the N400 component occurs at 445msec. The source is similiar to the N100 component and seen in right posterior areas (Figure 77 (A)), specifically in the right occipital gyrus bordering the fusiform and extending superiorly into the inferior and middle temporal gyri (Figure 77 (B)).

A

B

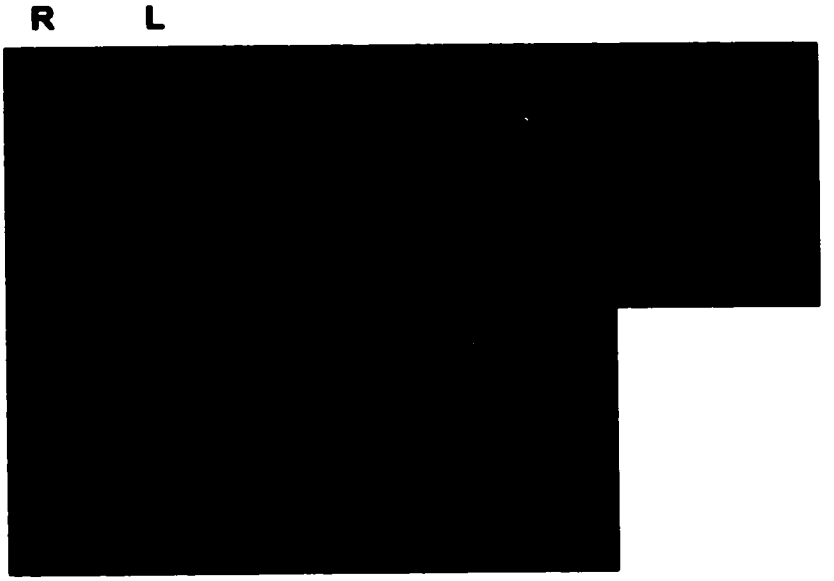

Figure 77. (A) Source maps at 445msec for Pixelated Objects. Pixels = $1cm^3$, direction is inferior to superior (L-R), axial views (B) The source is seen in the right OcG bordering with the fusiform, extending superiorly to the ITG/MTG when overlayed onto structural MRI scans.

A summary of sources for the Object and Pixelated Object conditions are listed in the table below (Table 19). Common sources for the N100 component across conditions include the right occipital gyrus and middle temporal gyrus. There are no common sources for the N400 component across conditions. The Objects condition shows bilateral sources, while the Pixelated Objects condition shows mainly right-lateralized

sources, with a weak left source in the middle temporal gyrus. Although the N100 source occurs posteriorly for both conditions, occipital N400 sources are more inferior and posterior than expected; superior sources in the supramarginal gyrus are consistent with regions described for visual object naming.

Table 19. Summary of ERP sources across conditions.

Objects	**Pixelated Objects**
N100	*N100*
Right ITG/MTG	Right OcG/fusiform
Right OcG	Right MTG
Left OcG/cuneus	
N400	*N400*
Left/midline OcG/striate	Right OcG/fusiform
Right SMG/sup parietal	Right ITG/MTG

Comparison across modalities

Two main sets of comparisons are made below. These comparisons are between: 1) CSM sites and MR volumes (fMRI and PEPSI), and 2) fMRI, PEPSI, and ERP sources, which is further divided into comparisons for the Objects vs. Pixelated Objects, Objects vs. Baseline, and Pixelated Objects vs. Baseline conditions. Comparison 1 is made between CSM sites and the PEPSI volume as well as between CSM sites and six MR volumes: a) Objects (*t*- and *F*-contrasts) b) Pixelated Objects (*t*- and *F*-contrasts) c) Objects vs. Pixelated Objects (*t*-contrast). These volumes are displayed below (Figure 78) on the 3-D reconstructions of this subject's brain. CSM sites and MR volumes are

both displayed on the surface; activations with high intensities are displayed as brighter areas.

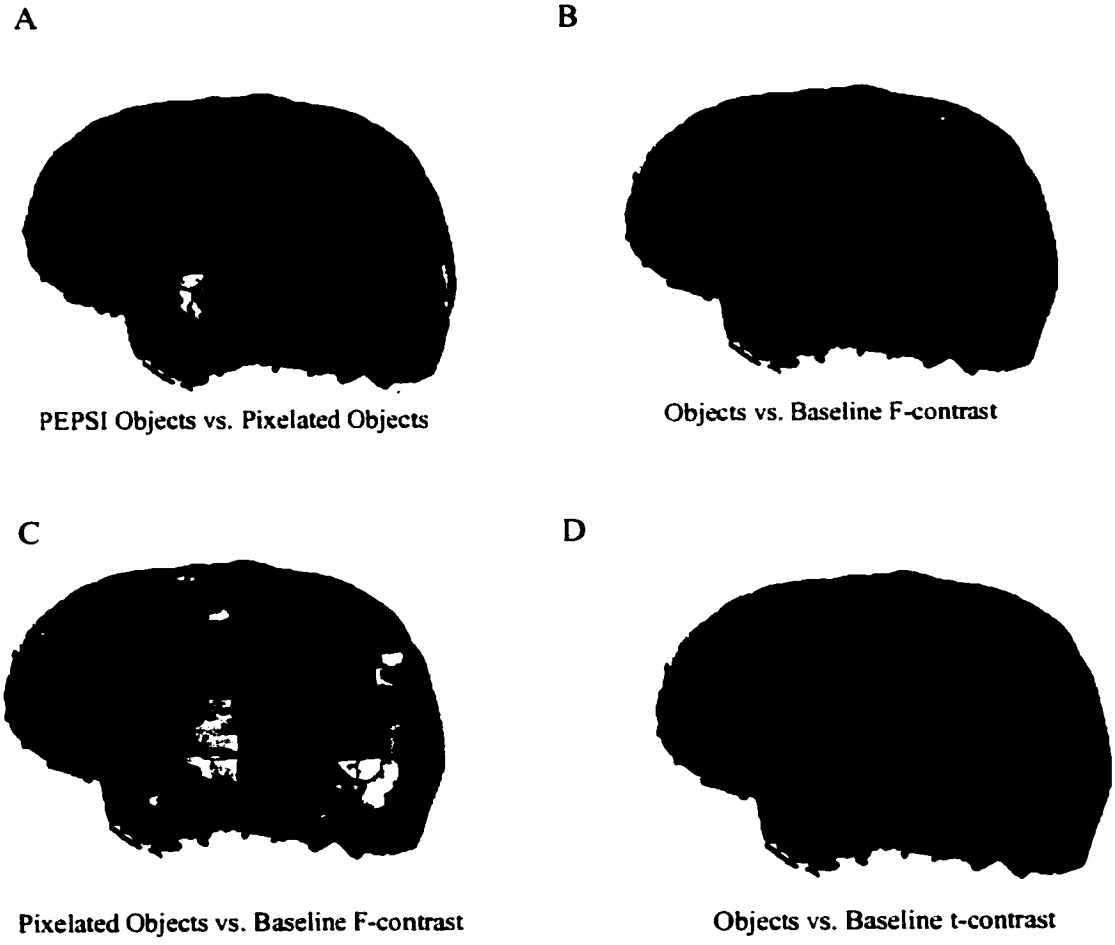

Figure 78. CSM maps and MR volumes considered for comparison analysis.

E

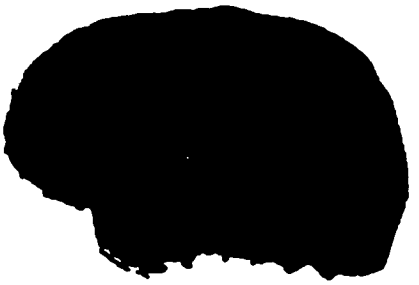

Objects vs. Pixelated Objects

Figure 78. Continued.

The analytical tool and radius/depth parameters described for P136 are also used here for this comparison and are shown in Table 20. Volumes are thresholded. Only those CSM sites that fall within the PEPSI slice location are considered for that volume.

Table 20. Weighted sums of voxel intensities for MR volumes of interest. CSM sites significant for language disruption are shaded.

CSM sites	PEPSI	F-Obj	F-Pix	T-Obj	T-Obj vs. Pix
Radius = 1 Depth = 5					
44		0.000	0.000	0.005	0.000
43		0.000	0.000	0.000	0.000
50		0.000	0.000	0.000	0.000
47	0.258	0.000	0.000	0.000	0.000
46	0.410	0.000	0.000	0.000	0.000
42	0.000	0.000	0.005	0.000	0.000
40	0.000	0.000	0.004	0.000	0.000
41		0.000	0.000	0.000	0.005
37	0.030	0.000	0.000	0.000	0.000
34		0.000	0.040	0.000	0.000
33	0.321	0.000	0.000	0.000	0.000
39	0.000	0.000	0.454	0.000	0.056

Table 20. Continued.

38	0.000	0.000	0.321	0.000	0.085
45		0.000	0.000	0.000	0.000
48		0.000	0.000	0.000	0.000
49		0.000	0.000	0.000	0.000
35		0.000	0.000	0.112	0.000
36		0.000	0.000	0.007	0.000
32		0.000	0.000	0.000	0.000
31		0.000	0.000	0.000	0.000
30		0.000	0.000	0.000	0.000
5		0.000	0.000	0.000	0.000
6		0.000	0.000	0.000	0.000
7		0.000	0.024	0.000	0.000
8		0.000	0.000	0.000	0.000
9	0.060	0.000	0.000	0.000	0.000
10		0.000	0.000	0.000	0.000
11		0.000	0.000	0.000	0.000
12	0.725	0.000	0.001	0.000	0.000
13		0.000	0.036	0.000	0.020
14		0.000	0.001	0.000	0.000
15	0.001	0.000	0.000	0.000	0.000
16		0.000	0.000	0.000	0.000
17		0.000	0.000	0.000	0.000
CSM sites	**PEPSI**	**F-Obj**	**F-Pix**	**T-Obj**	**T-Obj vs. Pix**
Radius = 1 Depth = 10					
44		0.000	0.001	0.006	0.000
43		0.000	0.057	0.000	0.000
50		0.000	0.000	0.000	0.000
47	0.716	0.000	0.000	0.000	0.000
46	0.774	0.000	0.000	0.000	0.000
42	0.000	0.000	0.116	0.000	0.000
40	0.064	0.000	0.023	0.000	0.001
41		0.000	0.008	0.000	0.037
37	0.642	0.000	0.093	0.000	0.003
34		0.000	0.567	0.000	0.026
33	2.120	0.000	0.003	0.000	0.000
39	0.003	0.000	0.747	0.000	0.073
38	0.068	0.000	0.575	0.000	0.122

Table 20. Continued.

45		0.000	0.000	0.000	0.000
48		0.000	0.000	0.000	0.000
49		0.000	0.000	0.000	0.000
35		0.000	0.000	0.141	0.000
36		0.000	0.000	0.008	0.000
32		0.000	0.000	0.000	0.001
31		0.000	0.000	0.000	0.020
30		0.000	0.000	0.000	0.002
5		0.000	0.000	0.000	0.000
6		0.000	0.001	0.000	0.007
7		0.000	0.082	0.000	0.002
8		0.000	0.000	0.000	0.000
9	0.101	0.000	0.000	0.000	0.000
10		0.000	0.000	0.000	0.000
11		0.000	0.000	0.000	0.001
12	2.877	0.000	0.129	0.000	0.000
13		0.000	0.186	0.000	0.124
14		0.000	0.032	0.000	0.000
15	0.002	0.000	0.058	0.000	0.000
16		0.000	0.000	0.000	0.000
17		0.000	0.000	0.000	0.000
CSM sites	**PEPSI**	**F-Obj**	**F-Pix**	**T-Obj**	**T-Obj vs. Pix**
Radius = 1 Depth = 15					
44		0.000	0.004	0.006	0.000
43		0.000	0.166	0.000	0.000
50		0.000	0.208	0.000	0.000
47	0.809	0.000	0.001	0.000	0.000
46	0.867	0.000	0.003	0.000	0.000
42	0.029	0.000	0.215	0.000	0.000
40	0.474	0.000	0.037	0.000	0.004
41		0.000	0.016	0.000	0.043
37	1.904	0.000	0.177	0.000	0.006
34		0.000	0.652	0.000	0.030
33	3.052	0.000	0.004	0.000	0.000
39	0.519	0.000	0.839	0.000	0.081
38	0.464	0.000	0.636	0.000	0.158
45		0.000	0.000	0.000	0.000

Table 20. Continued.

48		0.000	0.000	0.000	0.000
49		0.000	0.000	0.000	0.000
35		0.000	0.000	0.153	0.003
36		0.000	0.000	0.009	0.005
32		0.000	0.000	0.004	0.004
31		0.000	0.000	0.004	0.023
30		0.000	0.000	0.000	0.002
5		0.000	0.000	0.000	0.033
6		0.000	0.001	0.000	0.102
7		0.000	0.094	0.000	0.050
8		0.000	0.020	0.000	0.000
9	0.114	0.000	0.064	0.000	0.000
10		0.000	0.004	0.000	0.000
11		0.000	0.000	0.000	0.010
12	4.169	0.000	0.149	0.000	0.000
13		0.000	0.211	0.000	0.253
14		0.000	0.040	0.000	0.003
15	0.002	0.000	0.130	0.000	0.001
16		0.000	0.001	0.000	0.000
17		0.000	0.000	0.000	0.000
CSM sites	**PEPSI**	**F-Obj**	**F-Pix**	**T-Obj**	**T-Obj vs. Pix**
Radius = 5 Depth = 1					
44		0.000	0.000	0.012	0.000
43		0.000	0.000	0.000	0.000
50		0.000	0.000	0.000	0.000
47	0.024	0.000	0.000	0.004	0.000
46	0.061	0.000	0.000	0.000	0.000
42	0.000	0.000	0.015	0.000	0.001
40	0.000	0.000	0.026	0.000	0.002
41		0.000	0.000	0.000	0.002
37	0.004	0.000	0.014	0.000	0.002
34		0.000	0.005	0.000	0.001
33	0.038	0.000	0.000	0.000	0.000
39	0.000	0.000	0.160	0.000	0.014
38	0.000	0.000	0.180	0.000	0.036
45		0.000	0.000	0.000	0.000
48		0.000	0.000	0.000	0.000

Table 20. Continued.

49		0.000	0.000	0.000	0.000
35		0.000	0.000	0.029	0.000
36		0.000	0.000	0.005	0.000
32		0.000	0.000	0.000	0.000
31		0.000	0.000	0.000	0.000
30		0.000	0.000	0.000	0.000
5		0.000	0.000	0.004	0.000
6		0.000	0.002	0.000	0.000
7		0.000	0.002	0.000	0.000
8		0.000	0.000	0.000	0.000
9	0.008	0.000	0.000	0.000	0.000
10		0.000	0.000	0.000	0.000
11		0.000	0.000	0.000	0.000
12	0.045	0.000	0.003	0.000	0.000
13		0.000	0.015	0.000	0.002
14		0.000	0.000	0.000	0.000
15	0.030	0.000	0.000	0.000	0.000
16		0.000	0.000	0.000	0.000
17		0.000	0.000	0.000	0.000

No significant correlations were found between CSM sites and PEPSI or fMRI peak activations at the depths and radii tested. Qualitative comparisons show that lower-level PEPSI activation in the posterior superior temporal gyrus occurs below non-significant sites 46 and 47 and just posterior to language site 15. Anteriorly, higher-level activation from the left insula to the middle temporal gyrus sits below language site 12 and just posterior to non-significant site 33 in the anterior superior temporal gyrus. The PEPSI occipital activation falls outside the sampled area of CSM sites. Figure 79 below displays these qualitative relationships.

Figure 79. PEPSI activations and CSM sites at progressively greater depths from the surface of the cortex. Higher intensity PEPSI activations are in yellow, lower intensities are in orange; significant CSM sites are represented by orange dots, non-significant sites are shown with blue dots.

For fMRI activations in the Objects vs. Pixelated Objects condition, activation in the mesial superior and middle temporal gyri sit below non-significant sites 38 and 39 respectively. Activation also sits below non-significant site 37 in the anterior middle temporal gyrus, non-significant site 32 in the inferior frontal gyrus (operculum), and language site 13 in the ventral post-central gyrus. For the Objects vs. Baseline (*t*-contrast) condition, activation occurs below non-significant site 44 in the mesial inferior temporal gyrus, and below non-significant sites 35 and 36 in the inferior frontal gyrus (operculum). Remaining activations occur outside the sampled area of CSM sites. For the Objects vs. Baseline (*F*-contrast) condition, activations in the left middle temporal gyrus and post-central gyrus occur outside the sampled CSM area. For the Pixelated vs. Baseline condition, activation occurs below non-significant sites 38 (mesial superior temporal gyrus) and 39 (mesial middle temporal gyrus), more deeply below non-significant site 34 in the anterior inferior temporal gyrus, and just inferior and posterior to

language site 12 in the anterior middle temporal gyrus. Deeper activations occur below non-significant sites 46 and 47 in the posterior middle temporal gyrus and just inferior and posterior to language site 15. Remaining activations fall outside the sampled CSM area. These qualitative comparisons are shown below in Figure 80.

A Objects vs. Pixelated Objects

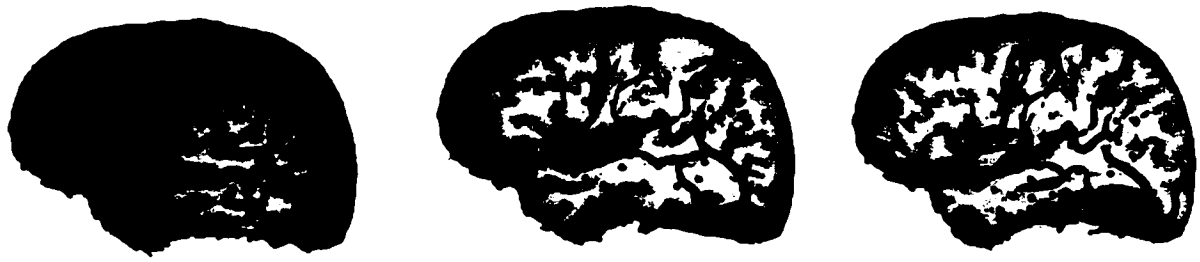

B Objects vs. Baseline (*t*-contrast)

Figure 80. CSM sites and fMRI activation for Objects vs. Pixelated Objects (A), Objects vs. Baseline (B), and Pixelated Objects vs. Baseline (C).

C Pixelated Objects vs. Baseline

Figure 80. Continued.

ERP sources for the N100 and N400 components for Objects are posterior to the sampled area of CSM sites. No left-sided sources are seen for the N100 or N400 components for Pixelated Objects.

Comparison 2 is made between fMRI, PEPSI, and ERP sources. Three comparisons are made: a) Objects vs. Pixelated Objects, b) Objects vs. Baseline, c) Pixelated Objects vs. Baseline.

A Objects vs. Pixelated Objects

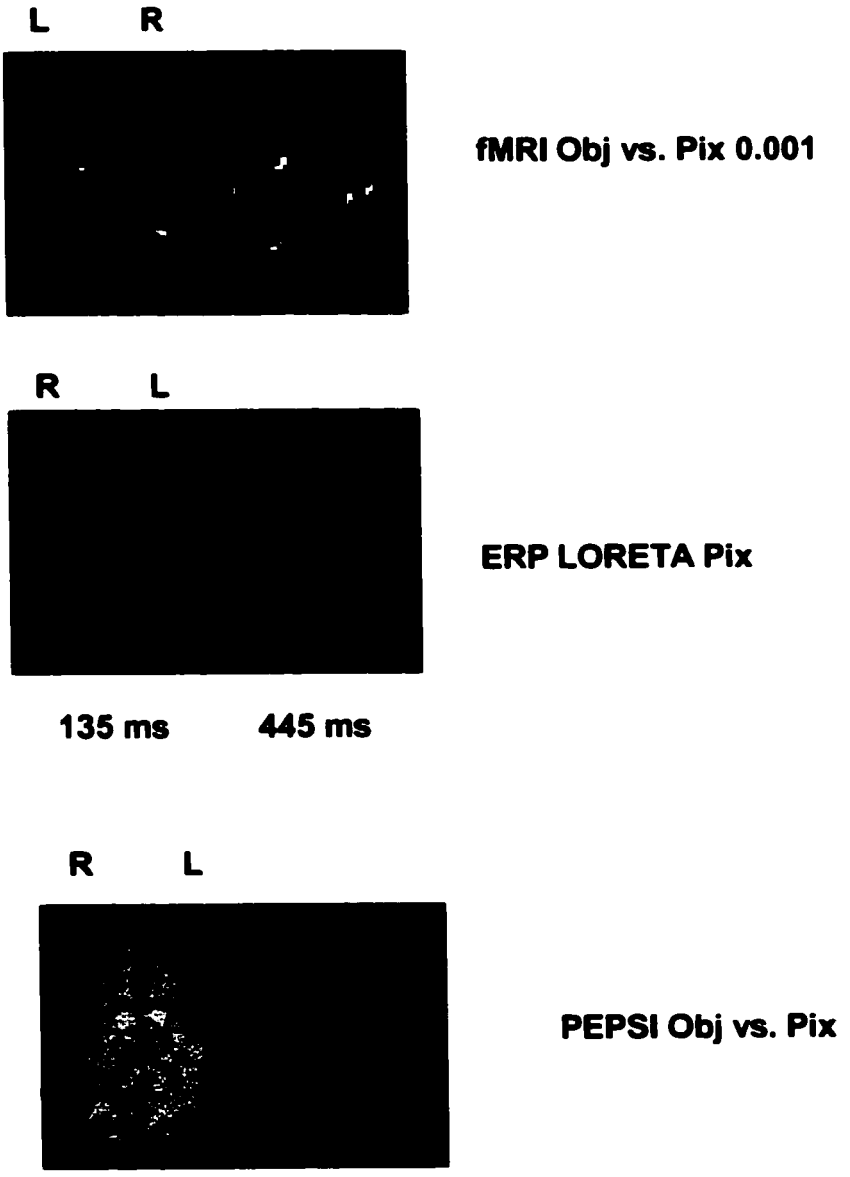

Figure 81. Comparison across imaging modalities for Objects vs. Pixelated Objects.

Matches are seen in the right middle temporal gyrus between fMRI, PEPSI, and ERP Pixelated Objects N100 and N400 sources (blue circles), the left insula between fMRI and PEPSI (green), and the right insula between fMRI and PEPSI (grey voxels, orange).

B Objects vs. Baseline

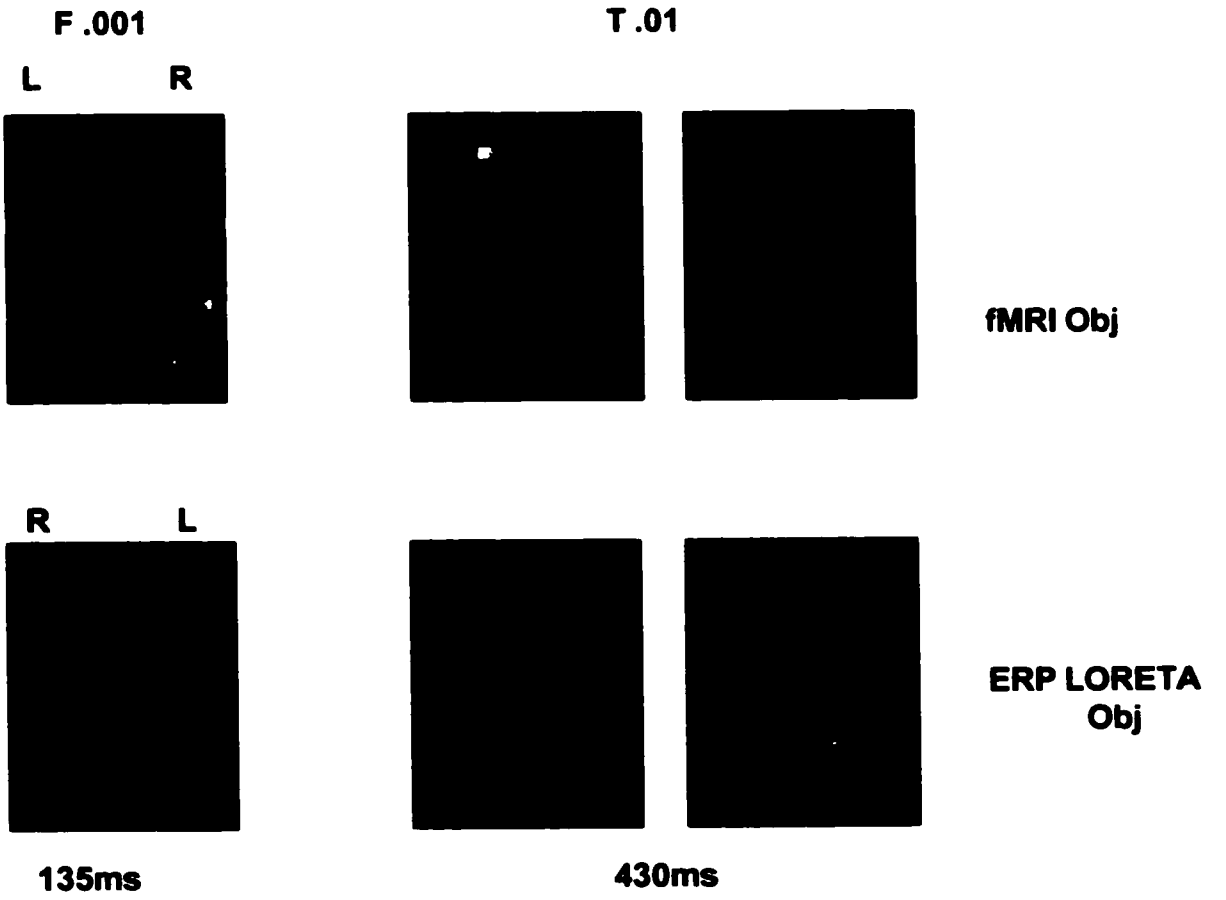

Figure 82. Comparison across modalities for Objects vs. Baseline.

Matches occur in the right inferior temporal gyrus between fMRI (*F*-contrast, blue circle) and ERP Objects N100 and in the right midline striate/occipital gyrus between fMRI (*t*-contrast, green) and ERP Objects N400. No matches occurred between PEPSI activations and fMRI or ERP sources for this condition.

C Pixelated Objects vs. Baseline

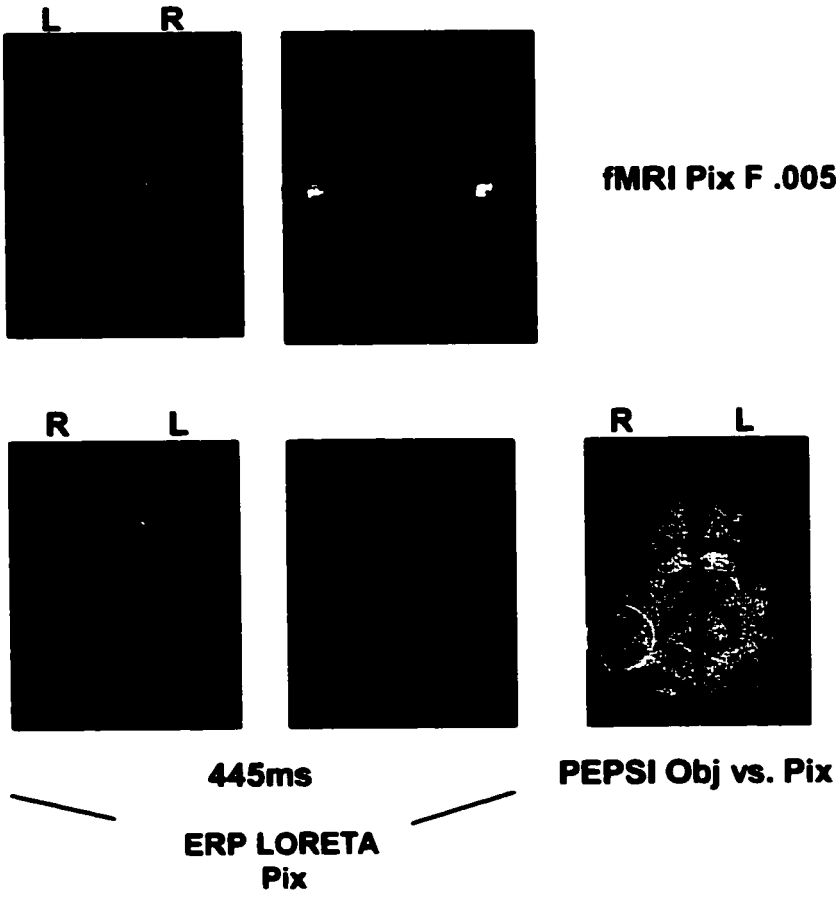

Figure 83. Comparison across modalities for Pixelated Objects vs. Baseline.

Matches occur in the white matter in the vicinity of the right lateral ventricle between fMRI (blue circle) and the ERP Pixelated Objects N400 source, in the left insula between fMRI and PEPSI (green), and the right middle temporal gyrus between between PEPSI and ERP Pixelated Objects N400 (yellow). Anterior and posterior distinctions between N100 and N400 sources are not seen here.

The left insula was identified as a common area of activation in fMRI and PEPSI, but the cortical surface projecting from this area was not sampled with CSM, so it is unknown whether this area would have produced a language disruption.

Chapter 5 Discussion

The use of a visual object-naming paradigm with PEPSI and ERP techniques in this study is novel. Before examining how activations across techniques compare to each other, it is important to consider whether the activations or sources within each technique are consistent with previous studies of visual object naming. Following this discussion, the implications of how and where these activations compare across techniques will be examined.

PEPSI

No other PEPSI studies with visual object naming have been reported before now. As mentioned above, only the posterior two-thirds of the slice are examined for activations. Left occipital activation occurred for all subjects, reflecting basic visual processing of stimuli. Although PEPSI analysis relies on a subtraction method in an attempt to segregate semantic processing of objects from visual processing of pixelated objects, visual processing that was common to both tasks was still seen. This effect was also seen by Price et al. (1997), who showed that left visual extrastriate cortex remained in a subtraction task using words and objects. It was postulated that differences between two tasks may include not only the addition of the cognitive component of interest, but the effect of that added component to baseline processes as well. Left-dominant subjects (P138, P137) tended to show more lateralized activations in structures associated with object processing, such as inferior temporal and inferior frontal gyri, than the right-

dominant subject (P136), who showed bilateral activation in temporal areas. Left inferior and middle temporal activations are consistent with several visual object imaging studies (eg. Martin et al., 1995; Menard et al., 1996; Damasio et al., 1996; Murtha et al., 1999); right middle temporal gyrus activations are less common, though still seen (Menard et al., 1996; Price et al., 1996b; Moore and Price 1999a). Competing interpretations for middle temporal gyrus activation during object naming center on semantic processing and visual perceptual processing specific to shape analysis. Superior temporal activations are more often associated with phonological processing (Demonet et al., 1992; Paulesu et al., 1993) or picture versus word comparisons (Menard et al., 1996; Moore and Price, 1999b), though Murtha et al. (1999) found left superior temporal activation in an object naming/semantic judgment task. Left insula activation is also consistent with object naming, possibly reflecting structural and semantic aspects of object recognition during object naming and/or to the phonological retrieval of object names (eg. Price et al., 1996b). Overall, PEPSI activations are consistent with areas described for visual object naming in the PET and fMRI literature.

fMRI

Visual areas (occipital gyrus and/or precuneus/cuneus) are activated in all conditions for all subjects. As with the PEPSI results, visual areas are commonly activated in visual object processing and naming studies, despite a wide variety of experimental and control tasks (see summary in Chapter 1), including object versus

scrambled object conditions (eg. Malach et al., 1995; Martin et al., 1996; Grill-Spector et al., 1998). Bilateral fusiform activation was seen in the Objects vs. Pixelated Objects condition in both left-dominant subjects (P138, P137), and in the Pixelated Objects vs. Baseline condition for the right-dominant subject (P136). Bilateral fusiform activation is common in visual object processing studies, including face processing (Puce et al., 1995, 1996), object categorization (Op de Beeck et al., 2000; Sergent et al., 1992a; Gauthier et al., 1997), and naming (Bookheimer et al., 1995; Martin et al., 1996; Price et al., 1996b; Moore and Price, 1999b; Murtha et al., 1999). Left-lateralized fusiform activation was seen in the Objects vs. Baseline condition for P136 and in the Pixelated Objects vs. Baseline condition for P138 and P137. Although left fusiform activation has been seen with generalized naming (Price et al., 1996b), it has also been seen with scrambled objects (Kanwisher et al., 1997), causing competing interpretations as to whether the fusiform in general is more strongly associated with visual perceptual processing rather than semantic processing. On the surface, activation in the fusiform in all three conditions supports the position of a visual perceptual processing role. However, it is likely that scrambled objects stimulate some automatic semantic processing in an attempt to attach a verbal label to the stimulus, much in the same way visual words and pronounceable pseudowords activate not only orthographic codes, but implicit semantic and phonological codes as well (Price et al., 1994; Price et al., 1996a).

Left inferior temporal areas external to the fusiform showed limited activation in these subjects, appearing only in the Objects vs. Baseline condition for P136 and in the

Pixelated vs. Baseline condition for P138. The posterior inferior temporal activation for P136 is consistent with object naming, as is the anterior inferior temporal activation for P138 (Vandenburghe et al., 1996; Price et al., 1996b). Again, since the activation for P138 is in the Pixelated Objects vs. Baseline condition, it suggests that some level of automatic attempts at naming these stimuli was taking place.

Middle temporal gyrus activation is seen for left-dominant subjects (P138, P137), occuring in the Objects vs. Pixelated Objects and Objects vs. Baseline conditions. The grid patient (P137) also showed middle temporal gyrus activation in the Pixelated vs. Baseline condition. This area is commonly activated in object categorization (Sergent et al., 1992a, 1992b), naming (Martin et al., 1995; Damasio et al., 1996; Murtha et al., 1999) and semantic categorization studies using words and pictures (Binder et al., 1995, 1996, 1997; Shaywitz et al., 1995; Vandenburghe et al., 1996; Murtha et al., 1999), suggesting that it plays a role in semantic processing. Some investigators, however, argue that the middle temporal gyrus is responsible for perceptual processes specific to visual shape analysis (Corbetta et al., 1990; Martin et al., 1995), while others assign it the role of accessing the name of an object during the recognition process rather than visual processes inherent in its recognition (Sergent et al., 1992a, 1992b). Lesions in this area do not appear to result in disruptions of object recognition or in deficits in describing an object's function, but rather the naming of these objects (Flude et al., 1989; Damasio et al., 1990), suggesting only that phonologic rather than semantic or visual processes are being affected. The activation pattern across conditions does not clarify whether visual

or semantic processes are represented in this area, particularly if subjects automatically attempted to attach semantic meaning to pixelated stimuli. Discussion of the ERP source localization results below may help to clarify the issue.

Superior temporal gyrus activation was seen for all subjects in the Objects vs. Pixelated Objects condition. Both superior temporal and supramarginal activations were seen in all conditions for P138. Superior temporal and supramarginal gyri are more often associated with word versus picture comparisons (Menard et al., 1996; Moore and Price, 1999b), being relatively more active for words, suggesting that its primary role may be in orthographic-to-phonologic processing. Murtha et al. (1999), however, also found superior temporal activation to object naming when compared to viewing plus signs, implying that although these areas are relatively more active for words when compared to objects, they may still be involved in phonologic processes associated with naming objects.

Left or bilateral inferior and middle frontal gyri activation was seen in left-dominant subjects across conditions. These frontal areas are found during a variety of object recognition and naming tasks, being similarly attributed to a variety of cognitive functions, including phonology with implicit (Menard et al., 1996) or explicit naming (Bookheimer et al., 1995; Martin et al., 1995; Price et al., 1996b), knowledge-guided searches during semantic categorization tasks (Kosslyn et al., 1994, 1995), and implicit or explicit semantic retrieval during object naming (Vandenberghe et al., 1996; Menard et al., 1996; Murtha et al., 1999). Frontal activations in this study were present with

superior temporal and supramarginal areas, suggesting an articulatory, phonological network; frontal activations were also present with inferior and middle temporal and fusiform gyri, suggesting a semantic network. Activations across conditions implies that both semantic and phonological processes were active for left-dominant subjects, which is reasonable since the task was not designed to segregate these processes. Across conditions, frontal areas for the right-dominant subject (P136) were consistently limited to the orbitofrontal gyrus and right or bilateral insula. Insular activation is consistent with object naming studies (eg. Price et al., 1996b); the role of the orbitofrontal gyrus in this context is probably related to the prefrontal attentional system that includes the cingulate and gyrus rectus, which were all seen across conditions for this subject.

ERP Scalp Distributions

Scalp distributions for the N100 component in the Objects condition are consistent across subjects. Peaks occur between 130-160msec, and are most prominent at midline and bilateral anterior sites, while amplitudes are reduced at lateral sites and severely reduced or absent at posterior sites. This distribution is unlike a study by Kiefer (2001), which examined perceptual and semantic characteristics of category-specific picture categorization. In this study peak amplitudes of the N100 component were distributed over posterior electrode sites, but only a limited number of frontal electrode sites were analysed. Several other studies, however, show peak amplitudes of the N100 component at bilateral frontal sites in response to pictures in sentences (Federmeier and

Kutas, 2002), correctly-identified fragmented pictures (Schendan and Kutas, 2002), and object decision tasks (Holcomb and McPherson, 1994). The pattern in the present study is consistent with these latter reports. Scalp distributions for the Pixelated Objects condition are also fairly consistent across subjects for this component. Peaks occur between 135-160msec, and are most prominent at midline and right anterior sites (P138, P136) or across all anterior sites (P137). Amplitudes are reduced at left lateral anterior sites (P138, P136) and either severely reduced or absent across all posterior sites. This pattern is also consistent with studies of object decision (Holcomb and McPherson, 1994) and picture semantic priming tasks (McPherson and Holcomb, 1999), which show distributions for non-objects or unidentifiable objects being more prominent at anterior sites.

Scalp distributions for the N400 component in the Objects condition vary across subjects. The distribution of the control subject (P138) shows the largest amplitudes for this component at left posterior and midline/right centro-temporal sites. Amplitudes are reduced at mesial lateral sites and absent at anterior sites bilaterally. This distribution is fairly consistent with the distribution of the N400 in the picture categorization task of Kiefer (2001), which was observed at occipito-temporal, centro-parietal, and fronto-central sites (over the motor cortices). Prominent right-sided centro-parietal sites, however, are more commonly associated with the N400 to words (eg. Holcomb and Neville, 1990) and sentences (eg. Kutas and Hillyard, 1980), while several studies show that N400 amplitudes to pictures are as prominent (Barrett and Rugg, 1990) or more

prominent (Holcomb and McPherson, 1994; Ganis et al., 1996) in left frontal sites. The anterior distributions of P136 and P137 are both consistent with this latter description of the picture N400, having the largest amplitudes in mesial midline (P137) and left anterior (P136) sites and being severely reduced or absent across posterior sites. An N400 component for the Pixelated Objects condition was not found for P136. In addition, a P300 effect was seen in right posterior areas for both patients (P136, P137), but not the control subject (P138). The pilot study described in Chapter 2 showed that a blocked presentation design prevented P300 effects from occurring in normal control subjects. It was expected that this outcome would have carried over to the patients as well, but it did not in this study. Whether this effect can be generalized to epilepsy patients as a population is not known because this study used a within-subjects design and only a small number of patients were utilized. Additionally, P300 effects in normals have been reported elsewhere. For example, a P300 effect for non-object pictures is seen in the study of Holcomb and McPherson (1994), who attribute it to extra effort in working memory processes. P300 effects are commonly attributed to surprise, or the occurrence of a low-probability event (Hagoort et al., 1999), but between the blocked design and instructions, subjects could clearly foresee whether an upcoming item was an object or a pixelated object. It is possible that extra effort was made in working memory processes to match a pixelated object with similarly-featured items in the memory store, but this conjecture predicts that normals and patients both would engage in this strategy. At present, it is unclear whether epileptic patients as a group are uniquely sensitive to novel

non-object stimuli in a way that normals are not. Future study is required to answer this question. Additionally, how the P300 in the Pixelated Objects condition affects the scalp distribution, amplitude, or robustness of the N400 component is unclear. As it stands, the largest amplitudes of the N400 component in this study are most prominent at midline/right anterior sites for P138 and midline/left anterior sites for P137. In both cases amplitudes are reduced or absent at posterior sites. This pattern is consistent with responses to non-objects or incomplete objects in other studies, which show prominent negative amplitudes with incomplete (Stuss et al., 1992) or unidentifiable pictures at anterior sites (Holcomb and McPherson, 1994; McPherson and Holcomb, 1999), often with a larger negativity than for objects.[8]

ERP Sources

Source localizations using LORETA with an object naming task have not been reported before now. Sources for the N100 component across Objects and Pixelated Objects conditions are found consistently in posterior areas for all subjects. A left occipital gyrus source is found for all subjects in the Objects condition, and bilateral occipital gyri sources are found for P138 and P136 in the Pixelated Objects condition;

---

[8] A greater negativity to non-objects than to objects at these sites is considered analogous to the greater negativity seen in response to pseudowords compared to related or unrelated words (Holcomb and Neville, 1990). Although the mean peak amplitude across the scalp for the N400 component did not significantly differ across conditions for P138 in a Paired Samples test (M (SE) [mV]= 0.129 (0.013), 0.132 (0.014) (Objects, Pixelated Objects), $t = -0.0133$, $p = 0.894$), it did for P137 (M (SE) = 0.17 (0.016), 0.29 (0.041) (Objects, Pixelated Objects), $t = -3.15$, $p = 0.002$). A larger number of subjects would be needed to determine whether the mean amplitude of the N400 response to Pixelated Objects is consistently more negative than that for Objects.

P137 had a right-sided occipital gyrus source for this condition. Sources in occipital areas across conditions very likely reflect relatively low-level visual perceptual processing during object detection. Sources in the inferior and middle temporal gyri were also found across subjects, but were more bilateral in the Pixelated Objects condition. As suggested by imaging studies (eg. Price et al., 1996b), these temporal sources may relate to structural aspects of object recognition, which should take place for both Object and Pixelated Object conditions at early stages of processing as reflected by the N100 component. As mentioned above, the role of the middle temporal gyrus has two competing interpretations: 1) perceptual processing relating to visual shape analysis (Corbetta et al., 1990), and 2) accessing the name of an object during the recognition process (Sergent et al., 1992a, 1992b). Lesion evidence in this area points to disruptions in naming objects rather than visual object recognition (Flude et al., 1989; Damasio et al., 1990), suggesting its role is accessing object names. However, a middle temporal neural generator for such an early component argues in favor of a more visual perceptual processing role, possibly in processes inherent in attempting to recognize an object, which would explain its presence in both conditions. Interestingly, P136 showed a source in the superior temporal gyrus in both conditions, again more bilaterally in the Pixelated Objects condition. Superior temporal activations have been reported in object naming paradigms (Murtha et al., 1999), but are considered to be involved in relatively later stages of phonologic processing during naming rather than early visual perceptual processes. The interpretation for this source across conditions at this early stage is

unclear, other than to fall into a broad, relatively ventral pathway from occipital areas, which has been linked to the encoding of shape or color properties (Maunsell and Newsome, 1987).

Sources for the N400 component vary widely across subjects. Sources are found in frontal areas for P138 across conditions. Sources are right-lateralized in the Objects condition to the middle and superior frontal gyri and the cingulate; sources are bilateral in the Pixelated Objects condition, localizing to the left inferior and middle frontal gyri in addition to the right superior frontal gyrus and cingulate. Why sources are lateralized to the right side when the subject is presumably left-dominant is unclear; considering this subject showed bilateral frontal activation for Objects vs. Baseline with fMRI, it is possible that left-sided activity was simply not reflected in scalp potentials and hence not found as a source. This question aside, cingulate areas are likely associated with attentional mechanisms (Petersen et al., 1988; Frith et al., 1991; Raichle et al., 1994), while superior frontal areas may be associated with effortful searches through memory for words (Demonet et al., 1994). Lesions in the superior frontal gyrus has been associated with an inability to generate word lists (Rubens, 1976; Alexander and Schmitt, 1980; Freedman et al., 1984; Stuss and Benson, 1986; Costello and Warrington, 1989), and significant naming errors have been shown to occur in superior frontal gyri of cortical stimulation patients (Ojemann, 1992), suggesting this area plays a role in object naming that is relatively later than processing the structure of an object or in object recognition. In ERP studies, the N400 component is considered sensitive to post-lexical

semantically based processes (see Rugg, 1990 and Holcomb, 1993 for reviews). In imaging studies, frontal areas, albeit left-sided, are found during a variety of object recognition and naming tasks. Competing interpretations for the role of inferior and middle frontal gyri have focused on a) phonological processes during naming, b) knowledge-guided searches, and c) semantic retrieval or semantic working memory. The overall pattern of imaging studies (see Chapter 1) suggests that frontal areas are considered part of an articulatory, phonological network when active concurrently with superior temporal and supramarginal gyri, and a semantic network when active with inferior and middle temporal gyri and fusiform regions. It is possible that a search for an appropriate label is the basis for these sources in the Pixelated Objects condition, which is consistent with the view that "more effortful semantic retrieval procedures" take place in frontal areas (Whatmough et al., 2002). In the Objects condition, the pattern of frontal sources for the N400 component together with inferior/middle temporal gyri sources for the N100 component argues for assigning a semantic processing role rather than a phonological role to frontal sources for the N400 component for this subject.

N400 sources for P136 in the Objects condition are left-lateralized to the inferior frontal gyrus (operculum), insula, pre- and post-central gyri, and the superior temporal gyrus. Like P138, sources for the N400 component are more anterior than those for the N100 component. The lateralization of this source, however, is also unexpected, since this patient was known to be right-dominant for language. Again, it is possible that right-sided activity was simply not reflected in scalp potentials and hence not found as a

source. Another possibility is that scalp potentials are affected in some way by epileptic activity. The scalp distribution for this patient showed that the most prominent amplitudes for the N400 component was left-lateralized to fronto-temporal sites, which is contralateral to the side of the epileptic focus. The lateralization of the scalp distribution pattern is consistent with a study by Lalouschek et al. (1998), where epilepsy patients showed larger negativities contralateral to the seizure focus in lateral fronto-temporal scalp sites in a continuous memory paradigm using pseudowords and spatial patterns. It is also consistent with results from Grunwald et al. (1995), who found smaller N400 amplitudes in intracranial temporal recordings ipsilateral to the epileptogenic focus in a visual oddball paradigm. A large sample of patients could determine whether these scalp distribution and source lateralizations could be generalized to the epileptic population. At this time, the paucity of LORETA source localization studies in either patient or normal populations renders these lateralization effects a matter of speculation. It is also interesting that the N400 source falls within the superior temporal gyrus, as it did for the N100 source for this subject. In imaging studies, this area is usually associated with visual word or phonological processing (see Chapter 1). Since the task required the covert naming of objects and the covert response of "scrambled" to pixelated objects, it is possible that such phonological processes are reflected here for this subject. It has been also been noted in imaging studies that the inferior frontal gyrus together with the precentral gyrus are involved with phonetic encoding or articulation (eg. Price et al., 1996c). In isolation, the involvement of the superior temporal gyrus in sources for both

the N100 and N400 components makes the interpretation of this area non-specific at the present time, but together with the involvement of the inferior frontal gyrus and pre-central gyrus, a phonological role for these sources may be argued for this subject. Phonological ERP effects have been examined relatively less than semantic effects, though some studies have reported similar latency and polarity effects for phonological manipulations in the N400 as for semantic manipulations (Praamstra et al., 1994; Rugg and Barrett 1987). Praamstra et al. (1994), for example, found a reduction in the amplitude of what appears to be an N400 component when a target word phonologically overlaps (i.e., rhymes) with a preceeding prime compared to when it does not. Differences in topography between phonological and semantic N400 effects are still a matter of debate (Hagoort et al., 1999); future ERP and source localization studies may clarify whether the N400 and/or its sources reflect semantic as well as phonologic effects.

N400 sources for P137 in the Objects condition are found in the left/midline occipital gyrus/striate area and in the right supramarginal gyrus and superior parietal lobule; sources are right-lateralized to the occipital gyrus/fusiform area as well as the inferior and middle temporal gyri in the Pixelated Objects condition. Unlike P138 and P136, the N400 sources for this subject were not anterior to those for the N100. The posterior sources are very similar in both location and lateralization across conditions to those found for this subject's N100 sources. The basis for these posterior sources in what is widely considered a semantic component is problematic. The novelty of source localization, particularly for components across time, makes it unclear whether such an

occurrence may be due to individual variability, some sort of sustained period of visual processing, or some kind of feedback mechanism between ventral and dorsal sources. A sustained period of visual processing would be consistent with reports of occipital-temporal activation for abstract patterns, reflecting processing at the structural description level (eg. Whatmough et al., 2002). How long such processing may be maintained, however, is unknown at this time and requires future study. The lateralization of the superior sources to the right side also deserves comment. The relatively weak lateralization of the scalp distribution is likely due to the bilateral nature of the inferior left and superior right sources. Like P136, these sources are contralateral to the side of the epileptic focus. Superior sources are more consistent with localizations in object naming imaging studies, though not strictly for semantic-specific processing. Superior parietal activation has been found for category-level matching for both words and pictures (Kosslyn et al., 1995), suggesting a semantic-based processing role. The supramarginal gyrus, however, is usually found to be more active for words than objects in imaging studies, such as passively viewing words and pictures (Menard et al., 1996), in naming or viewing words and objects (Moore and Price, 1999b), and in generating action-words for objects (Martin et al., 1995). As reviewed in Chapter 1, these studies suggest that like the superior temporal gyrus, the supramarginal gyrus is involved in tasks that call for relatively robust phonological processing. Again, it is likely that task requirements reflect phonological processing and possible that the N400 component and sources reflect the same.

The ERP source data raises two main issues for the N400 component and its sources: 1) the specificity of the N400 as a semantic component, and 2) the variable location of its source. The sources for the control subject (P138) argue strongly for a semantic-specific interpretation. However, the results from the two patients raise the prospect that the N400 may reflect processes that combine both semantic and phonological processing. Phonological ERP effects have been given relatively little attention compared to semantic effects, particularly for the N400. Some studies have reported that phonological manipulations have N400-like effects in terms of polarity and latency. Rugg and Barrett (1987) have shown that the N400 component is affected by phonemic similarities of rhyming words, and Praamstra et al. (1994) reported a reduction in the amplitude of an N400-like component when a target word shows rhyme overlap with a preceding prime compared to when there is no rhyme overlap. Although there were no specific phonological manipulations in the present study, the task demands of covertly generating a name for a picture may be reflected in the N400 component that was seen and may be responsible for sources that are consistent with phonological processing.

Attempts to find the neural generator for the N400 have been made by several investigators through the use of intracranial electrodes, and there is a large body of evidence indicating that the temporal lobe plays an important role in generating the N400 component. This evidence includes the observation that the N400 is severely attenuated following unilateral anterior temporal lobectomy (Rugg et al., 1991; Smith and Halgren,

1988, 1989), and intracranial N400 waveforms show similar characteristics and responses to semantic manipulations as the scalp N400 (eg. Nobre and McCarthy, 1995). However there is also evidence from the intrcranial study of Guillem et al. (1995) to suggest other anatomical structures generate the N400 component as well. Using picture stimuli in a continuous recognition memory task, they found N400 components in the anterior and posterior temporal lobe, prefrontal regions (gyrus rectus), and parietal structures (superior parietal lobule, supramarginal gyrus) that displayed large amplitudes, steep voltage gradients, and local polarity reversals, which they interpreted as evidence that the N400 component was generated locally from these structures rather than volume-conducted activity from one distant generator. Their conclusion that the scalp-recorded N400 component reflects synchronous activity occurring across widely distributed neural systems is consistent with the source localization data shown here. If the N400 reflects different cognitive activities such as semantic and phonological processing as postulated above, then it is reasonable to predict that local generators for this component would differ as well. Although the current study does not offer definitive evidence that the N400 component and its sources reflect distinct cognitive activities, i.e. semantic and phonologic processing, the task requirements and the distinct network of sources suggest this possibility.

Comparison across PEPSI, FMRI, ERP

Matches across modalities occur to some degree for all subjects, and common areas fall within the visual object and semantic processing networks described in Chapter 1. The most common posterior area found across techniques is the middle temporal gyrus, lateralized to the left for the control subject (P138) and to the right for patients (P136, P137). The most common anterior areas found across techniques are bilateral superior frontal gyri for the control subject (P138) and bilateral insula for the patients (P136, P137). Several other areas match across a subset of the techniques used, most notably occipital, inferior, and superior temporal gyri in posterior areas and inferior and middle frontal gyri in anterior areas.

For the control subject (P138), a primary result to note is that concurrent posterior and anterior fMRI activations appear to be functionally distinguishable based on the ERP source data. For all conditions, posterior fMRI activations match with sources for the ERP N100 component, which are consistently found in occipital, and posterior middle and superior temporal gyri. Anterior fMRI activations match with sources for the ERP N400 component, in inferior, middle, and superior frontal gyri. This division has implications for the interpretation of the role of several areas. It is perhaps unsurprising that occipital fMRI activations match with sources for the visual-processing based N100 component, but since source localization as a technique is so novel, it lends confidence to its ability to identify structures that are readily interpretable.

Middle temporal gyrus sources for the N100 component have a larger implication for the debate surrounding the role of this area in visual object naming. Recall that competing interpretations for middle temporal gyrus activation during object naming center on semantic processing and visual perceptual processing specific to shape analysis. As demonstrated in Chapter 1, several studies suggest that temporal activations become more prominent when semantic tasks are emphasized. Category-specific object naming studies also point to a semantic role for this area. Studies such as Moore and Price (1999a) and Whatmough et al. (2002), for example, found that the left posterior middle temporal gyrus was active for man-made objects, especially tools, while bilateral anterior temporal areas were more active for natural objects such as animals or fruit. It has been postulated by Humphrey and colleagues (eg. Humphreys et al., 1995) that non-biological categories such as tools require less visual analysis than biological items such as animals because tools have more distinct perceptual features, allowing for easier recognition. In addition, lesion data has shown that the posterior middle temporal area produces semantic conceptual deficits (Chertkow et al., 1997) and electrical stimulation in this region produces impaired access to semantic information (Hart et al., 1992). For P137, the middle temporal gyrus is found as a source in the Pixelated Objects condition for the semantically-linked N400 component, which supports this view on the surface. However, the middle temporal gyrus is also found as a source for the early visual processing N100 component for this subject, introducing some doubt for a purely semantic role for this area. Additional evidence exists to suggest that the posterior

middle temporal gyrus may be involved in structural processing of visual objects. In addition to the category effects described above, Whatmough et al. (2002) also found that activation in the posterior middle temporal gyrus increased when object stimuli were less familiar, possibly requiring increased structural processing for successful naming, and lesions close to this area have been shown to impair retrieval of object knowledge (Hart and Gordon 1990) and the specific identification of visually presented objects (Warrington and Shallice 1984). In contrast to a semantic role for this area, these latter results suggest that this area may reflect structural processing of objects. While matches between PEPSI and fMRI in the posterior middle temporal gyrus do not clarify a role for this area, the fact that these activations match with the source for the N100 component for P137, the Objects as well as Pixelated Objects conditions for the control subject (P138), and the Pixelated Object condition for P136, is consistent with an earlier, structural-processing role for this area. Future studies with a larger number of subjects and tasks that distinguish structural and semantic processing for objects using fMRI and ERP source localization for N100 and N400 components are needed to provide a clearer role for this area.

The strongest confirmation for demonstrating semantic processing across techniques occurs for P138 in inferior, middle, and superior frontal gyri. Sources for the N400 component for this subject are found reliably across conditions in anterior areas that are consistent with semantic and visual object naming networks described in Chapter 1. Anterior and posterior distinctions between fMRI and PEPSI activations and early/late

ERP sources are also found for P136. In particular, the matches in the right posterior inferior and middle temporal gyri with the N100 source in the Pixelated Objects condition and the matches in the left insula between fMRI and the N400 source in the Objects condition are consistent with visual structural processing and semantic aspects of object naming respectively. This distinction again lends confidence to the reliability of source localization, providing a unique opportunity to design future multi-modality studies that can clarify the timecourse of anterior and posterior activations in fMRI studies. As mentioned above, the lack of anterior and posterior distinctions between N100 and N400 sources for P137 is unexpected, though sources for the N400 are found more superiorly relative to N100 sources, suggesting that phonological processing was robust for this subject in parietal areas.

In addition to anterior and posterior distinctions, fMRI shows matches to other techniques in both *t*-contrasts, which show signal increases, and *F*-contrasts, which show signal decreases. The plots below in Figure 84 show the hemodynamic signal for specific voxels for P138 in the Objects condition that are representative of the difference between signal increases found in *t*-contrasts and signal decreases found in *F*-contrasts:

A

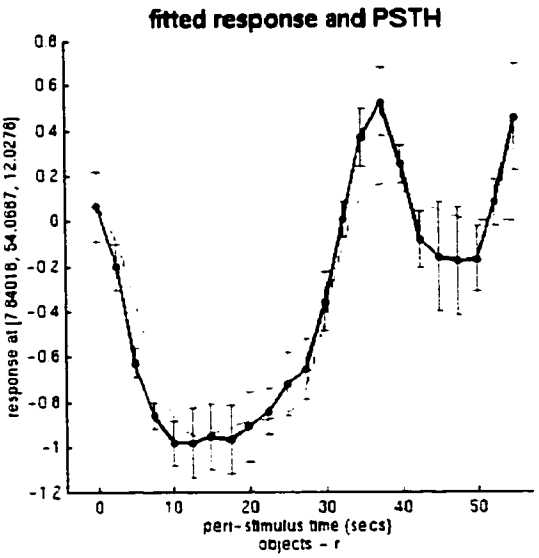

B

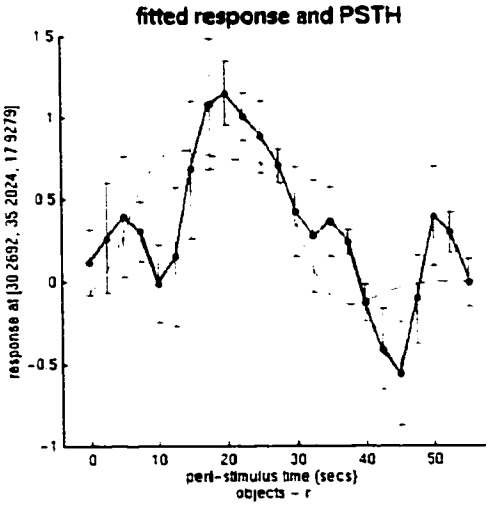

Figure 84. Peri-stimulus time histograms for P138 showing signal decreases for *F*-contrast at SPM coordinates (7, 53, 12) (Right SFG) (A) and signal increases for *t*-contrasts at (30, 35, 18) (Right MFG) (B).

As reviewed in Chapter 1, the physiological basis of negative correlations or activation decreases in unclear. Interpretations that have been considered but deemed unlikely are the redistribution or shunting of the blood supply from areas of decreased activity to increased activity, inhibition, and data analysis procedures. PET methods have determined that when the oxygen extraction fraction (OEF) increases, i.e. when oxygen utilization increases more than blood flow, a deactivation results. It has been suggested that an OEF increase may reflect a decrease in the activity of thalamic or other basal ganglia cells that project to deactivated areas (Gusnard and Raichle, 2001), or reflect the suppression of information processing in areas not engaged in task performance, such as unattended sensory input (Drevets et al., 1995). Areas of visuospatial processing such as medial parietal cortex, posterior cingulate, and precuneus regions have been shown in meta-analyses of PET data to consistently show decreases in activation when more complex cognitive tasks are engaged in (Shulman et al., 1997; Mazoyer et al., 2001). While some signal decreases in the present study are found in visual areas such as striate and occipital gyri (eg. Objects vs. Baseline for P137), fMRI decreases in this study are also found in a wider network of areas, including temporal and frontal regions for all subjects across conditions. If signal decreases were the result of the redistribution of the blood supply from areas of decreased activity to increased activity, one would predict that fMRI signal decreases would not match with PEPSI lactate increases or ERP source localizations, which presumably reflect increased or synchronous activity. Although the physiological basis of fMRI signal decreases is not clarified by this study, the

observations made here, that decreases occur in semantic and visual object naming networks and match with localizations from PEPSI and ERP sources, do provide indirect evidence that the decreases are not due to a shunting of the blood supply from areas of decreased activity to increased activity.

An additional observation made here concerns the subtraction paradigm used in PEPSI and fMRI techniques in an attempt to segregate visual and covert speech-motor processing from semantic processing. Finding baseline tasks that activate all but the process of interest is a common approach to both fMRI and PET studies, but has inherent limitations (see Price et al., 1997 for a review). The advantage of the analysis techniques used in the present study is that the subtraction between Objects and Pixelated Objects in fMRI and PEPSI could be compared to ERP sources for each condition separately, revealing whether activations could be attributed to the processing of one type of stimuli over another. For example, fMRI activations for Objects vs. Pixelated Objects matched with ERP sources from both conditions separately (P138), or mainly from Pixelated Objects (P137). The PEPSI subtraction (for P136 in particular) also clearly show that ERP sources from the Objects and the Pixelated Objects conditions were both represented in the PEPSI volume. These results support the notion made by Price et al. (1997) that differences between the two tasks include not only the addition of the cognitive component of interest, in this case semantic processing of object stimuli, but the effect of that added component to baseline processes as well, in this case showing visual processing common to both conditions. In general, an Objects vs. Pixelated Objects

comparison shows a combination of processing areas for each condition rather than a subtraction between common areas of processing.

The data here are consistent with the hypothesis made for this study that some common neuroanatomical areas would be found across techniques and that these areas would fall into the established network of visual object naming areas. It is clear, however, that some areas of activation are found only within a specific technique. These differences can be likely attributed to the various physiological mechanisms that each technique measures. Changes in both PEPSI and fMRI signals depend on the interaction of lactate and glucose metabolism as well as changes in blood flow and blood oxygenation rates. Studies to date indicate that upon stimulation, a transient period of nonoxidative glycolysis occurs where lactate concentration increases, glucose concentration decreases, and $CMRO_2$ increases, followed by a recoupling of glucose and $CMRO_2$ consumption. If CBF increases rapidly compared to $CMRO_2$, then an increase in the BOLD signal is seen. PEPSI is believed to capture increases in intracellular lactate concentrations, though the temporal resolution of the PEPSI signal make the relative contributions of the early nonoxidative glycolysis period and later oxidative glycolysis (recoupling) period unclear. Positive fMRI signal changes capture decreases in deoxyhemoglobin when CBF increases quickly relative to $CMRO_2$, but it is not presently known what specific conditions need to exist for these changes to be sufficiently large as to be measurable. Although single-voxel lactate comparisons to EPI-BOLD fMRI show similar signal magnitude changes using a two-second temporal resolution (Menon and

Gati, 1997), the PEPSI and fMRI techniques used here may measure relevant metabolic and hemodynamic changes at different temporal resolutions. Additionally, the spatial organization of capillaries and pial arterioles, which are relevant to the fMRI signal, compared to neuronal ensembles, which are relevant to PEPSI and ERP signals, are dramatically different (Mchedlishvili and Kuridze, 1984). Studies up to now show there is both some anatomical overlap (Serafini et al., 2001) and comparable signal magnitude changes (Menon and Gati, 1997) between lactate and the BOLD signal, suggesting that these techniques are measuring different but related aspects of stimulus-induced activation. If PEPSI reflects relatively faster metabolic events from neurons and glia while fMRI reflects secondary hemodynamic effects, it can be expected that some overlap, though not a one-to-one correspondence, would occur between these two techniques. Taking the ERP data into account, scalp-recorded electrophysiological activity must also meet several conditions before a signal can be detected. Neuronal populations must be geometrically oriented in roughly the same direction so individual dipole moments summate into an open-field, and the population must activate synchronously to specific stimuli. Only those field potentials meeting these criteria can be used as the basis for calculating low-resolution source localizations, implying that a subset of areas involved in a task will be identified as neural generators for that task. As such, the prediction that some overlap, but not a one-to-one correspondence, would occur across techniques is reasonable. Given these caveats, anatomical structures that are

common across techniques should be considered as playing important roles in the cognitive task under study.

CSM semantic category effects

In lesion studies, it has been well-documented that selective impairments can be found between specific semantic categories (eg. Warrington and Shallice, 1984; Hillis and Caramazza, 1991; Sartori et al., 1993). The most common dissociations are between categories of natural or living versus non-living things such as animals versus tools. Semantic category was not controlled for in this study, but post-hoc analyses show some category-specific effects for the left-dominant patient P137. At sites significant for language, the occurrence of an error was more likely if the semantic category of the item was natural or animal than if it was an artifact. Site 15, which sits in the mesial superior temporal gyrus, was just short of being significant for this effect. This effect is the opposite to what one would expect based on imaging and lesion data, which predict that artifacts are more susceptible to lesions in the left hemisphere. During direct cortical stimulation, Ilmberger et al. (2002) found that stimulation of the left superior temporal and inferior/superior frontal gyri increased naming errors for tool items relative to animal items. In imaging studies, the categories of natural and man-made objects do not appear to consistently activate posterior or anterior regions even when visual complexity is controlled for, but it does appear that natural categories activate more diffuse or bilateral temporal areas than artifacts, which activate more restricted areas in the left hemisphere. This pattern is consistent with lesion data, which shows that naming living items such as

animals appear to be impaired especially after bilateral lesions, in contrast to impairments in non-living items, which appear to be more restricted to the left hemisphere.

CSM vs. MR Volumes and ERP sources

Using the comparison method between CSM and fMRI/PEPSI volumes described, no significant correlations were found between sites significant for language and peak activations for either patient. Qualitatively, CSM sites that are closest to PEPSI activations for P136 are found in the posterior middle temporal gyrus, though these sites are both significant (site 29) and non-significant (sites 28 and 32) for language disruption. Anterior PEPSI activation found in the basal ganglia sits below significant language site 24, but the relationship between such deep activations and cortical stimulation on the surface is unclear. Across fMRI conditions, middle and superior temporal gyri activations sit below CSM sites, but these sites are mainly non-significant for language, while deep thalamic activation sits most in line with significant site 36 in the post-central gyrus. Similarly, ERP sources for the N100 component were found in inferior, middle, and superior temporal gyri, but only a non-significant site in the posterior superior temporal gyrus (site 30) could be considered in line with these sources. For P137, superior temporal areas also provide the closest matches between PEPSI activations and significant CSM sites (site 15 posteriorly and site 12 anteriorly), but these activations are proximal to non-significant CSM sites in this area as well (sites 33, 46, and 47). Across fMRI conditions, the only significant CSM language sites proximal to peak activations occur in the ventral post-central gyrus (site 13) and middle temporal gyrus (sites 12 and

15). Non-significant sites correspond to activations in inferior, middle, and superior temporal gyri as well as the inferior frontal gyrus (operculum). ERP sources for this patient were either outside the sampled CSM area or not lateralized to the dominant hemisphere.

Overall, non-correspondence between sources for the N100 component and CSM sites for P136 are perhaps not surprising given that this component measures early sensory processing while CSM purportedly disrupts object-naming abilities related to semantic processing. Correspondence between CSM language disruption and fMRI/PEPSI peak activations was extremely limited. Activations were both more extensive and deeper than the discrete areas of language cortex identified by CSM on the cortical surface. The physiological mechanism measured by cortical stimulation as presently understood (see Lesser et al., 1994 and Nathan et al., 1993 for reviews) differs from the other techniques used in this study on several fronts, particularly between the limited size of the area sampled by stimulation currents compared to entire or partial brain volumes taken into account by fMRI, ERP, and PEPSI. Bipolar square-wave stimulation is believed to cause activation in neurons and en passage fibers of both excitatory and inhibitory systems in primary motor and sensory cortices, and causing hyperpolarization of neuronal tissue when disrupting higher functions such as language (Ojemann, 1993); these effects occur directly under or between the two electrodes with little current spread, as evidenced by optical imaging in the monkey (Haglund et al., 1993) and human cerebral cortex (Haglund et al., 1992), and from simulations which

indicate a rapid drop in current both laterally and in depth from the area under the stimulating electrodes (Nathan et al., 1993). These differences in both physiological mechanisms and the sampled area of tissue that leads to the identification of language areas implies that CSM assesses language functions in a way that is markedly different from fMRI, PEPSI, or ERP techniques. Visual object naming using non-CSM techniques identify a much larger spatial extent of activation than CSM, which likely reflect differences in identifying involved versus essential areas associated with visual object naming task.

Although there have been no other reports comparing CSM and PEPSI or ERP source localization, several investigators have found a greater degree of correspondence between fMRI and CSM. The best correspondences seem to occur when several language tasks are used and neuroanatomical areas common across tasks are compared to CSM sites of language disruption. In this study, areas that were common across non-CSM techniques were reasonably proximal to CSM sites significant for language disruption for P136. For this subject, the right insula was identified as a common area of activation in both fMRI and PEPSI and this area sits reasonably in line with language site 24 in the anterior superior temporal gyrus, while the right posterior middle temporal gyrus, common to PEPSI and an N100 ERP source sits just inferior to site 29 in the posterior middle temporal gyrus. For P137, however, the left insula was identified as a common area of activation in fMRI and PEPSI, but the cortical surface projecting from this area was not sampled with CSM. It is important to take into account that

comparisons between activations and sources were only made to CSM sites that were sampled independently from the knowledge of where these activations occurred. Whether language disruptions would have occurred above areas identified by fMRI, PEPSI, or ERP sources is unknown.

This study provides the first report of a direct comparison between cortical stimulation mapping, fMRI, PEPSI, and ERP source localization in two patients during a visual object naming task. Results show that while CSM sites do not correlate significantly with peak areas identified with these other techniques, matches do occur within fMRI, PEPSI, and ERP sources which give insights regarding the timecourse of fMRI and PEPSI activations during a visual object naming task. As the physiological mechanisms captured by each technique are better understood, future studies using multi-modality imaging techniques can elucidate where and when the cognitive processes involved in this task take place.

References

Ackerman, R. F., D. M. Finch, et al. (1984). "Increased glucose utilization during long-duration recurrent inhibition of hippocampal pyramidal cells." Journal of Neuroscience 4: 251-264.

Afifi, A. K. and R. A. Bergman (1998). Functional Neuroanatomy: Text and Atlas. New York, McGraw-Hill Companies, Inc.

Alexander, M. P. and M. A. Schmitt (1980). "The aphasia syndrome of stroke in the left anterior cerebral artery territory." Archives of Neurology 37: 97-100.

Allison, T., G. McCarthy, et al. (1994). "Human extrastriate visual cortex and the perception of faces, words, numbers, and colors." Cerebral Cortex 4(5): 544-54.

Anderson, J. L. (1997). "How to estimate global activity independent of changes in local activity." NeuroImage 6(4): 237-244.

Baddeley, A. (1986). Working memory. Oxford, Oxford University Press.

Baddeley, A. (1990). Human memory: Theory and practice. Needham Heights, Allyn and Bacon.

Baddeley, A. (1992). "Working memory." Science 255: 556-559.

Barch, D. M., F. W. Sabb, et al. (1999). "Overt verbal responding during fMRI scanning: Empirical investigations of problems and potential solutions." NeuroImage 10(6): 642-57.

Barrett, S. E. and M. D. Rugg (1990). "Event-related potentials and the semantic matching of pictures." Brain and Cognition 14: 201-212.

Battini, C. F. Benedetti, et al. (1984). "Metabolic activity of intracerebellar nuclei in the rat: efects of inferior olive inactivation." Experimental Brain Research 54: 259-265.

Bavelier, D., D. Corina, et al. (1997). "Sentence reading: A functional MRI study at 4 Tesla." Journal of Cognitive Neuroscience 9(5): 664-686.

Beauvois, M. F. (1982). "Optic aphasia: A process of interaction between vision and language." Philosophical Transactions of the Royal Society London, Series B 298: 35-47.

Beisteiner, R., R. Lanzenberger, et al. (2000). "Improvement of presurgical patient evaluation by generation of functional magnetic resonance risk maps." Neuroscience Letters 290: 13-16.

Benson, D. F., W. A. Sheremata, et al. (1973). "Conduction aphasia: a clinicopathological study." Archives of Neurology, Chicago 28: 339-346.

Benson, F. (1985). Aphasia. Clinical Neuropsychology. K. M. Heilman and E. Valenstein. New York, Oxford University Press: 11-47.

Benson, R. R., D. B. FitzGerald, et al. (1999). "Language dominance determined by whole brain functional MRI in patients with brain lesions." Neurology 52: 798-809.

Bentin, S., G. McCarthy, et al. (1985). "Event-related potentials, lexical decision and semantic priming." Electroencephalography and Clinical Neurophysiology 60(4): 343-355.

Berger, M. S., J. Kincaid, et al. (1989). "Brain mapping techniques to maximize resection, safety, and seizure control in children with brain tumors." Neurosurgery 25: 786-792.

Biederman, I., P. C. Gerhardstein, et al. (1997). "High level object recognition without an anterior inferior temporal lobe." Neuropsychologia 35: 271-287.

Binder, J. R., S. M. Rao, et al. (1994). "Functional magnetic resonance imaging of human auditory cortex." Annals of Neurology 35: 662-672.

Binder, J. R., S. M. Rao, et al. (1995). "Lateralized human brain language systems demonstrated by task subtraction functional magnetic resonance imaging." Archives of Neurology 35: 662-672.

Binder, J. R., S. J. Swanson, et al. (1996). "Determination of language dominance using functional MRI: A comparison with the Wada test." Neurology 46: 978-984.

Binder, J. R., J. A. Frost, et al. (1997). "Human brain language areas identified by functional magentic resonance imaging." Journal of Neuroscience 17(1): 353-362.

Binder, J. R. (1997). "Neuroanatomy of language processing studies with fMRI." Clinical Neuroscience 4: 87-94.

Blumstein, S. E., E. Baker, et al. (1977). "Phonological factors in auditory comprehension in aphasia." Neuropsychologia 15: 19-30.

Bly, B. M. and S. M. Kosslyn (1997). "Functional anatomy of object recognition in humans: Evidence from Positron Emission Tomography and functional Magnetic Resonance Imaging." Current Opinion in Neurology 10: 5-9.

Bookheimer, S., T. Zeffiro, et al. (1995). "Regional cerebral blood flow changes during object naming and word reading." Human Brain Mapping 3: 93-106.

Bookheimer, S. Y., T. A. Zeffiro, et al. (1997). "A direct comparison of PET activation and electrocortical stimulation mapping for language localization." Neurology 48(4): 1056-65.

Brown, C. M. and P. Hagoort (1993). "The processing nature of the N400: Evidence from masked priming." Journal of Cognitive Neuroscience 5: 34-44.

Bub, D., S. Black, et al. (1988). "Semantic encoding of pictures and words: Some neuropsychological observations." Cognitive Neuropsychology 5: 27-66.

Buchel, C., C. Price, et al. (1998). "A multimodal language region in the ventral visual pathway." Nature 394: 274-276.

Burani, C., G. Vallar, et al. (1991). "Articulatory coding and phonological judgements on written words and pictures: The role of the phonological output buffer." European Journal of Cognitive Psychology 3: 379-398.

Burnstine, T. H., R. P. Lesser, et al. (1990). "Characterization of the basal temporal language area in patients with left temporal lobe epilepsy." Neurology 40: 966-970.

Caplan, D., D. Gow, et al. (1995). "Analysis of lesions by MRI in stroke patients with acoustic-phonetic processing deficits." Neurology 45: 293-298.

Caramazza, A. and J. R. Shelton (1998). "Domain-specific knowledge systems in the brain: The animate-inanimate distinction." Journal of Cognitive Neuroscience 10: 1-34.

Carr, T. H. and A. Pollatsek (1985). Recognizing printed words: A look at current models. Reading Research. D. Besner, T. G. Weller and G. E. MacKinnon. New York, Academic Press: 2-73.

Chertkow, H., D. Bub, et al. (1997). "On the status of object concepts in aphasia." Brain and Language 58(2): 203-232.

Coltheart, V., K. Patterson, et al. (1994). "When a ROWS is a ROSE: phonological effecs in written word comprehension." Quarterly Journal of Experimental Psychology 47A: 917-955.

Corbetta, M., F. M. Miezin, et al. (1990). "Attentional modulation of neural processing of shape, color and velocity." Science 248: 1556-1559.

Corina, D. (2000). fMRI test of visual object naming. Seattle, WA, Cognitive Neuropsychology laboratory, Dept. of Psychology, University of Washington.

Corina, D. (2001). Coding for Ojemann Speech Error. Seattle, WA, Cognitive Neuropsychology laboratory, Dept. of Psychology, University of Washington.

Corina, D., K. Steury, et al. (2001, personal communication). A comparison of language maps derived from cortical stimulation and fMRI: Data from Object Naming. Manuscript in preparation.

Costello, A. L. and E. K. Warrington (1989). "Dynamic aphasia: The selective impairment of verbal planning." Cortex 25: 103-114.

Coughlan, A. K. and E. K. Warrington (1978). "Word-comprehension and word-retrieval in patients with localized cerebral lesions." Brain 101: 163-185.

Cuenod, C. A., S. Y. Bookheimer, et al. (1995). "Functional MRI during word generation, using conventional equipment: A potential tool for language localization in the clinical environment." Neurology 45(10): 1821-1827.

D'Esposito, M., J. A. Detre, et al. (1997). "A functional MRI study of mental image generation." Neuropsychologia 35: 725-730.

Damasio, H. and A. R. Damasio (1980). "The anatomical basis of conduction aphasia." Brain 103: 337-350.

Damasio, A. R., H. Damasio, et al. (1982). "Prosopagnosia: Anatomic basis and behavioral mechanisms." Neurology 32: 331-341.

Damasio, A. R. and H. Damasio (1983). "The anatomical basis of pure alexia." Neurology Cleveland 33: 1573-1583.

Damasio, A., H. Damasio, et al. (1990). The neural regionalization of knowledge access: Preliminary evidence. The Brain., Cold Spring Harbor Symposium Series.

Damasio, H. and A. R. Damasio (1990). "The neural basis of memory, language and behavioral guidance: Advances with the lesion method in humans." Seminars in the Neurosciences 2: 277-286.

Damasio, H., T. J. Grabowski, et al. (1996). "A neural basis for lexical retrieval." Nature 380: 499-505.

Davies, K. G., R. E. Maxwell, et al. (1994). "Language function following subdural grid-directed temporal lobectomy." Acta Neurologica Scandinavica 90: 201-206.

Demb, J. B., J. E. Desmond, et al. (1995). "Semantic encoding and retrieval in the left inferior prefrontal cortex: A functional MRI study of task difficulty and process specificity." Journal of Neuroscience 15(9): 5870-5878.

Demonet, J. F., F. Chollet, et al. (1992). "The anatomy of phonological and semantic processing in normal subjects." Brain 115: 1753-1768.

Demonet, J. F., C. J. Price, et al. (1994). "A PET study of cognitive strategies in normal subjects during language tasks: Influence of phonetic ambiguity and sequence processing on phoneme monitoring." Brain 117: 671-682.

Demonet, J. F., J. Fiez, et al. (1996). "PET studies of phonological processing: A critical reply to Poeppel." Brain and Language 55: 352-379.

DeRenzi, E. and F. Lucchelli (1994). "Are semantic systems separately represented in the brain? The case of living category impairment." Cortex 30: 3-25.

Desimone, R. and L. G. Ungerleider (1990). Handbook of Neuropsychology. F. Boller and J. Grafman. Amsterdam, Elsevier. 2: 267-299.

Desmond, J. E., J. M. Sum, et al. (1995). "Functional MRI measurement of language lateralization in Wada-tested patients." Brain 118: 1411-1419.

Devinsky, O., K. Perrine, et al. (2000). "Relation of cortical language distribution and cognitive function in surgical epilepsy patients." Epilepsia 41(4): 400-404.

Devlin, J. T., L. Gonnerman, et al. (1998). "Category specific deficits in focal and widespread damage: A computational account." Journal of Cognitive Neuroscience 10: 77-94.

Drevets, W. C. et al. (1995). "Blood flow changes in human somatosensory cortex during anticipated stimulation." Nature 373: 249-252.

Duchowny, M., P. Jayakar, et al. (1996). "Language cortex representation: Effects of developmental versus acquired pathology." Annals of Neurology 40: 31-38.

Farah, M. J. (1990). Visual Agnosia. Cambridge, MIT Press.

Farah, M. J. and J. L. McClelland (1991). "A computational model of semantic memory impairment: Modality specificity and emergent category specificity." Journal of Experimental Psychology: General 120: 339-357.

Federmeier, K. D. and M. Kutas (2002). "Picture the difference: Electrophysiological investigations of picture processing in the two cerebral hemispheres." Neuropsychologia 40: 730-747.

Fellows, L. K., M. G. Boutelle, et al. (1993). "Physiological stimulation increases nonoxidative glucose metabolism in the brain of the freely moving rat." Journal of Neurochemistry 60: 1258-1263.

Fiez, J., M. Raichle, et al. (1995). "PET studies of auditory and phonological processing: Effects of stimulus characteristics and task demands." Journal of Cognitive Neuroscience 7(3): 357-375.

Fiez, J. A., M. E. Raichle, et al. (1996). "PET activation of posterior temporal regions during auditory word presentation and verb generation." Cerebral Cortex 6: 1-10.

Fiez, J. A. (1997). "Phonology, semantics, and the role of the left inferior prefrontal cortex." Human Brain Mapping 5: 79-83.

FitzGerald, D. B., G. R. Cosgrove, et al. (1997). "Location of language in the cortex: a comparison between functional MR imaging and electrocortical stimulation." American Journal of Neuroradiology 18(8): 1529-39.

Flude, B. M., A. W. Ellis, et al. (1989). "Face processing and name retrieval in an anomic aphasic: Names are stored separately from semantic information about familiar people." Brain and Cognition 11: 60-72.

Forde, E. M., D. Francis, et al. (1997). "On the links between visual knowledge and naming: A single case study of a patient with a category-specific impairment for living things." Cognitive Neuropsychology 14: 403-458.

Fox, P. T. and M. E. Raichle (1986). "Focal physiological uncoupling of cerebral blood flow and oxidative metabolism during somatosensory stimulation in human subjects." Proceedings of the National Academy of Sciences USA 83: 1140-1144.

Fox, P. T., M. E. Raichle, et al. (1988). "Nonoxidative glucose consumption during focal physiologic neural activity." Science 241: 462-464.

Frahm, J., G. Drueger, et al. (1997). Dynamic NMR studies of perfusion and oxidative metabolism during focal brain activation. Optical Imaging of Brain Function and Metabolism II. A. Villringer and U. Dirnagl. New York, Plenum Press: 195-203.

Fray, A. E., R. J. Forsyth, et al. (1996). "The mechanisms controlling physiologically stimulated changes in rat brain glucose and lactate: a microdialysis study." Journal of Physiology (London) 496: 49-57.

Freedman, M., M. P. Alexander, et al. (1984). "Anatomic basis of transcortical motor aphasia." Neurology 40: 409-417.

Friederici, A. D., E. Pfeifer, et al. (1993). "Event-related brain potentials during natural speech processing: effects of semantic, morphological and syntactic violations." Brain Research. Cognitive Brain Research 1(3): 183-92.

Friederici, A. D. (1995). "The time course of syntactic activation during language processing: a model based on neuropsychological and neurophysiological data." Brain and Language 50(3): 259-81.

Friederici, A. D. and A. Mecklinger (1996). "Syntactic parsing as revealed by brain responses: first-pass and second-pass parsing processes." Journal of Psycholinguistic Research 25(1): 157-76.

Friederici, A. D. (1997). "Neurophysiological aspects of language processing." Clinical Neuroscience 4: 64-72.

Friedmann, T. E. and C. Barborka (1941). "The significance of the ratio of lactic acid to pyruvic acid in blood after exercise." Journal of Biological Chemistry 141: 993-994.

Frith, C. D., K. J. Friston, et al. (1991). "A PET study of word finding." Neuropsychologia 29(12): 1137-1148.

Gabrieli, J., R. Poldrack, et al. (1998). "The role of left prefrontal cortex in language and memory." Proceedings of the National Academy of Sciences USA 95: 906-913.

Gainotti, G. and M. C. Silveri (1996). "Cognitive and anatomical locus of lesion in a patient with a category-specific semantic impairment for living things." Cognitive Neuropsychology 13: 357-390.

Ganis, G., M. Kutas, M. I. Sereno (1996). "The search for 'common sense': an electrophysiological study of the comprehension of words and pictures in reading." Journal of Cognitive Neuroscience 8: 89-106.

Gauthier, I., A. W. Anderson, et al. (1997). "Levels of categorization in visual object recognition studied with functional MRI." Currents in Biology 7: 645-651.

Geddes, L. A. and L. E. Baker (1967). "The specific resistance of biological materials – a compendium of data for the biomedical engineer and physiologist." Medical and Biological Engineering 5: 271-293.

Gerlach, C., I. Law, et al. (1999). "Perceptual differentiation and category effects in normal object recognition". Brain 122: 2159-2170.

Geschwind, N. (1965). "Disconnection syndromes in animals and man." Brain 88: 237-294, 585-644.

Glaser, W. R. and M. O. Glaser (1989). "Context effects in Stroop-like word and picture processing." Journal of Experimental Psychology: General 118: 13-42.

Gonnerman, L. A., E. S. Anderson, et al. (1997). "Double dissociation of semantic categories in Alzheimer's disease." Brain and Language 57: 254-279.

Goodale, M. A. and D. Milner (1992). "Separate visual pathways for perception and action." Trends in Neuroscience 15: 20-25.

Gordon, B., S. Uematsu, et al. (1991). "Utility of intraoperative neuropsychological testing with stepwise resection." Epilepsia 32: 87.

Grill-Spector, K., T. Kushnir, et al. (1998). "A sequence of object-processing stages revealed by fMRI in the human occipital lobe." Human Brain Mapping 6: 316-328.

Grunwald, T. C. E. Elger, et al. (1995). "Alterations of intrahippocampal cognitive potentials in temporal lobe epilepsy." Electroencephalography and clinical Neurophysiology 95: 53-62.

Guillem, F., B. N'Kaoua, et al. (1995). "Intracranial topography of event-related potentials (N400/P600) elicited during a continuous recognition memory task." Psychophysiology 32: 382-392.

Gusnard, D. A., and M. E. Raichle (2001). "Searching for a baseline: Functional imaging and the resting human brain." Nature Reviews Neuroscience 2: 685-694.

Halijamae, H. (1987). "Lactate metabolism." Intensive Care World 4: 118-121.

Haglund, M. M., G. A. Ojemann, and D. W. Hochman (1992). "Optical imaging of epileptiform and functional activity in human cerebral cortex." Nature 358: 668-71.

Haglund, M. M., G. A. Ojemann, and G. G. Blasdel (1993). "Optical imaging of bipolar cortical stimulation." Journal of Neurosurgery 78: 785-793.

Haglund, M. M., M. S. Berger, et al. (1994). "Cortical localization of temporal lobe language sites in patients with gliomas." Neurosurgery 34(4): 567-576.

Hagoort, P. and M. Kutas (1995). Electrophysiological insights into language deficits. Handbook of Neuropsychology. F. Boller and J. Grafman. Amsterdam, Elsevier. 10: 105-134.

Hagoort, P., C. M. Brown, and J. Groothusen (1993). "The syntactic positive shift (SPS) as an ERP measure of syntactic processing." Language and Cognitive Processes 8: 439-483.

Hagoort, P., C. M. Brown, and L. Osterhout (1999). The neurocognition of syntactic processing. The Neurocognition of Language. C. M. Brown and P. Hagoort, Eds. New York, Oxford University Press: 273-318.

Hamberger, M. J. and T. R. Tamny (1999). "Auditory naming and temporal lobe epilepsy." Epilepsy Research(3): 229-243.

Hart, J. J., R. S. Berndt, et al. (1985). "Category-specific naming deficit following cerebral infarction." Nature 316: 439-440.

Hart, J. J. and B. Gordon (1990). "Delineation of single-word semantic comprehension deficits in aphasia with anatomical correlation." Annals of Neurology 27: 226-231.

Hart, J., R. P. Lesser, et al. (1992). "Selective interference with the representation of size in the human by direct cortical electrical stimulation." Journal of Cognitive Neuroscience 4: 337-344.

Hashemi, R. H. and W. G. Bradley (1997). MRI: The basics. Baltimore, Williams & Wilkins.

Haxby, J. V., C. L. Grady, et al. (1991). "Dissociation of object and spatial visual processing pathways in human extrastriate cortex." Proceedings of the National Academy of Sciences USA 88: 1621-1625.

Haxby, J. V., B. Horwitz, et al. (1994). "The functional organization of human extrastriate cortex: a PET-rCBF study of selective attention to faces and locations." Journal of Neuroscience 14(11 Pt 1): 6336-53.

Hayes, C. E. and C. M. Mathis (1996). Improved brain coil for fMRI and high resolution imaging. Proceedings of the 4th Annual Meeting of ISMRM, New York.

Herbster, A. N., M. A. Mintun, et al. (1997). "Regional cerebral blood flow during word and nonword reading." Human Brain Mapping 5: 84-92.

Herholz, K., H. J. Reulen, et al. (1997). "Preoperative activation and intraoperative stimulation of language-related areas in patients with glioma." Neurosurgery 41(6): 1253-62.

Hillis, A. E. and A. Caramazza (1991). "Category-specific naming and comprehension impairment: A double dissociation." Brain 114: 2081-2094.

Hillis, A. E. and A. Caramazza (1995). "Cognitive and neural mechanisms underlying visual and semantic processing: Implications from "optic aphasia"." Journal of Cognitive Neuroscience 7: 457-478.

Hillyard, S. A. and J. C. Hansen (1986). Attention: Electrophysiological approaches. In Psychophysiology: Systems, Processes, and Applications. M. G. H. Coles, E. Donshin, S. W. Porges, Eds. New York, The Guilford Press: 227-243.

Hirsch, J., M. I. Ruge, et al. (2000). "An integrated functional magnetic resonance imaging procedure for preoperative mapping of cortical areas associated with tactile, motor, language, and visual functions." Neurosurgery 47(3): 711-22.

Holcomb, P. J. (1988). "Automatic and attentional processing: An event-related brain potential analysis of semantic priming." Brain and Language 35: 66-85.

Holcomb, P. J. and H. J. Neville (1990). "Auditory and visual priming in lexical decision: A comparison using event-related brain potentials." Language and Cognitive Processes 5: 281-312.

Holcomb, P. J. and W. B. McPherson (1994). Event-related brain potentials reflect semantic priming in an object decision task." Brain and Cognition 24: 257-276.

Howard, D., K. Patterson, et al. (1992). "The cortical localization of the lexicons." Brain 115: 1769-1782.

Hu, Y. and G. S. Wilson (1997). "A temporary lacal energy pool coupled to neuronal activity: fluctuations of extracellular lactate levels in rat brain monitored with rapid-response enzyme-based sensor." Journal of Neurochemistry 69: 1484-1490.

Huettel, S. A., J. Singerman, et al. (2000). Spatial and Temporal Variability of the fMRI Hemodynamic Response in Young and Elderly Subjects. Society for Neuroscience, 30th Annual Meeting, New Orleans, LA.

Humphreys, G. W. and M. J. Riddoch (1984). "Routes to object constancy: Implications from neurological impairments of object constancy." Quarterly Journal of Experimental Psychology 26A: 385-415.

Humphreys, G. W. and M. J. Riddoch (1987). The fractionation of visual agnosia. Visual Object Processing: A Cognitive Neuropsychological Approach. G. W. Humphreys and M. J. Riddoch. London, Erlbaum: 281-306.

Humphreys, G. W., M. J. Riddoch, et al. (1988). "Cascade processes in picture identification." Cognitive Neuropsychology 5: 67-103.

Humphreys, G. W. and M. J. Riddoch (1993). "Object agnosias." Baillieres Clinical Neurology 2(2): 339-59.

Humphreys, G. W., C. Lamote, T. J. Lloyd-Jones (1995). "An interactive activation approach to object processing: Effects of structural similarity, name frequency, and task in normality and pathology." Memory 3(3-4): 535-586.

Humphreys, G. W., M. J. Riddoch, et al. (1997). "Top-down processes in object identification: Evidence from experimental psychology, neuropsychology and functional anatomy." Philosophical Transactions of the Royal Society London 352: 1275-1282.

Humphreys, G. W., C. J. Price, et al. (1999). "From objects to names: A cognitive neuroscience approach." Psychological Research 62: 118-130.

Hyder, F., J. R. Chase, et al. (1996). "Increased tricarboxylic acid cycle flux in rat brain during forepaw stimulation detected with 1H[13C] NMR." Proceedings of the National Academy of Sciences USA 93: 7612-7617.

Hyder, F. D. L. Rothman, et al. (1997). "Oxidative glucose metabolism in rat brain during single forepaw stimulation: a spatially localized 1H [13 C] nuclear magnetic resonance study." Journal of Cerebral Blood Flow and Metabolism 17: 1040-1047.

Ilmberger, J. R. Sabine, et al. (2002). "Naming tools and animals: Asymmetries observed during direct electrical cortical stimulation." Neuropsychologia 40: 695-700.

Inati, S. (2002). GE2SPM 3.2 Script. Dartmouth Brain Imaging Center, Dartmouth College.

Izumi, Y., A. M. Benz, et al. (1994). "Effects of lactate and pyruvate on glucose deprivation in rat hippocampal slices." Neuroreport 5: 617-620.

Jasper, H. H. (1958). "Report to the committee on methods of clinical examination in electroencephalography. Appendix: The ten-twenty system of the International Federation." Electroencephalography and Clinical Neurophysiology 10: 371-375.

Jueptner, M. and C. Weiller (1995). "Review: does measurement of regional cerebral blood flow reflect synaptic activity? Implications for PET and fMRI." Neuroimage 2: 148-156.

Kandel, E. R., J. H. Schwartz, et al., Eds. (1991). Principles of Neural Science. New York, Elsevier Science Publishing Co.

Kanwisher, N., J. McDermott, et al. (1997). "The fusiform face area: A module in human extrastriate cortex specialized for face perception." Journal of Neuroscience 17: 4302-4311.

Kapur, S., R. Rose, et al. (1994). "The role of the left prefrontal cortex in verbal processing: Semantic processing or willed action?" Neuroreport 5: 2193-2196.

Kay, J. and A. W. Ellis (1987). "A cognitive neuropsychological case study of anomia." Brain 110: 613-629.

Kiefer, M. (2001). "Perceptual and semantic sources of category-specific effects: Event-related potentials during picture and word categorization." Memory & Cognition 29(1): 100-116.

Klein, D., A. Olivier, et al. (1997). "Obligatory role of the LIFG in synonym generation: evidence from PET and cortical stimulation." Neuroreport 8(15): 3275-3279.

Kosslyn, S. M., N. M. Alpert, et al. (1994). "Identifying objects seen from different viewpoints: A PET investigation." Brain 117: 1055-1071.

Kosslyn, S. M., N. Alpert, et al. (1995). "Identifying objects at different levels of the heirarchy: A Positron Emission Tomography study." Human Brain Mapping 3: 107-132.

Kutas, M. and S. A. Hillyard (1980). "Reading senseless sentences: Brain potentials reflect semantic anomaly." Science 207: 203-205.

Kutas, M. and C. Van Petten (1988). Event-related brain potential studies of language. Advances in Psychophysiology. P. Ackles, J. R. Jennings and M. G. H. Coles. Greenwich, JAI Press: 139-187.

Kutas, M. and C. K. Van Petten (1990). Electrophysiological perspectives on comprehending written language. New trends and advanced techniques in clinical neurophysiology. P. M. Rossini, F. Maugiere, Eds. Amsterdam, Elsevier: 155-167.

Kutas, M. and C. Van Petten (1994). Psycholinguistics electrified: Event-related brain potential investigations. Handbook of Psycholinguistics. M. A. Gernsbacher. San Diego, Academic Press: 83-143.

Kutas, M., K. D. Federmeier, and M. I. Sereno (1999). Current approaches to mapping language in electromagnetic space. The Neurocognition of Language. C. M. Brown and P. Hagoort, Eds. New York, Oxford University Press: 359-392.

Kwong, K. K., J. W. Belliveau, et al. (1992). "Dynamic magnetic resonance imaging of the human brain activity during primary sensory stimulation." Proceedings of the National Academy of Sciences USA 89: 5675-5679.

La Heij, W., B. Happel, et al. (1990). "Components of Stroop-like interference in word reading." Acta Psychologica 73: 115-129.

Lai, S., A. L. Hopkins, et al. (1993). "Identification of vascular structures as a major source of signal contrast in high resolution 2D and 3D functional activation imaging of the motor cortex at 1.5T: Preliminary results." Magnetic Resonance in Medicine 30: 387-392.

Lalouschek, W. W. Gerschlager et al. (1998). "Event-related potentials in patients with temporal lobe epilepsy reveal topography specific lateralization in relation to the side of the epileptic focus." Electroencephalography and clinical Neurophysiology 108: 567-576.

Langfitt, J. T. and R. Rausch (1996). "Word-finding deficits persist after left anterotemporal lobectomy." Archives of Neurology 53: 72-76.

Larrabee, M. G. (1995). "Lactate metabolism and its effects on glucose metabolism in an excised neural tissue." Journal of Neurochemistry 64: 1734-1741.

Larrabee, M. G. (1996). "Partitioning of CO2 production between glucose and lactate in excised sympathetic ganglia, with implications for brain." Journal of Neurochemistry 67: 1726-1734.

Lauter, J., P. Herscovitch, et al. (1985). "Tonotopic organization in human auditory cortex revealed by positron emission tomography." Hearing Research 20: 199-205.

Law, I., I. Kannai, et al. (1991). "Left supramarginal/angular gyri activation during reading of syllabograms in the Japanese language." Journal of the Neurolinguist 6: 243-251.

LeBihan, D. and A. Karni (1995). "Applications of magnetic resonance imaging to the study of human brain function." Current Opinion in Neurobiology 5: 231-237.

Lebrun, Y. and C. Leleux (1993). "The effects of electrostimulation and of resective and stereotactic surgery on language and speech." Acta Neurochirurgica - Supplementum 56: 40-51.

Lesser, R., B. Gordon, et al. (1994). "Electrical stimulation and language." Journal of Clinical Neurophysiology 11: 191-204.

Levine (1982). Visual agnosia in monkey and man. Analysis of Visual Behavior. D. J. Ingle, M. A. Goodale and R. J. W. Mansfield. Cambridge, MIT Press.

Liberman, A. M. and I. G. Mattingly (1985). "The motor theory of speech perception revised." Cognition 21: 1-36.

Luders, H., R. P. Lesser, et al. (1986). "Basal temporal language area demonstrated by electrical stimulation." Neurology 36: 505-510.

Luders, H., R. P. Lesser, et al. (1991). "Basal temporal language area." Brain 114(2): 743-54.

Lupker, S. J. (1985). Relatedness effects in word and picture naming: Parallels, differences and structural implications. Progress in the Psychology of Language. A. W. Ellis. Hillsdale, Earlbaum: 109-142.

Macleod, C. M. (1991). "Half a century of research on the Stroop effect: An integrative review." Psychological Bulletin 109: 163-203.

Madsen, P. L., R. Linde, et al. (1998). "Activation-induced resetting of cerebral oxygen and glucose uptake in the rat." Journal of Cerebral Blood Flow and Metabolism 18: 742-748.

Magistretti, P. J., L. Pellerin, et al. (1995). Brain energy metabolism: an integrated cellular perspective. Psychopharmacology: the Fourth Generation of Progress. F. Bloom and D. Kupfer. New York, Raven: 657-670.

Magistretti, P. J., L. Pellerin (1996). "Cellular bases of brain energy metabolism and their relevance to functional brain imaging: evidence for a prominent role of astrocytes." Cerebral Cortex 6: 50-61.

Magistretti, P. J., L. Pellerin (2000). Regulation of cerebral energy metabolism. Functional MRI. C. T. W. Moonen and P. A. Bandettini, Eds. Berlin, Springer-Verlag: 25-34.

Malach, R., J. B. Reppas, et al. (1995). "Object-related activity revealed by functional magnetic resonance imaging in human occipital cortex." Proceedings of the National Academy of Sciences USA 92: 8135-8139.

Malow, B. A., T. A. Blaxton, et al. (1996). "Cortical stimulation elicits regional distinctions in auditory and visual naming." Epilepsia 37(3): 245-52.

Mangun, G. R. and S. A. Hillyard (1991). "Modulations of sensory-evoked brain potentials indicate changes in perceptual processing during visual-spatial priming." Journal of Experimental Psychology: Human Perception and Performance 17(4): 1057-1074.

Marin, O. S. M. (1980). CAT scans of five deep dyslexic patients (Appendix 1). Deep Dyslexia. M. Coltheart, K. E. Patterson and J. C. Marshall, Routledge: 407-433.

Martin, A., J. V. Haxby, et al. (1995). "Discrete cortical regions associated with knowledge of color and knowledge of action." Science 270: 102-105.

Martin, A., C. L. Wiggs, et al. (1996). "Neural correlates of category-specific knowledge." Nature 379: 649-652.

Maunsell, J. H. R. and W. T. Newsome (1987). "Visual processing in monkey extrastriate cortex." Annual Review of Neuroscience 10: 363-401.

Mazoyer, B. M., N. Tzourio, et al. (1993). "The cortical representation of speech." Journal of Cognitive Neuroscience 5: 467-479.

Mazoyer, B. M., et al. (2001). "Cortical networks for working memory and executive functions sustain the conscious resting state in man." Brain Research Bulletin 54: 287-298.

Mazziota, J. C., M. E. Phelps, et al. (1982). "Tomographic mapping of human cerebral metabolism: Auditory stimulation." Neurology 32: 921-937.

McCarthy, R. A. and E. K. Warrington (1986). "Visual associative agnosia: A clinico-anatomical study of a single case." Journal of Neurology, Neurosurgery, and Psychiatry 49: 1233-1240.

McCarthy, R. A. and E. K. Warrington (1988). "Evidence for modality-specific meaning systems in the brain." Nature 334: 428-430.

McCarthy, G., A. M. Blamire, et al. (1993). "Echo-planar magnetic resonance imaging studies of frontal cortex activation during word generation in humans." Proceedings of the National Academy of Sciences USA 90: 4952-4956.

McIlwain, H. (1953a). "Glucose level, metabolism, and response to electrical impulses in cerebral tissues from man and laboratory animals." Biochemical Journal 55: 618-624.

McIlwain, H. (1953b). "Substances which support respiration and metabolic response to electrical impulses in human cerebral tissues." Journal of Neurology, Neurosurgery, and Psychiatry 16: 257-266.

McIntosh, A. R., C. L. Grady, et al. (1994). "Network analysis of cortical visual pathways mapped with PET." Journal of Neurology 14: 655-666.

McPherson, B. W., and P. J. Holcomb (1992). "Semantic priming with pictures and the N400 component." Psychophysiology 29: S51.

McPherson, B. W., and P. J. Holcomb (1999). "An electrophysiological investigation of semantic priming with pictures of real objects." Psychophysiology 36: 53-65.

McRae, K., V. R. de Sa, et al. (1997). "On the nature and scope of featural representations of word meaning." Journal of Experimental Psychology: General 126: 99-130.

Mchedlishvili, G. and N. Kuridze (1984). "The modular organization of the pial arterial system in phylogeny." Journal of Cerebral Blood Flow and Metabolism 4: 391-396.

Menard, M. T., S. Kosslen, et al. (1996). "Encoding words and pictures: A Positron Emission Tomography study." Neuropsychologia 34: 185-194.

Meno, J. R., A. V. Crum, H. R. Winn (2001). "Effect of adenosine receptor blockade on pial arteriolar dilation during sciatic nerve stimulation." American Journal of Physiology: Heart and Circulatory Physiology 281(5): H2018-2027.

Menon, R. S. and J. S. Gati (1997). Two second temporal resolution measurements of lactate correlate with EPI BOLD fMRI timecourses during photic stimulation. International Society for Magnetic Resonance in Medicine, Vancouver, BC.

Mesulam, M. M. (1990). "Large-scale neurocognitive networds and distributed processing for attention, language, and memory." Annals of Neurology 28: 597-613.

Milberg, W. and S. E. Blumstein (1981). "Lexical decision and aphasia: Evidence for semantic processing." Brain and Language 14: 371-385.

Mishkin, M., L. G. Ungerleider, et al. (1983). "Object vision and spatial vision: Two cortical visual systems." Trends in Neuroscience 6: 414-417.

Modayur, B., J. Prothero, et al. (1997). "Visualization-based mapping of language function in the brain." Neuroimage 6: 245-258.

Mohr, J. P. (1976). Broca's area and Broca's aphasia. Studies in Neurolinguistics. H. Whitaker and H. Whitaker. New York, Academic: 201-236.

Mohr, J. P., M. S. Pessin, et al. (1978). "Broca aphasia: Pathologic and clinical." Neurology 28: 311-324.

Moore, C. J., C. J. Price, et al. (1996). Phonological retrieval and semantic processing during naming tasks. 2nd International Conference on Functional Imaging of the Human Brain, Abstract S449.

Moore, C. J. and C. J. Price (1999a). "A functional neuroimaging study of the variables that generate category-specific object processing differences." Brain 122: 943-962.

Moore, C. J. and C. J. Price (1999b). "Three distinct ventral occipitotemporal regions for reading and object naming." NeuroImage 10: 181-192.

Mueller, W. M., F. Z. Yetkin, et al. (1996). "Functional magnetic resonance imaging mapping of the motor cortex in patients with cerebral tumors." Neurosurgery 39(3): 515-21.

Murtha, S., H. Chertkow, et al. (1999). "The neural substrate of picture naming." Journal of Cognitive Neuroscience 11(4): 399-423.

Nathan, S. S., S. R. Sinha, et al. (1993). "Determination of current density distributions generated by electrical stimulation of the human cerebral cortex." Electroencephalography and Clinical Neurophysiology 86: 183-192.

Newcombe, F., G. Ratcliff, et al. (1987). "Dissociable visual and spatial impairments following right posterior cerebral lesions: clinical, neuropsychological and anatomical evidence." Neuropsychologia 25: 149-161.

Nigam, A., J. E. Hoffman, R. F. Simons (1992). "N400 to semantically anomalous pictures and words." Journal of Cognitive Neuroscience 4: 15-22.

Nobre, A. C. and G. McCarthy (1994). "Language-related ERPs: Scalp distributions and modulation by word type and semantic priming." Journal of Cognitive Neuroscience 6(3): 233-255.

Nobre, A. C. and G. McCarthy (1995). "Language-related field potentials in the anterior-medial temporal lobe: II. Effects of word type and semantic priming." Journal of Neuroscience 15(2): 1090-1098.

Nudo, R. J. and R. B. Masteron (1986). "Stimulation-induced [14 C] 2-deoxyglucose labeling of synaptic activity in the central auditory system." Journal of Comparative Neurology 245: 553-565.

Ogawa, S., T. M. Lee, et al. (1990). "Oxygenation-sensitive contrast in magnetic resonance image of rodent brain at high magnetic fields." Magnetic Resonance in Medicine 14: 68-78.

Ogawa, S., D. W. Tank, et al. (1992). "Intrinsic signal changes accompanying sensory stimulation: Functional brain mapping with magnetic resonance imaging." Proceedings of the National Academy of Sciences USA 89: 5951-5955.

Ogawa, S., R. S. Menon, et al. (1993). "Functional brain mapping by blood oxygenation level-dependent contrast magnetic resonancee imaging. A comparison of signal characteristics with a biophysical model." Biophysical Journal 64: 803-812.

Ojemann, G. A. and H. Whitaker (1978). "Language localization and variability." Brain and Language 6: 239-260.

Ojemann, G. A. (1979). "Individual variability in cortical localization of language." Journal of Neurosurgery 50(2): 164-9.

Ojemann, G. A. and C. Mateer (1979). "Human language cortex: Localization of memory, syntax, and sequential motor-phoneme identification systems." Science 205: 1401-1403.

Ojemann, G. A. (1983). "Brain organization for language from the perspective of electrical stimulation mapping." Behavior and Brain Research 6: 189-230.

Ojemann, G., J. Ojemann, et al. (1989). "Cortical language localization in left, dominant hemisphere: An electrical stimulation mapping investigation in 117 patients." Journal of Neurosurgery 71: 316-326.

Ojemann, G. A. (1991). "Cortical organization of language." Journal of Neuroscience 11(8): 2281-2287.

Ojemann, G. A. (1992). "Localization of language in frontal cortex." Advances in Neurology 57: 361-368.

Ojemann, G. A. (1993). "Functional mapping of cortical language areas in adults: intraoperative approaches." Electrical and Magnetic Stimulation of the Brain and Spinal Cord 13: 155-163.

Olson, R., B. Wise, et al. (1990). Organization, heritability, and remediation of component word recognition and language skills in disabled readers. Reading and it development: Component skills approaches. T. H. Carr and B. A. Levy. San Diego, Academic Press: 261-322.

Op de Beeck, H., E. Beatse, et al. (2000). "The representation of shape in the context of visual object categorization tasks." NeuroImage 12: 28-40.

Osterhout, L. and P. J. Holcomb (1992). "Event-related brain potentials elicited by syntactic anomaly." Journal of Memory and Language 31: 785-804.

Paivio, A. (1990). Mental representations: A dual coding approach. New York, Oxford University Press.

Pardridge, W. M. and W. H. Oldendorf (1977). "Transport of metabolic substrates through the blood-brain barrier." Journal of Neurochemistry 28: 5-12.

Pascual-Marqui, R. D., C. M. Michel, D. Lehmann (1994). "Low resolution electromagnetic tomography: a new method for localizing electrical activity in the brain." International Journal of Psychophysiology 18(1): 49-65.

Paulesu, E., C. D. Frith, et al. (1993). "The neural correlates of the verbal component of working memory." Nature 362: 342-345.

Pellerin, L. and P. J. Magistretti (1994). "Glutamate uptake into astrocytes stimulates aerobic glycolysis: a mechanism coupling neuronal activity to glucose utilization." Proceedings of the National Academy of Sciences USA 91: 10625-10629.

Penfield, W. and L. Roberts (1959). Speech and Brain Mechanisms. Princeton, Princeton University Press.

Penney, T. B., A. Mecklinger, et al. (2001). "Repetition related ERP effects in a visual object target detection task." Brain Research. Cognitive Brain Research. 10(3): 239-250.

Perani, D., S. F. Kappa, et al. (1995). "Different neural systems for the recognition of animals and man-made tools." Neuroreport 6: 1637-1641.

Petersen, S. E., P. T. Fox, et al. (1988). "Positron emission tomographic studies of cortical anatomy of single-word processing." Nature 331: 585-589.

Petersen, S., P. Fox, et al. (1989). "Positron Emission Tomographic studies of the processing of single words." Journal of Cognitive Neuroscience 1(2): 153-170.

Petersen, S. E., P. Fox, et al. (1990). "Activation of extrastriate and frontal cortical areas by visual words and word-like stimuli." Science 249: 1041-1044.

Petersen, S. E. and J. A. Fiez (1993). "The processing of single words studied with positron emission tomography." Annual Review of Neuroscience 16: 509-530.

Phelps, E. A., F. Hyder, et al. (1997). "FMRI of the prefrontal cortex during overt verbal fluency." Neuroreport 8: 561-565.

Poeppel, D. (1996). "A critical review of PET studies of phonological processing." Brain and Language 55: 317-351.

Poliakov, A. V., K. P. Hinshaw, et al. (1999). "Integration and visualization of multimodality brain data for language mapping." Proceedings / AMIA Annual Symposium: 349-53.

Poliakov, A. V. (2002). FMRI Calculator version 4. Structural Informatics Group, Dept. of Biological Structure, University of Washington.

Posse, S., S. R. Dager, et al. (1997). "In vivo measurement of regional brain metabolic response to hyperventilation using magnetic resonance proton echo planar spectro-scopic imaging (PEPSI)." Magnetic Resonance in Medicine 37: 858–865.

Potter, M. C. and B. A. Faulconer (1975). "Time to understand pictures and words." Nature 253: 437-438.

Praamstra, P., A. S. Meyer, and W. J. M. Levelt (1994). "Neurophysiological manifestations of phonological processing: Latency variation of a negative ERP component timelocked to phonological mismatch." Journal of Cognitive Neuroscience 6: 204-219.

Price, C. J. and G. W. Humphreys (1989). "The effects of surface detail on object categorization and naming." Quarterly Journal of Experimental Psychology 41A: 797-827.

Price, C. J., R. Wise, et al. (1994). "Brain activity during reading: The effects of exposure duration and task." Brain 117: 1255-1269.

Price, C. J., R. Wise, et al. (1996a). "Demonstrating the implicit processing of visually presented words and pseudowords." Cerebral Cortex 6: 62-70.

Price, C. J., C. J. Moore, et al. (1996b). "The neural regions sustaining object recognition and naming." Philosophical Transactions of the Royal Society London, Series B 263: 1501-1507.

Price, C. J., Wise, R. J. S., Warburton, E., Moore, C. J., Patterson, K., Howard, D., et al. (1996c). "Hearing and saying: the functional neuro-anatomy of auditory word processing." Brain 119: 919-31.

Price, C. J., C. J. Moore, et al. (1997). "Segregating semantic from phonological processes during reading." Journal of Cognitive Neuroscience 9(6): 727-733.

Price, C. J. and K. Friston (1997). "Cognitive conjunction: A new approach to brain activation experiments." NeuroImage 5: 261-270.

Price, C. J. (1998). "The functional anatomy of word comprehension and production." Trends in Cognitive Sciences 2(8): 281-288.

Prichard, J., D. Rothman, et al. (1991). "Lactate rise detected by 1H NMR in human visual cortex during physiologic stimulation." Proceedings of the National Academy of Sciences USA 88: 5829-5831.

Puce, A., T. Allison, et al. (1995). "Face perception in extrastriate cortex studied by functional MRI." Journal of Neurophysiology 74: 1192-1199.

Puce, A., T. Allison, et al. (1996). "Differential sensitivity of human visual cortex to faces, letterstrings, and textures: a functional magnetic resonance imaging study." Journal of Neuroscience 16(16): 5205-15.

Puce, A., T. Allison, et al. (1999). "Electrophysiological studies of human face perception. III: Effects of top-down processing on face-specific potentials." Cerebral Cortex 9(5): 445-458.

Pugh, K. R., B. A. Shaywitz, et al. (1996). "Cerebral organization of component processes in reading." Brain 119: 1221-1238.

Purves, D., G. J. Augustine, et al., Eds. (2001). Neuroscience. Sunderland, MA, Sinaurer Associates, Inc.

Raichle, M. E., J. A. Fiez, et al. (1994). "Practice-related changes in human brain functional anatomy during nonmotor learning." Cerebral Cortex 4: 8-26.

Randolph, C., A. R. Braun, et al. (1993). "Semantic fluency in Alzheimer's, Parkinson's, and Huntington's disease: Dissociation of storage and retrieval failures." Neuropsychology 7: 82-88.

Ravden, D. and J. Polich (1998). "Habituation of P300 from visual stimuli." International Journal of Psychophysiology 30(3): 359-65.

Ravden, D. and J. Polich (1999). "On P300 measurement stability: habituation, intra-trial block variation, and ultradian rhythms." Biological Psychology 51(1): 59-76.

Richards, T. L., J. D. Bowen, et al. (1996). "MR brain spectroscopy: basic concepts with emphasis on multiple sclerosis." International Journal of Neuroradiology 2: 123-133.

Richards, T. L., S. R. Dager, et al. (1997). "Functional MR spectroscopy during language activation: A preliminary study using Proton Echo-Planar Spectroscopic Imaging (PEPSI)." International Journal of Neuroradiology 3: 490-495.

Richards, T. L., S. R. Dager, et al. (1999). "Dyslexic children have abnormal brain lactate response to reading-related language tasks." American Journal of Neuroradiology 20: 1393-1398.

Riddoch, M. J. and G. W. Humphreys (1987). "Visual object processing in optic aphasia: A case of semantic access agnosia." Cognitive Neuropsychology 4: 131-185.

Roeltgen, D. P., S. Sevush, et al. (1983). "Phonological agraphia." Neurology 33: 755-765.

Roland, P., B. Larson, et al. (1980). "Supplementary motor area and other areas in organization of voluntary movements in man." Journal of Neurophysiology 43: 118-136.

Romero, R. and J. Polich (1996). " P3(00) habituation from auditory and visual stimuli." Physiology & Behavior 59(3): 517-22.

Roskies, A. L., J. E. Fiez, et al. (1996). "PET studies of semantic analysis." Society for Neuroscience Abstracts 22: 110.

Rubens, A. B. (1976). Transcortical motor aphasia. Studies in Neurolinguistics. H. Whitaker and H. Whitaker. New York, Academic: 293-306.

Ruge, M. I., J. Victor, et al. (1999). "Concordance between functional magnetic resonance imaging and intraoperative language mapping." Stereotactic & Functional Neurosurgery 72(2-4): 95-102.

Rugg, M. D. (1985). "The effects of semantic priming and work repetition on event-related potentials." Psychophysiology 22(6): 642-7.

Rugg, M. (1990). "Event-related brain potentials dissociate repetition effects of high- and low-frequency words." Memory and Cognition 18: 367-379.

Rugg, M. D. and S. E. Barrett (1987). "Event-related potentials and the interaction between orthographic and phonological information in a rhyme-judgement task." Brain and Language 32: 336-61.

Rugg, M. D., R. C. Roberts, et al. (1991). "Event-related potentials related to recognition memory: Effects of unilateral temporal lobectomy and temporal lobe epilepsy. Brain 114: 2313-2332.

Rumsey, J. M., B. Horwitz, et al. (1997). "Phonological and orthographic components of word recognition: A PET-rCBF study." Brain 120: 739-759.

Rush, S. and D. A. Driscoll (1986). "Current distribution in the brain from surface electrodes." Anesthesia and Analgesia 47: 717-723.

Rutten, G. J., P. C. van Rijen, et al. (1999). "Language area localization with three-dimensional functional magnetic resonance imaging matches intrasulcal electrostimulation in Broca's area." Annals of Neurology 46(3): 405-8.

Sacchett, C. and G. W. Humphreys (1992). "Calling a squirrel a squirrel but a canoe a wigwam: A category-specific deficit for artifactual objects and body parts." Cognitive Neuropsychology 9: 73-86.

Sappey-Marinier, D., G. Calabrese, et al. (1992). "Effect of photic stimulation on human visual cortex lactate and phosphates using 1H and 31P magnetic resonance spectroscopy." Journal of Cerebral Blood Flow and Metabolism 12: 584-592.

Sartori, G. and R. Job (1988). "The oyster with four legs: A neuropsychological study on the interaction of visual and semantic information." Cognitive Neuropsychology 5: 130-152.

Sartori, G., R. Job, et al. (1993). "Category-specific form-knowledge deficit in a patient with herpes simplex virus encephalitis." Journal of Clinical and Experimental Neuropsychology 15: 280-299.

Sasanuma, S. (1971). "Selective impairment of phonetic and non-phonetic transcription of words in Japanese aphasic patients: Kana vs. Kanji in visual recognition and writing." Cortex 7: 1-18.

Sasanuma, S. (1975). "Kana and Kanji processing in Japanese aphasics." Brain and Language 2: 369-383.

Schacter, D. L., E. Reiman, et al. (1995). "Brain regions associated with retrieval of structurally coherent visual information." Nature 376: 587-590.

Schaffler, L., H. O. Luders, et al. (1996). "Quantitative comparison of language deficits produced by extraoperative electrical stimulation of Broca's, Wernicke's, and basal temporal language areas." Epilepsia 37(5): 463-75.

Schendan, H. E. and M. Kutas (2002). "Neurophysiological evidence for two processing times for visual object identification." Neuropsychologia 40: 931-945.

Schendan, H. E., G. Ganis, M. Kutas (1998). "Neurophysiological evidence for visual perceptual categorization of words and faces within 150ms." Psychophysiology 35: 240-251.

Schlosser, M. J., M. Luby, et al. (1999). "Comparative localization of auditory comprehension by using functional magnetic resonance imaging and cortical stimulation." Journal of Neurosurgery 91(4): 626-35.

Schurr, A., C. A. West, et al. (1988). "Lactate-supported synaptic function in the rat hippocampal slice preparation." Science 240: 1326-1328.

Schurr, A., J. J. Miller, et al. (1999). "An increase in lactate output by brain tissue serves to meet the energy needs of glutamate-activated neurons." Journal of Neuroscience 19: 34-39.

Segebarth, C. M., V. Belle, et al. (1994). "Functional MRI of the human brain: predominance of signals from extracerebral veins." Neuroreport 5: 813-816.

Serafini, S., K. Steury, et al. (2001). "Comparison of fMRI and PEPSI during language processing in children." Magnetic Resonance in Medicine 45: 217-225.

Sergent, J., E. Zuck, et al. (1992a). "Positron Emission Tomography study of letter and object processing: Empirical findings and methodological considerations." Cerebral Cortex 2: 68-80.

Sergent, J., S. Ohta, et al. (1992b). "Functional neuroanatomy of face and object processing." Brain 115: 15-36.

Shallice, T. (1981). "Phonological agraphia and the lexical route in writing." Brain 104: 413-429.

Shallice, T. and G. Vallar (1990). Neuropsychological impairments of short-term memory. T. Shallice and G. Vallar. New York, Cambridge University Press: 11-53.

Shaywitz, B. A., K. R. Pugh, et al. (1995). "Localization of semantic processing using functional magnetic resonance imaging." Human Brain Mapping 2: 10-20.

Sheridan, J. and G. W. Humphreys (1993). "A verbal-semantic category-specific recognition impairment." Cognitive Neuropsychology 10: 143-184.

Shulman, R. G., A. M. Blamire, et al. (1993). "Nuclear magnetic resonance imaging and spectroscopy of human brain function." Proceedings of the National Academy of Sciences USA 90: 3127-3133.

Shulman, G. J., J. A. Fiez, et al. (1997). "Common blood flow changes across visual tasks: II. Decreases in cerebral cortex." Journal of Cognitive Neuroscience 9(5): 648-663.

Sibson, N. R., A. Dhankhar, G. F. Mason, et al. (1998). Stoichiometric coupling of brain glucose metabolism and glutamatergic neuronal activity. Proceedings of the National Academy of Science USA 95: 316-321.

Sittsworth, J. D. J. and T. H. Lanthorn (1993). "Lactate mimics only some effects of D-glucose on epileptic depolarization and long-term synaptic failure." Brain Resonance 630: 21-27.

Smith, E. E. and L. Magee (1980). "Tracing the time course of picture-word processing." Journal of Experimental Psychology: General 109: 373-392.

Smith, M. E., and E. Halgren (1988). "Attenuation of a sustained visual processing negativity after lesions that include the inferotemporal cortex." Electroencephalography and Clinical Neurophysiology 70: 366-369.

Smith, M. E., and E. Halgren (1989). "Dissociation of recognition memory components following temporal lobe lesions." Journal of Experimental Psychology: Learning, Memory, and Cognition 15: 50-60.

Snodgrass, J. G. and M. Vanderwart (1980). "A standardized set of 260 pictures: norms for name agreement, image agreement, familiarity, and visual complexity." Journal of Experimental Psychology: Human Learning and Memory 6(2): 174-215.

Spitzer, M., M. E. Bellemann, et al. (1996). "Functional MR imaging of semantic information processing and learning-related effects using psychometrically controlled stimulation paradigms." Cognitive Brain Research 4: 149-161.

Springer, J. A., J. R. Binder, et al. (1999). "Language dominance in neurologically normal and epilepsy subjects." Brain 122: 2033-2045.

Stapleton, S. R., E. Kiriakopoulos, et al. (1997). "Combined utility of functional MRI, cortical mapping, and frameless stereotaxy in the resection of lesions in eloquent areas of brain in children." Pediatric Neurosurgery 26: 68-82.

Steinmetz, H., U. Ebeling, et al. (1990). "Sulcus topography of the parietal opercular region: an anatomic and MR study." Brain and Language 38: 515-533.

Steinmetz, H. and R. J. Seitz (1991). "Functional anatomy of language processing: neuroimaging and the problem of individual variability." Neuropsychologia 29(12): 1149-1161.

Steury, K., D. Corina, et al. (2001). A comparison of fMRI and fMRS during an auditory monitoring task. Abstract submitted to Cognitive Neuroscience Society.

Stromswold, K., D. Caplan, et al. (1996). "Localization of syntactic comprehension by Positron Emission Tomography." Brain and Language 52: 452-473.

Strother, S. C., J. R. Anderson, et al. (1995). "Principal component analysis and the scaled subprofile model compared to intersubject averaging and statistical parametric mapping: I. "Functional connectivity of the human motor system studied with [15O] water PET"." Journal of Cerebral Blood Flow and Metabolism 15(5): 738-753.

Stuss, D. T. and D. F. Benson (1986). The Frontal Lobes. New York, Raven.

Stuss, D. T., T. W. Picton, et al. (1992). "Perceptual Closure and Object Identification: Electrophysiological responses to incomplete pictures." Brain and Cognition 19: 253-266.

Swinney, D., E. Zurif, et al. (1989) "The effects of focal brain damage on sentence processing: An examination of the neurological organization of a mental module." Journal of Cognitive Neuroscience 1: 25-37.

Tallal, P. and E. Newcomb (1978). "Impairment of auditory perception and language comprehension in dysphasia." Brain and Language 5: 13-24.

Thompson-Schill, S. L., M. D'Esposito, et al. (1997). "Role of left inferior prefrontal cortex in retrieval of semantic knowledge: A reevaluation." Proceedings of the National Academy of Sciences USA 94: 14792-14797.

Turner, R., P. Jezzard, et al. (1993). "Functional mapping of the human visual cortex and 4 and 1.5 tesla using deoxygenation contrast EPI." Magnetic Resonance in Medicine 29: 277-279.

Ungerleider, L. G. and M. Mishkin (1982). Two cortical visual systems. Analysis of visual behavior. D. J. Ingle, M. A. Goodale and R. J. W. Mansfield. Cambridge, MIT Press: 549-586.

Ungerleider, L. G. and J. V. Haxby (1994). "'What' and 'where' in the human brain." Current Opinion in Neurobiology 4(2): 157-65.

Vallar, G. and A. D. Baddeley (1984). "Fractionation of working memory: Neuropsychological evidence for a phonological short-term store." Journal of Verbal Learning and Verbal Behavior 23: 151-161.

Van Orden, G. C., J. C. Johnston, et al. (1988). "Word identification in reading proceeds from spelling to sound to meaning." Journal of Experimental Psychology: Human Learning and Memory 14: 371-386.

Vandenberghe, R., C. J. Price, et al. (1996). "Functional anatomy of a common semantic system for words and pictures." Nature 383: 254-256.

Vanier, M. and D. Caplan (1985). CT scan correlates of surface dyslexia. Surface Dyslexia. K. E. Patterson, J. C. Marshall and M. Coltheart, Erlbaum: 511-525.

Vellutino, F. R., D. M. Scanlon, et al. (1995). The increasingly inextricable relationship between orthographic and phonological coding in learning to read: Some reservations about current methods of operationalizing orthographic coding. The varieties of orthographic knowledge II: Relationships to phonology, reading, and writing. V. W. Berninger. Dordrecht, Kluwer Academic Publishers: 47-111.

Villringer, A. (2000). Physiological changes during brain activation. Functional MRI. C. T. W. Moonen and P. A. Bandettini. Berlin, Springer-Verlag: 3-13.

Vitkovich, M. and G. W. Humphreys (1991). "Perseverant responding in speeded picture naming: It's in the links." Journal Of Experimental Psychology: Learning, Memory, and Cognition 17: 664-680.

Votaw, J. R., T. L. Faber, et al. (1999). "A confrontational naming task produces congruent increases and decreases in PET and fMRI." NeuroImage 10: 347-356.

Wada, J. and T. Rasmussen (1960). "Intracarotid injection of sodium amytal for the lateralization of cerebral speech dominance: experimental and clinical observations." Journal of Neurosurgery 17: 266-282.

Wang, J., T. Zhow, et al. (1999). "Relationship between ventral stream for object vision and dorsal stream for spatial vision: an fMRI + ERP study." Human Brain Mapping 8: 170-181.

Warburton, E., R. J. S. Wise, et al. (1996). "Noun and verb retrieval by normal subjects: Studies with PET." Brain 119: 159-179.

Warrington, E. K. and A. Taylor (1973). "Contribution of the right parietal lobe to object recognition." Cortex 9: 152-164.

Warrington, E. K. (1982). "Neuropsychological studies of object recognition." Philosophical Transactions of the Royal Society London, Series B 298: 15-33.

Warrington, E. K. and R. A. McCarthy (1983). "Category specific access of dysphasia." Brain 106: 859-878.

Warrington, E. K. and T. Shallice (1984). "Category specific semantic impairments." Brain 107: 829-854.

Warrington, E. K. and R. A. McCarthy (1987). "Categories of knowledge: Further fractionations and an attempted integration." Brain 110: 1273-1296.

Whatmough, C., H. Chertkow, et al. (2002). "Dissociable brain regions process object meaning and object structure during picture naming." Neuropsychologia 40: 174-186.

Wise, R., F. Chollet, et al. (1991a). "Distribution of cortical neural networks involved in word comprehension and word retrieval." Brain 114: 1803-1817.

Wise, E., U. Hadar, et al. (1991b). Language activation studies with positron emission tomography. Exploring brain functional anatomy with positron emission tomography. Chichester, Wiley: 218-234.

Zattore, R., A. Evans, et al. (1992). "Lateralization of phonetic and pitch discrimination in speech processing." Science 256: 846-849.

Zattore, R., E. Meyer, et al. (1996). "PET studies of phonetic processing of speech: Review, replication, and reanalysis." Cerebral Cortex 6: 21-30.

Zhang, X. L., H. Begleiter, et al. (1995). "Event related potentials during object recognition tasks." Brain Research Bulletin 38(6): 531-538.

Ziegler, J. C., M. Besson, et al. (1997). "Word, pseudoword, and nonword processing: A multitask comparison using event-related brain potentials." Journal of Cognitive Neuroscience 9(6): 758-775.

Appendix A

Object Stimuli

Airplane Ant Apple Astronaut Bagpiper Banana

Baseball Basket Bat Bathrobe Batteries Bear

Bed Bee Bell Belt Bicycle Bird

Book Bowl Box Briefcase Broom Buffalo

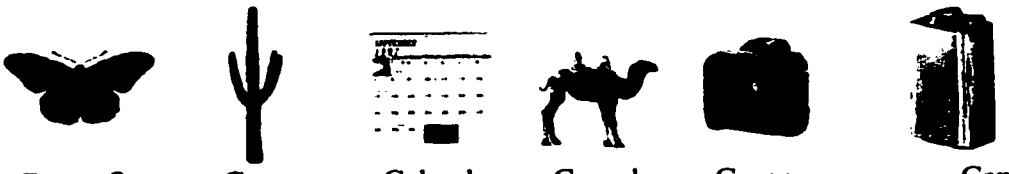

Butterfly Cactus Calendar Camel Camera Can

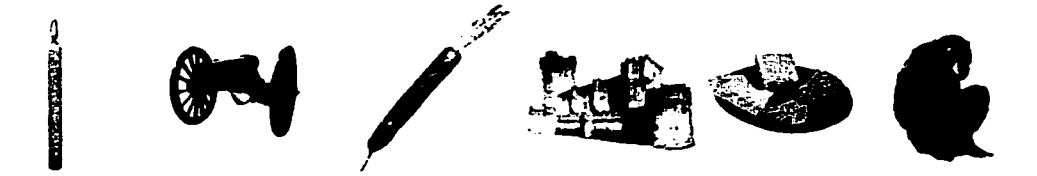

Candle Cannon Carrot Castle Cheese Chimpanzee

Cigarette Clipboard Clock Clown Comb Cookies

Couch Crab Crackers Credit Cards Crown Cup

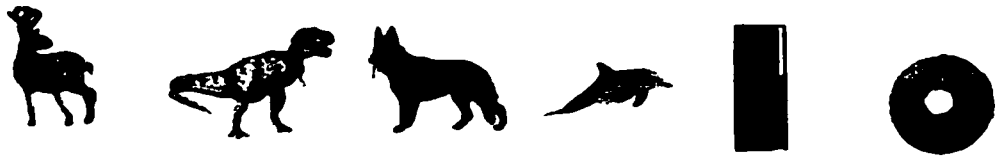

Deer Dinosaur Dog Dolphin Door Doughnut

Dress Duck Earth Eggs Elephant Eye


Fan


Fire Hydrant


Fish


Flowers


Fly


Football


Frog


Giraffe


Globe


Goggles


Grapes


Grasshopper


Hairbrush


Hamburger


Hammer


Hand


Hat


Hatchet


Helicopter


Helmut


Hiker


Hinge


House


Ice Cream


Igloo


Iron


Jar


Jug


Key


Knife


Ladybug


Lamp


Lemon

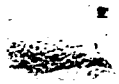
Letter


Lettuce


Lighthouse


Lizard


Lock


Mirror


Moon


Mushroom


Nail


Newspaper


Octopus


Onion


Orange


Paintbrush


Paperclip


Pen


Pencil


Penguin


Phone


Piano


Pig


Piggybank


Pizza


Plaid


Plant


Pliers


Plug


Pumpkin


Rainbow


Razor


Ring


Rollerskate


Scissors


Screw


Screwdriver


Shark


Shell


Sink


Skateboard


Skillet


Snail


Snake


Soap


Sodapop


Speghetti


Spoon


Stapler


Star


Statue


String


Suitcase


Sunglasses


Tape


Teapot


Thumbtack


Tissue


Toast

Toothbrush Tractor Train Tree Truck Trumpet

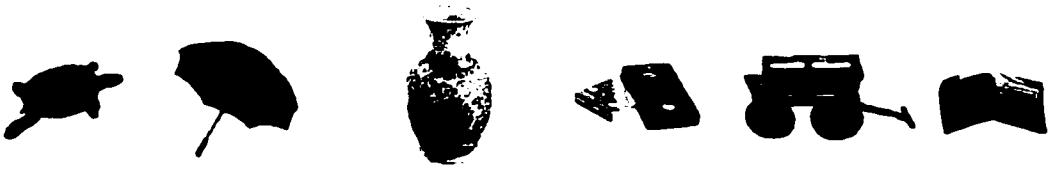

Turtle Umbrella Vase Videotape Wagon Wallet

Watch Wheelbarrow Windmill Wine Wrench Zebra

Pixelated Objects

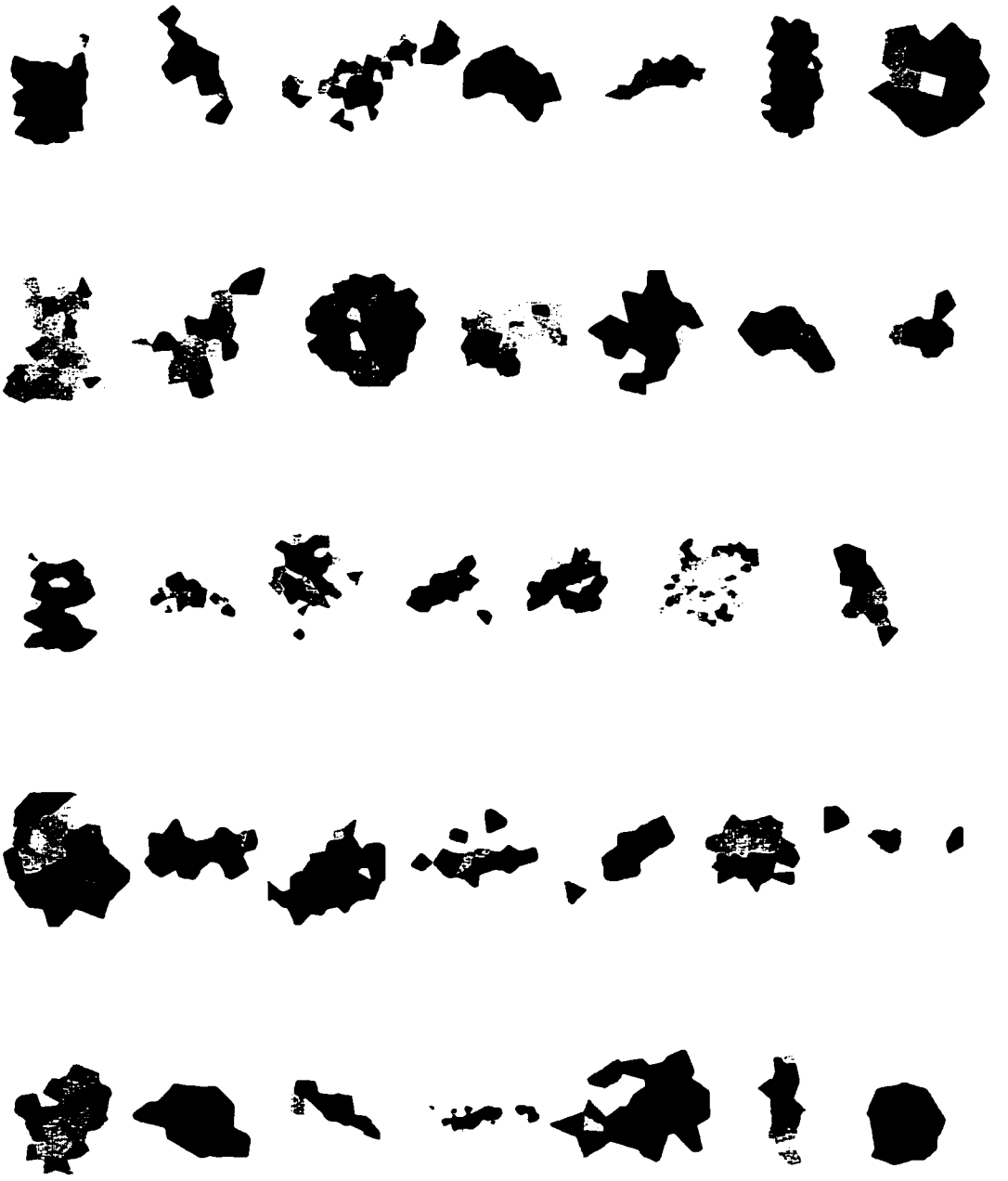

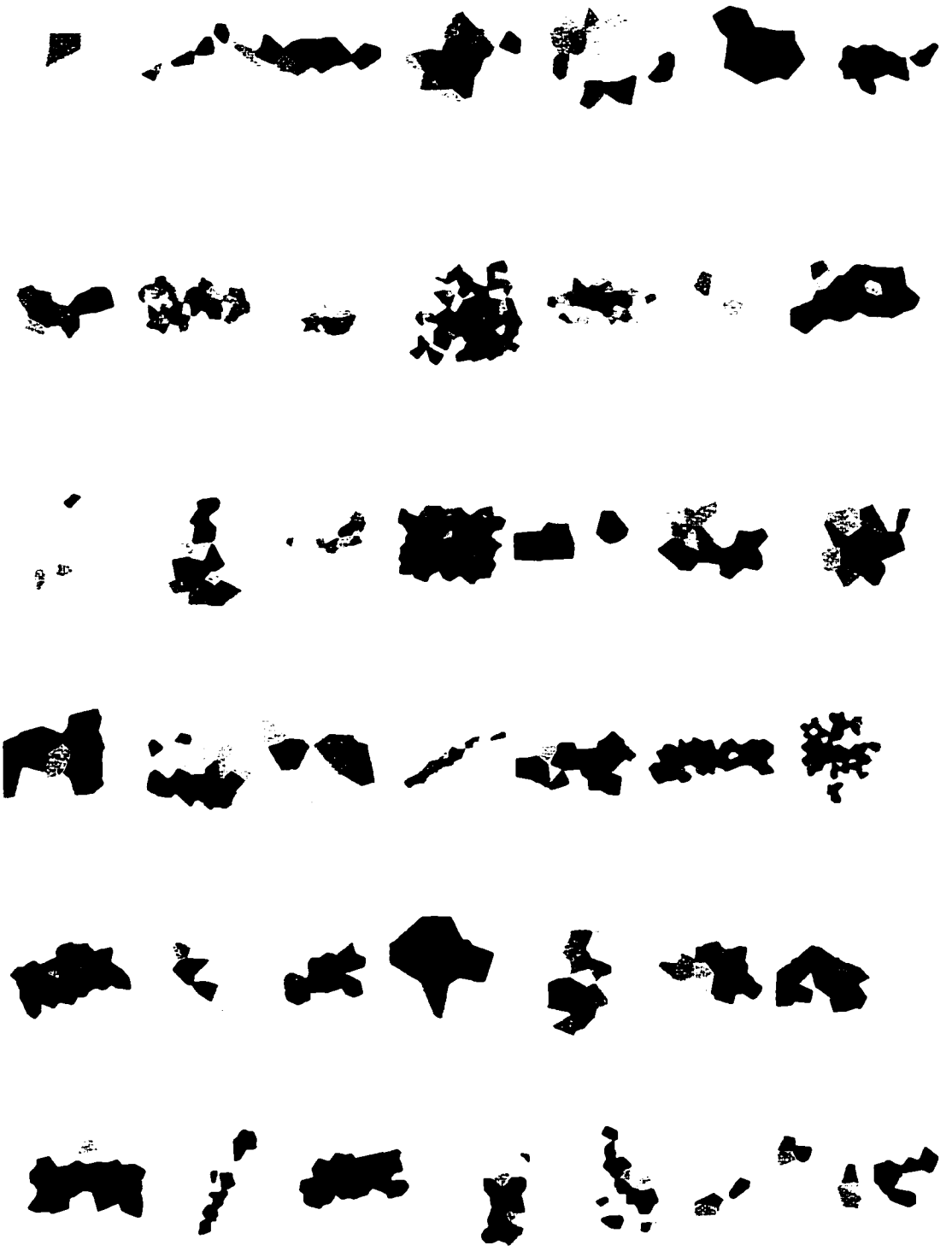

APPENDIX B

Coding for Ojemann Speech Error – David Corina, UW Dept. of Psychology

Temporal Characteristics

A	normal naming rate
B	ahh/umm...(filler)
C	short delay
D	long delay

Content Characteristics

1	target
2	semantic paraphasia (e.g., cow → horse, chair → sit)
3	phonological paraphasia (**clear substitution** e.g., /f / → /v /, /t / → /d /)
4	neologism – an unrecognizable word (e.g., cow → zobluch)
5	perseveration – portion or all of preceding word
6	semantic/phonological blends (e.g., oyster → lobster, train → plane)
7	morphological anomaly (e.g., mouse → mice)
8	phonological reduction – drop a syllable (e.g., dresser → dress, candle → can)
9	apraxic error – slur, stutter, motor issue
10	off target
11	no target

Miscellaneous Diacritics

R	repeated successive attempts/approximations
FSE	error followed a stimulation error, but not stimulated itself
!	comment – see comment box
S	self-corrects/resolves to a correct response

Confidence Rating

5	very confident
1	not confident at all

VITA

Sandra Serafini

Degree	Year	Field	Institution
B.A.	1990	Honours Music	University of Waterloo
M.A.	1993	Ethnomusicology	University of British Columbia
Ph.D.	2002	Speech & Hearing Sciences	University of Washington

Publications

Corina, D., Richards, T., Serafini, S., Richards, A., Steury, K., Abbott, R.D., Echelard, D., Maravilla, K.R., Berninger, V.W. (2001). FMRI auditory language differences between dyslexic and able reading children. *Neuroreport* 12: 1195-1201.

Serafini, S., Steury, K., Richards, T., Corina, D., Abbott, R., Dager, S.R., Berninger, V. (2001). Comparison of fMRI and PEPSI during language processing in children. *Magnetic Resonance in Medicine* 45: 217-225.

Richards, T.L., Corina, D., Serafini, S., Steury, K., Dager, S.R., Marro, K., Abbott, R.D., Maravilla, K.R., Berninger, V.W. (2000). The effects of a phonologically-driven treatment for dyslexia on lactate levels as measured by proton MRSI. *American Journal of Neuroradiology* 21: 916-922.

Richards, T.L., Dager, S.R., Corina, D., Serafini, S., Heide, A.C., Steury, K., Strauss, W., Hayes, C.E., Abbott, R.D., Craft, S., Shaw, D., Posse, S., Berninger, V.W. (1999). Dyslexic children have abnormal brain lactate response to reading-related language tasks. *American Journal of Neuroradiology* 20: 1393-1398.

Heide, A.C., Kraft, G.H., Slimp, J.C., Gardner, J.C., Posse, S., Serafini, S., Bowen J.D., Richards, T.L. (1998). Cerebral N-Acetyl Aspartate is low in MS patients with abnormal visual evoked potentials. *American Journal of Neuroradiology* 19: 1047-1054.

Richards, T.L., Dager, S.R., Panagiotides, H.S., Hayes, C.E., Posse, S., Serafini, S., Nelson, J.A., Maravilla, K.R. (1997). Functional magnetic resonance spectroscopy during language activation: A preliminary study using Proton Echo-Planar Spectroscopic Imaging. *International Journal of Neuroradiology* 3: 490-495.

Richards, T.L., Gates, G.A., Gardner, J.C., Merrill, T., Hayes, C.E., Panagiotides, H., Serafini, S., Rubel, E.W. (1997). Functional magnetic resonance spectroscopy of the auditory cortex in patients with sudden sensorineural hearing loss. *American Journal of Neuroradiology* 18: 611-620.

Serafini, S. (1995). Timbre judgments of Javanese gamelan instruments by trained and untrained adults. *Psychomusicology* 14: 137-153.